ESTABLISHING AND APPLYING SPEED-FLOW RELATIONSHIPS FOR TRAFFIC ON RURAL TWO-LANE TWO-WAY HIGHWAYS IN THE WESTERN CAPE

By

Janvier Twagirimana

(REB Scholar)

Thesis presented in partial fulfilment of the requirements for the degree of Masters of Engineering in the Faculty of Engineering at Stellenbosch University

Supervisor: Prof. Christo J. Bester

December 2013

Declaration

By submitting this thesis electronically, I declare that the entirety of the work contained therein is my own, original work, that I am the sole author thereof (save to the extent explicitly otherwise stated), that reproduction and publication thereof by Stellenbosch University will not infringe any third party rights and that I have not previously in its entirety or in part submitted it for obtaining any qualification.

December 2013

Abstract

Speed-flow-density relationships are the most useful tools in the highway design and planning process. They are useful in predicting the roadway capacity, in determining the adequate level-of-service of traffic flow and in determining travel time for a given roadway.

Two-lane two-way rural highways constitute the vast majority of the rural road network in South Africa. Nowadays in the Western Cape and other provinces of South Africa, the speed-flow-density relationships normally used for rural transportation studies are derived from the Highway Capacity Manual, which reflects the traffic conditions in the North American situation. Since the North American traffic conditions may be different from the South African conditions, a need to investigate speed-flow-density relationships on these highways in South Africa arises in order to justify any investment made on these roads.

In this context, a video technique was used to collect traffic flow data during morning peak hours on two rural two-lane two-way highways in the Western Cape Province in order to investigate these relationships. Through the use of Adobe premiere C.S 6 software, travel time of individual vehicles and distance headways were measured and used in computation of average speed and average density.

Several researchers have developed models to describe the relationships between traffic characteristics on uninterrupted flow facilities. In this study, some of these models were tested using collected data in order to investigate which model fits the data satisfactorily. Statistical methods were used to evaluate the ability of each model to predict the flow characteristics over the whole range of data. Average speed and density data were used through regression analysis to perform curve fitting and testing of these developed models. In the next stage, the model which provided a best representation of the data on each section was selected and through the application of the steady-state equation (2.1), flow-density and speed-flow relationships were established on these sections. The available data were also used to investigate the

impact the observation time has on the speed-flow curve and the resulting capacity value.

Finally, the developed speed-flow curves were used to determine the capacities of the study sections. These capacity values were used to determine if the shoulder usage contributes in increasing the capacity of two-lane two-way highways by comparing them to the capacity provided by HCM.

Opsomming

Spoed-vloei-digtheid verhoudings is baie handig in die beplanning en ontwerp van paaie. Dit kan ook gebruik word in die voorspelling van kapasiteit, diensvlak en reistyd. Twee-laan twee-rigting paaie maak die grootste deel van die Suid-Afrikaanse padnetwerk uit en vir die beplanning daarvan word van Amerikaanse spoed-vloei-digtheid verhoudings gebruik gemaak aangesien daar nog nie voorheen ‘n studie hiervan in SA gemaak is nie.

Video-opnames is gebruik om verkeersvloeidata op twee paaie in die omgewing van Stellenbosch te versamel. Die reistyd en digtheid van individuele voertuie is tydens spitstye waargeneem. Die data is gebruik om te bepaal watter modelle die beste is om die spoed-vloei-digtheid verhoudings vir hierdie paaie te modelleer. Die beste modelle is dan gebruik om die kapasiteit van die paaie te bepaal en dit te vergelyk met die Amerikaanse waardes.

Acknowledgments

First and foremost, I would like to express my sincere appreciation to my Supervisor and promoter, Professor Christo J. Bester for his continuous support and encouragement for this thesis. Without his valuable guidance and instruction, this work would not have been finished on time. He always made himself available whenever I needed him, and spent his precious time to review and correct the drafts of this thesis. Besides the unlimited and priceless academic assistance from him, I was also attracted by his generous personality. He is a very humble, heart-warming person and generous not only to me but also to all students. He showed me a good example and I respect him.

Appreciation also goes to the Rwandan Government, which through the Rwandan Education Board funded my studies and makes my endeavour a success. I wish to express my heartfelt thanks to the Department of Civil Engineering and the technicians of structural laboratory who helped me to get all the equipment I needed for successful data collection process.

I want to deeply acknowledge my family's endless love and support for me. No words can describe my appreciation to my beloved wife, Olive Imanizabayo, who encouraged me to continue my postgraduate studies. I owe a great debt to her. I also want to express great appreciation to my mother, brother and sisters and friends who give me enormous love and prayer and always proud of me. I believe that they congratulate my achievement the most in the world.

Finally, I would like to acknowledge each and every person who has contributed to the success of this thesis. May God the almighty continue to bless each and every one in your everyday life.

Once again, thank you very much from the bottom of my heart. Without you, this achievement could not be possible.

Table of Contents

List of Figures

Chapter 1

Chapter 2

Chapter 3

Chapter 4

APPENDIX C

List of Tables

Chapter 2

Appendix A

List of Abbreviations

HCM	Highway Capacity Manual
PHF	Peak-hour Factor
USA	United States of America
ATS	Average Travel Speed
PTSF	Percent Time-Spent-Following
PFFS	Percent of Free-Flow Speed
FFS	Free Flow Speed
Pcph	Passenger car per hour
Pcphpl	Passenger car per hour per lane
LOS	Level of Service
SSE	Sum of Squares of Errors
SSR	Regression Sum of Squares
CBD	Central Business District
N	National road
Min	minute
R	Regional road

CHAPTER 1: INTRODUCTION

1.1 Background

The analysis of traffic conditions in macroscopic models are governed by fundamental relationships between flow, speed and density. Speed-flow-density relationships are the most useful tools in highway design and planning process. They are useful in predicting the roadway capacity, in determining the adequate level-of-service of traffic flow and in determining travel time for a specific roadway.

Travel demand models which constitute a part of the planning process use speed-flow relationships to assign traffic flows on different links of the highway network. Since the highway network are kept changing due to the establishment of new developments along it, these relationships need to be understood, and revised to accommodate changing conditions and new volumes.

In South Africa as well as in many countries of the world, two-lane highways constitute the vast majority of the rural road network (Van As & Van Nierkerk, 2004; Dey et al., 2008).Two-lane two-way rural highways being uninterrupted flow roadways, they exhibit traffic operations different from those of other uninterrupted flow facilities (e.g. freeways), since motorists are constrained to use the lane of conflicting traffic for lane switching and passing purposes. This implies that the relationships developed empirically or for other types of uninterrupted facilities cannot be applied to this type of highways.

The theory of traffic flow helps in description of the relationships between speed, flow and density for all conditions of traffic flow on different highways. Once a particular relationship between two traffic characteristics is established, unknown characteristic can be estimated. Mathematical relationships used to describe traffic flow can be classified into two approaches, the macroscopic approach and microscopic approach. The macroscopic approach considers the flow as a stream and it is concerned with macroscopic speed, flow and density, while the microscopic approach which considers traffic as a mixture of individual vehicles deals with individual speed, time and distance

headways. Research has however shown that the two approaches are interrelated (Garber & Hoel, 2002; Gazis et al., 1961).

Many studies have been conducted overseas since 1930s, to explain the relationships between speed, flow and density of traffic more specifically for uninterrupted flow facilities, and the factors that affect these relationships. In spite of their constituting a significant proportion, very few researches were carried out to describe these relationships on two-lane two-way rural highways in South Africa.

1.2 Problem statement

As noted previously, the South African road network presents a vast majority of two-lane highways especially in rural areas. The understanding of relationships between traffic speed, flow, and density is proved to be important considering the impact the shape of the resultant curves have on the highway design and planning processes. These relationships clearly give quantitative estimates of the change in speed as a function of anticipated or projected changes in traffic demand. Therefore, ignoring these relationships may lead to unjustified decisions regarding road construction, upgrading, and evaluation of effectiveness of implemented traffic engineering measures, hence causing serious problems for transportation policy.

Nowadays in all South African provinces including the Western Cape, the speed-flow-density relationships normally used for rural transportation studies are derived from the Highway Capacity Manual, which reflects the traffic conditions in the North American situation. Since the North American traffic conditions may be different from the South African conditions, a need for investigation of these relationships has arisen to account for traffic conditions on South African two-lane two-way highways, in order to ensure that it is justified to maintain the application of the relationships derived by the Highway Capacity Manual in the South African context. The purpose of this study is to come up with models that explain those relationships on two-lane two-way rural roads in the Western Cape.

1.3 Objectives of the Study

The main objective of this study is:

- To establish speed-flow-density models on two-lane rural roads in the Western Cape using different models established overseas to describe relationships between uninterrupted traffic stream parameters.

Along with the main objective, the subsidiary objectives are:

1. To evaluate the suitability of the developed models in congested and uncongested regime.
2. To develop travel time-density and travel time–flow relationships on rural two-lane highways
3. To investigate whether the use of paved shoulders can assist in increasing road capacity.

1.4 Research design

This part illustrates the main components of the present study and procedures followed in conducting this study. The following figure shows schematically the relationships between different components of this study.

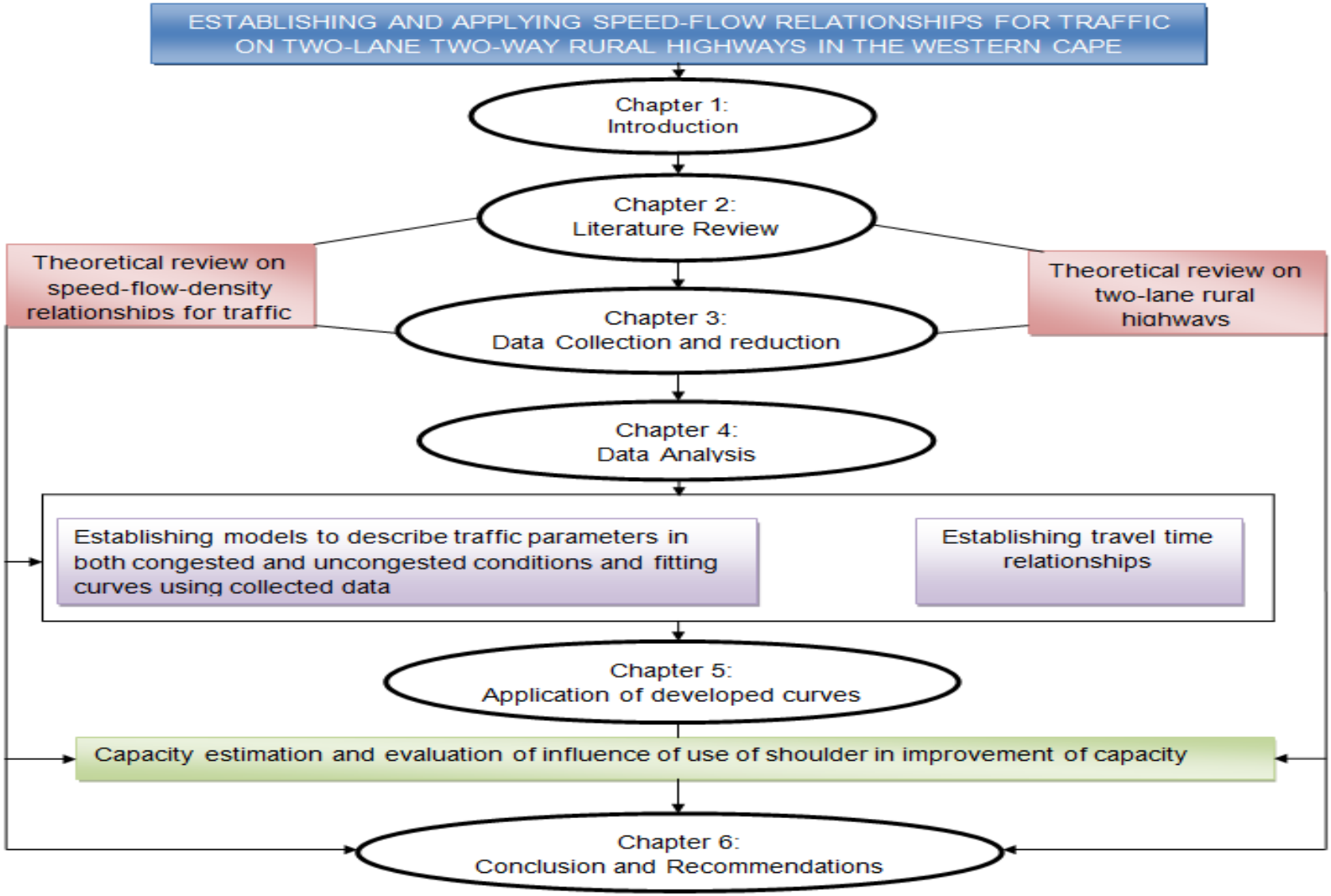

Figure 1. 1: Research design

1.5 Outline of the Thesis

Chapter 1 presents the background of the study, problem statement and objectives of research. The remainder of the study is organized as follows:

Chapter 2 consists of the literature review on the theory of traffic flow relationships on uninterrupted flow facilities, capacity related theory on two-lane two-way rural highways, and finally the concept of regression analysis.

Chapter 3 provides in detail the methodology used in the study and description of the study areas. Traffic data collection and reduction processes at different study areas are discussed in detail and data on traffic are gathered to be analysed.

In Chapter 4, traffic data are analysed and various models explaining relationships between traffic parameters are established.

Chapter 5 consists of evaluation of highway performance where the effect of shoulder use on capacity is investigated by using the developed curves.

In Chapter 6, Conclusions drawn from results and recommendations are presented.

CHAPTER 2: LITERATURE REVIEW

2.1 Introduction and structure

Transport forms one of the primary needs in all categories of the population in modern society, because everyone needs to travel for different purposes namely working, studying, shopping, recreational, commuting, and so on. Since a great proportion of daily trips are done by road, road traffic flow and all related parameters are deemed necessary to be understood in order to improve the highway performances. Therefore, understanding the entire range of relationships between traffic parameters leads in achieving an enhancement of quality of traffic operations, hence an improvement of highway performances.

In developed countries and some developing countries including South Africa, many studies has been done and well documented on speed-flow-density models and relationships on freeways and expressways, however, a little amount of literature is available on these relationships applied to two-lane rural highways. With reference to this, and the objectives of this study, this literature review has a following structure:

i. A brief overview on basic terms used in traffic flow theory.
ii. Relationships between traffic flow characteristics
iii. Review on theoretical conventional speed-flow-density models
iv. More research and interpretation of traffic characteristics relationships
v. Theory on two-lane two-way highways
vi. A brief description on regression analysis, given that it will mostly be used in this study.

2.2 A brief overview on basic terms used in Traffic flow theory

Traffic flow theory is one of the disciplines of transportation engineering which uses mathematical analysis and modelling to explain road traffic flow mechanisms.
The theory of traffic flow uses mainly three interrelated parameters for which relationships are worthy to be understood. In order to establish these relationships on

two-lane highways, it is essential to understand those parameters for which the steady-state flow fundamental relationship is shown in the following equation:

$$Q = u_s . K \quad (2.1)$$

Where:

Q = Flow (Veh /h)

u_s = Macroscopic speed (Km/h)

K = Density (Veh/km)

Different terms used in analysis of traffic flow are defined in the following part as described in the Highway Capacity Manual (TRB, 2000). These terms are grouped into two categories according to the relative approach in which they are used, as shown in Figure 2.1.

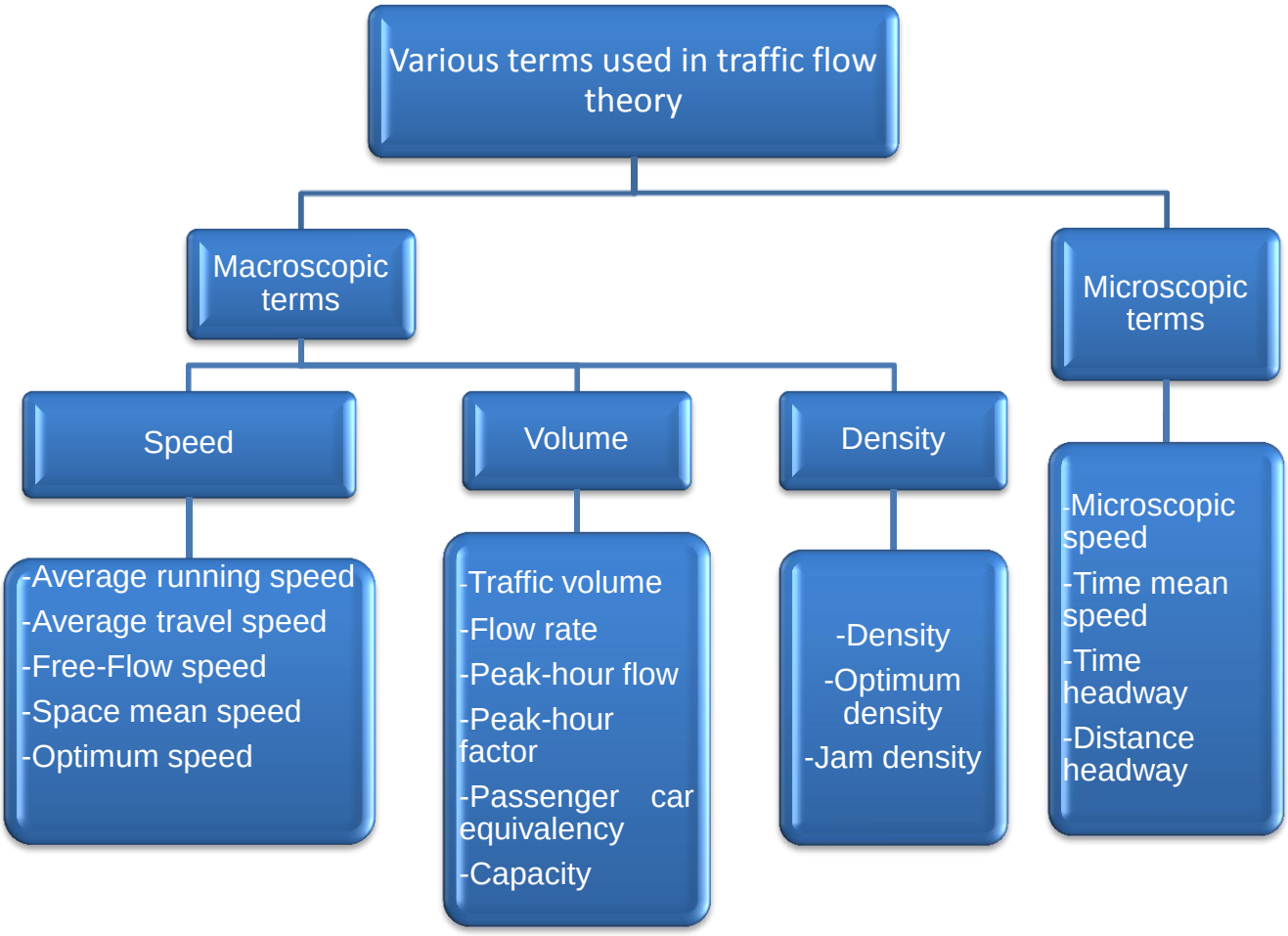

Figure 2. 1: Most used terms in traffic theory

2.2.1 Macroscopic approach

When traffic is studied at the macroscopic level, following traffic characteristics are considered:

2.2.1.1 Speed

Speed can be defined as the rate at which vehicles move along a given roadway and it is expressed as distance per unit of time.

In the analysis of traffic stream, following speed parameters can be considered depending on the purpose of the study:

- **Average running speed** is a speed computed when vehicles are only in motion and is obtained by dividing the length travelled by the time a platoon of vehicles uses to travel a given length.
- **Average travel speed** is the speed calculated by dividing the distance travelled by the average travel time required for a stream of vehicle not excluding the time the vehicles were stopped.
- **Free-flow speed** is defined as the average speed of vehicles traveling over a roadway, measured under low-volume traffic conditions, that is, when density and flow rate on particular section of the roadway are both zero. In this case, the drivers are free to drive at their desired speed and are not embedded by the presence of others.
- **Space mean speed** also termed macroscopic speed is defined as a speed of a traffic stream measured under basis of the average travel time of vehicles traveling over a given length. This speed draws this name from the fact that the average travel time weights the average to the time each vehicle spends in a given roadway. The following formulae is used to compute the space mean speed:

$$u_s = \frac{n}{\sum(\frac{1}{u_i})} = \frac{nL}{\sum t_i} \qquad (2.2)$$

Where:

u_s= Space mean speed (km/h)

n = Number of vehicles (vehicles)

t_i= The time it takes the individual vehicle *i* to travel a given highway section (sec).

u_i= speed of the individual vehicle *i* (m/sec)

L= length of section of the highway (m)

- **Optimum speed** is defined as the speed which occurs when the level of traffic flow is at capacity.

2.2.1.2 Volume

Traffic volume is the total number of vehicle passing a point on a roadway within a given time period; volumes are expressed in terms of annual, daily, hourly or sub hourly periods.

Following terms are used to characterize traffic volume (flow) on a given portion of the road:

- **Flow rate** is defined as a rate at which vehicles pass over a given point of roadway during the sub hourly time period, usually 15 minutes. And it is expressed as number of vehicles per unit of time mostly hour or second.
- **Peak hour flow** is defined as the highest traffic flow which is obtained during any successive 60 minutes. This flow is mostly considered in capacity and other traffic studies since it provides the most critical period which can affect the operation of a given highway, thereby capacity.
- **Peak hour factor** is defined as the ratio of total hourly volume to the maximum rate of flow within the hour. The peak hour factor can be computed as shown in the following equation:

$$\textbf{Peak hour factor} = \frac{\text{Hourly Volume}}{\text{Peak flow rate(within the hour)}} \qquad (2.3)$$

- **Capacity** can be defined as maximum rate of flow that can be achieved on a given roadway facility under prevailing roadway, traffic and control conditions.
- **Passenger car equivalency** can be defined as the equivalent value which is representative of a number of passenger cars that would use the same amount of capacity of a given highway as heavy vehicles under the prevailing conditions.

2.2.1.3 Density

Density is defined as average number of vehicles occupying a given length of a roadway at a particular instant; density is expressed as vehicle per kilometre.

Density is an important parameter for uninterrupted-flow facilities since it characterizes the quality of traffic operations of a given facility, also describing the proximity between vehicles and reflecting the freedom to manoeuvre within the traffic stream.
Following density parameters are of great importance in defining relationship between traffic characteristics:

- **Optimum density** can be defined as a density which corresponds to the maximum flow.
- **Jam density** is defined as the maximum density that may be found on any road. This density is obtainable for stopped vehicles on a given road, that is, when flow rate is zero.

2.2.3 Microscopic analysis

In microscopic analysis of traffic stream, following terms are used to characterize and study the state of the traffic flow.

Microscopic speed also called spot speed is defined as a rate of motion at which an individual vehicle uses travelling a certain distance over time. It can be computed as shown in the following formula:

$$u_i = \frac{\mathrm{dx}}{\mathrm{dT}} \tag{2.4}$$

Where:

u_i = Microscopic speed of vehicle i

dx = Short distance travelled

dT = Short time interval

Time mean speed is defined as the arithmetic mean of the speeds of vehicles passing a point on a highway during an interval of time. The time mean speed is computed as follows:

$$u_t = \frac{1}{n}\sum u_i \qquad (2.5)$$

Where:

u_t = time mean speed (km/h)

u_i = speed of the *i*th vehicle (km/h)

From the field data, the research carried out by Wardrop (1952) has shown that a relationship exists between time mean speed and the space mean speed. That relationship is formulated as follows:

$$u_t = u_s + \frac{\sigma^2}{u_s}$$

With σ is the standard deviation of macroscopic speed which is obtained as shown in the following formula:

$$\sigma = \frac{\sum D_i (u_i - u_s)^2}{K} \qquad (2.6)$$

K_i = Density of vehicles in each individual stream

K = Total density

u_i *and* u_s are as previously determined.

Time headway is defined as a difference between the time the front of a vehicle arrives at a point on a highway and the time the front of the next following vehicle arrives at the same point. Time headway is expressed in seconds.

Distance headway can be defined as the longitudinal distance between the front bumper of lead vehicle and the front bumper of the following vehicle. This distance includes the length of the lead vehicle and the gap distance between the lead and the following vehicles. Space headway is expressed in meters.

Moreover, it is worthy to note that the distance headway can be obtained either photographically or by computation using individual speed measurement and time headway as follows:

$$e_{n+1}=h_{n+1}\dot{x}_n \quad (2.7)$$

Where:

e_{n+1}= Distance headway of following vehicle (m)

h_{n+1}= Time headway of the following vehicle at a given point (sec)

$\dot{x}_n$ = Speed of lead vehicle during the time period h_{n+1} (m/sec)

It can also be noted that there is a relation between average distance headway between successive vehicles and density as shown in the following formulae (Leutzbatch, 1988):

$$k=\frac{1}{a} \quad (2.8)$$

Where:

k = density

a = average distance headway

With average distance headway computed by averaging the individual distance headways as shown in the following equation:

$$a=\frac{\sum a_n}{N} \quad (2.9)$$

Where:

a_n=Individual distance headway (m/ Veh)

N = Number of observed distance headways

2.3 Relationships between traffic flow characteristics

First and foremost, in order to simplify the representation of relationships between traffic flow parameters, the basic stream flow relationships were developed under the assumption of a linear relationship between speed and density.

The resulting Speed-Density relationship is shown in the following equation:

$$u = u_f\left(1 - \frac{k}{k_j}\right) \tag{2.10}$$

Where:

u = Space mean speed

u_f = Free flow speed (km/h)

k = Density (veh/km)

k_j = Jam density (veh/km)

Applying the steady-state flow relationship between traffic parameters (Equation 2.1) to the linear speed-density relationship, the parabolic shaped speed-flow curve was obtained as shown in the following formula (Mannering et al., 2007):

$$q = k_j\left(u - \frac{u^2}{u_f}\right) \tag{2.11}$$

Where:

q = Flow rate, veh/h

u, k_j and u_f are defined as previously.

In a similar way, by the use of the equation 2.1 to the speed-density relationship shown in equation 2.10, a parabolic shaped flow-density curve was obtained. The curve presents a peak point corresponding to the maximum flow with intermediate levels of speed and density. The resultant curve is shown in the following equation:

$$q = u_f \left(k - \frac{k^2}{k_j}\right) \tag{2.12}$$

All parameters are as previously determined.

The speed-density-flow relationships discussed in previous section can be illustrated in Figure 2.2. The figure shows a generalized representation of relationships between traffic flow characteristics on uninterrupted flow facilities, developed under assumption of linear speed-density.

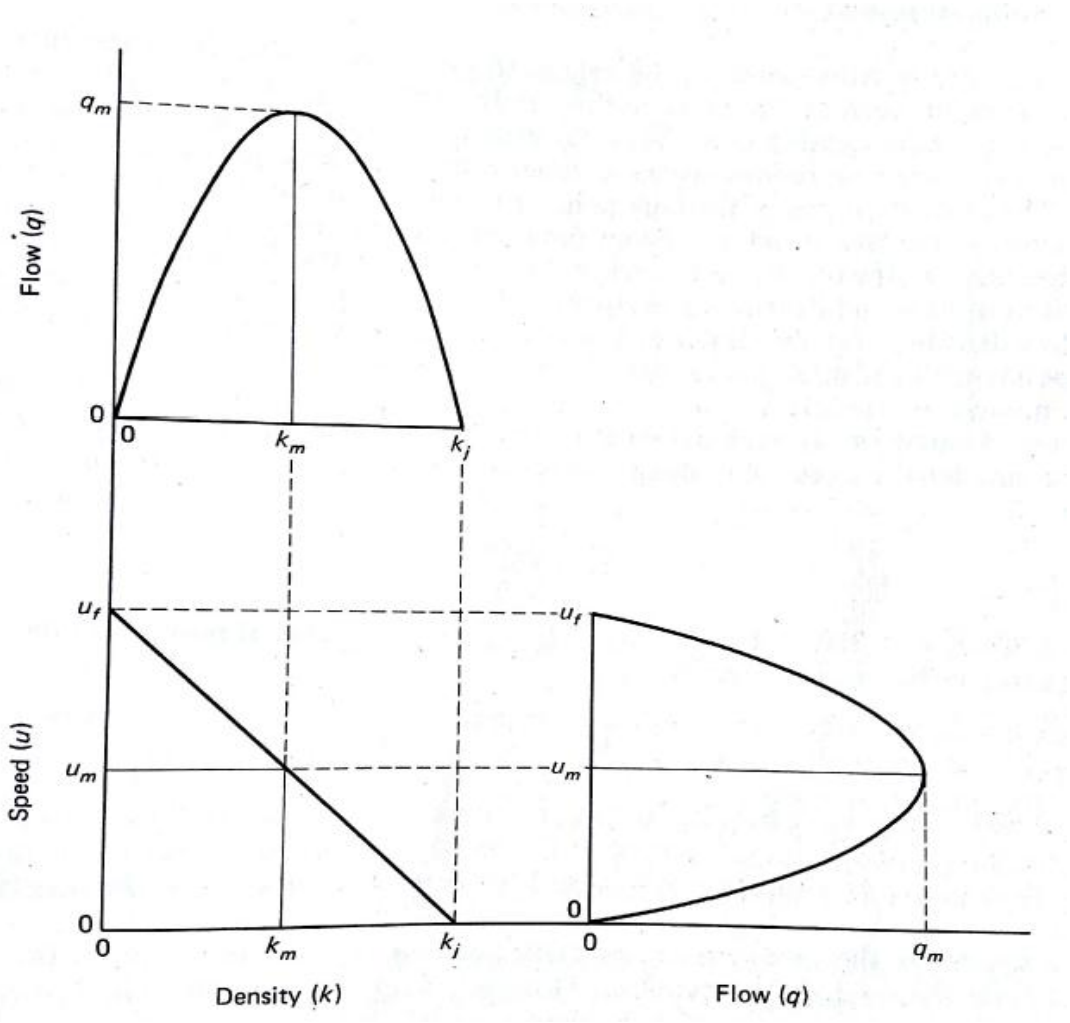

Figure 2. 2 : Generalized relationships among speed, density, and flow rate on uninterrupted-flow facilities (Baerwald, 1976)

Some points on the curves are of great importance in understanding traffic behaviour on a given facility. There are two situations, under which the flow rate is zero. The first

situation occurs when there are no vehicles on the highway. Under this condition, the attributed speed is theoretical and corresponds to the maximum speed (u_f) which can occur on a given highway. This speed termed free-flow speed is the speed with which vehicles will be travelling on highway without hindrance by the presence of other vehicles.

The second situation in which flow rate is zero corresponds to a high density in which vehicles arrive at a complete stop. Under this condition, there is no movement of vehicles. Vehicles will tend to line up end to end, the speed is zero and the corresponding density is called jam density (k_j).

As density increases from zero, the flow also increases progressively from zero to a maximum value. After the flow reaches that value, a further increase in density will then result in decrease in flow which will eventually reach zero when the density is equal to jam density. That maximum value of flow under prevailing conditions corresponds to the capacity of a given highway.

Furthermore, the flow conditions corresponding to low density (density less than optimum density) and high speed are referred to as no congested regime, and flow condition with higher density (density greater than density at which flow is at the maximum) and low speed indicates congested regime. Moreover, it is worthy to note that the slope of any line drawn from origin of the speed-flow curve to any point on the curve indicates density, and in the same way, the slope of any line drawn from the origin of the flow-density curve gives speed (Roux, 2001).

2.4 Review on theoretical conventional speed-flow-density models

Since the 1935's pioneering work of Greenshields in traffic studies, many researchers have developed various models aiming to describe the relationships between traffic characteristics on uninterrupted flow facilities. These models were developed following two main approaches, macroscopic approach and microscopic approach. The first approach is macroscopic approach that uses traffic average speed, flow and density in flow analysis. The second approach which is microscopic approach also termed car-

following theory deals with individual vehicle spacing and speed. The following part discusses some of the most pertinent traffic flow models developed by those researchers.

2.4.1 Macroscopic traffic model

While investigating traffic characteristics on two-lane highways, Greenshields (1935) found that speed decreases linearly with increasing of density on such highways. He subsequently proposed a model shown as follows:

$$u = u_f \left(1 - \frac{k}{k_j}\right) \tag{2.13}$$

Where:

u = Speed (km/h)

u_f = Free flow speed (km/h)

k = Density (Veh/km)

k_j = Jam density (Veh/km)

The findings from the Greenshields' (1935) study showed that the speed-density relationship presents significant changes when the density on highway is heavy, which is logical since entire stream of vehicles is likely to be hindered by any form of delay or slow vehicles.

The Greenshields (1935)'s study constitutes one single and general case. This model was found to be simple and satisfy all boundary conditions (u =0 at k =k_j and u = u_f at k=0) as shown in the previous section. However, many other researchers found non-linear relationship between speed and density and they developed more complex models which are ranged from single to three regime models using either statistical approach or hydrodynamic analogy to traffic flow phenomenon.

Using the applied fluid dynamic principles, as proposed by Lighthill and Withmam (1955) who postulated that traffic flow can be treated as a fluid flow in different traffic

situations, Greenberg (1959) obtained a logarithmic flow-density curve which presents a maximum value of flow when k_j/k =e and optimum speed when speed= c.

To achieve this, Greenberg applied the equation of motion of one-dimensional fluid together with the equation of continuity (conservation of flow) to the traffic flow situation. The two used equations are shown as follows:

$$\frac{du}{dt} = -\frac{C^2}{k}\frac{\partial k}{\partial t} \tag{2.14}$$

$$\frac{\partial k}{\partial t} + \frac{\partial q}{\partial x} = 0 \tag{2.15}$$

Where:

u = Traffic velocity (miles per hour)

k = Traffic density (vehicles per mile)

x = Distance on the roadway (m)

t = Time (hour)

c = Parameter

q = Traffic flow rate (vehicles/hour)

The obtained speed-density curve is shown in the following equation:

$$u = c\ ln\left(\frac{k_j}{k}\right) \tag{2.16}$$

Where:

$c = u_o$ (Speed at maximum flow, miles/hour)

k = Traffic density (vehicles per mile)

k_j = Jam density (vehicles per mile)

From Equation 2.16, flow-density curve can be obtained using the fundamental relationship (Equation 2.1).The resultant curve is presented in following equation:

$$q = c\ k\ \ln\left(\frac{k_j}{k}\right) \tag{2.17}$$

The Greenberg (1959)'s study showed that the headway between lead and following vehicles can be computed as a function of the velocity. This relationship is shown as follows:

$$h = h_j . e^{\frac{u}{c}} \tag{2.18}$$

Where:

h = Headway (foot)

h_j = Headway at the jam=5280/k_j,

$c = u_o$ (Speed at maximum flow, miles/hour)

Underwood (1961) compared the curve established by Greenshields, Norman and Greenberg and found that the Greenberg model provided a best representation of traffic data in a congested regime. However, the Greenberg model was found unsuitable in free-flow regime, due to its inability to provide a realistic free-flow speed. This incited Underwood to propose another model formulated as follows:

$$u = u_f . exp[-\frac{k}{k_o}] \tag{2.19}$$

Where:

u = Speed (km/hour)

u_f = Free-flow speed (km/hour)

k_o = Optimum density (veh/km)

k = Density (veh/km)

In the Underwood (1961)'s study, the speed-volume curve was also developed. In this model the traffic flow was found to be better described in terms of three different zones specified in terms of probabilities. The three zones were found to be the zone of normal flow, zone of unstable flow and finally a zone of forced flow (Underwood, 1961).

While investigating speed-density curve on Eisenhower expressway, (Drake, Schofer & May 1965), found that the curve presents concavity at low density, they then proposed a bell-shaped curve of the form:

$$u = u_f . exp\left[-\frac{1}{2}\left(\frac{k}{k_0}\right)\right] \quad (2.20)$$

All parameters are as previously determined.

Drew (1968) proposed a model which provides a generalized form of the speed-density curve by introducing a new parameter in the Greenshields' model. The proposed model is formulated as follows:

$$u = u_f\left[1-\left(\frac{k}{k_j}\right)^{n+1/2}\right] \quad (2.21)$$

Where:

n= additional parameter with values -1, 0 and +1, giving the form of the model to be respectively exponential, parabolic and linear model.

All other parameters are as previously determined.

In the study carried out by Edie (1960) with the purpose of examining different established speed-density curves, he found the existence of discontinuities from the traffic data on many empirical curves. These discontinuities were marked by a sharp capacity drop at some critical densities, where the maximum flow rate achievable in free-flow regime were found to be considerably higher than that in congested regime; this gave birth to a dual-regime traffic stream model. He subsequently hypothesized that Underwood model can be used for the free-flow regime and the Greenberg model be used for the congested-flow regime (Edie, 1960).

Drake et al. (1965) also examined different developed models and proposed that the speed density models are better presented under multi regime models. They suggested three additional representations of speed-density curves. The first representation was the use of separated Greenshields'-type model for the free-flow regime and the congested-flow regime. The second was the use of constant-speed model for the free-flow regime and a Greenberg model for congested-regime. And finally, the third representation which is slightly different from the two previous representations was a three-regime model where the Greenshields' model was applied to free-flow, transitional, and congested-flow regimes separately. However, researchers showed that there exists a problem associated with the use of multi regime models which is to determine the exact point where the breakpoint between regimes occurs.

2.4.2 Microscopic traffic models (Car-following theories)

Understanding car following theories contributes significantly to a deep understanding of traffic flow, since these theories provide a better description of a one-by-one vehicle following process on the same lane in traffic flow. Moreover, the basic element of this theory resides on knowledge of average distance headway between vehicles in a platoon.

Chandler et al. (1958) proposed a linear model based on stimulus-response concept, where they hypothesized that the response of a driver is proportional to the stimulus he received. Further on, in the study which resulted into the development of car following model, the researchers associated with General Motors group have proposed five generations of car-following models (May, 1990). All these models were established working under the above stated stimulus-response concept, presented as shown in the following statement (May, 1990).

Response=function [Sensitivity, Stimuli]

The response and stimuli are the common components of those models. The response is indicated by the acceleration or deceleration of the following vehicle depending on the fluctuation of velocity of the lead vehicle, while the difference in velocity between the

lead and following vehicle corresponds to stimuli, the sensitivity term is the only variable term of those models which differentiates one generation to another (May, 1990).

At the early stage of development of these models, the sensitivity term was considered constant. The equation was given a following form:

$$\ddot{X}_{n+1}(t+\Delta t)=\alpha\,[\dot{X}_n(t) - \dot{X}_{n+1}(t)] \qquad (2.22)$$

Where:

$\ddot{X}_{n+1}$= Acceleration/deceleration of the following vehicle (ft/sec^2)

$\dot{X}_n$ = Velocity of the lead vehicle (ft/sec)

$\dot{X}_{n+1}$= Velocity of the following vehicle (ft/sec)

α = Sensitivity term (sec^{-1})

t = at time t

t+Δt = Variation of time after t time

In developing the second generation model, the research group incorporated the distance headway in the sensitivity term. The model was developed with two different sensitivity terms, one used for traffic situation associated with low spacing and other used for the situation associated with a high spacing.

Due to difficulties to determine which sensitivity value to be use in the model, the research group proposed to measure the sensitivity term as an inverse function of the distance headway. After multiple transformations, they established a third generation model shown as follows:

$$\ddot{X}_{n+1}(t+\Delta t)=\frac{\alpha o}{x_n(t)-x_{n+1}(t)}\,[\dot{X}_n(t)- \dot{X}_{n+1}(t)] \qquad (2.23)$$

Where:

α_o= Sensitivity parameter (ft/sec)

And other terms are as previously defined.

As the speed of the vehicle platoon increases, the drivers of individual vehicles within the platoon are likely to be sensitive to the relative distance between them and the vehicle in front of them, an attempt was made therefore, to insert the speed in the car-

following model. Thus, in the light of incorporating the speed of the following vehicle to the sensitivity term of the model, the fourth model was established as shown in the following equation:

$$\ddot{X}_{n+1}(t+\Delta t)=\frac{\alpha'[\dot{x}_{n+1}(t+\Delta t)]}{x_n(t)-x_{n+1}(t)}\ [\dot{X}_n(t)-\dot{X}_{n+1}(t)] \quad (2.24)$$

Where:

α' = Constant (dimensionless)

x_n = Position of the lead vehicle

x_{n+1} = Position of the following vehicle

And other terms are as previously defined.

The final generalized car-following model was developed by raising the speed and distance headway components of the sensitivity term to certain exponents. The resulting model known as the general model of car-following theories is shown as follows:

$$\ddot{X}_{n+1}(t+\Delta t)=\frac{\alpha_{l,m}[\dot{x}_{n+1}(t+\Delta t)]^m}{[x_n(t)-x_{n+1}(t)]^l}\ [\dot{X}_n(t)-\dot{X}_{n+1}(t)] \quad (2.25)$$

Where:

l = The distance headway exponent

m = The speed exponent

And other terms are as previously defined.

When the traffic stream is moving in a steady state, it was found that the speed, flow and density of this traffic stream can be determined using equation 24 (Garber & Hoel, 2010).

Apart from the General motor research team, some other researchers have undertaken several works regarding this important traffic issue. Pipes (1953) had previously postulated that vehicles are separated by a legal distance and time as shown in the following equation:

$$x_n - x_{n+1} = L + T(\dot{x}_{n+1}) \quad (2.26)$$

Where:

L= Legal distance headway between two vehicles

T= Legal time headway between two vehicles

The transformation of Equation 2.26 leads to the basic response-stimuli concept of the car-following theories, from which Pipes (1953) developed a model similar to Equation 2.22, shown as follows:

$$\ddot{X}_{n+1}(t+T)=\lambda\,[\dot{X}_n(t)-\dot{X}_{n+1}(t)] \tag{2.27}$$

Where:

λ = Sensitivity factor

According to May (1990) and Baerwald et al. (1976), the general expression of λ proposed by Gazis et al. (1961) is given in the following form

$$\lambda = a\frac{\dot{x}_{n+1}{}^{m}(t+T)}{[x_n(t)-x_{n+1}(t)]^{l}} \tag{2.28}$$

Inserting the expression of λ from Equation 2.28 into Equation 2.27, results into the general equation of car-following theory (Equation 2.25) developed by General Motors research group.

2.4.3 Interrelationship between Macroscopic and Microscopic models

Research has shown that macroscopic models can be obtained from the generalized car-following equation (Equation 2.25) when proper integers are selected for the *m* and *l* exponents of the latter (Gazis et al., 1961). Besides, the integration of the general car-following model established by the research group associated with General Motors, in which the sensitivity factor exhibiting m and l exponents gives an expression presented in the following equation:

$$\mathrm{f_m(u)} = \mathrm{c'} + \mathrm{c.\,f_l(s)} \tag{2.29}$$

Where

u = Steady-state speed of traffic stream,

s = Constant average spacing,

c and c'= appropriate constants consistent with physical restrictions.

In the study carried out by May and Keller (1967) investigating the relationships between macroscopic and microscopic flow models, they came out by establishing a matrix resulting in different steady-state equations in which different models were embodied. May and Keller (1967) provided also a way of attributing some non-integer values to the *m* and *l* exponents of the general car-following model to define some deterministic flow models. The derived matrix shows different combinations of m and l constants as illustrated in the following table.

Table 2. 1: Steady-state flow equations for different *m* and *l* values (May & Keller, 1967)

	m < 1	m = 1	m > 1
$l < 1$	$U^{1-m} = c\left(K^{l-1} - K_j^{l-1}\right)$	No solution	$U^{1-m} = U_f^{1-m} + c.K^{l-1}$
$l = 1$	$U^{1-m} = c.Ln\left(\frac{K_j}{K}\right)$	$Ln(U) = c.Ln\left(\frac{K_j}{K}\right)$	$U^{1-m} = c.Ln\left(\frac{K_j}{K}\right)$
$l > 1$	$U^{1-m} = c\left(K^{l-1} - K_j^{l-1}\right)$	$Ln\left(\frac{U_f}{U}\right) = c.K^{l-1}$	$U^{1-m} = U_f^{1-m} + c.K^{l-1}$

May and Keller(1967)'s study underlined that the matrix provided not only the representation of the previously developed speed-density model, but also that it has the ability to accommodate several other possible models in terms of *m* and *l* combinations. The examination of the matrix presented in Table 2.1 show that, the yet developed macroscopic and microscopic speed-density models can be obtained in terms of *m* and *l* combination (Roux, 2001). For example, the Greenshields model is obtained when *m*=0 and *l*=2, the Greenberg model is obtained when *m*=0 and *l*=1, the Drew model is obtained when *m*=0 and *l*= 3/2, the Underwood model is obtained when *m*=1 and *l*=2

and finally the bell-shaped curve model by Drake, May and Schofer is obtained when *m*=1 and *l*=3. The matrix of the yet developed macroscopic models is shown in Table 2.2.

Table 2. 2: Matrix of yet developed macroscopic models (May & Keller, 1967)

	$m=0$	$m=1$
$l=0$	$u=\frac{1}{s}\left(\frac{1}{k}-\frac{1}{k_j}\right)$ with s = constant	-
$l=1$	$u=u_0.\ln\left(\frac{k_j}{k}\right)$	-
$l=1.5$	$u=u_f\left(1-\left(\frac{k}{k_j}\right)^{1/2}\right)$	-
$l=2$	$u=u_f\left(1-\frac{k}{k_j}\right)$	$u=u_f e^{-k/k_0}$
$l=3$	-	$u=u_f e^{-\frac{1}{2}\left(\frac{k}{k_0}\right)^2}$

The May and Keller (1967)'s study has also shown that the non-integer values of *m* and *l* can be utilized and can more effectively represent the actual speed-density relationships. That is, the shape of the speed-density curve is likely to be changed by keeping one of *m* and *l* exponents constant and changing the other in such a way that it provides a better fit with the actual data (May &Keller, 1967). The example illustrated in the Figure 2.3 shows the modification of the shape of the curve and a progressive change from the exponential model (*m*=1 and *l*=2 to the bell-shaped model (*m*=1, *l*= 3) when the exponent *m* is given a constant unit value and the exponent *l* is changing in increment of 2/10.

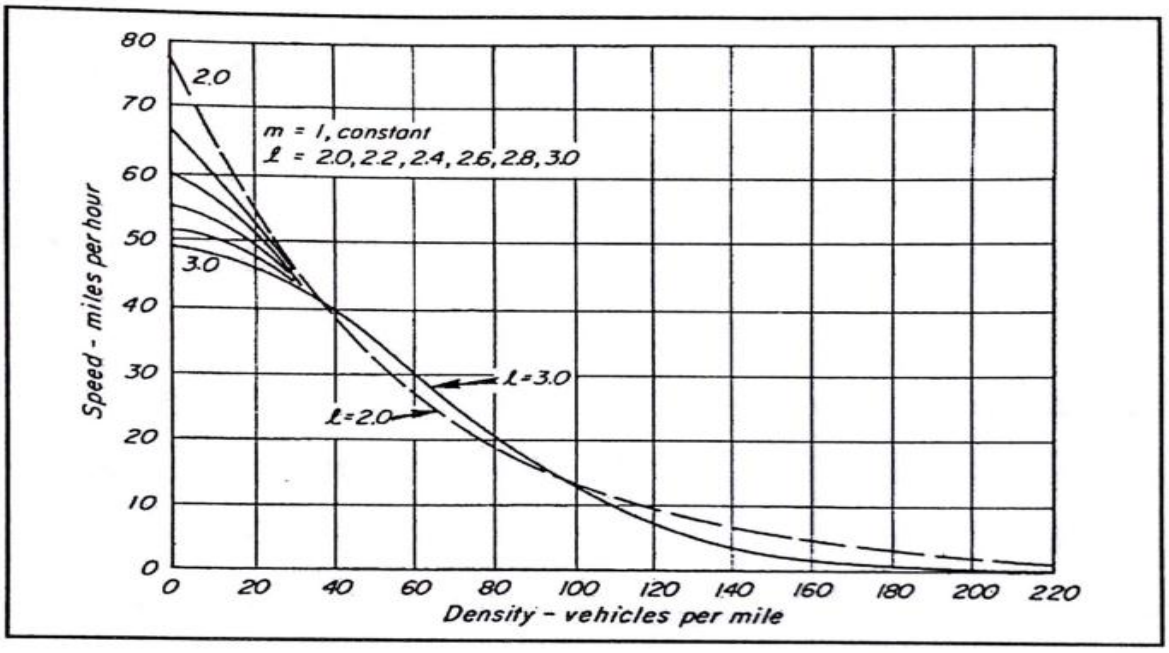

Figure 2. 3: Effect of using non-integer exponents on the shape of the speed-density relationship (May and Keller, 1967)

2.5 More research and interpretation of relationships between traffic characteristics

Speed-volume relationships were investigated in a study carried out in Israel, on two rural two-lane highways. This study showed on one of the study site a clear parabolic shape with a sharp peak indicating capacity, while on other site the relationship was devoid of a peak since the data were obtained only on the upper part of the curve. This research showed that the flow data do not always present the theoretical parabolic model and that capacity is not a clear single value for all two-lane roads (Polus et al., 1991).

While investigating the speed-flow relationships on two-lane rural highways in Finland, Pursula and Enberg (1991) considered first one direction and two directions combined afterwards, they then found that the relationship was linear in both cases since the increase in flow resulted in a linear decrease of speed.

Chin and May (1991) reviewed previous works of Hurdle and Datta (1983) and that of Allen et al., (1985). They pointed out that the form of the speed-flow curves cannot be

attributed to the observed data alone but also on the choice of speed-flow function. They noted that in order to obtain a model which fits satisfactorily the data, the speed-flow curve can be examined in two portions; with the first portion corresponding to the uncongested regime where the speed was seen to be less sensitive to the flow and the second portion corresponding to the congested regime (Chin & May, 1991).

Hall et al. (1992) reviewing the works of different authors, noticed a drop of speed of about 20 to 25 percent of free-flow speed on different freeway systems. They suggested another way of interpreting the speed-flow data by not focusing on the speed drop only but also to consider the speed corresponding to the end point of the curve, since the values were seen to be different for different authors. This finding also underlined that in order to identify the shape of speed-flow-density relationships, data must be taken on several locations since no only one location was able to cover the full range of operations, hence resulting in composite curves (Hall et al., 1992).

2.6 Theory on two-lane two-way rural highways

2.6.1 Introduction

Two-lane two-way highways form one of the type of highways which present certain particularities, since the vehicles behind are constrained to use the lane of oncoming vehicles during overtaking process due to low speed of the vehicles ahead. Moreover, since rural highways serve mainly two functions in many national highway networks namely mobility and access, and that two-lane two-way highways constitute the largest portion of rural highways mileage in those networks, these result in their carrying a large portion of rural traffic in most developed and developing countries including South Africa. Again due to today's growing awareness of issues such as road safety and environment protection, the performance of rural roads has attracted much attention of many researchers across the globe (Tapani, 2008). In this context, research is needed to understand rural traffic phenomenon, in order to enhance the quality of service provided by highways in rural environment especially for two-lane highways in the Western Cape.

The following section provides a brief description of different aspects to be considered when dealing with two-lane two-way highways and finally their analytical capacity determination.

2.6.2 Definition of two-lane highways

By definition, two-lane two-way highways are defined as undivided roadways composed of two lanes, one for use by traffic in each direction, and which overtaking process takes place in the lane of oncoming traffic, if adequate sight distance and a safe gap in the conflicting traffic are available(O'flaherty, 1997). Figure 4 shows a typical two-lane two-way rural highway in South Africa.

Figure 2. 4: Typical two-lane two-way highways in South Africa (Google earth)

The highway capacity manual classifies two-lane highways into three broad categories, where two first categories are found in pure rural environment and the last category is found in developed areas (TRB, 2010).The three categories of two-lane roads are defined as follows (TRB, 2010):

1. Class I: are two-lane highways in which the motorists' expectations are that they will drive at relatively high speeds. Those highways are generally major intercity routes, primary arterials connecting major generators of traffic, daily commuter routes, or primary links to the other arterial highways. These facilities are mostly used when long distance trips are to be undertaken.
2. Class II: are two-lane highways on which motorists' expectations are such that they can travel at relatively lower speeds than for class I. Those are two-lane highways which function is to provide access to class I two-lane highways and those which serve as scenic byways or recreational routes that are not primary arterials. In general, these routes serve relatively short trips, and their average trip lengths are relatively shorter than those for Class I two-lane highways.
3. Class III: Two-lane highways which serve moderately developed areas. They may be part of the class I or class II highway which pass through a developed area or small town and are more associated to reduced speed limits.

2.6.3 Methods of analysis of two-lane two-way highways

The highway capacity manual being a document that provides capacity analysis procedures and methodologies for different types of highways in the United States is adopted in South Africa. In this manual, a study of performance measures for two-lane two-way highways could be conducted either by directional segment procedure, that is, an operational assessment for one direction of travel at time, or by two-way segment methodology where performance measures are studied over both directions of travel combined (TRB, 2000). However, the latest version of HCM came out with a method of analysis of two-lane highways, in which the performance of these highways can only be studied using only one direction methodology, and that results obtained are to be expanded to two lanes by applying a weighted average procedure(TRB, 2010).

2.6.3.1 Evaluation of traffic performance on two-lane two-way highways

The analysis of traffic performance for two-lane two-way highways is one of the most important aspects to consider while undertaking the planning, design and operation of

these facilities. The evaluation of traffic performance is therefore, a major input to important decisions on public investments made regarding different stages of the life of these highways. However, highway performance study is normally done within the capacity analysis for various highway facilities, by the use of Highway Capacity Manual procedures, where highway performance measures are described in terms of level of service (TRB, 2010).

Two-lane two-way highways exhibit operation characteristics different to that of other uninterrupted facilities, resulting from higher interactions between vehicles travelling not only in the same direction but also in the direction of oncoming vehicles. Due to this characteristics uniqueness, measuring traffic performance at such highways becomes a complex problem. Currently, three performance measures are proposed by Highway Capacity Manual (TRB, 2010).Those performance measures are respectively Average Travel Speed (ATS), Percent Time-Spent-Following (PTSF) and Percent of Free-Flow Speed (PFFS).

The first measure is obtained by dividing the length of the highway section travelled by the average travel time used by all vehicles to traverse it, during a defined period of time (TRB, 2010). Figure 2.5 illustrates typical average travel speeds and flow relationships for two-lane highways in United States obtainable under the ideal conditions namely lane width greater than or equal to 3.6m, clear shoulders with width equal or greater than 1.8m, absence of no-passing zones, traffic stream composed of only passenger cars, level terrain, and absence of obstruction to through traffic (TRB, 2010).

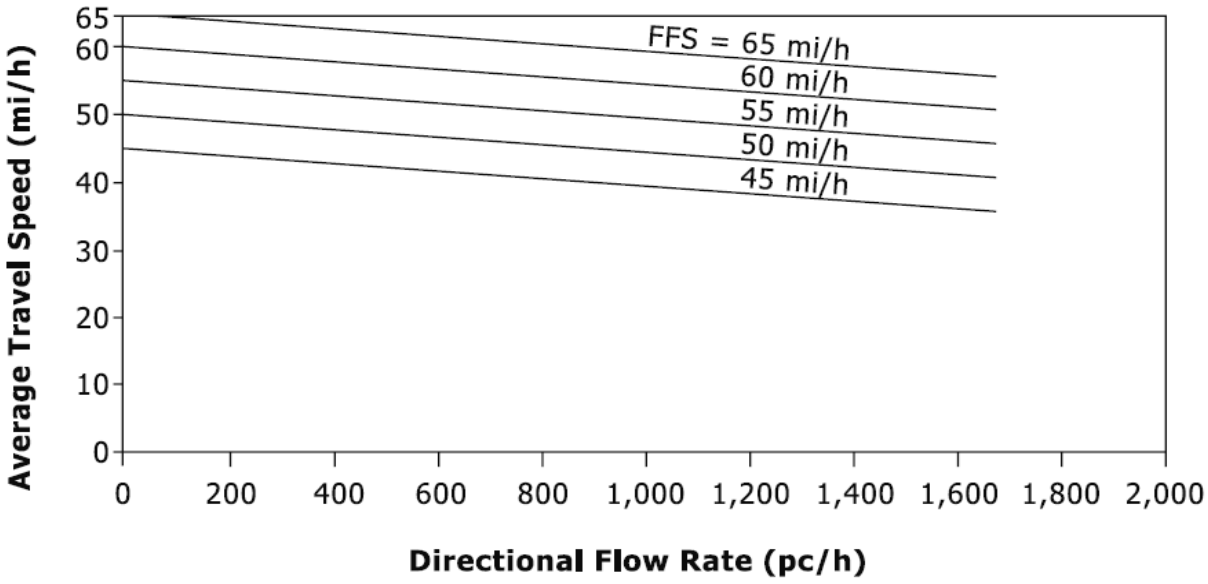

Figure 2. 5: Average Travel Speed versus direction flow rate relationships (TRB, 2010)

The second measure is defined as the average percentage of travel time that vehicles spent travelling in formed platoons behind slower vehicles due to lack of passing possibility (TRB, 2010). Figure 2.6 illustrates typical percent time-spent-following and flow relationships under the ideal conditions as stated in previous section, for two-lane highways in the United States.

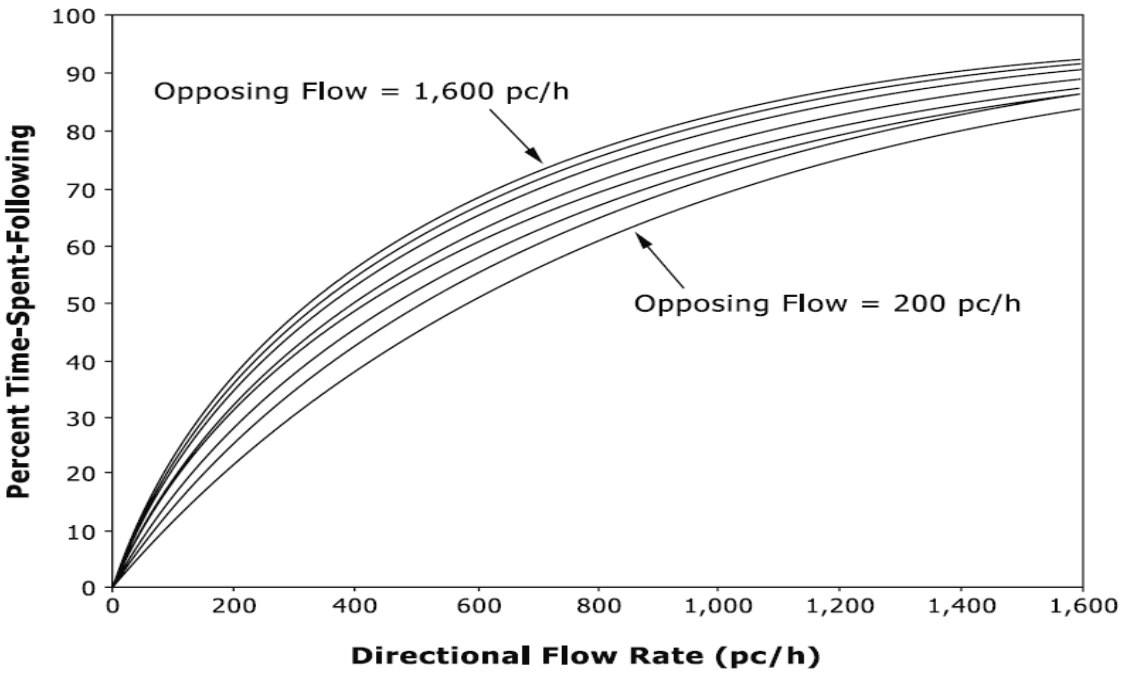

Figure 2. 6: Percent -Time-Spent-Following versus direction flow rate relationships (TRB, 2010)

The third measure reflects the degree at which drivers are traveling in accordance to the posted speed limit. This measure is used to evaluate service quality on class III two-lane highways since high speeds are not expected on these highways, and drivers are more likely to travel at or near the speed limit (TRB, 2010).

Since on-site determination of PTSF is found difficult or impractical, the HCM (TRB, 2000; TRB, 2010) propose a surrogate estimate of PTSF, that is, percent followers which are the proportion of vehicles traveling at headway less than a critical value, say 3 seconds, as observed at a fixed location within a certain time interval.

However, the use of percent followers alone was found inadequate in decision making with respect to the upgrading and improving processes of two-lane highways since it does not accurately reflect the effect of traffic level (Shawky & Hashim, 2010). As percent follower measure is dependent on increase of flow and speed variation, it may be possible that in certain conditions, low traffic levels associated with high variations in speed will result in reduced passing opportunities and consequently, they will present high values of percent followers, in these cases the road upgrading or improvement

decision based on PTSF measure alone can be proved erroneous and unjustified (Shawky & Hashim, 2010).

Due to the above mentioned limitations in determination of the PTSF measure, many researchers in different countries have introduced different alternative performance measures other than PTSF to fit local conditions found in their countries. Examples of those alternative measures are follower density, average travel speed of passenger cars, platoon percentage, density, percentage of vehicle impeded, and so on (Hashim & Abdel-Wahed, 2011).

Van As (2003) was the first to propose the use of follower density as an alternative performance measure to evaluate the service quality for two-lane roads in South Africa. In this study, the limiting values of follower density for different levels of service were proposed as shown in Table 2.3.

Table 2. 3: Proposed values of follower density on different level of service on two-lane roads (Van As, 2003)

LOS	"Typical" Follower Density	Range of Follower Densities
A	1.0	0.3 – 1.4
B	2.0	1.3 – 3.3
C	4.0	3.0 – 6.7
D	8.0	6.3 – 9.5

Furthermore, in a study carried out by Kaisy and Karjala (2008) with the purpose to examine performance indicators on two-lane roads and establish their relationships with platooning variables such as flow rate in the direction of travel, opposing flow rate and percentage of heavy vehicles. The traffic flow in the direction of travel was found highly correlated with performance indicators more significantly to follower density and percent followers (Kaisy & Karjala, 2008). This study also underlined that the follower density measure was found to be more easily estimable in the field than the HCM Percent Time-Spent-Following performance measure (Kaisy & Karjala, 2008).

Similar results were found in the study conducted in Egypt undertaking the evaluation of performance measures for two-lane rural roads, Hashim and Abdel-Wahed (2011) investigated the relationship between performance measures and platooning variables such as previously cited. Their study showed that the follower density performance measure was strongly correlated with platooning variables especially the flow rate in the direction of travel (Hashim & Abdel-Wahed, 2011). Moreover, it was found that the relationship between flow rate in the direction of travel and follower density is better presented in a quadratic form (Hashim & Abdel-Wahed, 2011).

Besides, the role of using a performance measure is to be able to evaluate the quality of service for a given length of a two-lane road in order to determine whether road improvement or upgrading processes may be envisaged. The use of the average measure of effectiveness over the full length of a two-lane highway is not justified because it is not evident that the total road length shows signs of poor performance, this however, implies that road improvement or upgrading may only be required for the section of the two-lane road where the level of service was found poor not the road as a whole (Van As, 2003).

2.6.3.2 Capacity determination of Two-lane two-way highways

The capacity of two-lane two-way highway in a given condition can be determined either by analytical methods, which include methods provided by Highway Capacity Manual published in 2000, Models developed by the Finnish National Road Administration published in 2000, Methods developed by Brilon and Weisner in 1994 and 1998, and Luttinen in 2001 or by the use of Simulation tools, since there are some complex situations which require simulation as the only solution for their evaluations (Van As, 2003).

However, capacity conditions of two-lane two-way highway are difficulty to be observed in the field, since very few two-lane roads operate at or near capacity and most of times road improvement or upgrading are done prior to operations at capacity conditions are at hand(Harwood et al., 1999: TRB, 2000).

Since the second version of HCM (1965 HCM publication) which provided a value of 2000pcph as capacity of two-lane rural highways, many studies have been conducted to determine the capacity of these highways across the globe (Rozic, 1992).The third version of HCM published in 1985 defined the value of capacity of two-lane highways as 2800pcph with corresponding speed of 72km/h and critical density of 19.4veh/km (TRB, 1985). Furthermore, the 2000 HCM proposed the capacity values under ideal conditions for two-lane two-way roads as 1700pc/h for each direction of travel and 3200 pc/h for both direction of travel combined (TRB, 2000). Mathematically, the capacity of the two-lane two-way highways was found to take the following form (Luttinen, 2001).

$$C = \min \left\{ \frac{1700}{P_d} ; 3200 \right\} \quad (2.30)$$

Where

C = Capacity of two-lane two-way highways,

P_d = The proportion of traffic in the major direction.

Prior the publication of the latest version of HCM, the capacity of a two-way two-lane highway was defined in terms of the total two-way traffic that a given facility is likely to accommodate: since it was believed that the traffic in one direction being in close interaction with traffic moving in the other direction more often when the traffic is heavy, the determination of the capacity for single direction only was very difficult (Mc Shane & Roess, 1990).

The latest version of HCM underlined that the capacity can only be determined separately for each direction and that total roadway capacity is to be determined by weighted average of the one-direction results (TRB, 2010).Therefore in this manual, the capacity under ideal condition is given as 1700 Veh/km per one direction and a limit of 3200veh/h for the total of two directions as previously mentioned in the 2000 HCM version (TRB, 2010). From the value of capacity under ideal condition, some

adjustments are applied on it to obtain the capacity under prevailing conditions of a given roadway (TRB, 2010).

However, some researchers have shown that the capacity values provided by HCM underestimate the capacity likely to be obtainable on two-lane highways since it can ideally be estimated by 3600pcph, if the demand is high in both directions (Yagar, 1983). And also the value of capacity of 4000 pcph can be achieved on these highways under base conditions in both directions (Rozic, 1992). In this regard, Kim and Elefteriadou (2009) in their study investigating the capacity of two-lane two-way highways using simulation method, found that the capacity under ideal conditions as defined previously vary with the average free-flow speeds, since capacity is likely to be 1800pcphpl when the average free-flow speed is 64Km/h, while it is 2000 pcphpl when the average free-flow speed is 80Km/h.

2.6.4 Effect of geometric design features on traffic flow characteristics, performance and capacity on two-lane two-way highways

Highway geometric features being either longitudinal section characteristics such as the average percentage of the highway with no-passing zones in both direction, or cross-sectional characteristics such as lane and usable shoulder widths are considered in estimation of one of the most important parameter of the speed-density-flow model which is the driver's desired speed under free-flow condition. On the other hand, research showed that the possibility to drive at the desired speed on two-lane two-way highways is more dependent on the ability to overtake slower vehicles ahead, which in turn is a function of conflicting traffic level and geometry characteristics such as curve radius, tangent length, and so on (Shawky & Hashim, 2010).

The study conducted by Kim and Elefteriadou (2009) using simulation software" TWOSIM" has shown that some geometric factors namely the length of the road section, and the presence of passing zones do not have any significant impact on capacity, while others such as maximum superelevation rate in the horizontal curve, driveway, curb radius and grade of the upgrade segment exhibit a considerable negative impact on the highway capacity. One of the reason found in this research is

that, during operation at capacity, there are very few gaps available in the direction under consideration as well as in the opposing direction and, therefore, very few opportunities to overtake (Kim & Elefteriadou, 2009).

The Kim and Elefteriadou (2009)'s study has shown that two-lane road capacity is strongly influenced by driver characteristics namely standard variation among driver desired speed and delay of safety reaction time. This study showed that traffic composition was also found to influence capacity of these highways, since the increase in percentage of trucks particularly in the presence of horizontal curve, driveway and upgrade resulted in significant capacity reduction. However, the capacity was found to be less influenced by the opposing volume even if the interaction between vehicles moving in both directions may be significant (Kim & Elefteriadou, 2009).

2.7 Regression analysis

Regression analysis is a statistical technique that is used to explore and define the relationships between two or more variables, where dependent variables also called output variables are related to independent variables called predictor variables (Montgomery & Runger, 2007). For the sake of this project, regression analysis will be used to determine some parameters of traffic flow models since their determination on site is difficult or even impractical.

2.7.1 Regression procedure

The available values of variables under consideration are drawn in the graph called scatter plot in which the dependent variable is presented on the y-axis and independent variable on x-axis, in such a way that each pair of variable values is represented by a point plotted in a two-dimensional coordinate system. The reason for this step is to provide a way of visualizing the relationship between variables with the purpose to define a suitable model which provides the best fit to the observed data.

Once the form of the model is obtained, the parameters needed must be determined. These parameters are estimated by the method of least squares which consists of

minimizing the discrepancies between observed values and estimated values of the output variable. The following example depicts the above mentioned method as follows:

Let *y* be a dependent variable and *x* an independent variable, it is further assumed that a linear relationship exists between *y* and *x*, as shown in the figure below.

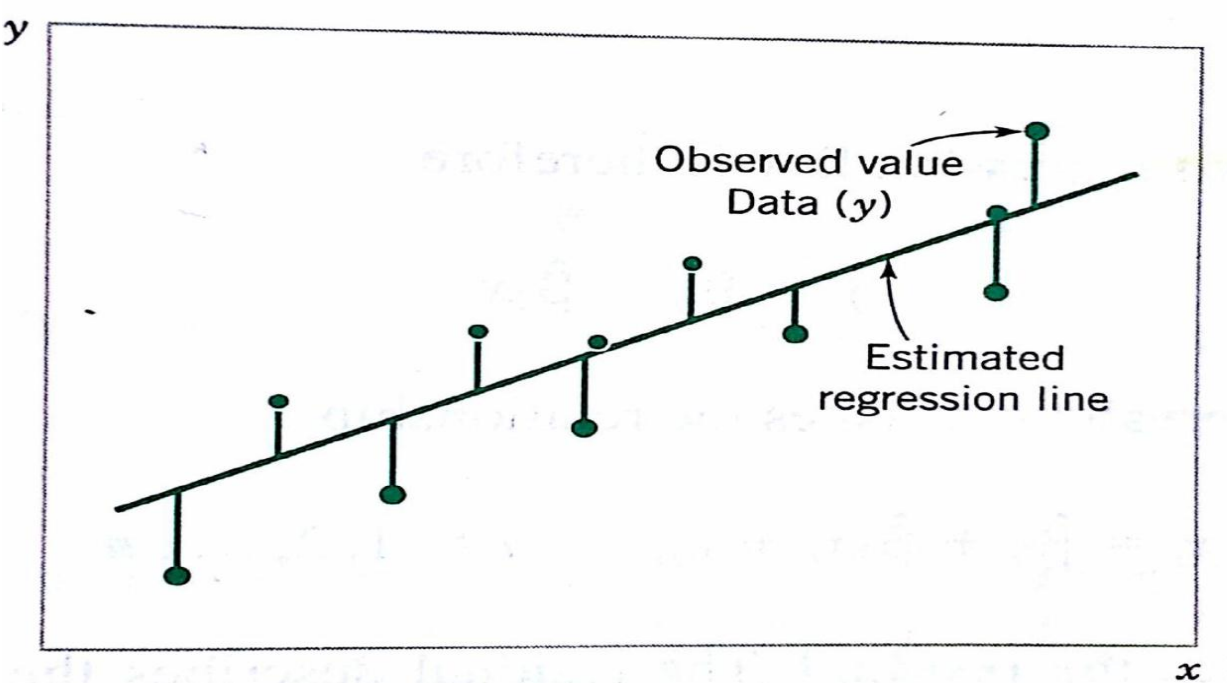

Figure 2. 7: Deviations of the data from the estimated regression model (Montgomery & Runger, 2007)

Since the mean of *y* is a linear function of *x*, and that actual observed values of *y* do not coincide to the straight line, an ad hoc method to generalize this to a probabilistic linear model is to assume that the expected value of *y* is a linear function of *x*, and that the determination of the actual value of *y* for a fixed value of *x* can be given as a linear model plus a random error term as shown as follows:

$$y= \beta_0 +\beta_1 x +\varepsilon \qquad (2.31)$$

Where:

β_0 and β_1= regression coefficients

ε= random error

Using Equation 2.31, each observation *i* can be expressed as follows:

$$y_i = \beta_0 + \beta_1 xi + \varepsilon_i \quad (2.32)$$

Where:

y_i = the observed value of dependent variable for *i*th observation

Other parameters are as previously determined.

As seen in the Figure 2.7, the estimates of β_0 and β_1 give rise to a line which is considered at a certain extent as a best fit for the given data. The estimated or fitted value of *y* for each value of *x* from the line is therefore given by the following formula:

$$\hat{y}\imath = \hat{\beta}_o + \hat{\beta}_1 x_i \quad (2.33)$$

Where:

$\hat{y}\imath$ = the estimated value of the dependent variable for *i*th observation

The residual (e_i) which is the vertical difference between the observed value and estimated value of the output variable is therefore an estimate of vertical deviation obtained from the prediction of the actual value for the particular observation *i*. For the above example, it is given by the following formula:

$$e_i = y_i - \hat{y}_\imath \quad (2.34)$$

It is worthy to note that, the best fitting model is obtained when the sum of the square of errors between observed values and the estimated values of output variables from the model is minimized, that is, when sum of residuals is minimized (Box et al., 1978; Montgomery & Runger, 2007). The sum of squares of residuals can be determined as follows:

$$SSE = \sum_{i=1}^{n} (e_i)^2 = \sum_{i=1}^{n} (y_i - \hat{y}_\imath)^2 \quad (2.35)$$

2.7.2 Analysis of adequacy of the regression model

In order to test the adequacy of regression model, a method called analysis-of-variance is used. In this method, the total variation in the output variable is subdivided into two main components: Regression sum of squares (SSR) and the Sum of squares of errors (SSE) which reflect respectively, the amount of variations of dependent variable accounted for by the model and the variations left unexplained by the model (Walpole & Myers, 1989). The Regression sum of squares is defined as follows:

$$SSR = \sum_{i=1}^{n} (\hat{y}_i - \bar{y})^2 \tag{2.36}$$

The total variation in the output variable (SST) can then be expressed symbolically in following equation:

$$SST = SSR + SSE \tag{2.37}$$

Furthermore, the coefficient of determination, R^2, which is the ratio of sum of squares, is more often used to judge the adequacy of the developed model. This coefficient uses relative sizes of variation of dependent variables and the total variation of the latter to quantify the overall adequacy of the model (Roux, 2001). R^2 coefficient can be computed as shown in the following expression:

$$R^2 = \frac{SSR}{SST} = 1 - \frac{SSE}{SST} = \frac{SST - SSE}{SST} \tag{2.38}$$

It is noteworthy to indicate that the values of R^2 vary between 0 and 1. For models that fit well the available data, R^2 is near 1, otherwise, the values of R^2 are close to 0.For instance, if the computed value of R^2 for a set of data is x, this implies that the model explains x % of the total variation of data.

CHAPTER 3: DATA COLLECTION AND PROCESSING

3.1 Introduction

This study was carried out through a series of field data collection from two different study sites located on rural two-lane highways in the Western Cape Province. The data were collected by means of a video technique. During all filming sessions, the camera was set up some distance away from the highway sections to obtain sufficient segment lengths, and to prevent that drivers are influenced and change their driving habit. With the purpose of examining if both directions of traffic on these highways have similar relationships between traffic parameters, the data were taken in both directions during peak morning and afternoon hours.

For each vehicle, data was recorded on direction of travel, travel time, vehicle class, and spacing measured from front bumper to front bumper of the following vehicle. Later on, the measured travel time was averaged for a specified time interval to determine the average mean speed for that particular time interval, and in the similar way, the density was computed from vehicular spacing for the corresponding time-interval.

This chapter provides information on the selection of the study sites, the site description, the processing methodology of field data into the suitable format appropriate for analysis, and finally the type and amount of data collected.

3.2 Study sites selection

With the aim of establishing acceptable and accurate speed-flow relationships and to meet the objectives of the study, some criteria were taken into consideration as a basis in the selection of the study sites.

The main criterion was the availability of all conditions of traffic namely free-flow, moderate and heavy traffic conditions representing bumper to bumper situation. This criterion was deemed very important for site selection, to obtain traffic data which will produce speed-flow curves able to cover a full range of traffic conditions, varying from

free-flow to heavily congested (stop and go) conditions. Together with the above criterion, it was also necessary to determine suitable time and enough time period for collecting data, with the purpose to provide more reliable results from which conclusions drawn can be applicable to other roads with similar conditions. To this end, numerous study sites were proposed but only two amongst the proposed sites were found to satisfy these conditions during morning peak hours, and were therefore selected and used in this study.

The Highway capacity manual (TRB, 2010) specifies that uninterrupted flow conditions on a given section of highways occurs when it is located at a distance of 2 to 3 miles from the nearest signalized intersection. This serves as a second criterion which is the choice of location of the study sites, in the position where traffic cannot be influenced by a signalized intersection or any platoon of traffic formed upstream of traffic signals.

According to many studies, there are a number of other factors that are likely to influence driver behaviour on two-lane highways. These factors must be taken into account during selection of the study sections so as to reflect the true traffic behaviour under prevailing conditions. These other factors can be classified as follows:

Road geometric conditions

These conditions include various factors such as the lane widths, shoulder width and lateral clearance, design speed, speed limit, lane and shoulder conditions, horizontal and vertical alignments, and adjacent land use.

Traffic conditions

These include factors like traffic composition (mix), directional distribution, parking and presence of pedestrians.

Environmental conditions

These include factors like weather conditions, season, visibility, speed restrictions, and so on.

3.3 Description of the study sites

As previously mentioned, the data collection process was undertaken from the sections located on two rural two-lane two-way roads. The figure below shows the map of the study site segments and surrounding areas. In the section below, the detailed information of each study site are described.

Figure 3. 1: Map indicating the locations of the study sites (Google map)

Study site 1: R44 (In proximity of Stellenbosch Town)

This section is located on a rural regional two-lane highway (R44).The site is situated on the section of R44 between Stellenbosch and Wellington Towns. The study segment is located about 6 km north west of Stellenbosch Town CBD, and about 2 km from the nearest signalized intersection towards Stellenbosch. The figure below provides a screenshot of the study section.

Figure 3. 2: Study section 1(R44 towards Stellenbosch Town) (Google earth)

Site layout data

The on-site conditions are quite similar to the base conditions provided in the Highway Capacity Manual (TRB, 2010). This section is on a level terrain with grade <3%. It is comprised of two lanes of 3.6m width each and shoulders of 1.8m width on both sides. The passing opportunity is not restricted on this section, and the through traffic is not impeded by traffic signals or turning vehicles. The shoulders on either side are properly maintained and are in good riding conditions. The speed limit on this section is 100Km/h.

Study site2: R 304(Near Stellenbosch Town)

This section of highway is located on a regional rural two-lane road (R304) which connects Stellenbosch Town with the national road N1.The Study segment is located about 6 km North West of the CBD of Stellenbosch Town as well. This section is located about 4.5km from the nearest signalized intersection toward Stellenbosch. The figure below provides a presentation of the study section.

Figure 3. 3: Study section 2(R304 towards N1) (Google earth)

Site layout data

The prevailing conditions on this section are quite similar to the base conditions specified in the Highway Capacity Manual (TRB, 2010). This section is situated on a level terrain since the gradient is less than 3%. The section consists of two lanes of 3.6m width each, and shoulder of 1.8m width. The passing opportunity is allowed in both directions, and the through traffic is not impeded by traffic signals or turning vehicles. The shoulders on either side are properly maintained and are in good riding conditions. The speed limit on this particular section is 100Km/h.

3.4 Data processing

The data on both sites were taken during morning and afternoon peak hours on two different dates. During the playback of the video footage, it was observed that the morning peak hours provide the data which cover all traffic conditions for the traffic moving towards the town of Stellenbosch(South bound direction). But in the other direction, only the free-flow traffic was found for both morning and afternoon hours. Thus, in this study only data taken in the morning peak hours were considered for further analysis.

The methodology followed in this study to reduce data from the video footage and transform them in the format appropriate for further analysis can be viewed in 5 main steps presented as follows.

Step 1: Measuring travel time for a particular time-interval

The pattern of each vehicle was observed and travel time of each vehicle was measured directly from the video footage by calculating the difference between time the vehicle under observation enters the section and the time the vehicle arrives at the end point of the section. That is, the difference between the time when the front bumper of the vehicle reaches the entrance point and the time the same bumper reaches the exit point of the study section. The travel times of all individual vehicles in a given time interval (1 and 5 minutes in the case of this study) were then averaged.

Step 2: Computing the Average Speed

The average travel times obtained in Step 1 were subsequently used in computation of average speed using the following formulae:

$$\text{Average speed} = \frac{\text{Distance}}{\text{Average travel time}} \text{x } 3.6$$

Where:

Average speed is expressed in km/h

Distance is expressed in meters

Average travel time expressed in seconds

Step 3: Measuring spacing between vehicles for the given time-interval

The spacing between vehicles were measured from the footage by observing the positions of the front bumper of the vehicle ahead and the front bumper of the vehicle behind in a platoon. Once individual spacing measured, they were then averaged for the given time-interval (1 and 5 minutes for the sake of this project). Since spacing between

vehicles is not constant and varies all along the section length, three measurements of spacing were made throughout the time-interval and they were averaged to be used in the next step.

Step 4: Calculating the average density

In the same way as in step 2, the average spacing computed in previous step were used to calculate the average density for the corresponding time-interval (1 and 5 minutes in the case of this study). The average density was calculated using the following formulae:

$$\text{Average density} = \frac{1000}{\text{Average Spacing}}$$

Where:

Average density is expressed in veh/km

Average spacing is expressed in meters

Step 5: Computing the corresponding flow

The traffic flow for each time-interval was computed from the corresponding average speed (**Step 2**) and average density (**Step 4**) using the steady-state equation between traffic parameters (Equation 2.1).

3.5 Data collected

The following part provides the summary of the data collection procedure and the data collected on both study sites. The data obtained from both sections are presented below direction by direction. The full data set is shown in Table 1 through to Table 8 in Appendix A.

3.5.1 Section 1: (R44 near Stellenbosch Town)

The collection of data on this section was undertaken on 6th of May 2013 during morning peak hours. The data were taken on a stretch of road of 112m length. This

distance was the maximum possible achievable distance, due to the configuration of the area, which made it impossible to position the camera at a farther distance from the roadway to allow the observation of a large segment length. This length was measured with aid of standard land surveying equipment from physical objects available on the roadway section, readily recognizable on the footage such as telephone posts and trees. The playback of the video footage was performed with the use of Adobe premiere CS 6 software which displays up to 2 decimals of seconds, to obtain more accurate measurements in travel time determination.

The following figure shows a snapshot of the footage for Section 1 in which the position of the telephone posts were demarcated on the television screen to facilitate the measurements.

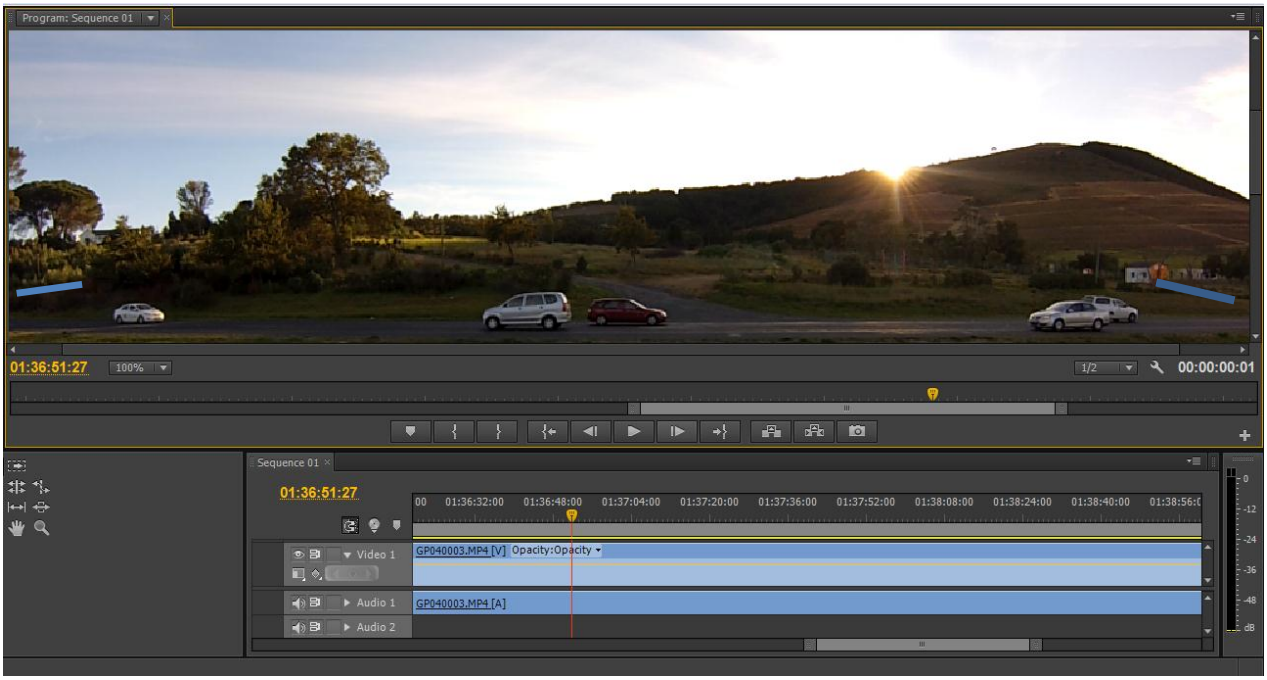

Figure 3. 4: Footage for section 1(R 44)

Due to weather conditions and the battery-life of the camera, the traffic was observed and filmed for a period of 2 hours and 20 minutes in both directions. The filming session started from 6:31 to 8:51.But due to weather conditions, the first 52 minutes of the footage were not clear; the data were then processed from 7:24 to 7:51. This means

that actual data were collected for a period of 91minutes. The total number of vehicles observed and from which data were collected are 1195 vehicles in the southbound direction towards Stellenbosch Town and 790 vehicles in the northbound direction towards Wellington Town.

The results are presented in graphical form in the section below, starting from vehicles moving in southbound direction towards Stellenbosch Town.

3.5.1.1 Speed Measurements

Once the travel time was measured from the footage and averaged for each one-minute of observation, the speed was calculated as shown in Step 2 of the methodology. Figure 3.5 illustrates the change in actual average speed for this section.

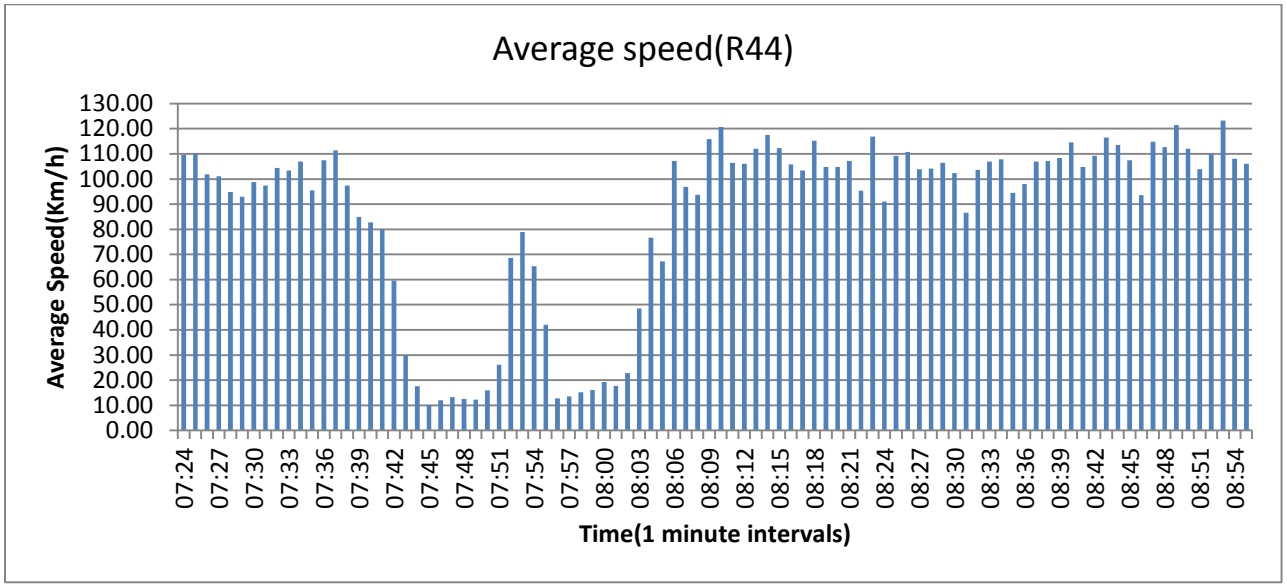

Figure 3. 5: Average speed measurements over consecutive 1min. intervals (R 44 south bound direction)

From Figure 3.5, it can be observed that during the early morning, vehicles travel at high speed varying between 100 and 110 km/h. This average speed stays relatively in this range for a couple of minutes up to the point where a sharp drop of speed occurs (about 7:43). This sudden change of speed indicates that the capacity of this section has abruptly been exceeded and the section starts to operate in congested condition.

During this interval, the average speed fluctuates since at 7: 51 a sharp increase of speed is experienced. In the next interval, speed starts to decrease again until 8:02 where the speed increases again to reach the maximum average speed attainable in this direction (123.3 km/h).

An inspection of Figure 3.5 also shows that the average speeds calculated for free-flow conditions before and after the congested period (07:42-8:05) shows a difference of 8Km/h. This difference is considered relatively high given that in both periods, the density is low in this direction (Figure 3.7). Many factors may contribute to this occurrence. Among these factors, the reduction of visibility was thought to be the main reason, provided that the data were taken during the start of winter season where in the early morning the visibility is restricted, and cause the drivers to lower their speed.

Another observation made is that during data collection, it was found that in this section, drivers travel at a high speed. A large difference of average speed ranging from 10km/h to 23 km/h was found during free-flow conditions, since the speed limit for this section is 100km/h. This large value was expected because the free-flow condition prevails on this section in both directions, and shoulders are in good riding condition. Thus, drivers are free to drive at their chosen speeds regardless of the maximum allowed speed.

3.5.1.2 Density measurements

As previously mentioned, the methodology utilized in this study to compute average density was to use the average of measured spacing between vehicles travelling on the highway section. Figure 3.6 provides an illustration of the change in average spacing during consecutive one-min time intervals of data collection period.

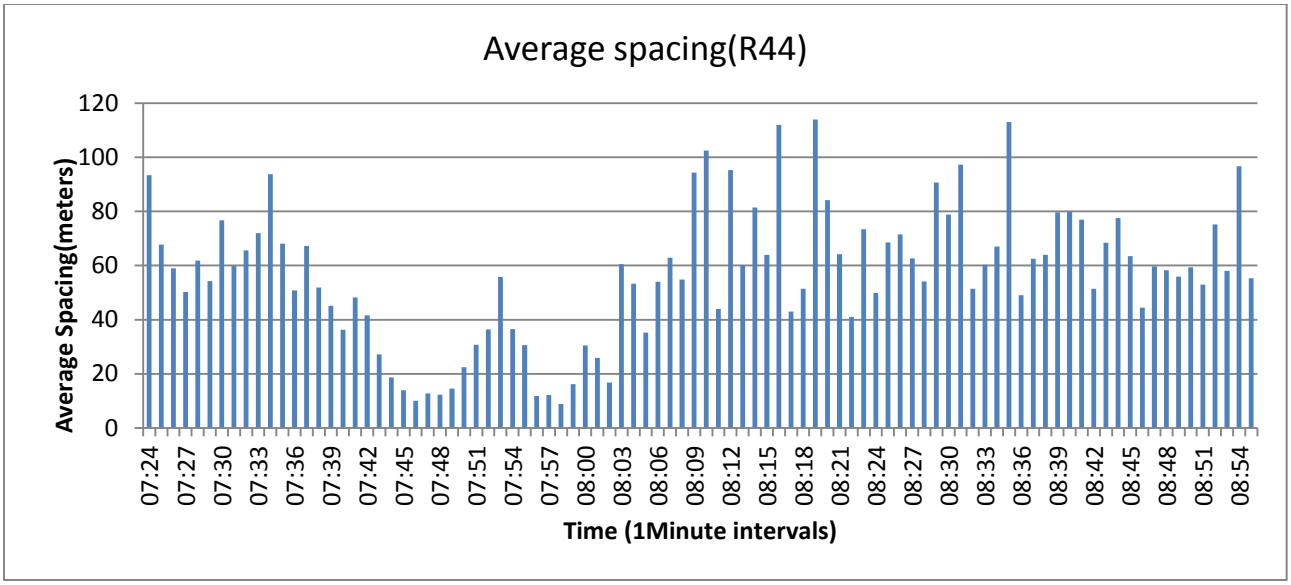

Figure 3. 6: Graphic presentation of the average spacing over consecutive 1min. intervals (R44 southbound direction)

Figure 3.7 illustrates the change in average density calculated from average spacing. The close inspection of this figure shows that during the early morning, traffic on this section is under free-flow condition, with maximum density achievable being below 20veh/km. The density starts to increase progressively in response to increasing in demand up to the point a heavy congestion occurs (about 7:46). From this point onwards, the density varies and a sudden decline occurs for few minutes after which the density increases again and attains a higher value of about 112 veh/ km. Through the visual inspection of Figure 3.7, that density can however to a certain extent be considered as jam density. The reason for this is that due to the variations of density during the congested condition, it is difficult to determine the exact value of jam density. Given the behaviour of traffic on this section, it is obvious that the capacity of this section is insufficient to meet the required demand.

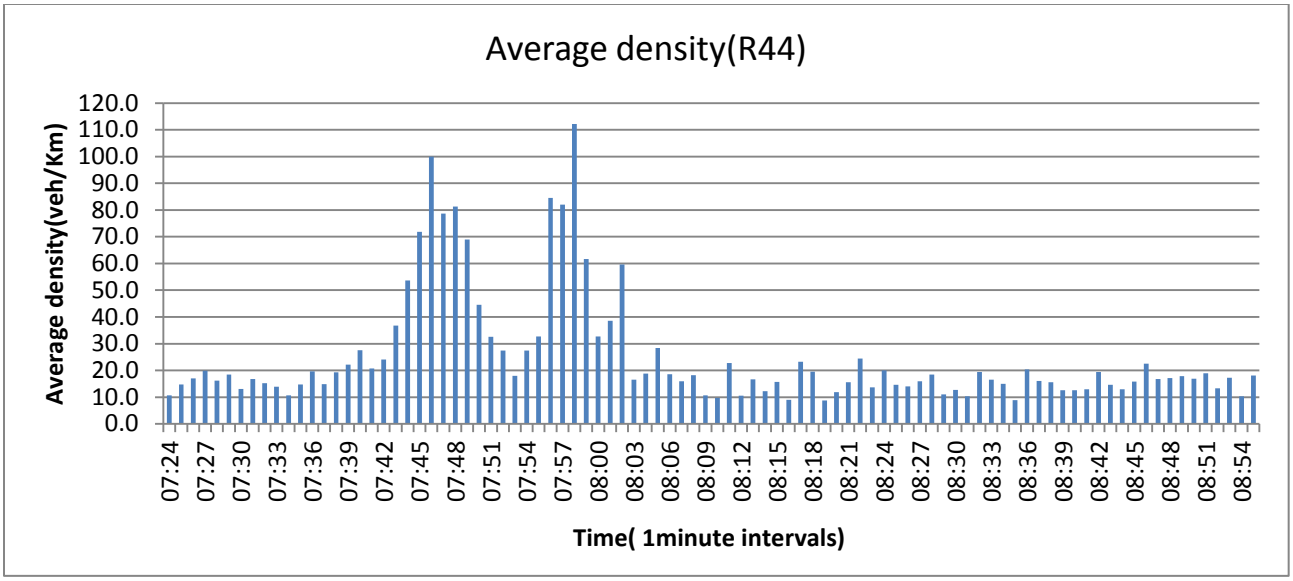

Figure 3. 7: Average density over consecutive 1 min. intervals (R44 southbound direction)

In the next interval, a sharp drop in average density is observed from 8:05 to the rest of the study period, where average density varies between 8veh/km to 25veh/km. This decrease in density is caused by the reduction of demand and results in the section to operate in free-flow condition during this interval.

The largest volume of traffic passed through this section between 7:36 and 7:42(Figure 3.8). The traffic density observed from Figure 3.7 for this period stayed relatively constant at a reasonably low value. This density is referred to as optimum density of the section, and it indicates the density at which the volume of the traffic passing a given section is close to its capacity. In this direction for this section, optimum density can be estimated to be about 23veh/km.

3.5.1.3 Flow measurements

The traffic flow over each one-min intervals was computed from corresponding average speed and density using the steady-flow equation(Equation 2.1) as described in methodology discussed above. Figure 3.8 gives an illustration of the change in flow during consecutive one-min intervals.

From Figure 3.8, it can be observed that traffic on this section during the whole study period is relatively high and it is comprised of alternate increase and decrease of flow. This results in a difficult prediction concerning the operating conditions of the section. However, in conjunction with Figure 3.5, the prediction can be made possible. In the early morning up to 7:42 the flow is at a high level with high speed greater than 88 km/h which corresponds to the level of service A (TRB, 2010). This indicates that this section operates in free-flow conditions.

It can be observed that the largest volume of traffic passes over this section during this interval from 7:36 to 7:42. This flow constitutes the optimum flow, which characterize the capacity of this section. The speed for this condition is known as optimum speed (Chapter 2). For this section, the optimum speed was calculated by averaging the speed observed over this period. A value of 89.08km/h was obtained.

In the next interval starting from 7:44 until 7:51, traffic flow decreases together with a decrease in average speed up to 10km/h. This indicates that the section operates in a congested condition. In the remaining interval, a series of alternative increase and decrease of flow is experienced with corresponding low average speed until 8:05 and then average speed starts to increase. This results in the section to operate first in congested condition up to 8:05 and from this point onwards, the section operates in free-flow condition.

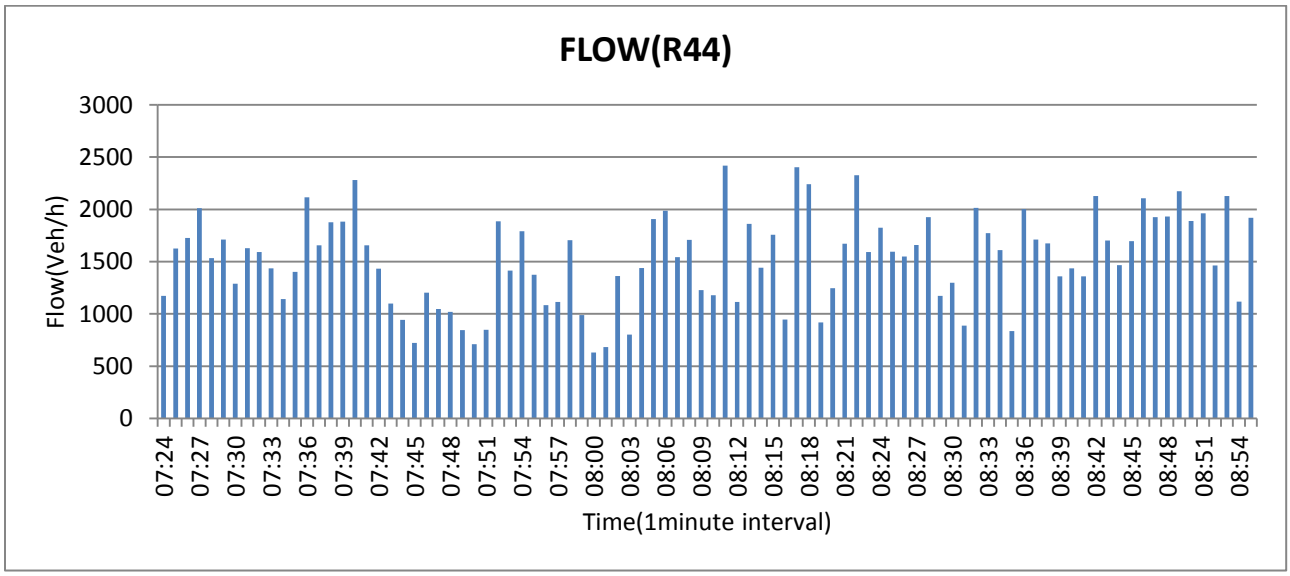

Figure 3. 8: Flow of traffic over consecutive 1 min. intervals (R44 southbound direction)

In this figure also, it can be seen that a maximum flow rate of 2418 veh/h in one direction can be reached. One of the factors contributing to such large amount of flow to occur on this section is due to the fact that some drivers use shoulders, to allow faster vehicles behind to overtake without using the lane of opposing vehicles.

As mentioned previously, data were taken also in the northbound direction towards Wellington town during the same time; the results in this direction are shown in the section below.

3.5.1.4 Speed measurements

Figure 3.9 illustrates the actual average speed measured during consecutive one-min intervals during morning hours in the northbound direction. A closer look at this figure reveals that in this direction, the average speed was very high throughout the observation period. The minimum and maximum speeds of 88km/h and 132.6km/h respectively were observed. From this figure, it can also be observed that the variations of speed in this direction consist of alternative slight increases followed by slight decrease of speed throughout the study period. Various factors can be the contributing factors to this occurrence. Among these factors, the presence of heavy vehicles in traffic stream is seen as main factor, given that in this direction, heavy vehicles were observed in a large number .This results in lowering of speed of the faster vehicles behind, and the increase of speed once the slower vehicles have cleared the section.

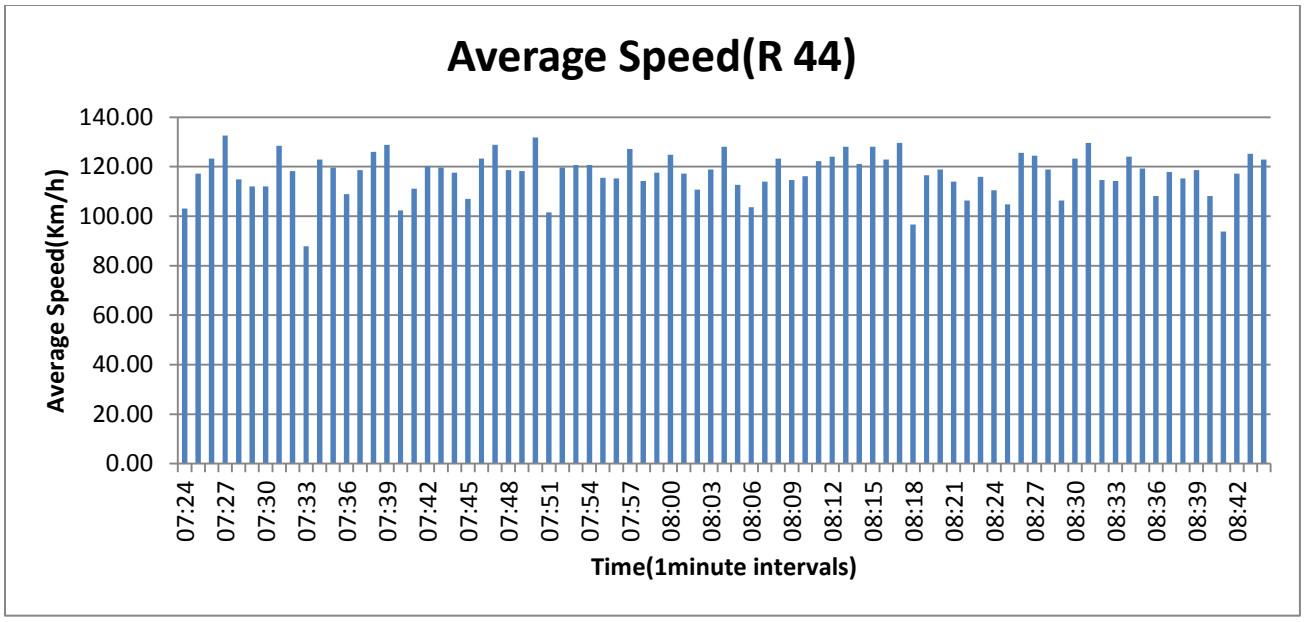

Figure 3. 9: Average speed measurements over consecutive 1min. intervals (R 44)

From this figure, it is worthy to note that a maximum speed in this section is achievable in this direction (133 km/h). A difference of about 10km/h was found when this value was compared to the maximum value obtained in the other direction of flow (Figure 3.5).

3.5.1.5 Density measurements

Figure 3.10 illustrates the change in average spacing over consecutive one-min intervals observed throughout the data collection period. A look at this figure shows that spacing varies between 40 to 80 m over a long period of data collection. This indicates that interaction between consecutive vehicles is very low, and drivers are not highly embedded by the presence of others.

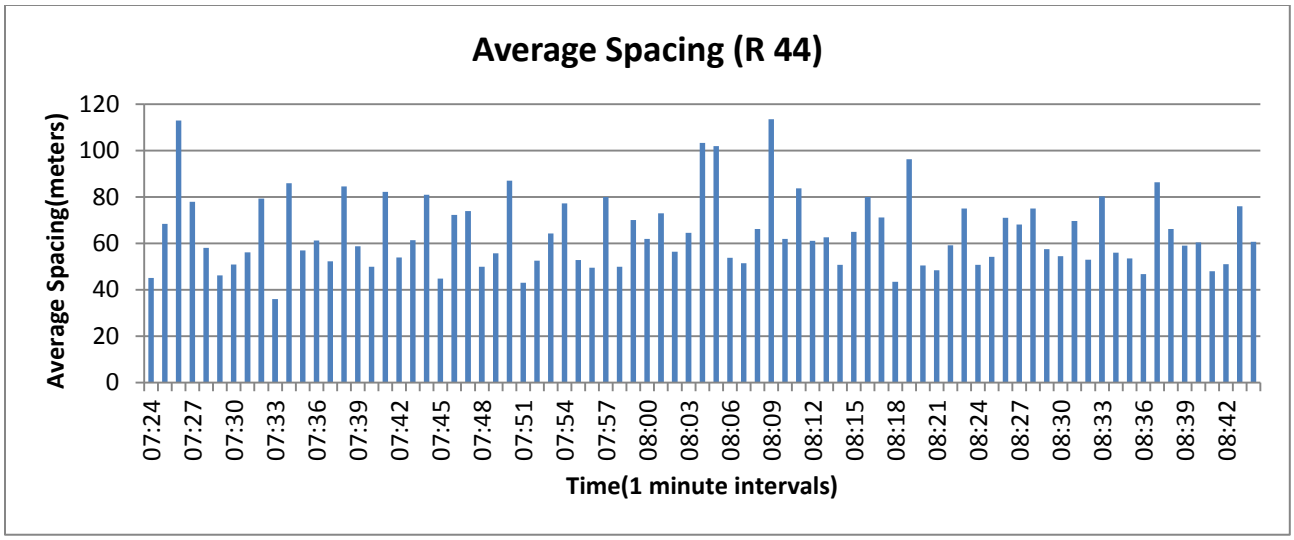

Figure 3. 10: Graphic presentation of the average spacing over consecutive 1min. intervals (R44 northbound direction)

Once average spacing was determined, the average density was computed and results are presented in Figure 3.11. From this figure, it can be observed that variations in average density for this direction is low compared to that in the other direction. An inspection of this figure also shows that the average density varies mainly between about 10veh/km to 23veh/km. This density is very low and with additional information from Figure 3.9, it can be seen that the average speed during the whole study period shows that LOS A prevails in this direction. This implies that the section operates in free-flow condition.

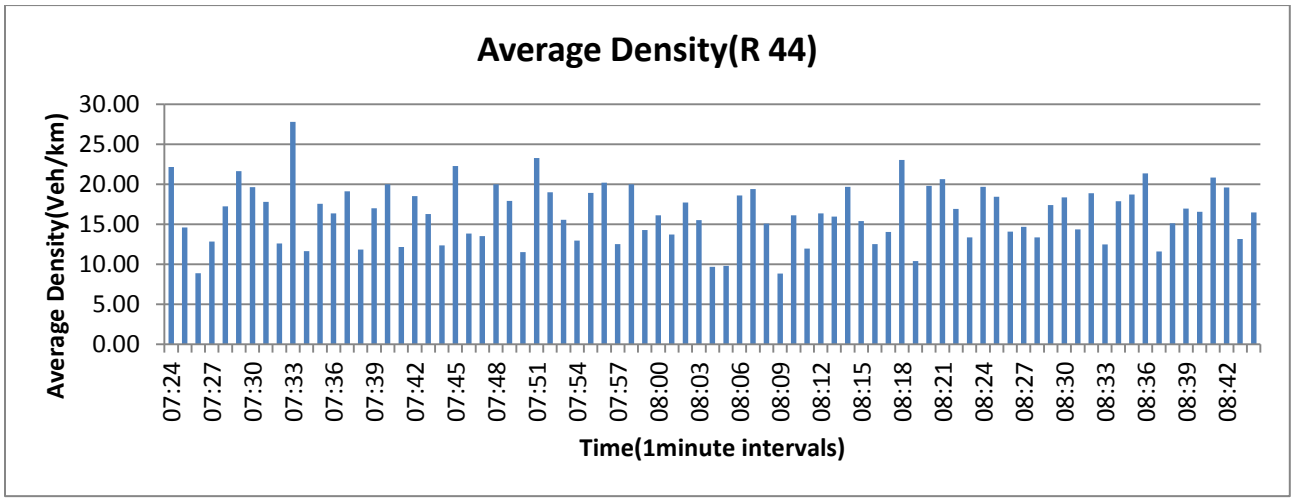

Figure 3. 11: Average density over consecutive 1 min. intervals (R44 northbound direction)

3.5.1.6 Flow measurements

Figure 3.12 provides an illustration of the change in traffic flow over consecutive one-min intervals for this section in the north bound direction. An inspection of this figure shows that flow in this direction remains at a relatively high level, during the whole study period with a minimum value of 1009 veh/h. The average flow throughout the whole period is 1897 veh/km. It is also possible to observe a maximum flow rate of 2440 veh/hr. This high value was expected since the drivers maintain high speed, even with relatively low spacing as observed during the video capturing process.

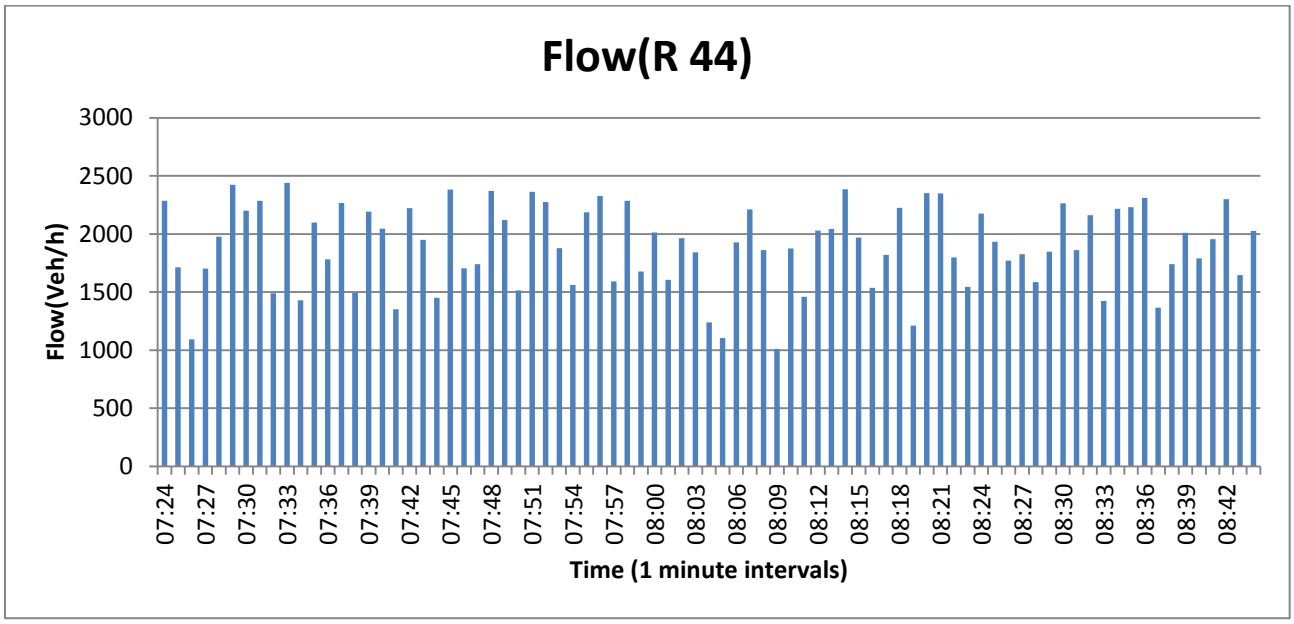

Figure 3. 12: Flow of traffic over consecutive 1min. intervals (R44 north bound direction)

3.5.2 Section 2: (R304)

The collection of data on this section was undertaken on 10th of May 2013 during morning peak hours. Since the configuration of the area could not allow the possibility to settle the camera to a farther distance from the roadway, to allow the observation of large section of highway, the data were taken on a road segment of 78m length. This length was measured using standard land surveying equipment from physical objects available on the road way section easily recognizable on the footage, such as telephone posts and fence posts of adjacent farms along the road section. The play back of the

video footage was performed using Adobe premiere CS 6 software as for Section1. This software can display up to 2 decimals of seconds, and it allows obtaining the accurate measurements in travel time determination. The following figure shows a screenshot of the footage for Section 2 in which the position of telephone post and one fence post were demarcated on the television screen during measurement.

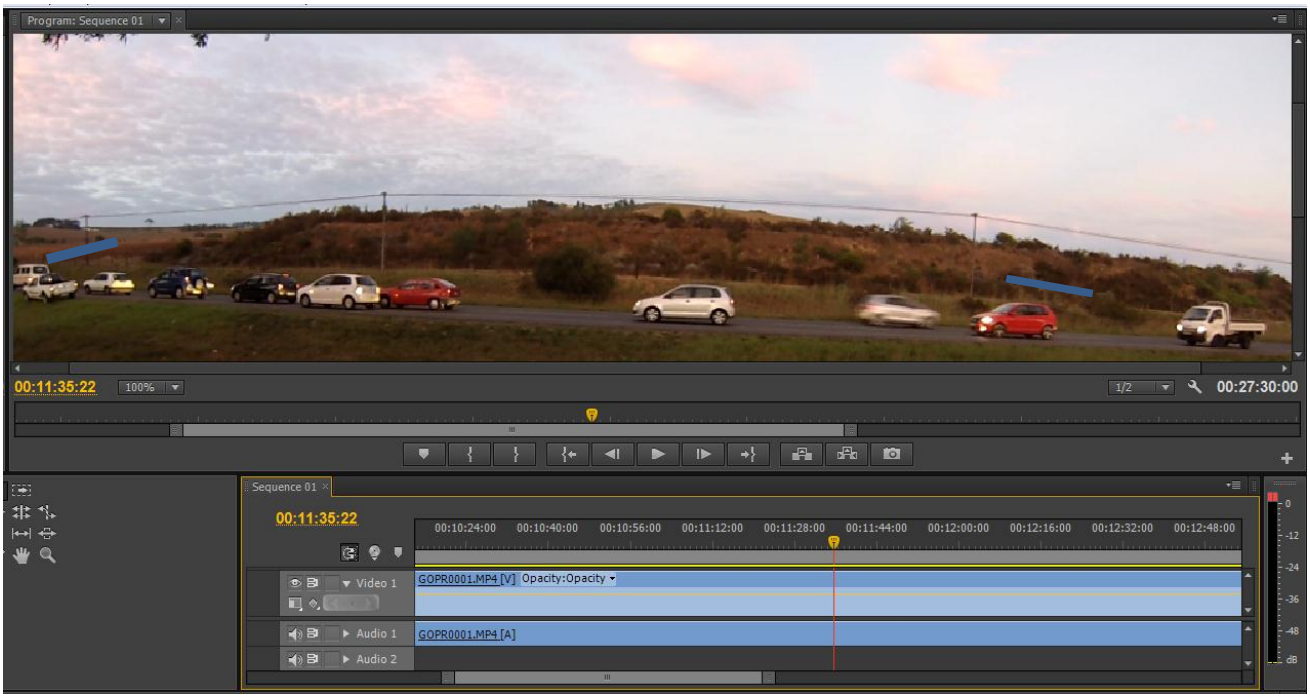

Figure 3. 13: Footage for section 1(R 304 toward Stellenbosch Town)

Due to limited battery-life of the camera, the traffic were observed and filmed for a period of 2 hour and 20 minutes for both directions. The filming session started from 7:31 to 9:51, this means that, the data were collected during a duration of 140 minutes. The number of vehicles observed was 2281 vehicles in southbound direction towards Stellenbosch Town and 1354 vehicles in northbound direction towards N1. The results are presented in graphical form in following section, starting from vehicles moving in the southbound direction towards Stellenbosch Town.

3.5.2.1 Speed measurements

The averages of travel time measured from footage were used to compute average speeds for this section. Figure 3.14 is an illustration of the change in actual average speed in the southbound direction towards Stellenbosch Town.

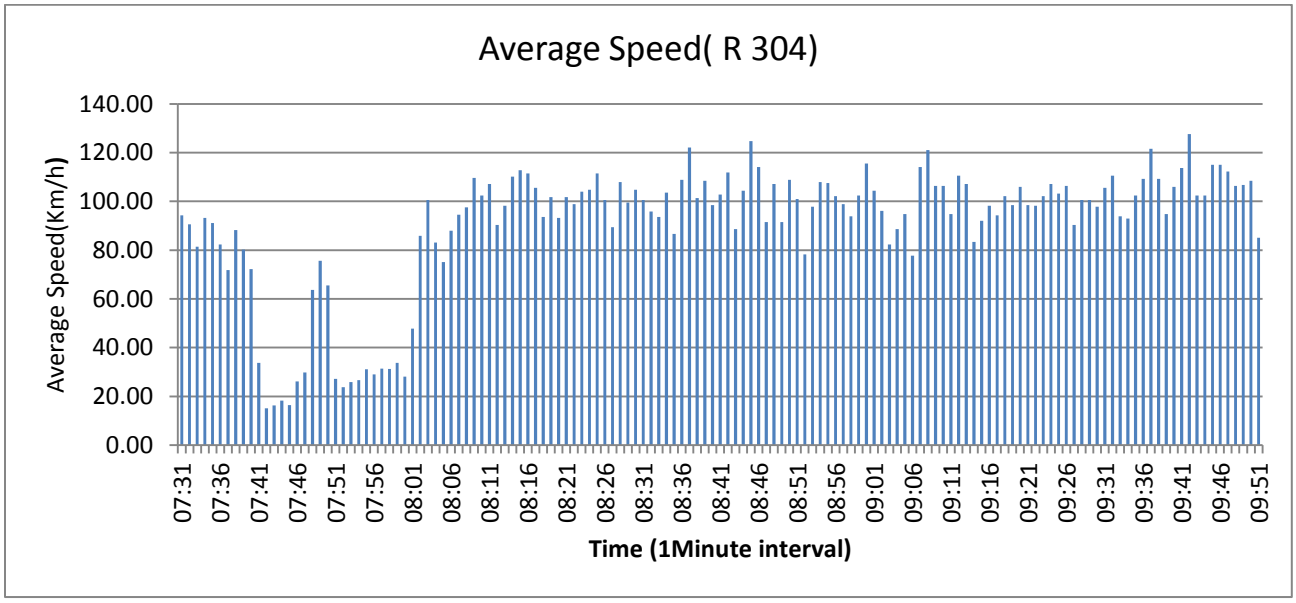

Figure 3. 14: Average speed measurements over consecutive 1min. intervals (R 304 south bound direction)

From Figure 3.14, it can be observed that during the early morning, vehicles travel at a relatively high speed of about 84km/h corresponding to the level of service B (TRB, 2010). This average speed stays in this range for a couple of minutes until 7:40 where a sharp drop of speed occurs. From this point to about 8:00, the average speed remains low but variable, since at 7:48 to 7:50 an abrupt increase of speed is experienced. In spite of this increase of speed, it can be seen that the section operates under congested condition, since an overall average speed of 32.42 km/h is observable in that interval. This speed corresponds to the level of service E which indicates heavy congestion (TRB, 2010).

In the next interval, the average speed increases again and reaches its maximum. During this interval, it can be seen that the section operates under free-flow condition

since the average speed of 102km/h obtained during this interval shows that the section falls in range of LOS A (TRB, 2010).

A similar observation as in Section 1 shows that the average speeds calculated for free flow condition before and after the congested period (07:41-8:00) shows a difference of 16.6km/h.

This difference is again considered high, given that in both periods the density was low on this section (Figure 3.16). Numerous factors may contribute to this occurrence. Among these factors, the reduction of visibility during early morning was seen to be the main reason as observed at Section1.

It is noteworthy to indicate that at this section, drivers travel at high speed during free flow conditions. A large difference ranging from 5 to 27km/h was found during free-flow conditions, since the speed limit for this section is 100Km/h. This was expected because the free-flow condition prevails on this section in both directions, thus, drivers are free to drive at their chosen speeds.

3.5.2.2 Observation of density

In a similar way as in Section 1, vehicular spacing was measured, and averages were calculated for each one-min intervals. Figure 3.15 is an illustration of change in average spacing in this direction.

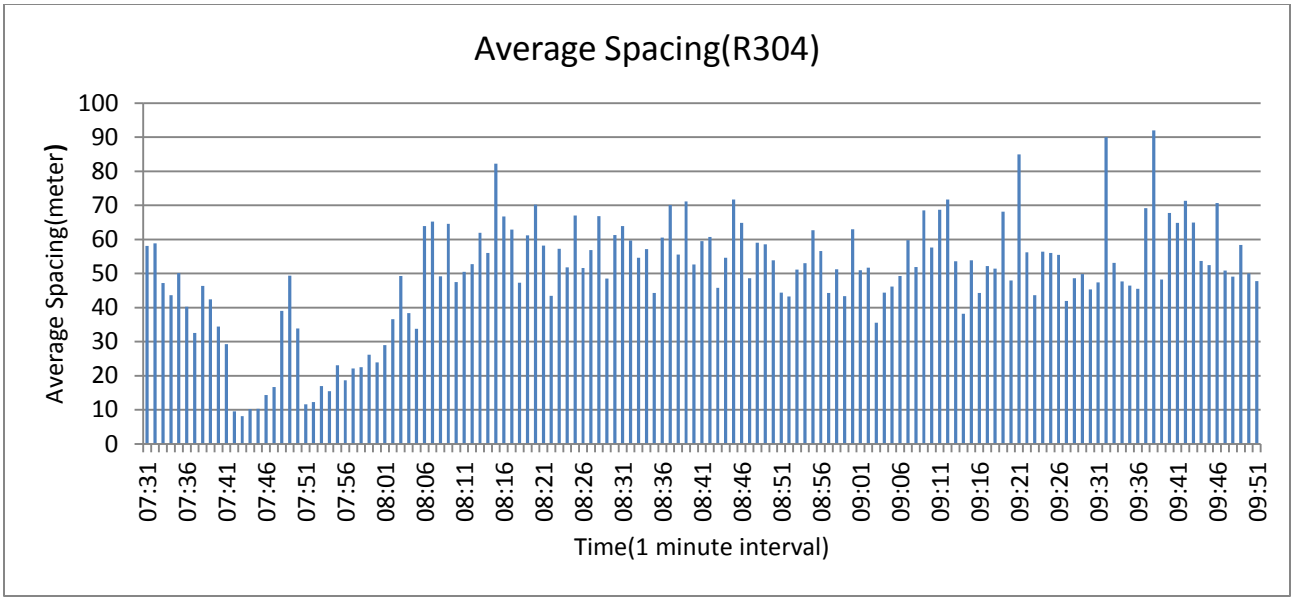

Figure 3. 15: Graphic presentation of the average spacing over consecutive 1min. intervals (R304 southbound direction)

Figure 3.16 provides an illustration of the variations in the average density calculated from average spacing obtained throughout the study period. It can be observed that the traffic on this section during the early morning is free-flow traffic. The density during this period varies between 17veh/km to 34veh/km.

The density starts to increase progressively in response to increase of demand up to the point a heavy congestion occurs at about 7:42. The onset of this congestion indicates that the capacity of the section has suddenly been exceeded. It can be seen that estimation of optimum density for this section from Figure 3.16 is not an easy task. The optimum density in this direction lies somewhere between 27 and 35veh/km.

From 7:43 onwards, a maximum density observable on this section is reached (121.8veh/km), with a corresponding speed of 9.54km/h. Through the visual inspection of Figure 3.16, that density can be considered as jam-density.

After the maximum density is reached, a series of sharp decrease and increase of average density is experienced until 8:06. From this point onwards, average density is very low and presents relatively small variations throughout this interval.

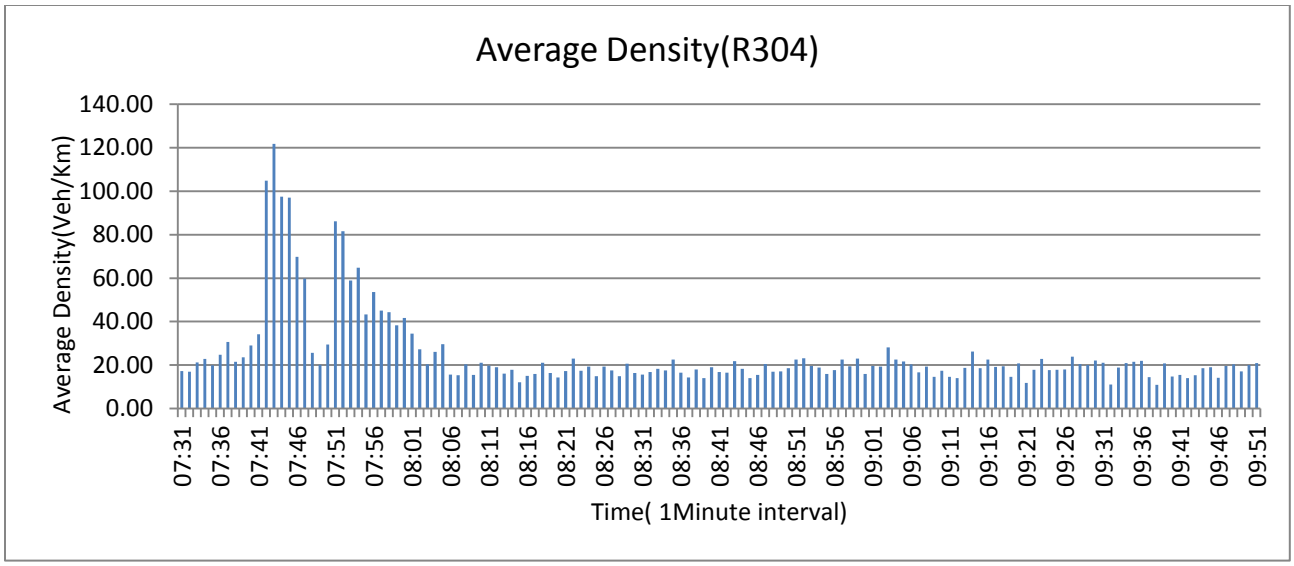

Figure 3. 16: Average density over consecutive 1min. intervals (R304 south bound direction)

3.5.2.3 Flow measurements

Figure 3.17 depicts the change in flow over consecutive one-min intervals for this section. From this figure, it can be observed that flow is relatively high throughout the whole study period, and its variations are not very pronounced. This leads to the prediction of the state of traffic in this direction being difficult as it was the case with the same direction in Section 1 discussed above.

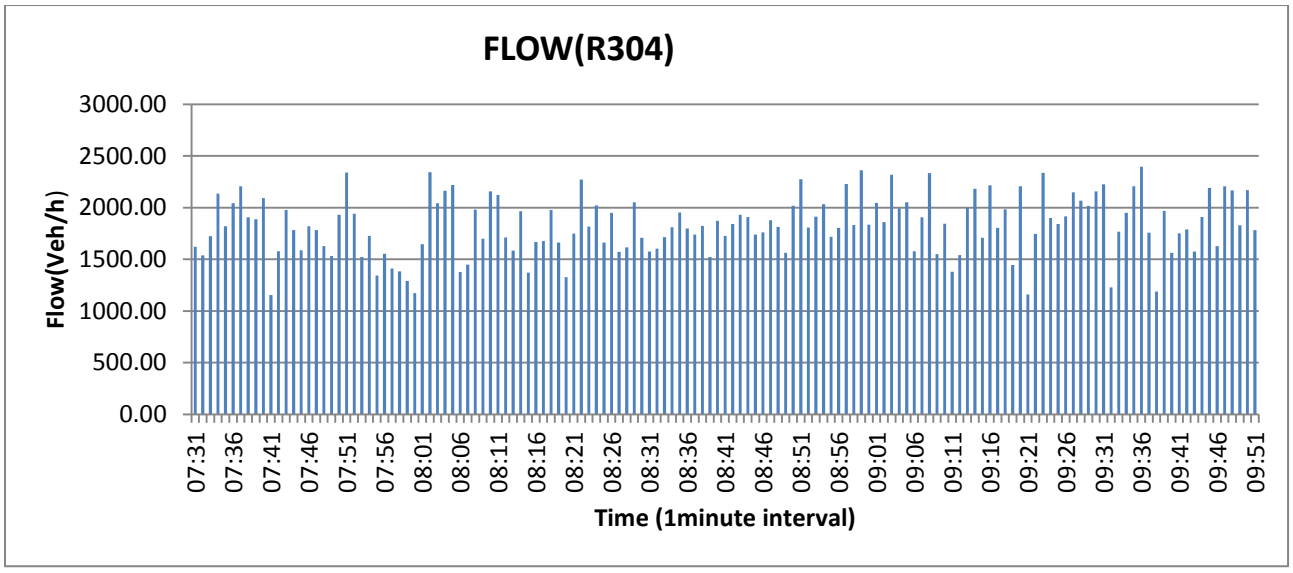

Figure 3. 17: Average flow measurements over consecutive 1min. intervals (R 304 south bound direction)

It can be noted that the largest volume of traffic observable over this section before congested period passes between 7:34 and 7:40. This flow constitutes the optimum flow, which characterize the capacity of this section. The corresponding speed called optimum speed can be calculated as average of speed obtained in this interval (refer to Figure 3.5). This optimum speed is estimated to be 82.76km/h.

An inspection of this figure gives an opportunity to observe a flow rate of 2397 veh/h in one direction. This value is very large. Several factors may contribute to occurrence of this large amount of flow. Among the factors contributing to such large amount of flow to occur on this section is that drivers use shoulders, to allow vehicles behind to overtake them. However, this value is small compared to the value obtained on Section 1(maximum value in Figure 3.8).

The data were taken in the other direction on this section as well; the results obtained in this direction (direction towards N1) are discussed in the following section.

3.5.2.4 Speed Measurements

Figure 3.18 is an illustration of the variations in actual average speed for this section during morning peak hours. The average speed is very high throughout the whole duration of observation, with minimum and maximum speeds of 84.58 and 130.6km/h respectively. It can be observed that the speed in this direction consists of series of consecutive slight increases and decreases of speed during the study period, as it was observed in the same direction for Section 1.

The average speed throughout the whole period is 111.74veh/h. This value falls in a range of a level of service A (TRB, 2010). This gives an indication that the section operates in a free-flow condition during the entire period of observation.

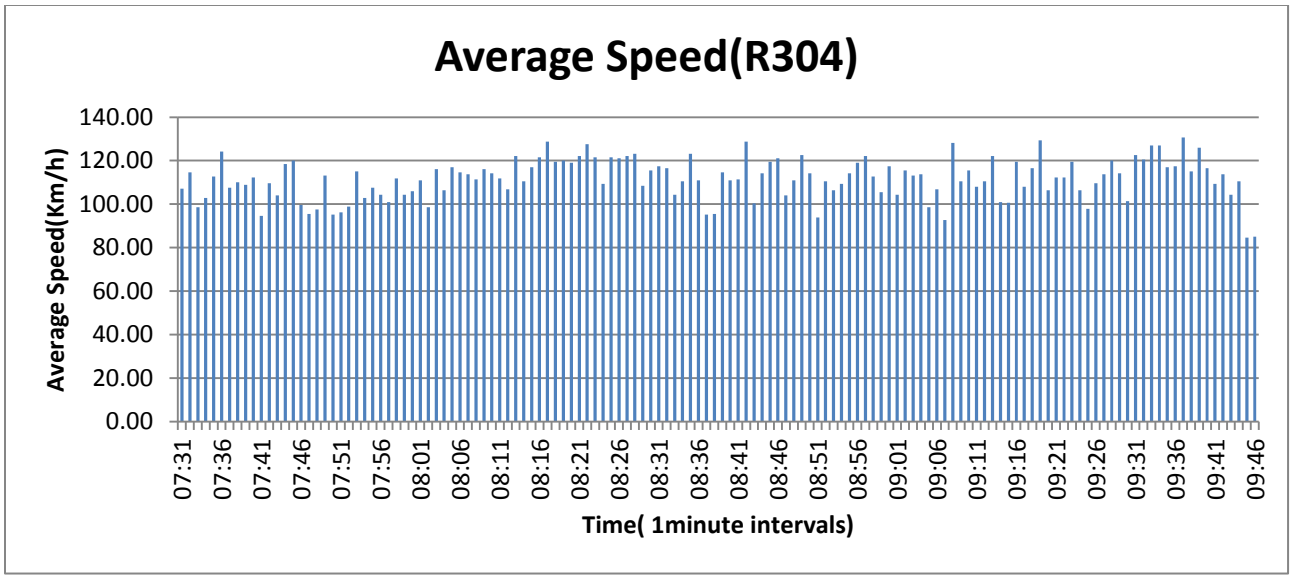

Figure 3. 18: Average speed measurements over consecutive 1min. intervals (R 304 north bound direction towards N1)

3.5.2.5 Density measurement

Figure 3.19 gives an illustration of the change in average spacing observed during the data collection period. An observation of this figure shows that spacing varies generally between 40 to 80 m over the long period of the data collection process as it was observed in the same direction in Section 1.

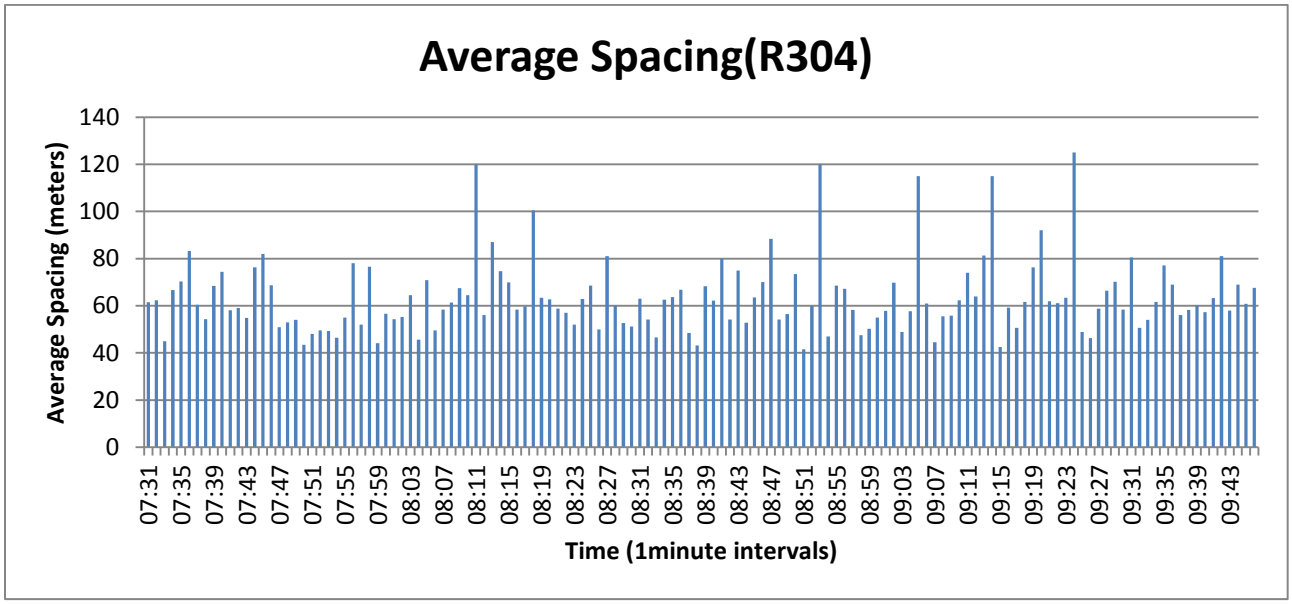

Figure 3. 19: Graphic presentation of the average spacing over consecutive one-min intervals (R 304 north bound direction)

From average spacing values, the average densities were computed and results are presented in Figure 3.20. From this figure, it can be observed that in this direction, the variations in average density are relatively low compared to that in the other direction of this section.

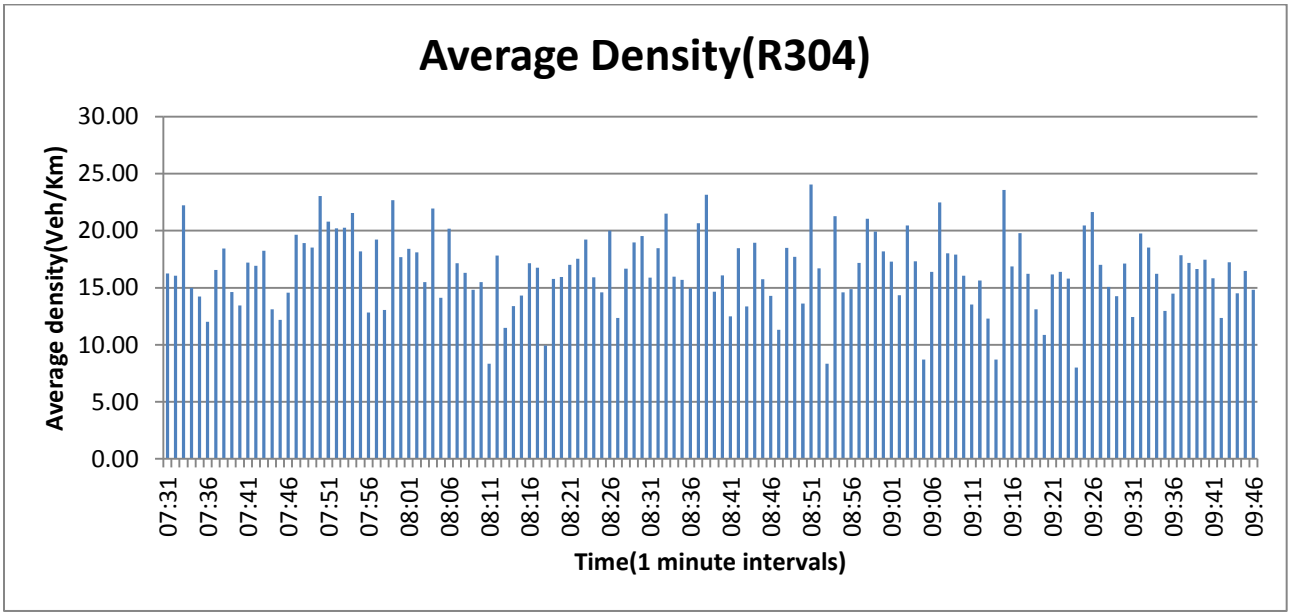

Figure 3. 20: Average density measurements over consecutive 1min. intervals (R 304 north bound direction)

It can be seen from Figure 3.20 that the average density varies mainly between about 8veh/Km to 24veh/km. This density is very low and with additional information from Figure 3.21, it may be concluded that this section operates in a free-flow condition in this direction throughout the whole duration of the study period.

3.5.2.6 Determination of flow

Figure 3.21 provides an illustration of the change in traffic flow over consecutive one-min intervals for this section in the northbound direction. It can be seen that flow in this direction is high with high variations throughout the entire study period. The average flow throughout the whole period was found to be 1837 veh/km with a maximum flow rate of 2420veh/h observable in this direction. This large value of flow was expected, since the vehicles travel at high speed even with relatively low spacing as observed during video capturing process.

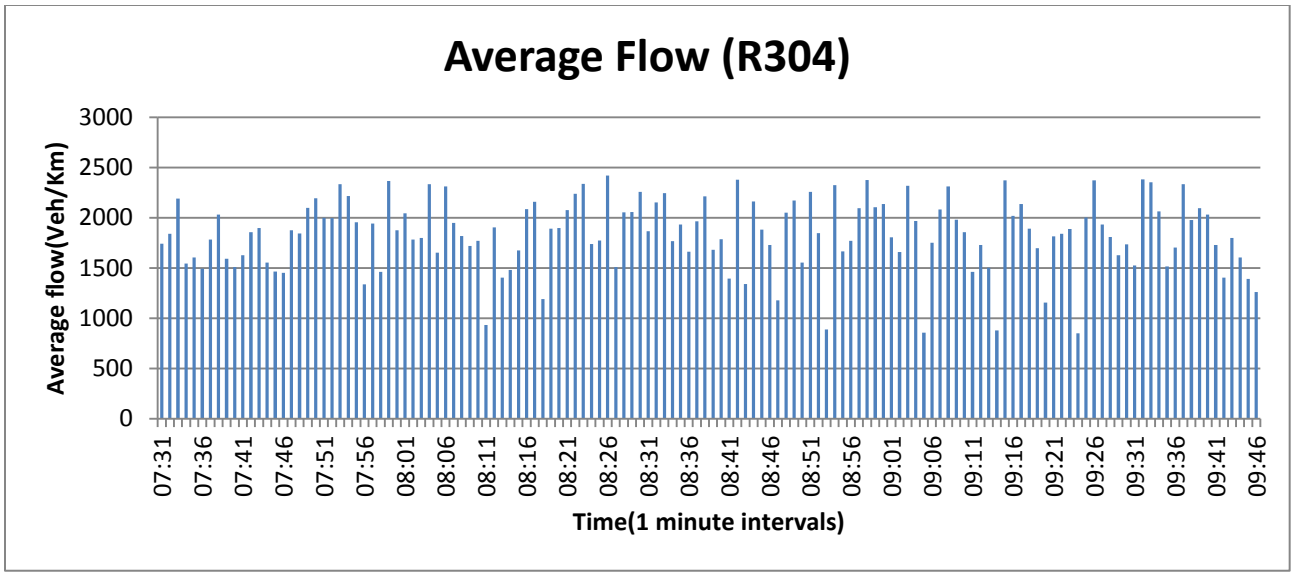

Figure 3. 21: Average flow measurements over consecutive 1min. intervals (R 304 north bound direction)

CHAPTER 4: DATA ANALYSIS

4.1 Introduction

As mentioned earlier in Chapter 2, several projects have been conducted to describe relationships between flow, density and speed on highways. However, most of these projects have been carried out on freeways and expressway in most countries. This resulted in development of theoretical models used worldwide for analysis of all types of highways. The basic purpose of this study resides in developing speed-density-flow relationships on rural two-lane highways in the Western Cape Province using some of the well-known models developed during previous projects. These models have been tested using actual data in order to find a model that fits the available data taken on rural two-lane highways.

To achieve this, a combination of regression analysis and personal judgement was used to derive practical models that provide a reasonable and reliable representation of the observed data on the Western Cape rural two-lane highways.

4.2 Model utilised

The following models were used in analysis of data obtained on both sections during the study period.

- The Greenshields Model

Greenshields (1935) as a first pioneer of traffic flow proposed a linear relationship between speed and density during his study on traffic characteristics on two-lane highways. This model is presented as follows:

$$u = u_f \left(1 - \frac{k}{k_j}\right) \qquad (2.13)$$

This model is very simple to use and satisfy all boundary conditions, namely free flow and congested conditions. However, other researchers have developed other models

which can describe the actual traffic data better since in most cases linear relationships between traffic parameters is not applicable.

- The Greenberg Model

Through the use of fluid dynamics principles, Greenberg (1959) proposed a logarithmic speed-density model of the form:

$$u = u_o \ln\left(\frac{k_j}{k}\right) \tag{2.16}$$

This model showed its strength in describing congested conditions. However, this particular formulation fails to satisfy the boundary condition of mean free speed at zero volume and density. This results in failure to provide realistic estimates during free-flow conditions as it will be shown later in this study.

- The Underwood Model

Underwood (1961) established a model relating speed to density by an exponential function. His model is shown in the following equation.

$$u = u_{f.} e^{-k/k_o} \tag{2.19}$$

The Underwood model seems to represent the observed data satisfactorily. However, in some cases, this model has failed to yield reasonable free-flow speed, as it will be shown later in this study.

- The Drake, May and Schofer Model

Drake et al., (1965) during their study found that the curve presents concavity at low density; they then proposed a bell-shaped curve of the form:

$$u = u_f e^{\frac{-1}{2}\left(\frac{k}{k_o}\right)^2} \tag{2.20}$$

This model was found suitable in describing low density field data. However, this model showed a shortcoming in prediction of data under congested conditions, since it underestimated the observed speed during this condition.

- The Drew Model

Drew (1965) using fluid analogy proposed a model similar to the Greenshields model where he incorporated another variable *n* which values are greater than -1. This model is represented by following equation:

$$u = u_f[1-(\frac{k}{k_j})^{n+1/2}] \quad (2.21)$$

- The Multi-regime Matrix Model

May and Keller (1967) proposed a series of steady-state flow equations using non integer values to describe traffic parameters (Chapter 2).

It was noticed that some of these equations do not result in zero speed for a jammed density. This results that these models provide ineffective description of the whole traffic range by the use of only one equation. They are therefore found to be effectively used to describe certain ranges of densities, instead of the whole traffic range from zero density to jam density. This observation was verified from the available data as will be shown later in this report.

Again, it is therefore worthy to note that with the use of these equations, those having an exponent *l*>1 with u_s incorporated in their formula were found effective in describing the field data.

- The composite Model

The observation of different curves obtained in many studies has shown that relationships between traffic parameters exhibit discontinuities between low and high density data. It was observed that there can be different regimes to describe these parameters.

In this context, Eddie (1960) came out with a method to describe traffic behaviour using two different models, one for the description of low density data and another one for representation of high density conditions. He suggested the use of the Underwood and Greenberg models for uncongested and congested conditions respectively.

In this study, different models were examined to obtain models which provide the best fit to actual data. Once the appropriate models are obtained, they were used in a further stage.

4.3 Curve fitting: Speed-Density relationship

As mentioned earlier, different developed models were tested with available data in order to identify which model fits the data best. This procedure has been carried out with the use of regression analysis. In this study, the speed-density curve was used for describing the available data. This curve was selected since it is easy to handle mathematically and once it is established, the other curves namely flow-density and speed-flow curves can be derived easily by applying the steady-state equation.

$$Q = u_s . K \qquad (2.1)$$

In search of the model which best predicts speed-density relationships based on available data, the known parameters were mentioned and unknown parameters were identified so as to find them through the method of least squares discussed in Chapter 2.

4.3.1 Relationships based on one-minute time intervals

With reference to the methodology developed in the 5th version of HCM (TRB, 2010) indicating that analysis of two-lane highways is done by considering only one direction. In this study each direction was investigated individually and analysis is based on one-min time intervals. The results of regression analysis for each model are provided in Tables 9 and 10 in Appendix A.

- **The Greenshields Model**

The linear model proposed by Greenshields is represented by Equation 2.13:

$$u = u_f \left(1 - \frac{k}{k_j}\right)$$

For this Model, the known parameters are the exponents *m* and *l* (*m*=0, *l*=2), while free-flow speed, u_f, and jam density,k_j, are identified as unknown parameters. Figure B-1 through B-4 in Appendix B are illustrations of curve fitting of available data using the Greenshields Model.

The regression analysis performed on Section 1 gave the following values:

South bound direction: u_f= 121.6 km/h, k_j= 86 veh/km, R^2=0.733.

North bound direction: u_f= 139.16 km/h, k_j= 104 veh/km and R^2=0.375.

Figure 4.1 illustrates the greenshields curve fitted to the data taken on section located on R44 in the south bound direction towards Stellenbosch.

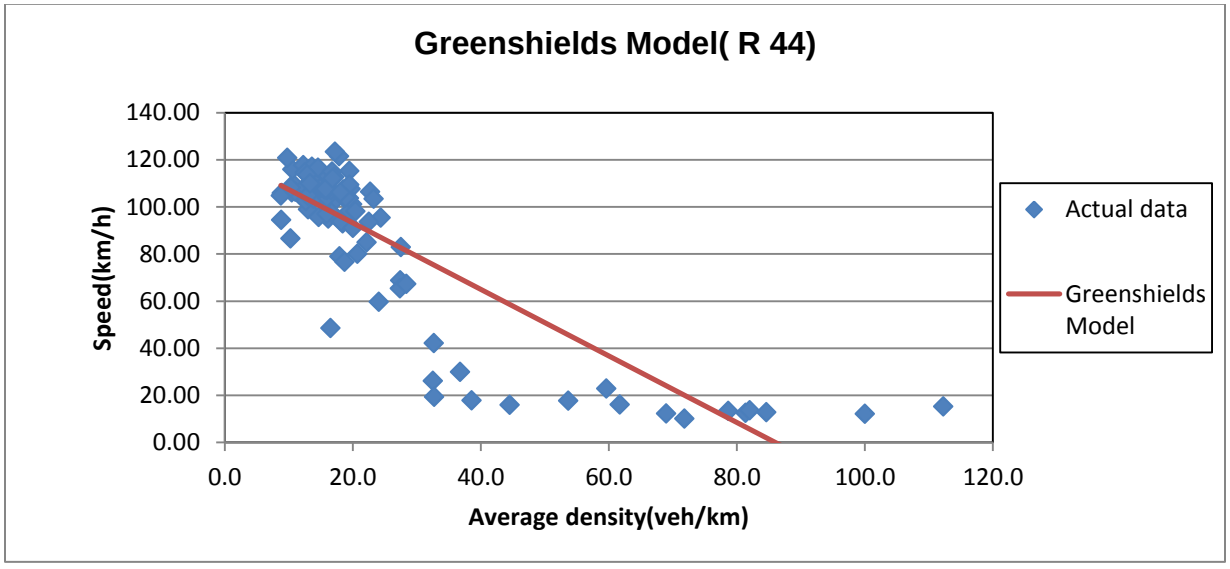

Figure 4. 1: Greenshields Model fitted to data taken on R44 in the south bound direction

The regression analysis performed on Section 2 provided the following values:

South bound direction: u_f= 121.27 km/h, k_j= 97.48 veh/km, R^2=0.740.

North bound direction: u_f= 122.94 km/h, k_j= 181.46 veh/km and R^2=0.059.

Figure 4.2 provides an illustration of the Greenshields curve fitted to the data taken on a section located on R304 in the south bound direction.

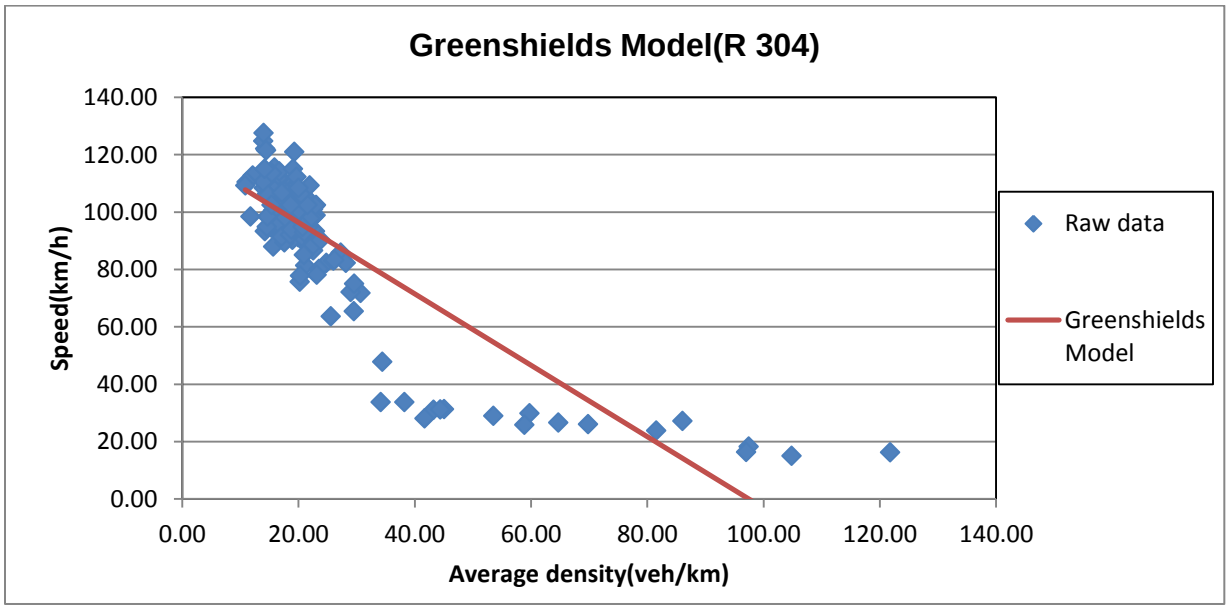

Figure 4. 2: Greenshields Model fitted to data taken on R304 in the south bound direction

From the results obtained through regression analysis, in all cases low values of R^2 were obtained more significantly in north bound direction. From the figures, it can be seen that although relatively good estimates of free-flow speed are achieved in most cases, certain areas of the data are not represented by this model and it underestimates the speeds at low densities. From the above considerations, it is more obvious that Greenshields Model failed to describe the whole range of traffic on both study sites. Therefore, this model is considered inadequate for describing traffic on rural two-lane highways under study.

- **The Greenberg Model**

The logarithmic model proposed by Greenberg is represented by Equation 2.16:

$$u = u_o \ln\left(\frac{k_j}{k}\right)$$

For this model, the known parameters are the exponents *m* and *l* which values are 0 and 1 respectively. The unknown parameters are optimum speed, u_o, and jam density, k_j. These parameters as well as the Coefficients of determination (R^2) relevant to each dataset are provided by regression analysis. Figure B-5 through B-8 in Appendix B are illustrations of curve fitting of available data using Greenberg Model.

On Section 1, the following values were obtained through regression analysis:

South bound direction: u_o= 52.72 km/h, k_j= 103 veh/km, R^2=0.786.

North bound direction: u_o= 19.68 km/h, k_j= 6168 veh/km and R^2=0.304.

Figure 4.3 provides an illustration of the Greenberg curve fitted to the data taken on section located on R44.

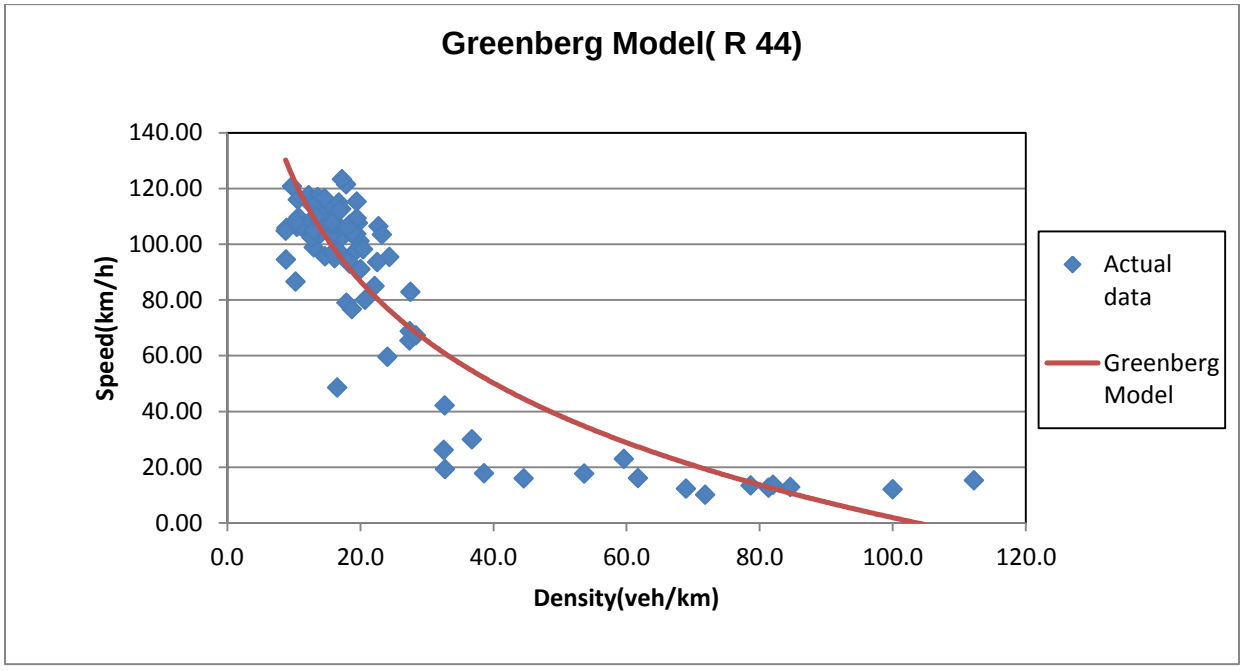

Figure 4. 3: Greenberg Model fitted to data taken on R44 in the south bound direction

On section 2, regression analysis provided the following values:

South bound direction: u_o= 53.45 km/h, k_j= 117.245 veh/km, R^2=0.842.

North bound direction: u_o= 7.85 km/h, k_j= 24461393 veh/km and R^2=0.0338.

Figure 4.4 provides an illustration the Greenberg curve fitted to the data taken on a section located on R304 in the south bound direction towards Stellenbosch.

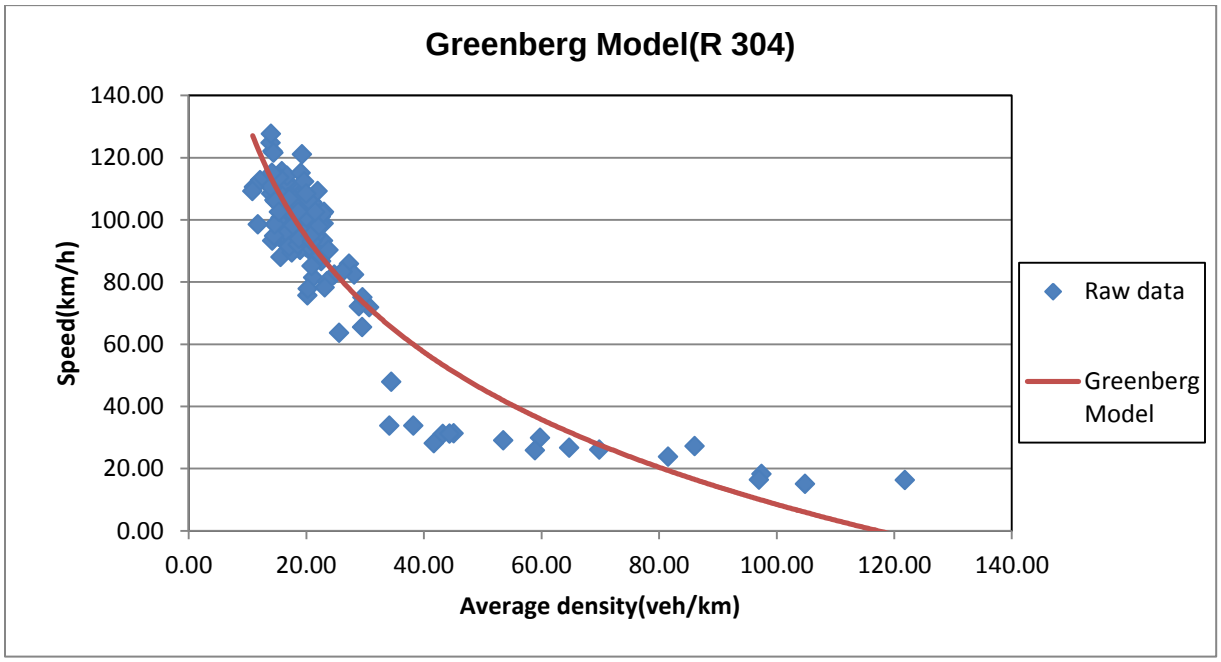

Figure 4. 4: Greenberg Model fitted to data taken on R304 in the south bound direction

It is clear that, despite relatively high value of R^2 compared to the values obtained for Greenshields Model, the model failed to describe the available data in low density area, since this model provides unrealistic speed for zero density. However, this model provided a relatively good description of high density regime for the traffic moving in south bound direction for both study sites.

An interesting observation can be made for the north bound direction (Figure B-6 and B-8 in Appendix B), in that this model yielded unreasonable values of jam density. This was expected since the free flow condition prevailed in that direction during the entire study periods and no sign of congested conditions were observed throughout that period.

Nevertheless, the values of coefficient of determination (R^2) in all cases remained relatively low more significantly in the north bound direction; this indicated that this model is not able to explain the total variability in the actual data for both directions. The Greenberg model is therefore found ineffective for representing the entire speed-density domain on these highways.

- **The Underwood Model**

The exponential model proposed by Underwood is represented by Equation 2.19:

$$u = u_f . e^{-k/k_o}$$

For this model, the exponents m and *l* are defined as known parameters with values of 1 and 2 respectively, while free-flow speed, u_f, and optimum density, k_o, are specified as unknown parameters. These parameters were obtained via regression analysis which provided also the corresponding coefficient of determination (R^2). Figures B-9 through B-12 in Appendix B are illustrations of curve fitting of available data using Underwood Model.

On Section 1, the following values were obtained:

South bound direction: u_f= 157.27km/h, k_o= 32 veh/km, R^2=0.824.

North bound direction: u_f= 142.56 km/h, k_o= 83 veh/km and R^2=0.391.

Figure 4.5 illustrates the Underwood curve fitted to the data taken on a section located on R44 in the south bound direction.

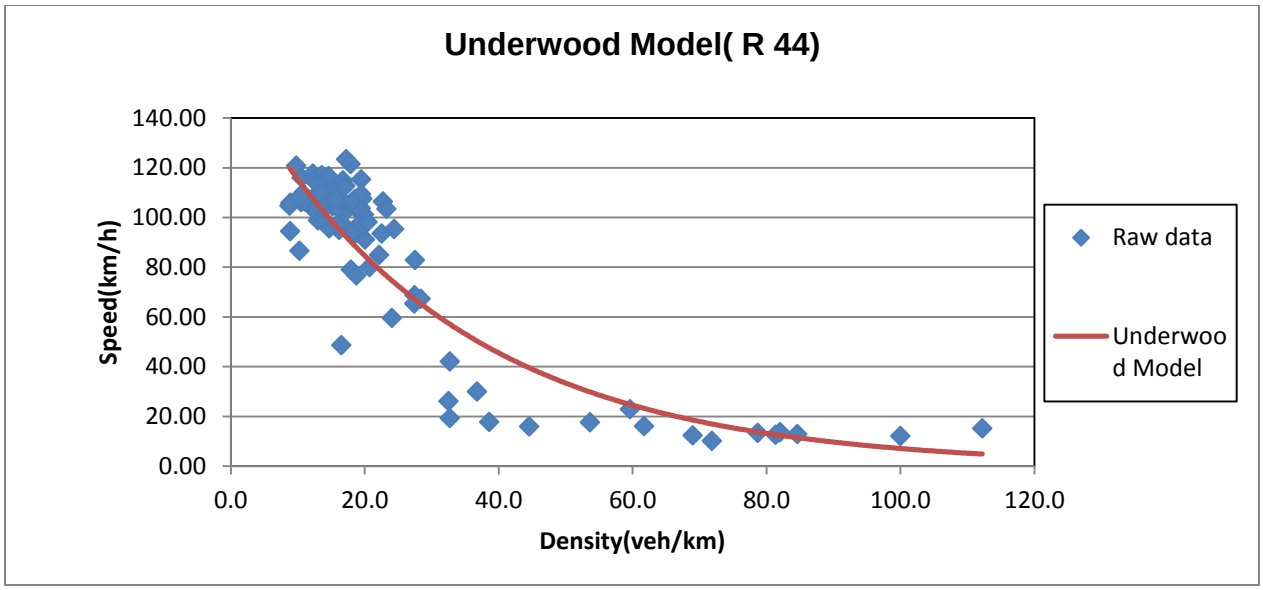

Figure 4. 5: Underwood model fitted to data taken on R 44 in the south bound direction

On Section 2, regression analysis provided the following values:

South bound direction: u_f= 150.3 km/h, k_o= 42 veh/km, R^2=0.861.

North bound direction: u_f= 123.68 km/h, k_o= 166.67 veh/km and R^2=0.0615.

Figure 4.6 provides an illustration the Underwood curve fitted to the data taken on a section located on R304 in the south bound direction towards Stellenbosch.

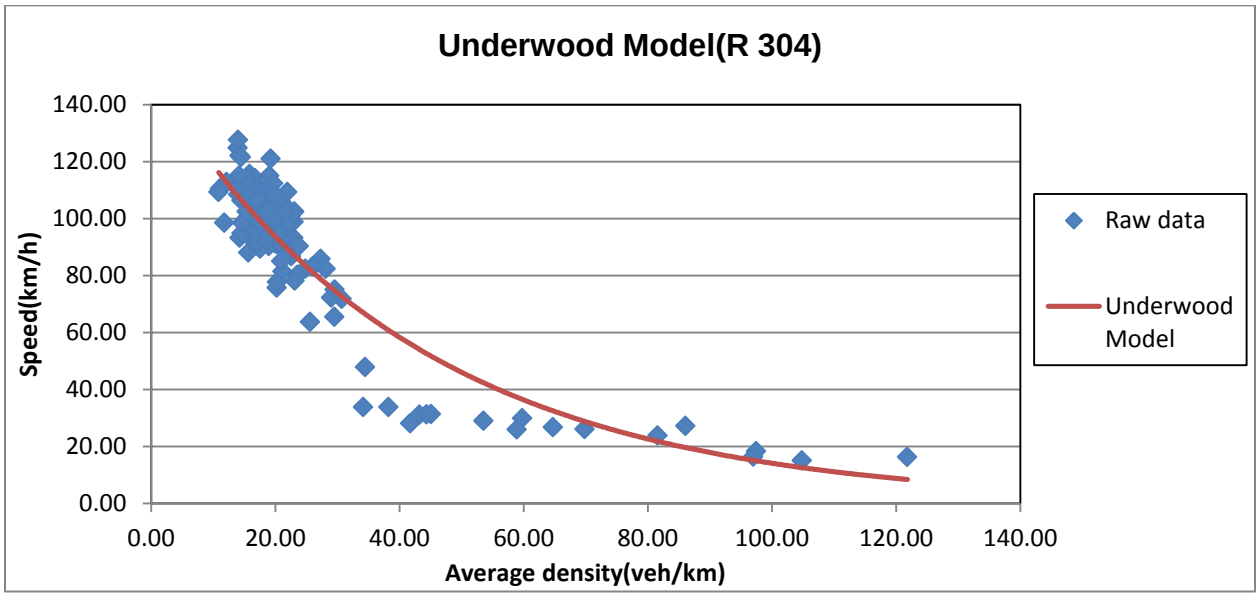

Figure 4. 6: Underwood model fitted to data taken on R 304 in the south bound direction towards Stellenbosch

This model provided a relatively better description of the high-density conditions for traffic moving in a south bound direction for both sections. High values of R^2 are also obtained in this direction.

A shortcoming of this model consists of the fact that it provided overestimated free-flow speed in all directions, and that it was unable to provide zero speed at high density. Therefore, this provides an indication that even if the model explained a significant part of the total variability in data, but it failed to satisfy all boundary conditions. From these observations, this model was found ineffective for description of the actual traffic data obtained on these highways.

- **The Drake, May and Schofer Model**

The Drake et al. model resulting in bell-shaped curve is represented by Equation 2.20:

$$u = u_f e^{\frac{-1}{2}(\frac{k}{k_o})^2}$$

In the Drake et al. model, the known parameters are the exponents *m* and *l* which values are respectively 1 and 3. Free-flow speed, u_f, and optimum density, k_o, were identified as unknown parameters. These variables as well as the coefficient of determination (R^2) for each data set were provided by regression analysis performed on available data. Figures B-13 through B-16 in Appendix B are illustrations of curve fitting of available data using the Drake et al. Model.

Regression analysis yielded the following values:

On Section 1:

South bound direction: u_f= 124.87km/h, k_o= 25.45 veh/km, R^2=0.860.

North bound direction: u_f= 130.15 km/h, k_o= 36.46 veh/km and R^2=0.402.

Figure 4.7 illustrates the Drake et al. curve fitted to the data taken on a section located on R 44 in the south bound direction.

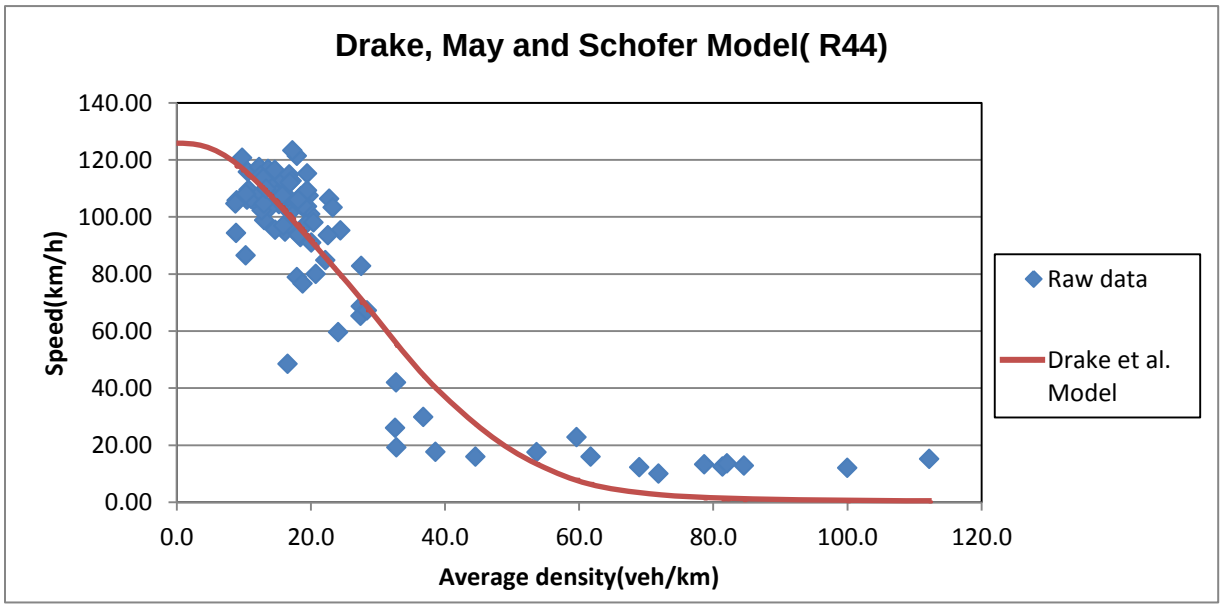

Figure 4. 7: The Drake et al. model fitted to data taken on R 44 in the south bound direction

On Section 2, regression analysis yielded the following values:

South bound direction: u_f= 124.19 km/h, k_o= 25.6 veh/km, R^2=0.874.

North bound direction: u_f= 119.04 km/h, k_o= 47.21 veh/km and R^2=0.087.

Figure 4.8 illustrates the Drake et al. curve fitted to the data taken on a section located on R 304 in the south bound direction.

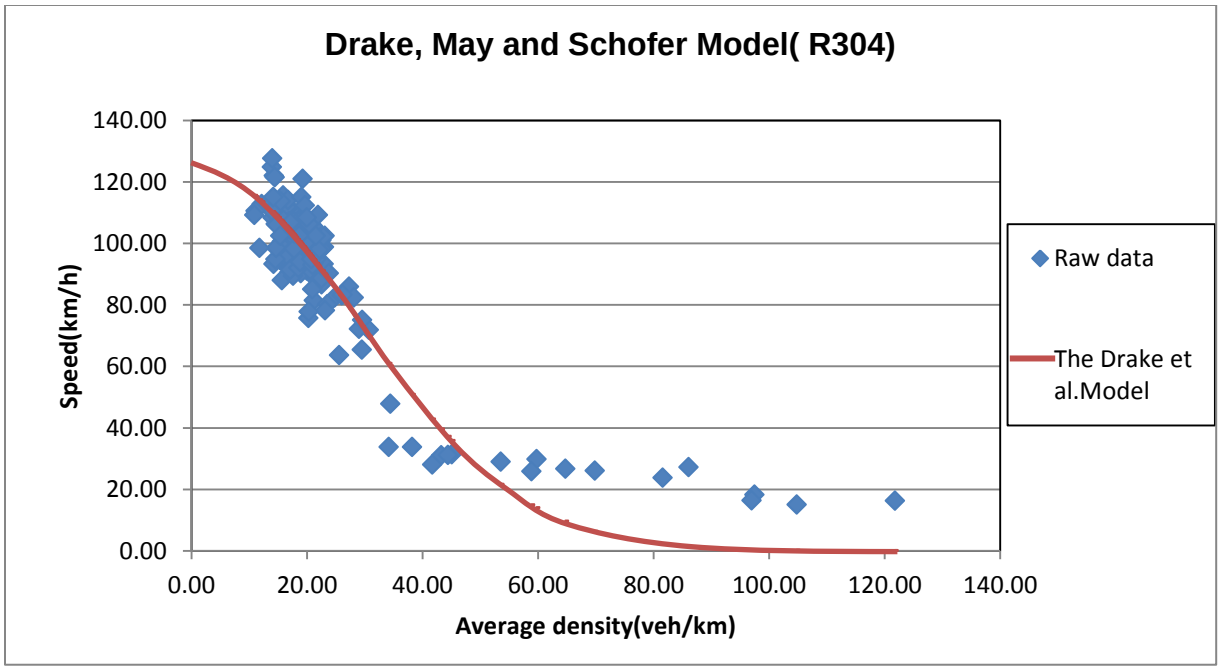

Figure 4. 8: The Drake et al. model fitted to data taken on R 304 in the south bound direction

This model seems to provide a better representation of low density traffic data, with an achievement of high values of R^2 in certain cases. However, the model failed to describe traffic under high density conditions since it underestimated the congested speed achievable in these conditions. Therefore, this model cannot be used to describe the entire speed-density data obtained from these sections.

- **The Drew Model**

The Drew model considered as generalized form of the Greenshields Model is represented by Equation 2.21:

$$u = u_f\left[1-\left(\frac{k}{k_j}\right)^{n+1/2}\right]$$

In Drew model, the known parameters are the exponents *m* and *l* which values are 0 and 2/3 respectively. Free-flow speed, u_f, jam density, k_j, and parameter n are identified as unknown parameters. Figures B-17 through B-20 in Appendix B are illustrations of curve fitting of available data using the Drew Model.

The regression analysis performed on available data yielded the following values:

On Section 1:

South bound direction: u_f= 173.4km/h, k_j= 88 veh/km, n=0, R^2=0.786.

North bound direction: u_f= 123.64 km/h, k_j= 36.46 veh/km, n=6.988 and R^2=0.465.

Figure 4.9 depicts the Drew model fitted to the data taken on a section located on R 304 in the south bound direction.

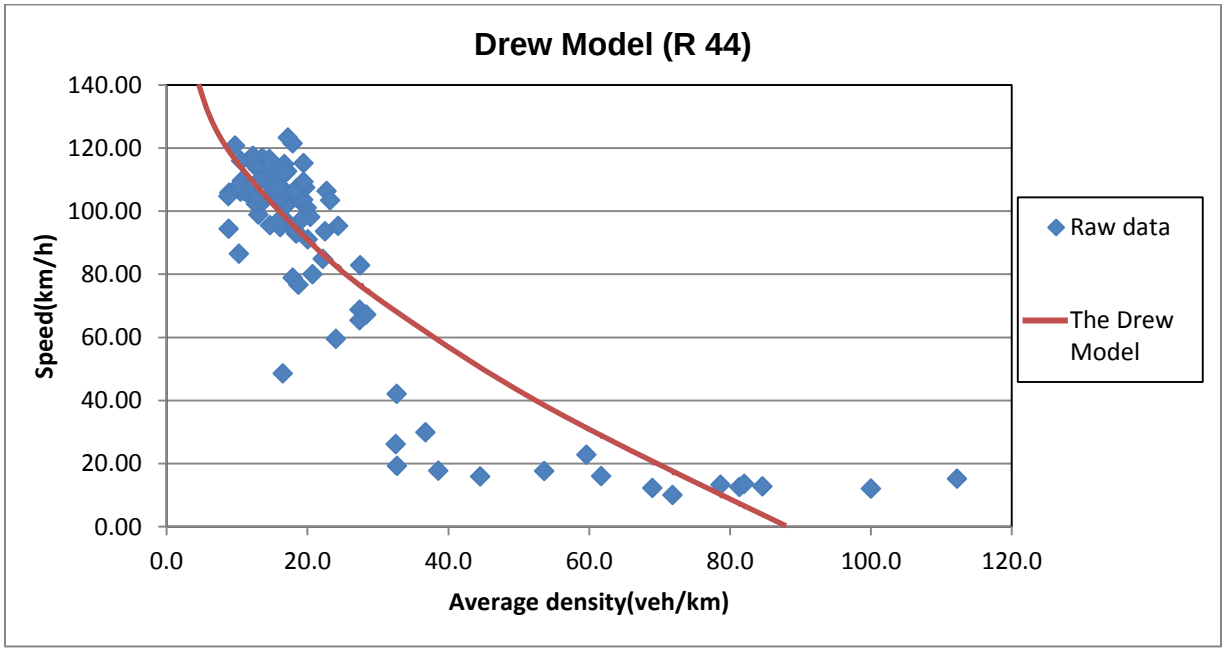

Figure 4. 9: The Drew model fitted to data taken on R 44 in the south bound direction towards Stellenbosch

On Section 2, regression analysis yielded the following values:

South bound direction: u_f= 173.38 km/h, k_j= 100.13 veh/km, n=0, R^2=0.813.

North bound direction: u_f= 114 km/h, k_j= 28.66, n= 17.18 veh/km and R^2=0.173.

Figure 4.10 depicts the Drew model fitted to the data taken on a section located on R 304 in the south bound direction.

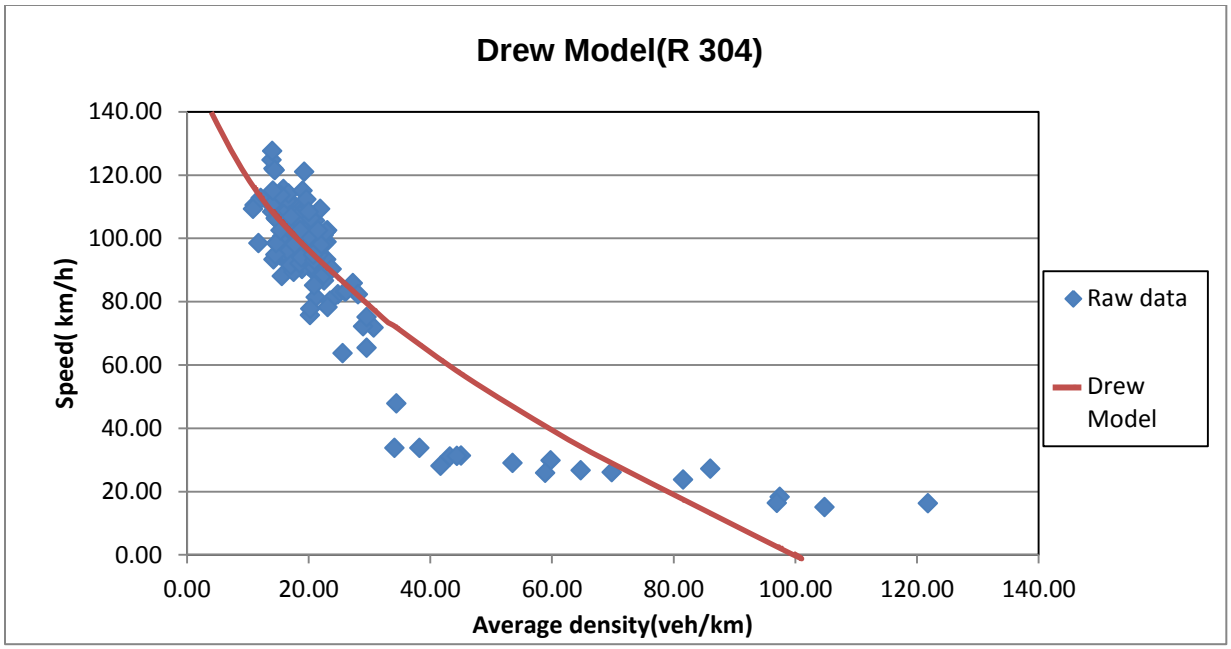

Figure 4. 10: The Drew model fitted to data taken on R 304 in the south bound direction towards Stellenbosch

The Drew model fitted on available data provided overestimated free-flow speed in certain cases and failed to describe traffic data in high density conditions. A closer look at Figures 4.9 and 4.10 also shows that there are certain areas of the data which are not sufficiently explained by the model. Despite high value of R^2 obtained in some cases, this model is qualified ineffective to use for describing traffic on these highway sections.

- **The multi-regime Model**

All the steady-state flow equations developed by May and Keller presented in matrix of *m* and *l* values (Table 2.1) were used to select which equations that provide a best fit of the available data. In each case, an equation which presented high value of R^2 and reasonable parameters which could result in a suitable curve was selected to be used in a further stage. As it was the case with the previous models, the unknown parameters were first identified and through regression analysis their values were determined.

In contrast to the previous models at the exception of the Drew model, some equations from the matrix presented more than 2 unknown parameters that needed to be

determined. Trial and error method of guessing initial values for parameters k_j, u_f, k_o and c was used to solve these equations through the use of Excel solver non-linear regression analysis. Figures B-21 through B-24 in Appendix B are illustrations of curve fitting of available data using the multi-regime Model.

On Section 1:

South bound direction

The data are represented by equation: $\ln\left(\frac{U_f}{U}\right) = c.K^{l-1}$ with *m*=1 and *l* >1

Unknown parameters: *l*=2.057, m=1, c=2.9483E-02, u_f= 124.9 km/h, R^2=0.818.

North bound direction:

The data are represented by equation: $U^{1-m} = U_f^{1-m} + c.K^{l-1}$ with *m* >1and *l*>1

Unknown parameters: *l*=3.523, m=1.1715, c=2.16.E-06, u_f=120 km/h and R^2=0.432.

Figure 4.11 gives an illustration of the multi-regime model fitted to the data taken on a section located on R 44 in the south bound direction.

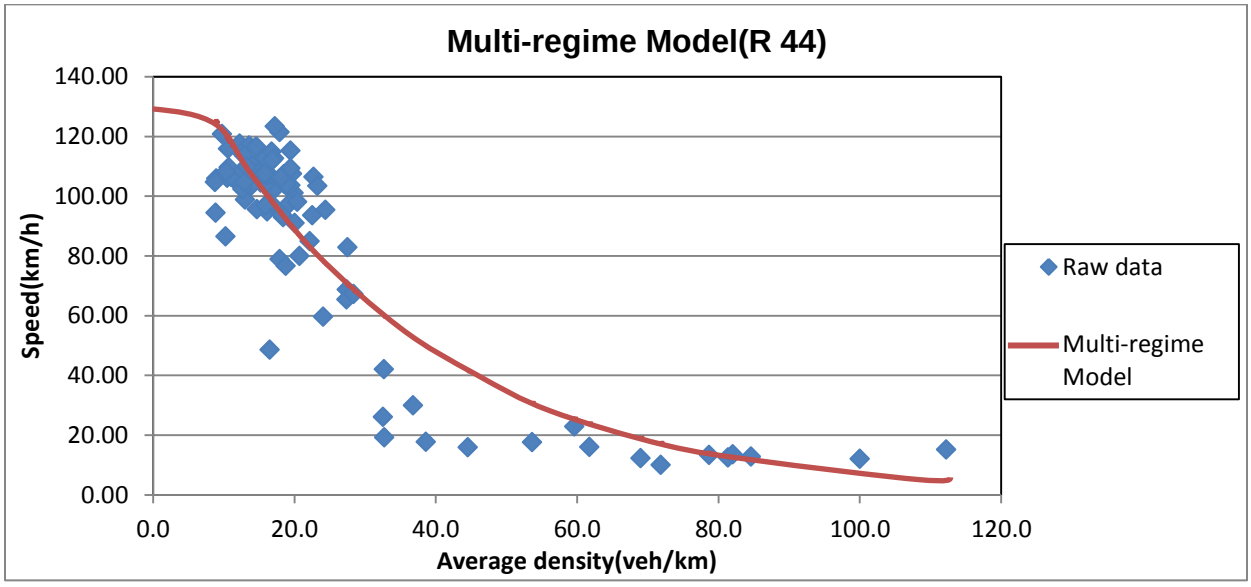

Figure 4. 11: The multi-regime model fitted to data taken on R 44 in the south bound direction towards Stellenbosch

On Section 2:

South bound direction:

The data are represented by equation: $U^{1-m} = U_f^{1-m} + c.K^{l-1}$ with m >1and l>1

Unknown parameters: l=2.99999, m=2, c=5.49.E-06, u_f= 120km/h and R^2=0.867.

North bound direction:

The data are represented by equation: $\ln\left(\frac{U_f}{U}\right) = c.K^{l-1}$ with m=1 and l >1

Unknown parameters: l=3.9568, c=1.24.E-05, u_f= 118.37 km/h and R^2=0.110.

Figure 4.12 gives an illustration of the multi-regime model fitted to the data taken on a section located on R 304 in the south bound direction.

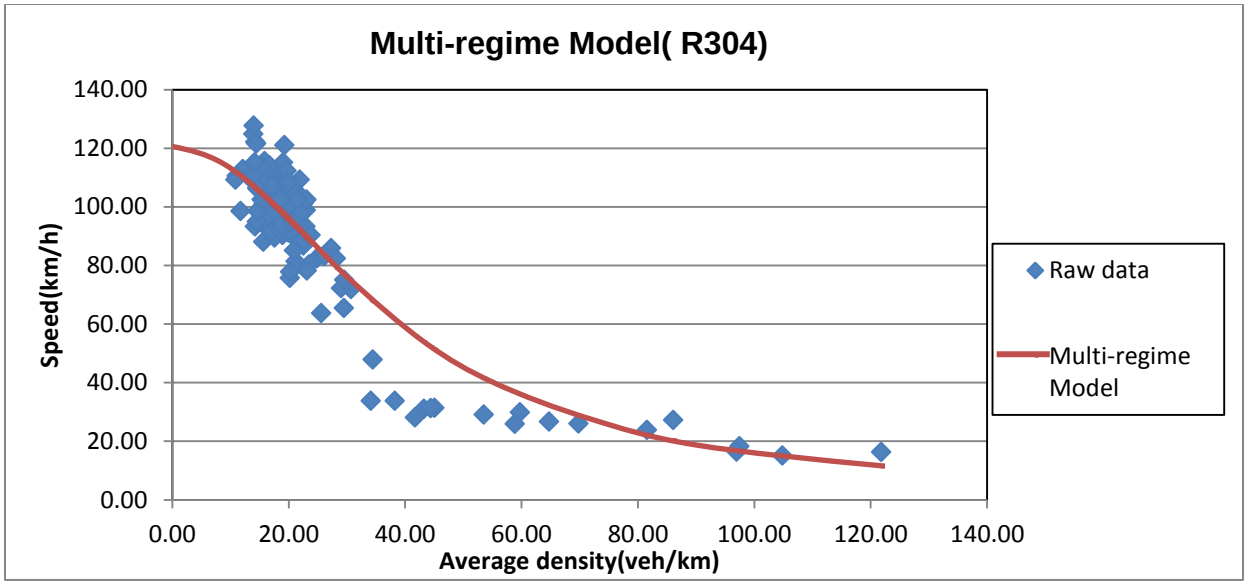

Figure 4. 12: The multi-regime model fitted to data taken on R 304 in the south bound direction towards Stellenbosch

This model provided relatively good representation of high density data. High values of R^2 were also achieved with the use of this model. This provides an indication that the model explains at a higher degree a significant number of variability in data. However the drawback of this model resides on the fact that, some areas of the data are not

sufficiently represented by the model and that low density data are poorly described in certain cases.

Although the coefficient of determination was found to be quite good in some cases and that this model provided a reasonable free flow speed, the multi-regime model failed to represent the entire speed-density curve. With the fact that this model did not satisfy the boundary condition for jammed density where corresponding speed must be zero, it may be concluded that this study shows a good agreement with observation made which indicated that some of the equations of multi-regime models do not result in zero speed for a jammed density, and consequently cannot be used to represent the whole spectrum of densities.

- **Composite Model**

The use of the composite model consists of representation of the traffic domain by use of different models, where each model defines a specific area (traffic regime) of the traffic data. When Eddie proposed the use of composite Model, he suggested the use of Underwood model and Greenberg model for uncongested and congested parts of the curve respectively.

In both study sections, it was observed that the traffic in the north bound direction consists of free flow traffic only, while south bound traffic consists of two regimes of traffic. Therefore, the composite model was applied to south bound traffic data where the Drake et al. model was selected to describe the uncongested regime, while high density regime (congested-flow regime) was represented by Greenberg model on both sections.

As has been mentioned previously, the use of the composite model requires a proper way of identification of the exact point of the breakdown between different regimes. In case of this study, the density corresponding to the capacity observed during uncongested period defines the point of separation between two regimes identified in this study. This was thought because after the capacity is reached, any increase of density marks the beginning of congested condition.

Through the regression analysis, unknown parameters of the composite model were obtained as well as overall coefficient of determination (R^2) as shown as follows:

Section 1: R 44 near Stellenbosch Town

Free-flow regime: $u = u_f e^{\frac{-1}{2}(\frac{k}{k_o})^2}$ (m=1, l=3)

Unknown parameters: u_f = 124.87km/h, k_o = 25.45veh/km

Congested flow regime: Greenberg Model: $u = u_f ln\left(\frac{k_j}{k}\right)$

Unknown parameters: u_o = 35.16 km/h, k_j=110.4 veh/km

Overall coefficient of determination: R^2= 0.876

Figure 4.13 provides an illustration of the composite model fitted to the data taken on a section located on R 44 in the south bound direction.

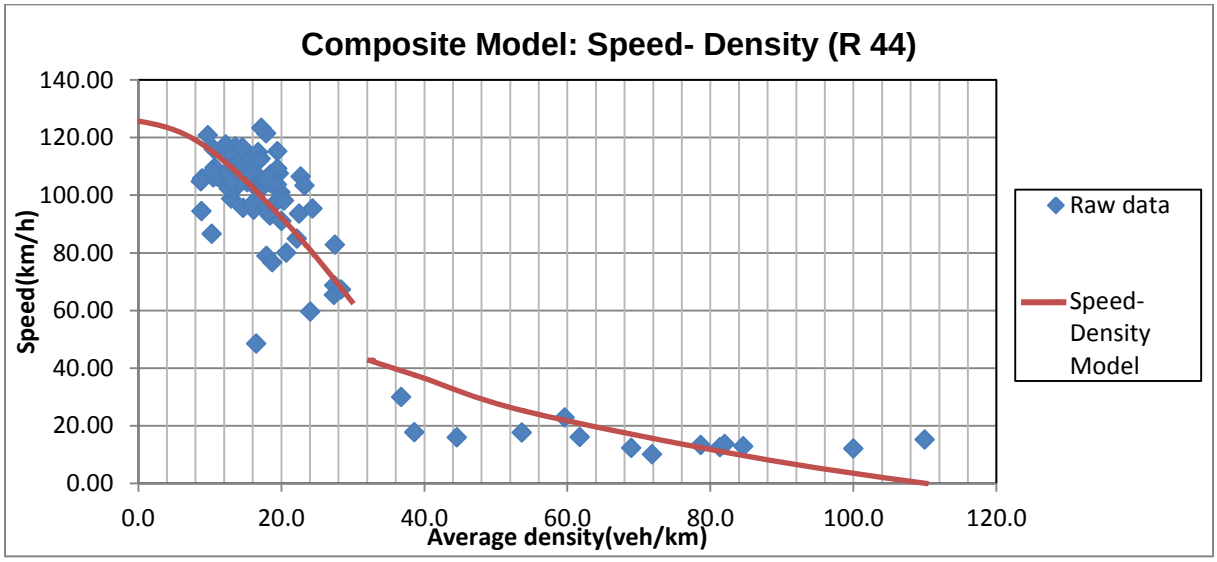

Figure 4. 13: The composite model fitted to data taken on R 44 in the south bound direction

With relatively high value of overall R^2 (0.876) achieved when fitting data using the composite model compared to the previously tested models, and a quite good representation of both low and high density traffic conditions in the south bound direction where the data are available for all traffic conditions. It is obvious that the

composite model is adequate for describing traffic flow in this section. Figure 4.14 provides an illustration of the composite model describing speed-density relationship in the south bound direction of Section 1.

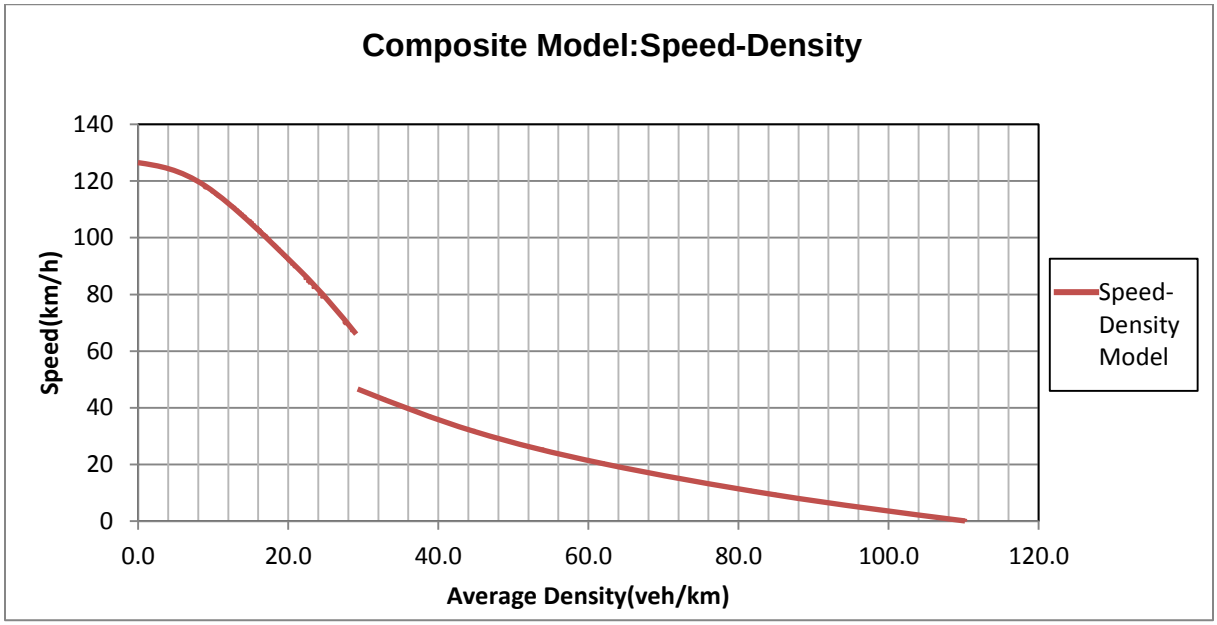

Figure 4. 14: Speed-Density relationship for traffic in the south bound direction on Section 1

From Figure 4.14, it can be seen that there is a clear discontinuity in data. This gives an indication that on this section, traffic is composed of two regimes. A difference in speed of about 20km/h was found between the minimum speed achieved under uncongested regime and maximum speed during congested condition.

As mentioned earlier, once the adequate speed-density relationships are established, the composite model in case of this section, the use of the steady-state equation of traffic (Equation 2.1) allowed us to establish the corresponding flow-density and speed-flow relationships. Figure 4.15 depicts the flow-density relationship derived from the composite model for Section 1.

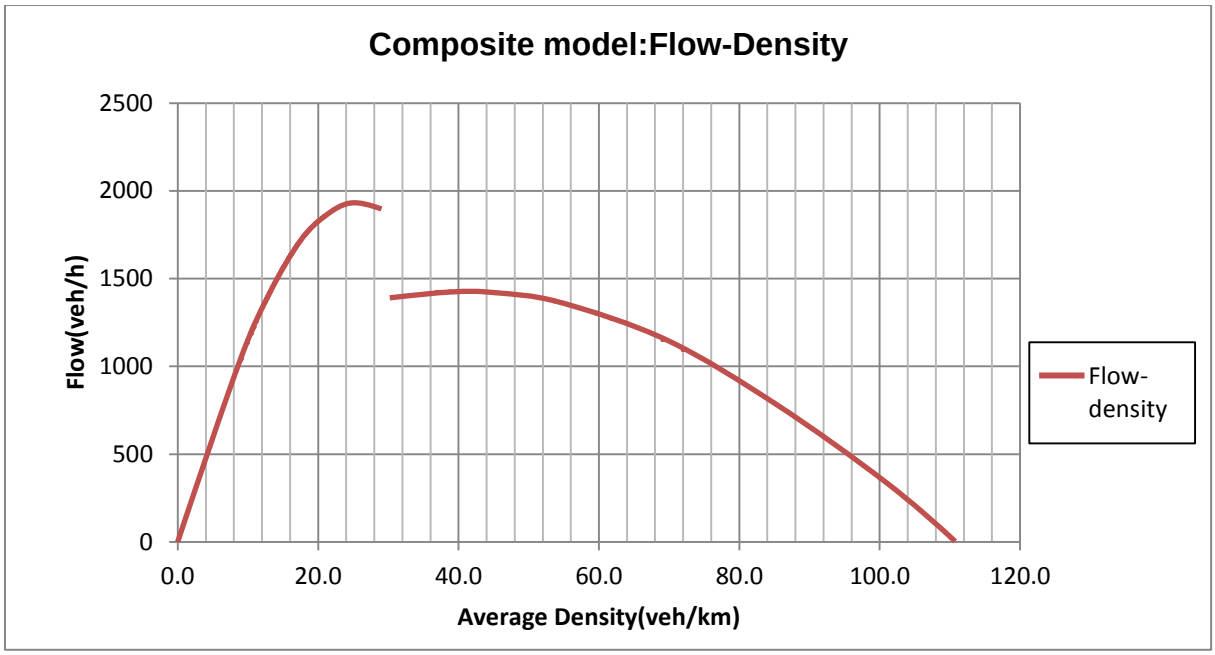

Figure 4. 15: Flow-Density relationship for traffic in the south bound direction on Section 1

From Figure 4.15, it can be observed that flow increases with increase in density starting from the origin of the curve up to the point where the maximum flow achievable on this section is reached. From that point onwards, further increase of density results in sudden drop of flow up to the point where flow becomes zero. This point corresponds to the condition where vehicles make a complete stop due to high interaction between them. The density in this condition is called jam density. The optimum density observed in this section is 25.45veh/km.

Figure 4.16 depicts the speed-flow relationship derived from the composite model for Section 1.

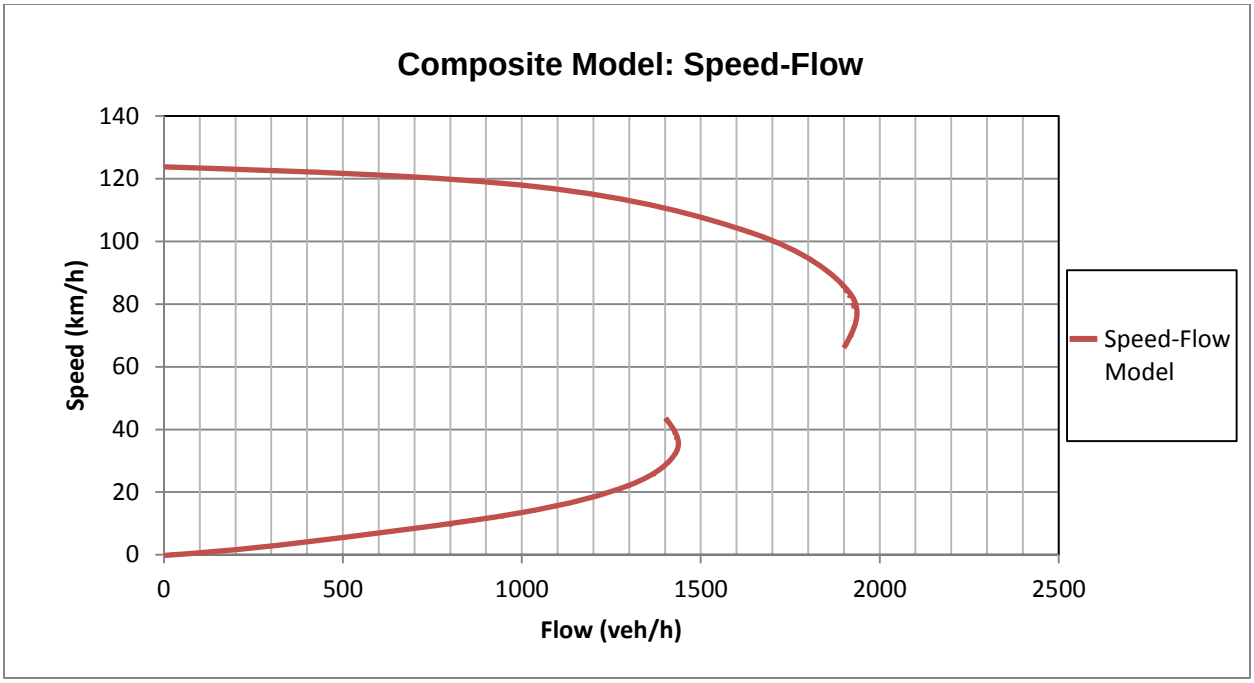

Figure 4. 16: Speed-Flow relationship for traffic in the south bound direction on Section 1

From Figure 4.16, it can be observed that the curve presents two points of zero flow, one at the maximum speed (124.87km/h) and another at the intersection of speed and flow axis. One point corresponds to the point of free-flow speed, where there is no vehicle on the section of the road. In this condition, the speed is theoretical and corresponds to the maximum achievable speed when vehicles travel without hindrance caused by other vehicles. The second point of zero flow corresponds to zero speed in congested conditions where vehicles are forced to stop due to restriction of the movement resulting from high interaction between vehicles.

There is one more point worth mentioning, and that is the existence of two road capacities, one associated to uncongested regime and another obtained in the congested regime. The difference between congested and uncongested capacities was found to be 500veh/h for this section.

Section 2: R 304 near Stellenbosch Town

Free-flow regime: $u = u_f e^{\frac{-1}{2}(\frac{k}{k_o})^2}$ (m=1, l=3)

Unknown parameters: u_f = 124.19km/h, k_o = 28.60veh/km

Congested flow regime: Greenberg Model: $u = u_f ln\left(\frac{k_j}{k}\right)$

Unknown parameters: u_f= 29.32 km/h, k_j=165 veh/km

Overall coefficient of determination: R^2= 0.898

Figure 4.17 provides an illustration the Composite model fitted to the data taken on a section located on R 304 in the south bound direction.

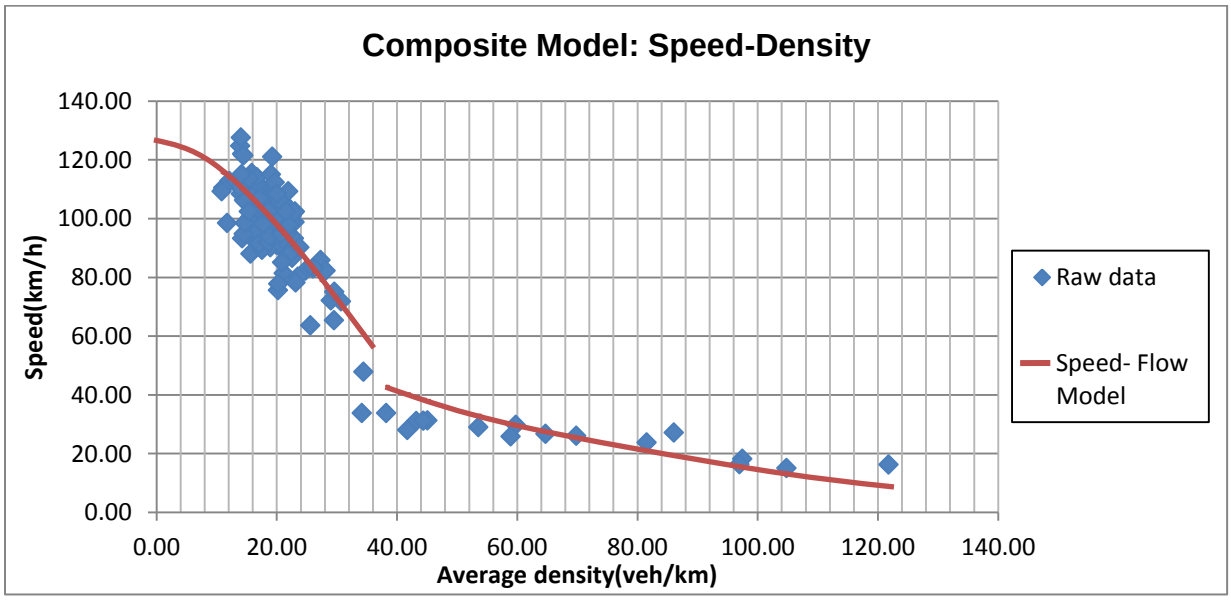

Figure 4. 17: The composite model fitted to data taken on R 304 in the south bound direction

An overall R^2 of 0.898 is obtained when fitting available data using the composite model. This model also provided a good representation of both free flow and congested traffic conditions in the south bound direction. Figure 4.18 provides an illustration of the composite model used to describe speed-density relationship in the south bound direction of Section 2.

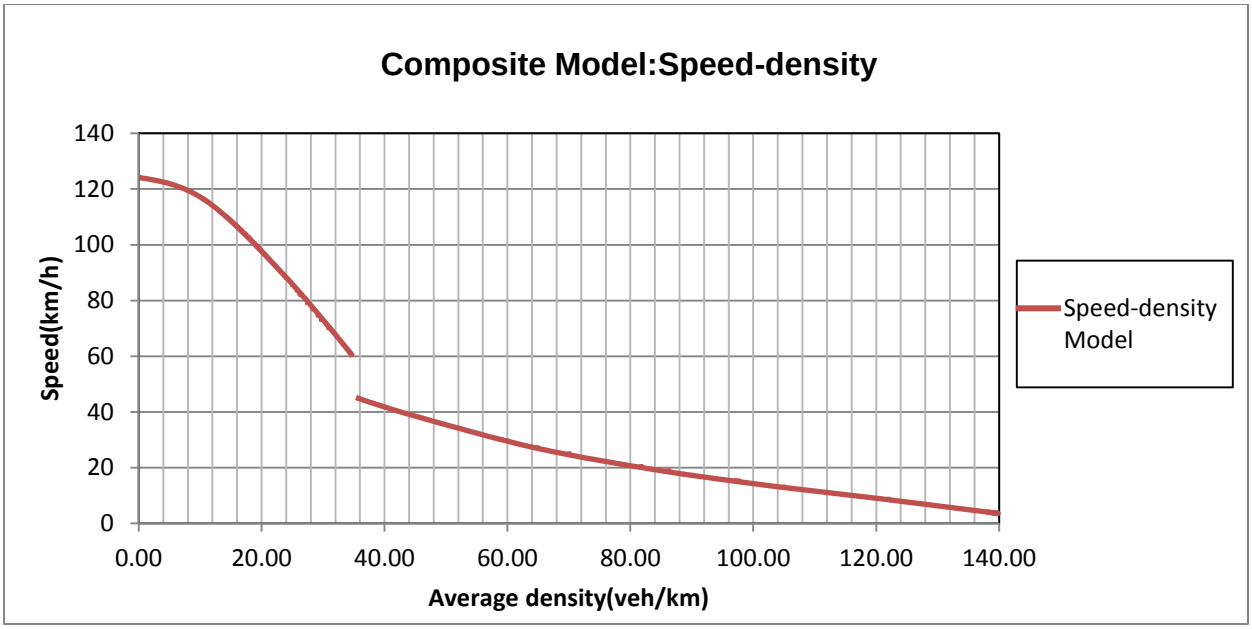

Figure 4. 18: Speed-Density relationship for traffic in the south bound direction on Section 2

In this section, a drop in speed of about 20 km/h was found between the uncongested and congested regimes as it was observed in Section 1. Also in this section, jam-density is estimated about 165veh/km and a free flow speed of 124.19km/h. The free flow speed obtained in this section is likely the same as the value obtained for Section 1. Figure 4.19 depicts the flow-density relationship derived from the composite model for Section 2.

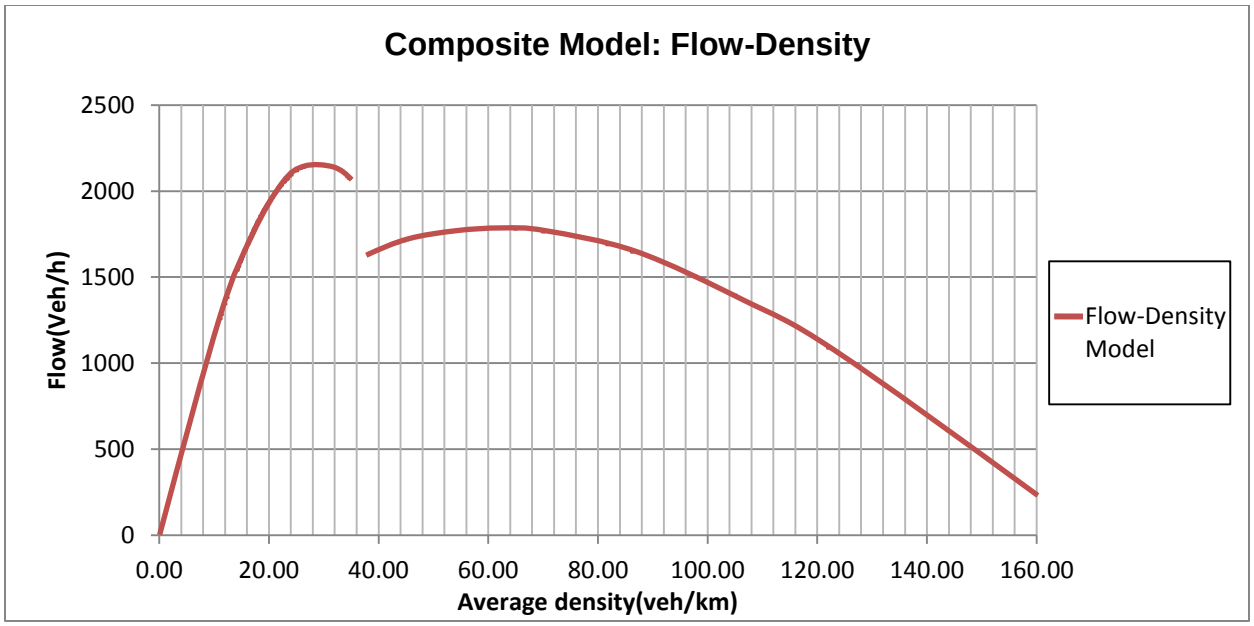

Figure 4. 19: Flow-Density relationship for traffic in the south bound direction on section 2

From Figure 4.19, a maximum flow rate of 2154veh/h is observed in the uncongested conditions while a value of 1780 veh/h is observed in congested conditions. The optimum density obtained in this section (28.6veh/km) is slightly higher than that observed in Section 1. Figure 4.20 depicts the speed-flow relationship derived from the composite model for Section 2.

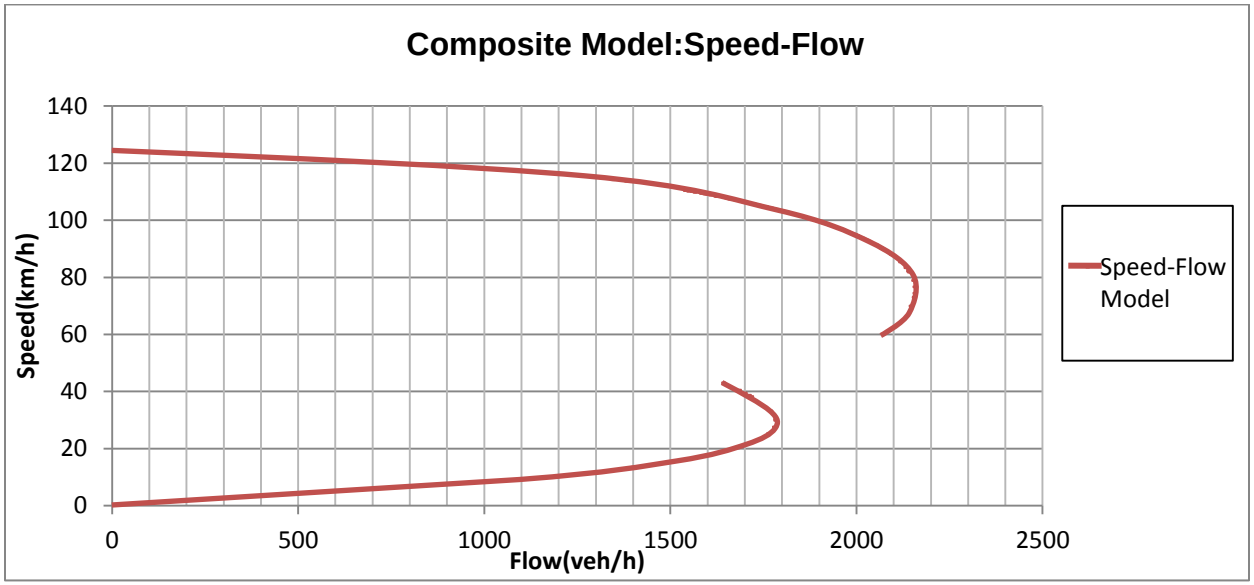

Figure 4. 20: Speed-Flow relationship for traffic in the south bound direction on Section 2

From Figure 4.20, it is possible to observe that the slope of the curve is less steep at low flow rate (somehow considered as linear curve) and start to be very steep when the flow is near to the capacity of the section. The difference of about 400veh/h was found between maximum flows achieved during congested and uncongested conditions in this section. Again, this difference was found to be slightly lower than the difference observed in Section 1.

4.3.2 Relationships based on 5-minute time intervals

Several researchers have shown that the two-lane highway analysis based on one-min time intervals may result in an overestimation of the speed-flow relationships and consequently derived road capacities of these highways. In this study, speed-flow relationships were investigated using data averaged over 5-min time intervals in order to verify if this observation is applicable to available data. In this analysis, data were tested using the same models used in analysis done previously in order to find a suitable model which can provide a best fit. The results of regression analysis for each model are summarised in Tables A-11 and A-12 in Appendix A.

- **Greenshields Model**

Regression analysis was used to determine the free-flow speed, u_f, and jam density, k_j, identified as unknown parameters. Figures C-1 through C-4 in Appendix C are illustrations of curve fitting of available 5-min time slices data using the Greenshields model on both study sites.

On Section 1, the regression analysis gave the following values:

South bound direction: u_f= 135.68 km/h, k_j= 63.55 veh/km, R^2=0.693.

North bound direction: u_f= 157.78 km/h, k_j= 77.13veh/km and R^2=0.586.

On Section 2, the regression analysis gave the following values:

South bound direction: u_f= 131.88km/h, k_j= 72.87 veh/km, R^2=0.874.

North bound direction: u_f= 142.2km/h, k_j= 76.61 veh/km and R^2=0.201.

Figure 4.21 provides an illustration of the Greenshields model fitted to the average 5-min time intervals data taken on R 44 in the south bound direction.

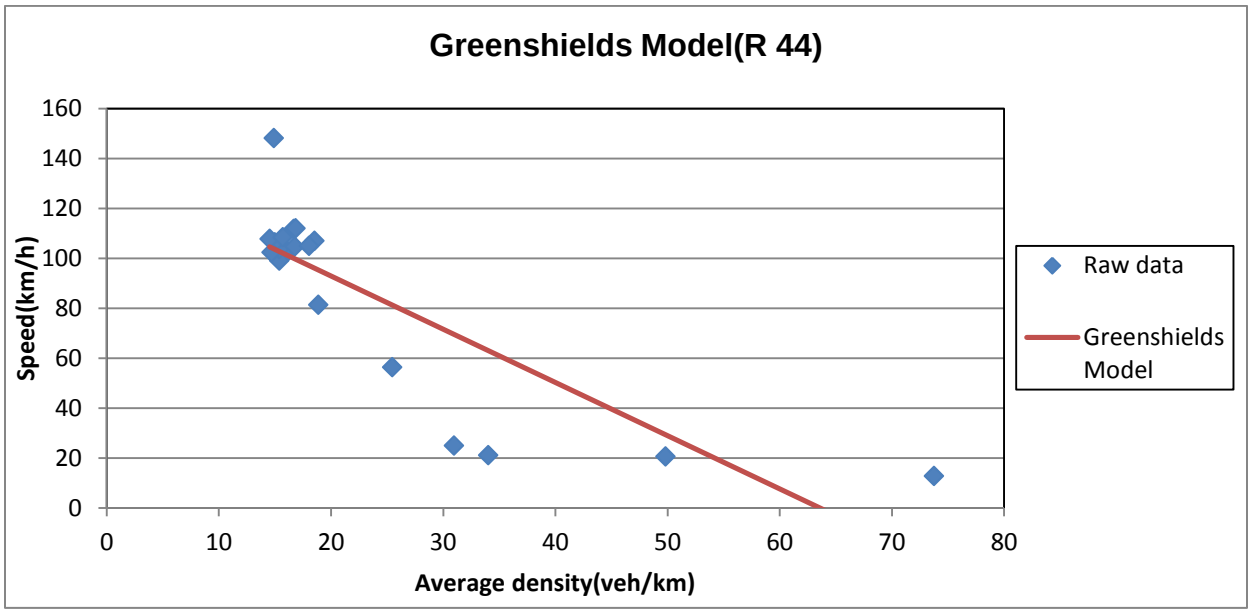

Figure 4. 21: The Greenshields model fitted to the 5-min speed-density data taken on Section 1 in the south bound direction

This model provided quite good estimates of free-flow speed in all cases. However, the model showed a weakness in describing some parts of the data as shown in Figure 4.21 and it failed to describe the data corresponding to congested conditions. Although a quite better estimation of free flow speed, this model provided low values of R^2. Again, as it was the case in analysis of one-min data, this model was found ineffective for representing the available data.

- The Greenberg Model

In Greenberg model, optimum speed,u_o, and jam density,k_j, are identified as unknown parameters. These parameters were determined through regression analysis. Figure C-5 through C-8 in Appendix C are illustrations of curve fitting of 5-min time intervals data using the Greenberg model.

On Section 1, the regression analysis gave the following values:

South bound direction: u_o= 77.5 km/h,k_j= 62.25 veh/km, R^2=0.831.

North bound direction: u_o= 35.3 km/h,k_j= 634.22 veh/km and R^2=0.587.

On Section 2, the regression analysis gave the following values:

South bound direction: u_o= 65.27km/h,k_j= 85.48 veh/km, R^2=0.922.

North bound direction: u_o= 31.49km/h,k_j= 586veh/km and R^2=0.194.

Figure 4.22 provides an illustration the Greenberg model fitted to the average 5-min speed-density data taken on R 44 in the south bound direction.

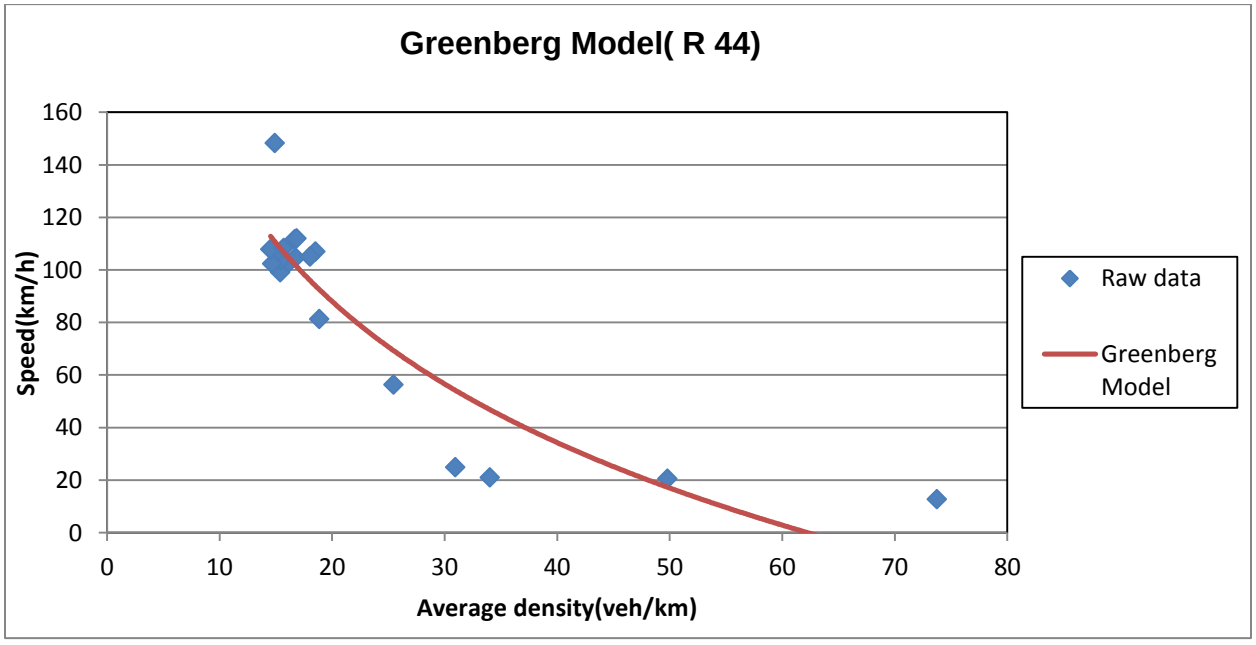

Figure 4. 22: The Greenberg model fitted to the 5-min speed-density data taken on Section 1 in the south bound direction

This model provided a quite good representation of available data with relatively high value of R^2 in most cases. But, this model failed to provide realistic values of free flow speed in all cases and jam densities more significantly in the north bound direction. This model was therefore judged inadequate for describing the actual data.

- **The Underwood Model**

Regression analysis was used to determine free flow speed, u_f, and optimum density, k_o, identified as unknown parameters in this model. Figure C-9 through C-12 in Appendix C are illustrations of curve fitting of 5-min time intervals data using the Underwood model.

On Section 1, the regression analysis gave the following values:

South bound direction: u_f= 199.04 km/h, k_o= 22.72 veh/km, R^2=0.832.

North bound direction: u_f= 163.2 km/h, k_o= 58.82 veh/km and R^2=0.598.

On Section 2, the regression analysis gave the following values:

South bound direction: u_f= 185.01km/h, k_o= 29.41 veh/km, R^2=0.941.

North bound direction: u_f= 147.17km/h, k_o= 58.82 veh/km and R^2=0.202.

Figure 4.23 provides an illustration of the Underwood model fitted to the average 5-min speed-density data taken on R 44 in the south bound direction.

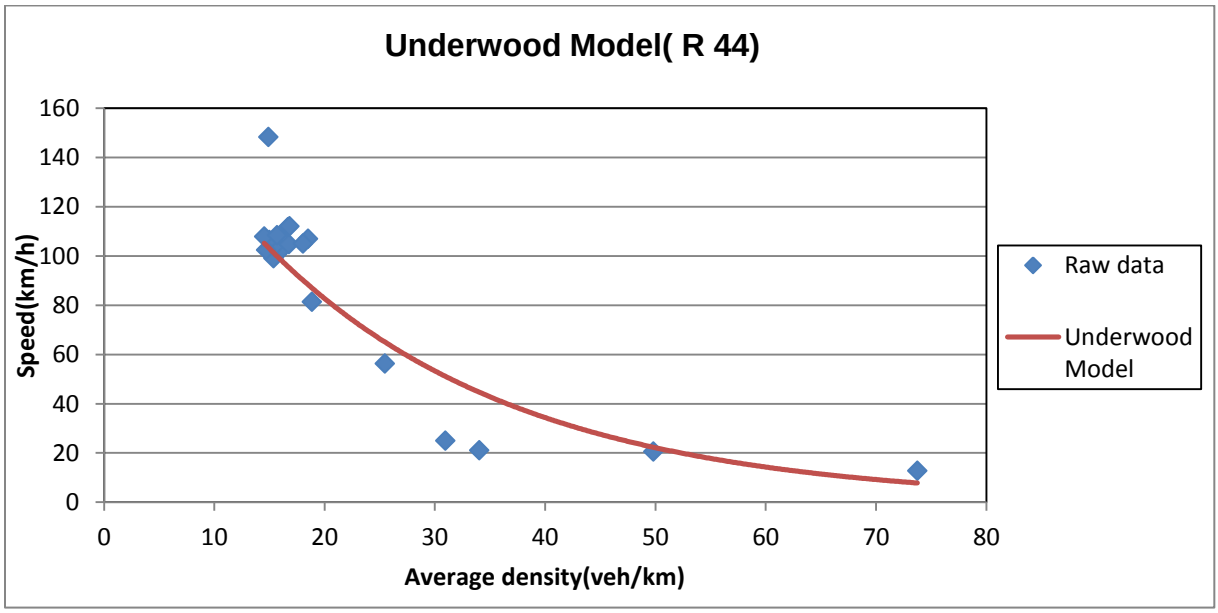

Figure 4. 23: The Underwood model fitted to the 5-min speed-density data taken on Section 1 in the south bound direction

High values of R^2 are obtained in most cases with the use of the Underwood Model. This shows that the model explains significant parts of the variability in data. However, this model was judged inefficient for representation of the data due to its inability to give reasonable free flow speed.

- **The Drake et al. Model**

In the Drake et al. Model, free-flow speed, u_f, and optimum density, k_o, are identified as unknown parameters like in the Underwood Model. These parameters were estimated through regression analysis. Figure C-13 through C-16 in Appendix C are illustrations of curve fitting of 5-min time intervals data using the Drake et al. model.

On Section 1, the regression analysis gave the following values:

South bound direction: u_f= 165 km/h, k_o= 17.33 veh/km, R^2=0.905.

North bound direction: u_f= 141.5 km/h, k_o= 32.28 veh/km and R^2=0.581.

On Section 2, the regression analysis gave the following values:

South bound direction: u_f= 125.12 km/h, k_o= 27.59 veh/km, R^2=0.928.

North bound direction: u_f= 127.57 km/h, k_o= 31.95 veh/km and R^2=0.206.

Figure 4.24 provides an illustration of the Drake et al. model fitted to the average 5-min speed-density data taken on R 44 in the south bound direction.

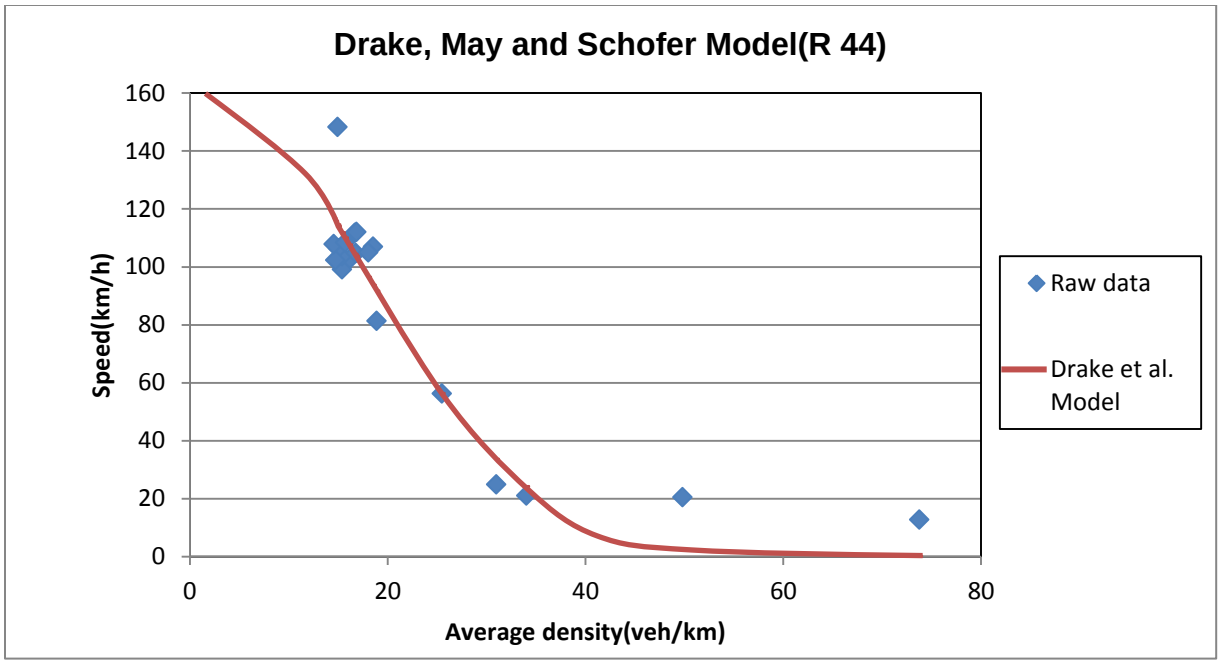

Figure 4. 24: The Drake et al. model fitted to the 5-min speed-density data taken on Section 1 in the south bound direction

The Drake et al. model provided high values of R^2 in most cases. With the use of this model, a reasonable free-flow speed is obtained in Section 2 while an overestimation of free-flow speed is observed in Section 1. However, this model slightly underestimates the speed obtainable in congested conditions in all cases.

- **The Drew model**

In the Drew model, free-flow speed, u_f, jam density, k_o, and parameter n are identified as unknown parameters. These parameters were estimated through regression analysis. Figure C-13 through C-16 in Appendix C are illustrations of curve fitting of 5-min time intervals data using the Drew model.

On Section 1, the regression analysis gave the following values:

South bound direction: u_f= 210.36 km/h, k_o= 62.12 veh/km, n=0, R^2=0.771.

North bound direction: u_f= 141.5 km/h, k_o= 52.24 veh/km, n=1.31and R^2=0.579.

On section 2, the regression analysis gave the following values:

South bound direction: u_f= 195.15km/h, k_o= 76.56 veh/km, n=0, R^2=0.906.

North bound direction: u_f= 114.94km/h, k_o= 27.48 veh/km, n=6.7 and R^2=0.222.

Figure 4.25 provides an illustration of the Drew model fitted to the average 5-min speed-density data taken on R 44 in the south bound direction.

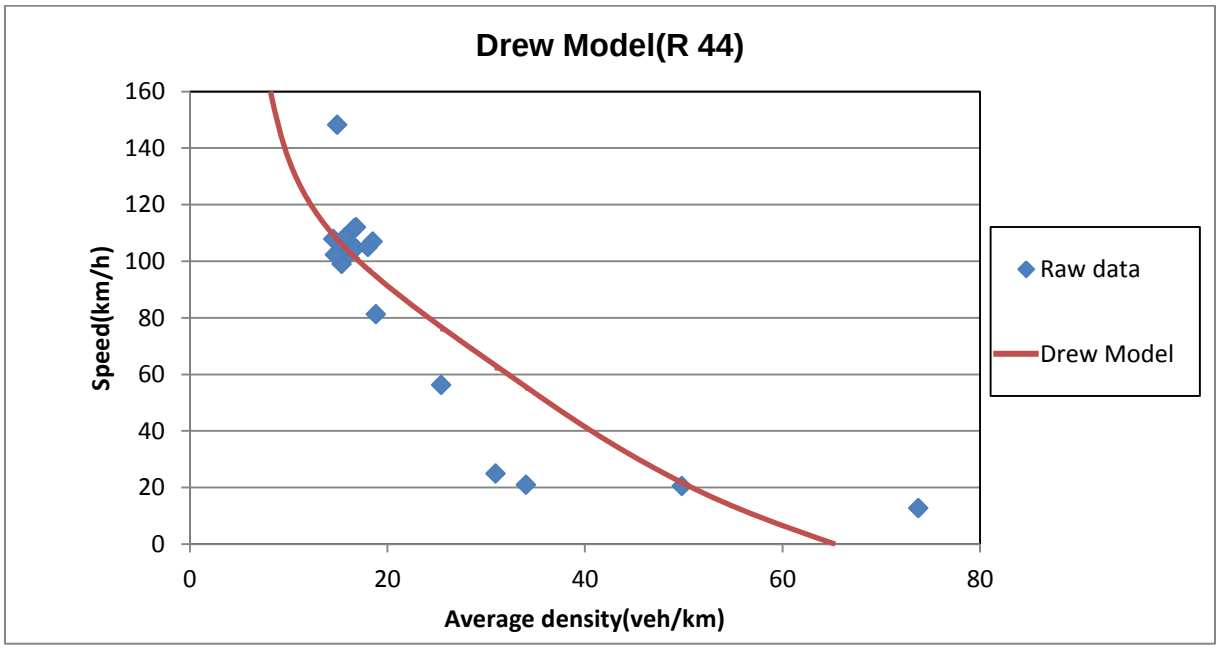

Figure 4. 25: The Drew model fitted to the 5-min speed-density data taken on Section 1 in the south bound direction

This model provided high values of R^2 in some cases. But this model showed some drawbacks, since it failed to represent well the congested part of the data and that it provided high and unrealistic free-flow speeds as it was observed with curve fitting using the Underwood Model.

- **The multi-regime Model**

In the multi-regime model, various parameters are defined as unknown depending on the specific equation chosen to be used. In the case of available data, the equation corresponding to the exponents *m*=1 and *l*>1 was found to provide a quite better representation of the data compared to other equations of the model. In this particular equation, free-flow speed, u_f, *l* and *c* are identified as unknown parameters.

Regression analysis was used to determine these parameters. Figure C-13 through C-16 in Appendix C are illustrations of curve fitting of 5-min time intervals data using the multi-regime model.

For Section 1, the regression analysis gave the following values:

In the south bound direction:

The data are represented by equation: $\ln\left(\frac{U_f}{U}\right) = c.K^{l-1}$ with m=1 and l >1

Unknown parameters: u_f= 143.07km/h, c= 1.8 E-04, l=3.643308, R^2=0.911.

In the north bound direction:

The data are represented by equation: $\ln\left(\frac{U_f}{U}\right) = c.K^{l-1}$ with m=1 and l >1

Unknown parameters: u_f= 144.39 km/h, c= 1.06 E-03, l=2.76791 and R^2=0.583.

For Section 2, the regression analysis yielded the following values:

In the south bound direction:

The data are represented by equation: $\ln\left(\frac{U_f}{U}\right) = c.K^{l-1}$ with m=1 and l >1

Unknown parameters: u_f= 173.4km/h, c= 1.91E-02, l=2.15028, R^2=0.933.

In the north bound direction:

The data are represented by equation: $\ln\left(\frac{U_f}{U}\right) = c.K^{l-1}$ with m=1 and l >1

Unknown parameters: u_f= 120km/h, c= 3.16E-05, l=3.764023 and R^2=0.210.

Figure 4.26 provides an illustration the multi-regime model fitted to the average 5-min speed-density data taken on R 44 in the south bound direction.

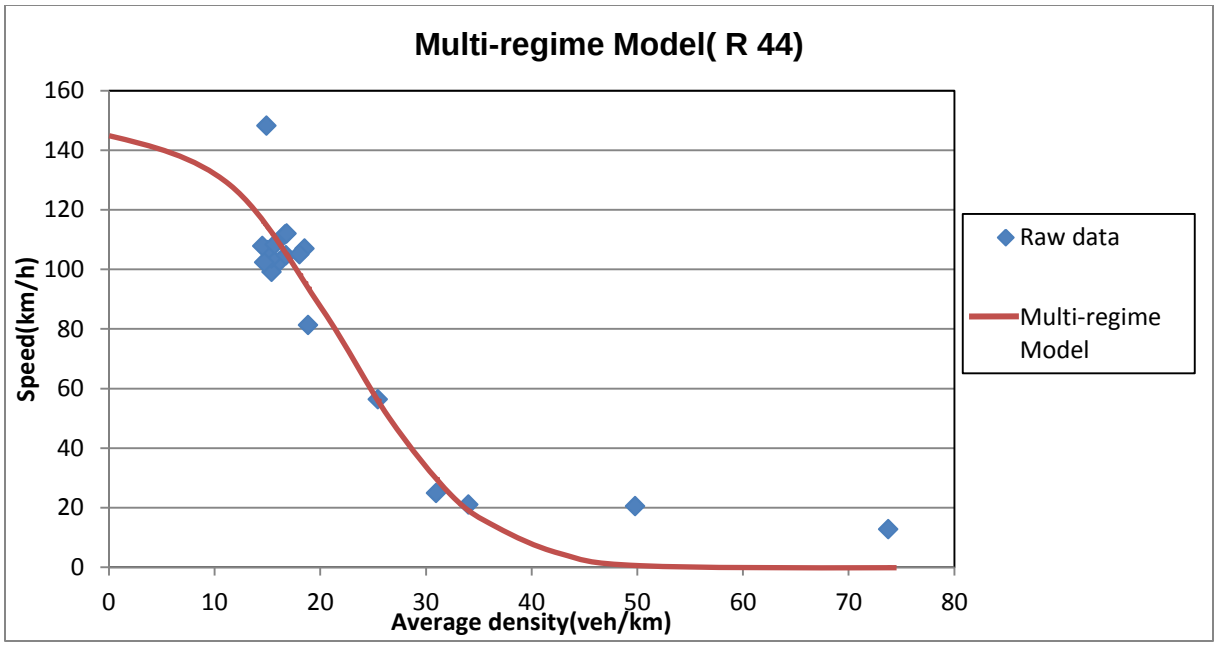

Figure 4. 26: The multi-regime model fitted to the 5-min speed-density data taken on Section 1 in the south bound direction

High values of R^2 are obtained in some cases with the use of the multi-regime model. However, this model yielded relatively good estimates of free-flow speed for Section 1 while a slightly overestimation of free-flow speed is noticeable in Section 2. Again, this model underestimated slightly the speed obtainable in congested conditions.

- **The composite Model**

In the composite model, two regimes were selected like in previous 1-min time intervals based analysis: the uncongested regime and the congested regime. In all cases, no any composite model was found to describe the available data satisfactorily, since the values of R^2 in all cases were found to be relatively low compared to some single regime models. This may be due to the reduction of points relating to congested conditions. Therefore, the composite model was not used for analysis of 5 min-time intervals speed-density data.

For Section 1, the multi-regime model was selected to describe the entire speed-density domain in the south bound direction.

This model was selected since it provided high value of R^2 and a quite good estimate of uncongested conditions compared to the other tested models.

As it was observed earlier, only free-flow traffic was found in the north bound direction on both sections. This resulted in further investigation to be carried out in the south bound direction only. Figure 4.27 provides an illustration of the multi-regime model describing speed-density relationship in the south bound direction of Section 1.

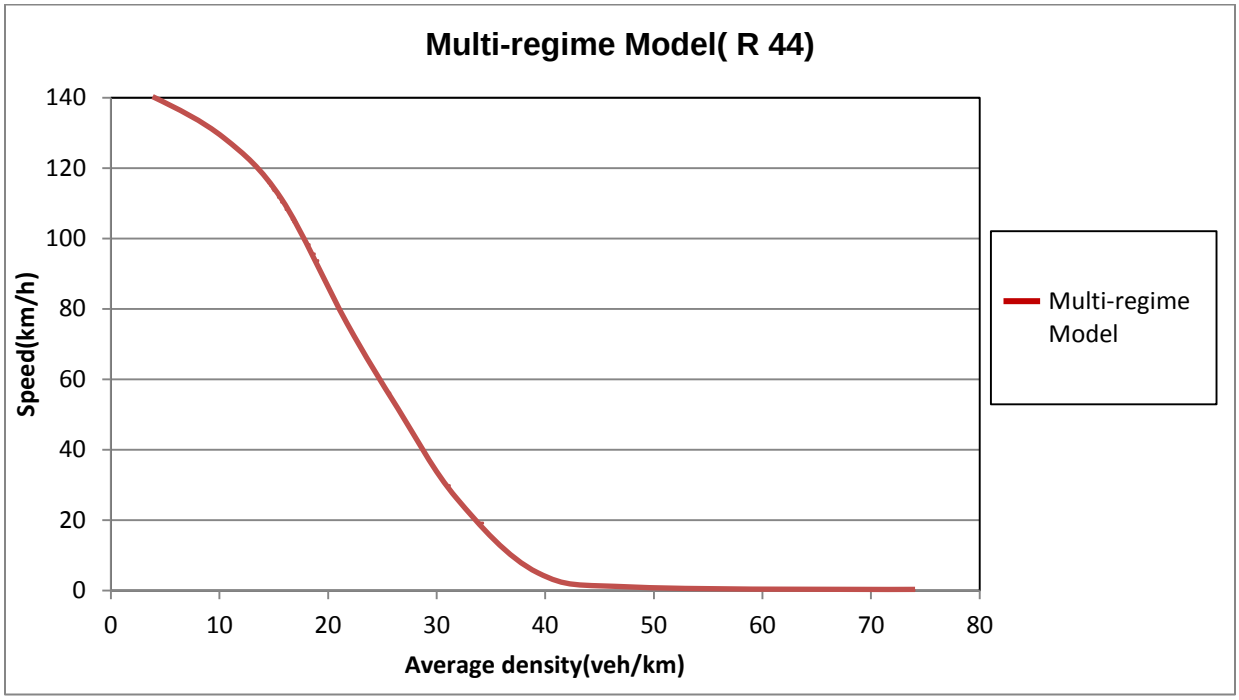

Figure 4. 27: The 5-min time intervals Speed-Density relationship for traffic in the south bound direction on Section 1

The use of multi-regime model to describe the entire speed-density data in this case was made possible since the effect of congestion is less pronounced with the available data. This provides somehow a different view of what has been observed in previous analysis based on one-min time intervals data, where the multi-regime model was judged inefficient to represent the whole domain of traffic data.

Applying the steady-flow equation to the 5-min time intervals speed-density data, the flow-density relationship was established. Figure 4.28 gives an illustration of the flow-density curve.

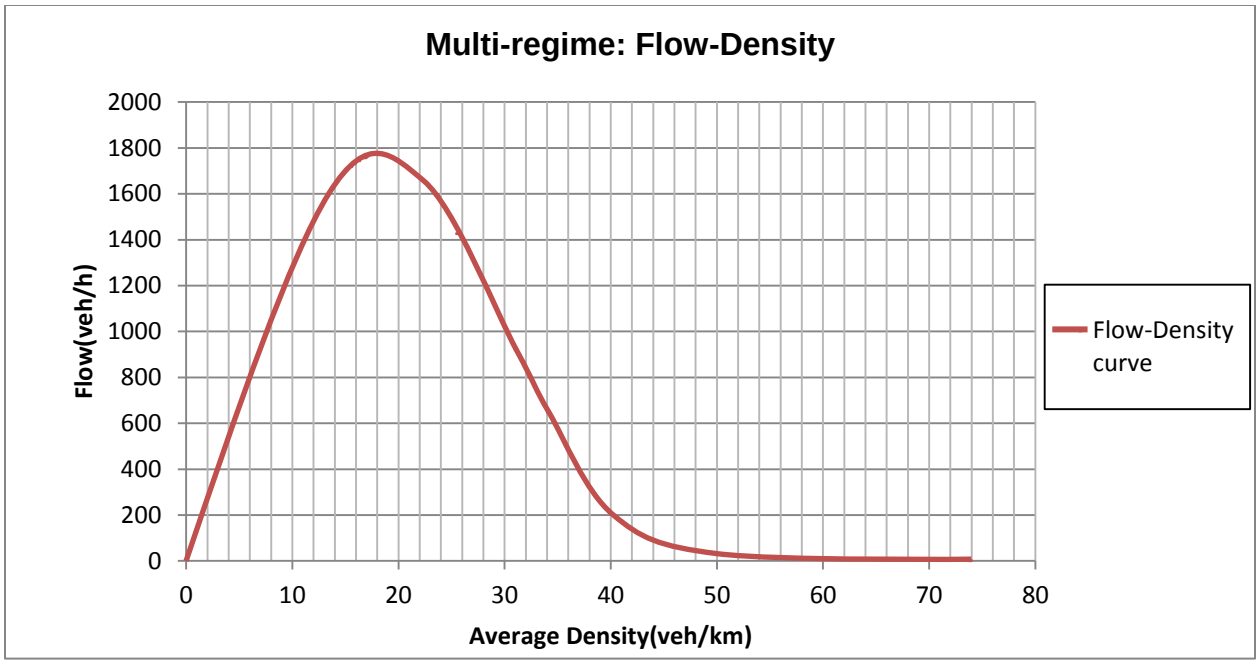

Figure 4. 28: The 5-min intervals Flow-Density relationship for traffic in the south bound direction on section 1

It can be seen that the maximum flow (1770veh/h) observed on the curve (Figure 4.28) is lower than the maximum flow obtained in previous analysis, when the data were observed in one-min time intervals (Figure 4.17). This gives a good agreement with previous studies which stipulated that the shorter the duration of observation, the higher the value of road capacity and vice versa.

Again, the speed-flow relationship was established using 5-min time intervals. Figure 4.29 gives an illustration of the speed-flow curve derived for Section 1.

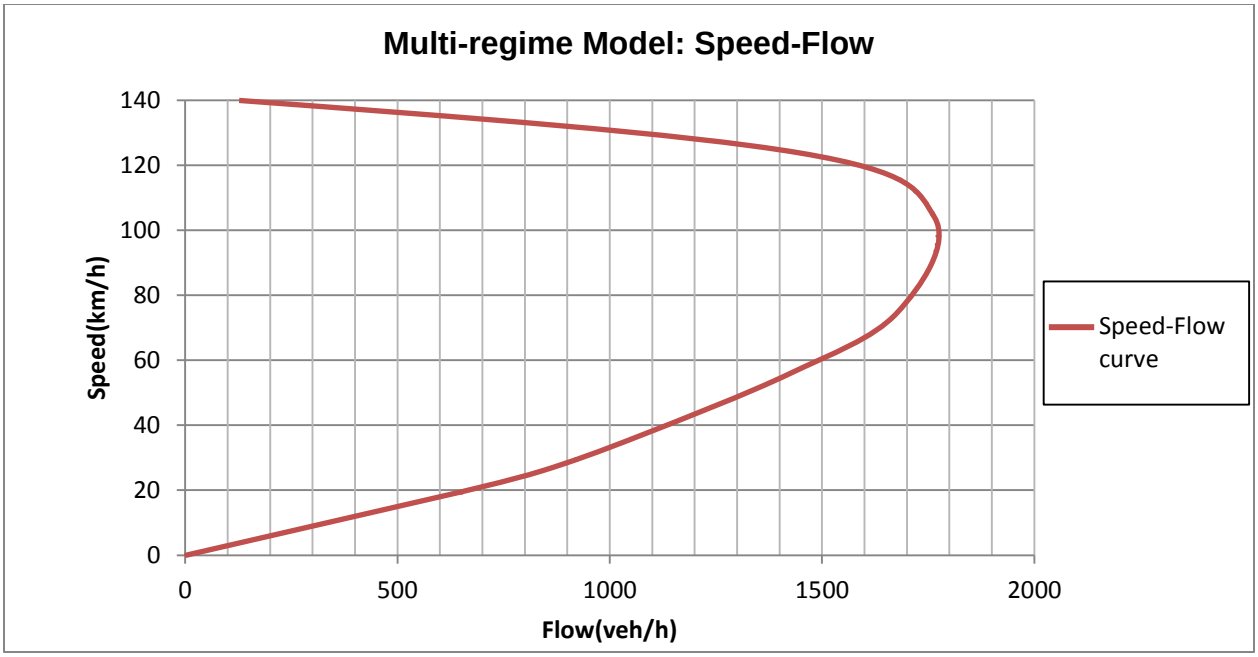

Figure 4. 29: The 5-min time intervals Speed-Flow relationship for traffic in the south bound direction on section 1

The slope of the curve is less steep at low flow rate. With increase of flow, the slope starts to be very steep when flow rate is close to the capacity of the section. The optimum speed achieved with this model is 96km/h. This value is surprisingly very close to the posted speed limit of the section and it is greater than the value obtained in previous analyses.

For Section 2, The Drake et al. model was selected to describe the available data, despite a high value of R^2 obtained with the multi-regime model. The reason of choosing the Drake et al. model was due to its reasonableness of the free-flow speed compared to the multi-regime model. Figure 4.30 provides an illustration the Drake et al. model fitted to the 5-min time intervals data taken on a section located on R 304 in the south bound direction.

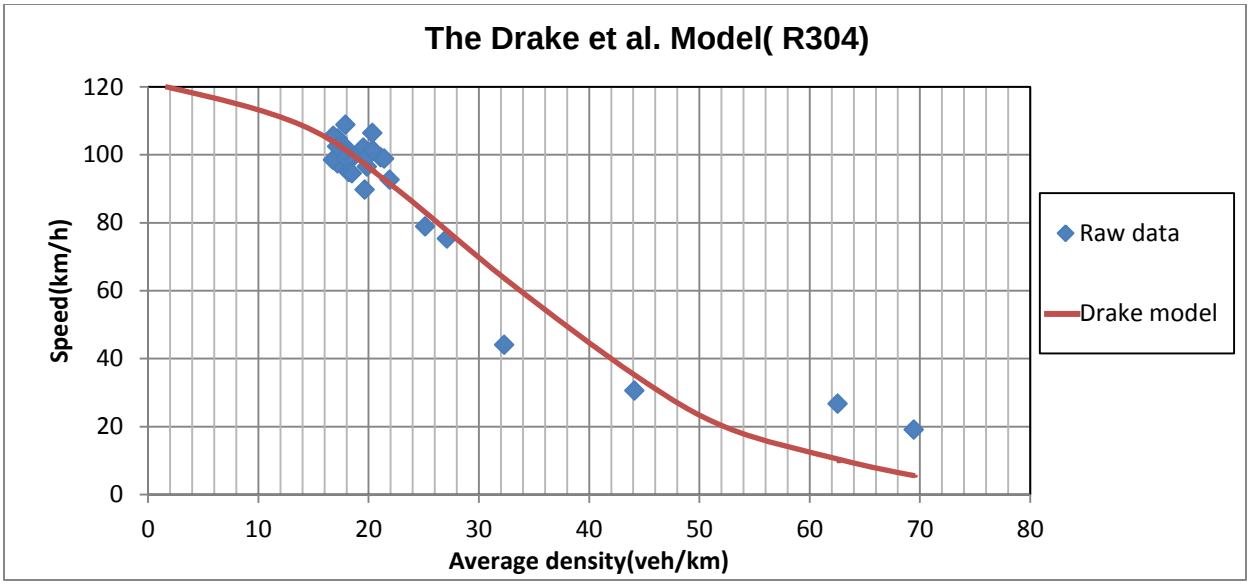

Figure 4. 30: The Drake et al. Model fitted to the 5-min. speed-density data taken on Section 2 in the south bound direction

Fitting the available data using the Drake et al. model provided an acceptable R^2, but the data relating to congested conditions are not well represented. The optimum speed achieved with this model is 78km/h. This value is slightly lower than the optimum speed obtained in Section 1.

Figure 4.31 provides an illustration of the multi-regime model describing speed-density relationship in the south bound direction of Section 2.

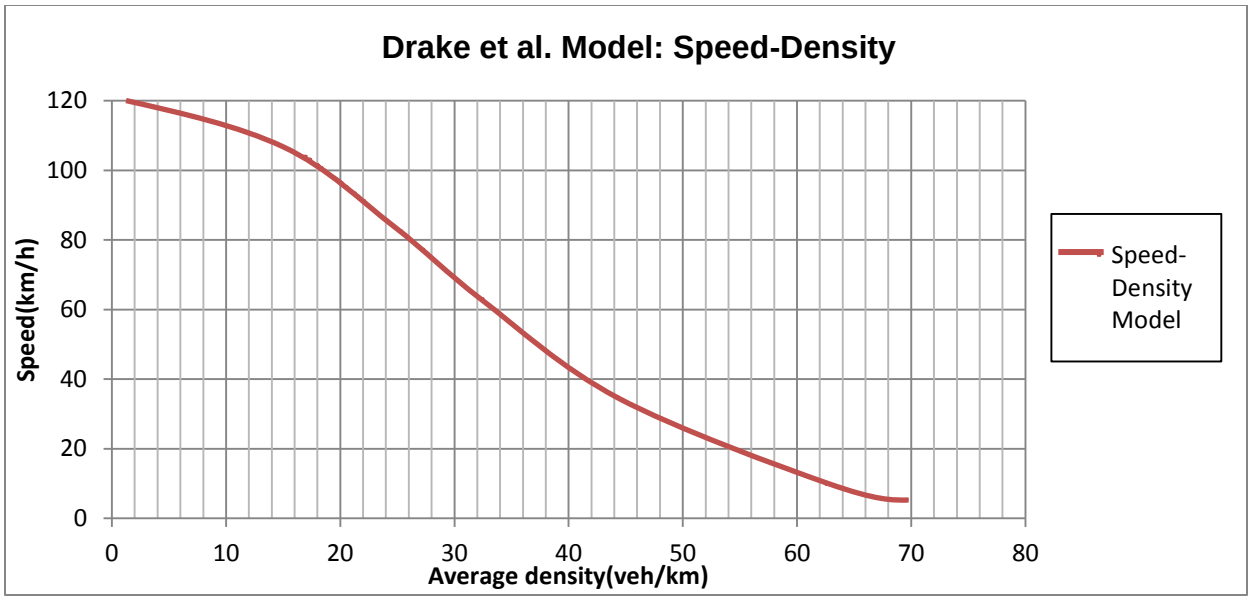

Figure 4. 31: The 5-min intervals Speed-Density relationship for traffic in the south bound direction on section 2

Again, the use of the Drake et al. model to describe the entire speed-density data in this section was made possible since the effect of congestion is not significant with the available data. Applying steady-flow equation (Equation 2.1) on speed-density data, flow-density and speed-flow curves were established. Figure 4.32 provides an illustration of 5-min flow-density relationship in the south bound direction of Section 2.

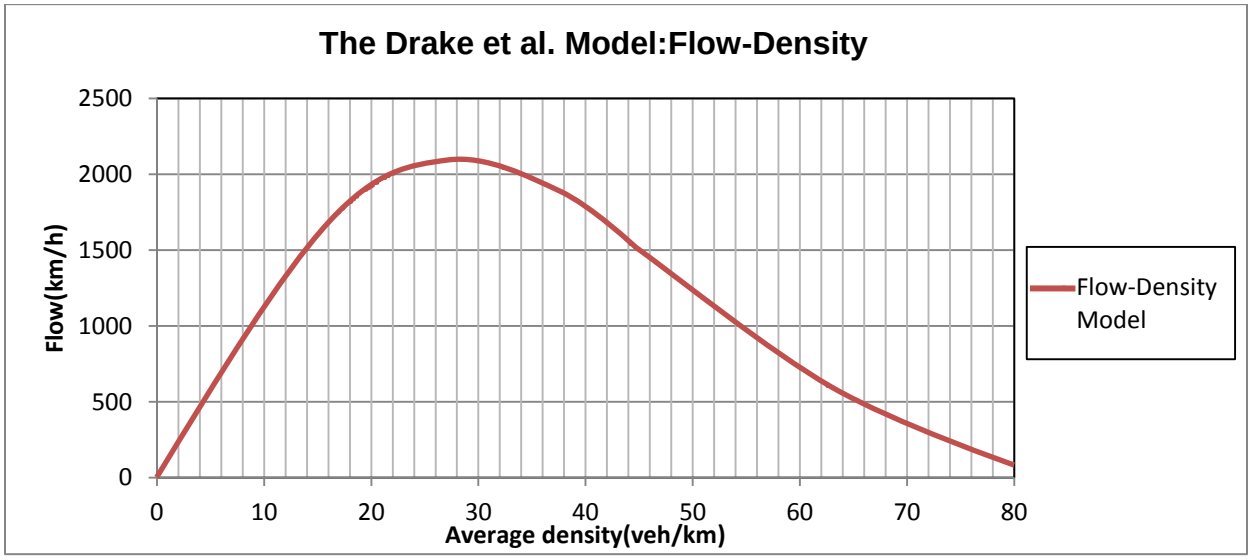

Figure 4. 32: The 5-min intervals Flow-Density relationship for traffic in the south bound direction on Section 2

Figure 4.33 provides an illustration of the 5-min speed-flow relationship in the south bound direction of Section 2.

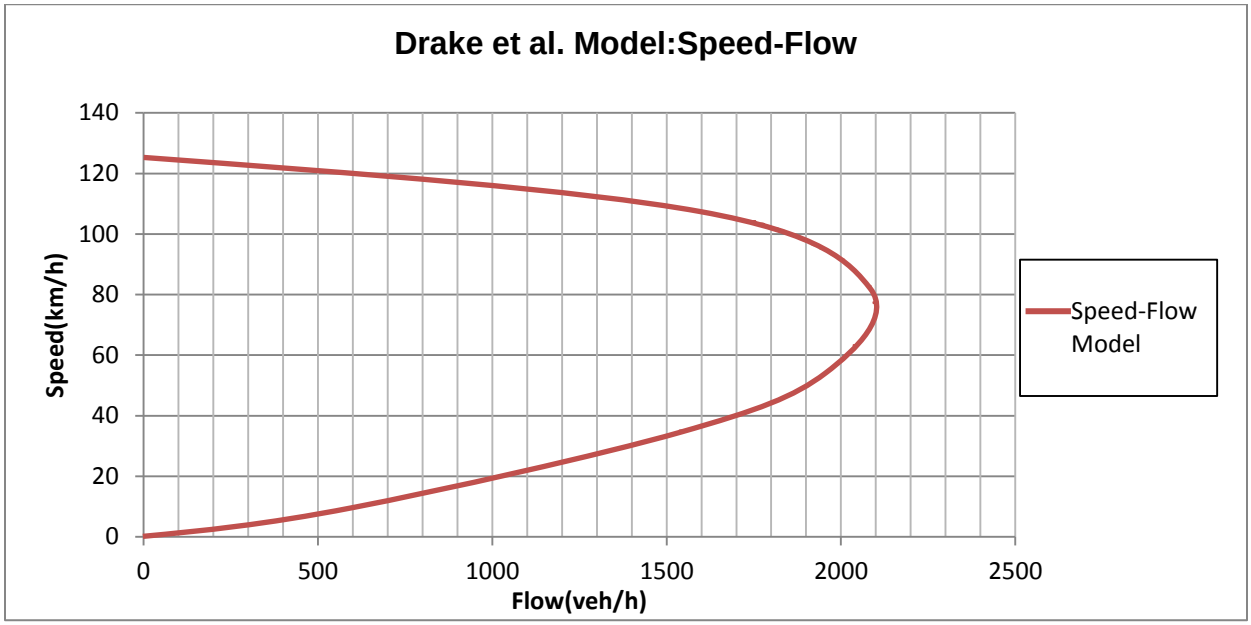

Figure 4. 33: The 5-min intervals Speed-Flow relationship for traffic in the south bound direction on Section 2

The maximum flow of 2093 veh/km is obtained on this curve. Again, this value is lower compared to the value obtained when the data were observed in one-min time intervals (Figure 4.20). Surprisingly, the difference in capacities for both scenarios (one-min and 5-min intervals) is higher for Section 1 compared to Section 2 even if Section 2 presented the highest value of capacity.

4.4 Travel time relationships

Travel time considered as one of the most easily visualized among traffic quality characteristics was extensively researched during past decades. In this study, apart from establishing speed-flow relationships, an investigation was made to explore the relationships between travel time and other traffic parameters namely density and flow on rural two-lane two-way highways in the Western Cape.

Using the conventional curves found in previous studies, as shown in Figure 4.34. Guerin (1958) investigated the travel time relationships on two-lane highways in USA. He subsequently constructed travel time-density relationships applied on traffic data.

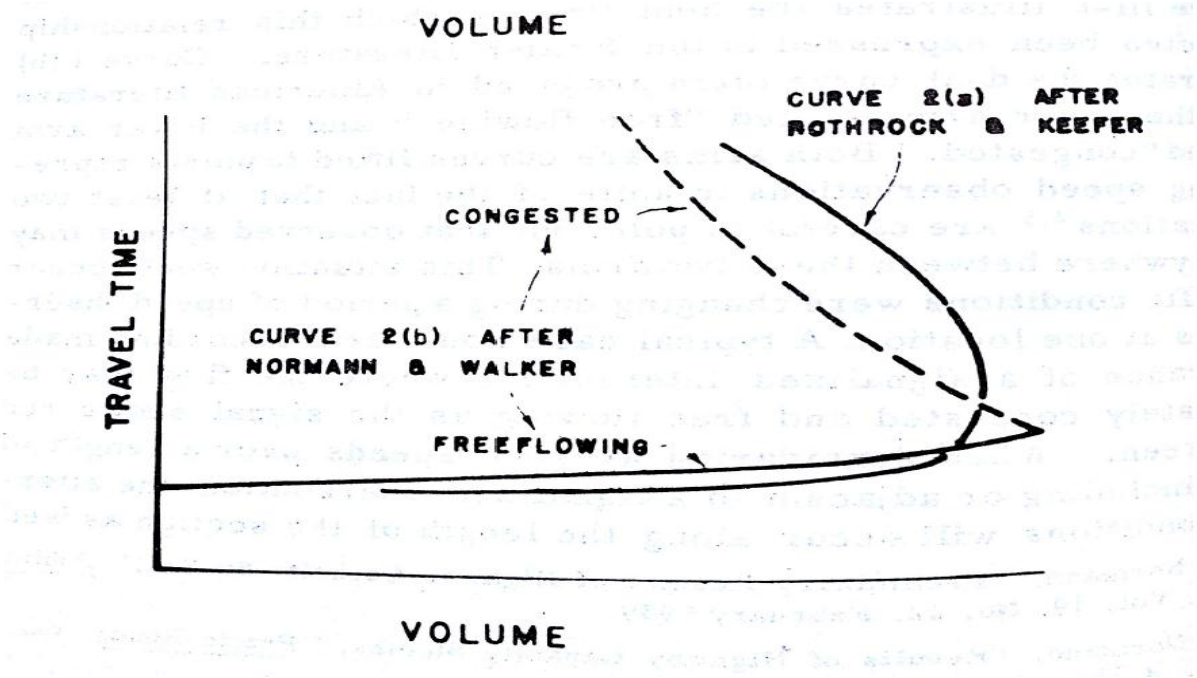

Figure 4. 34: Travel time relationships found in literature (Guerin, 1958)

Guerin (1958) suggested the use of boundary curve in describing relationship between travel time and density. The boundary curve proposed by Guerin has the following form:

$$T = \frac{a.K^2}{\sqrt{(b-K)}} + c$$

Where

a: a constant such that 2a is equal to the curvature of the time density curve at zero density

b: a constant equal to the maximum density obtained under bumper to bumper conditions

c: constant equal to the minimum travel time.

Figure 4.35 illustrates an example of travel time-density relationship after Guerin (1958) on Temple Street in USA.

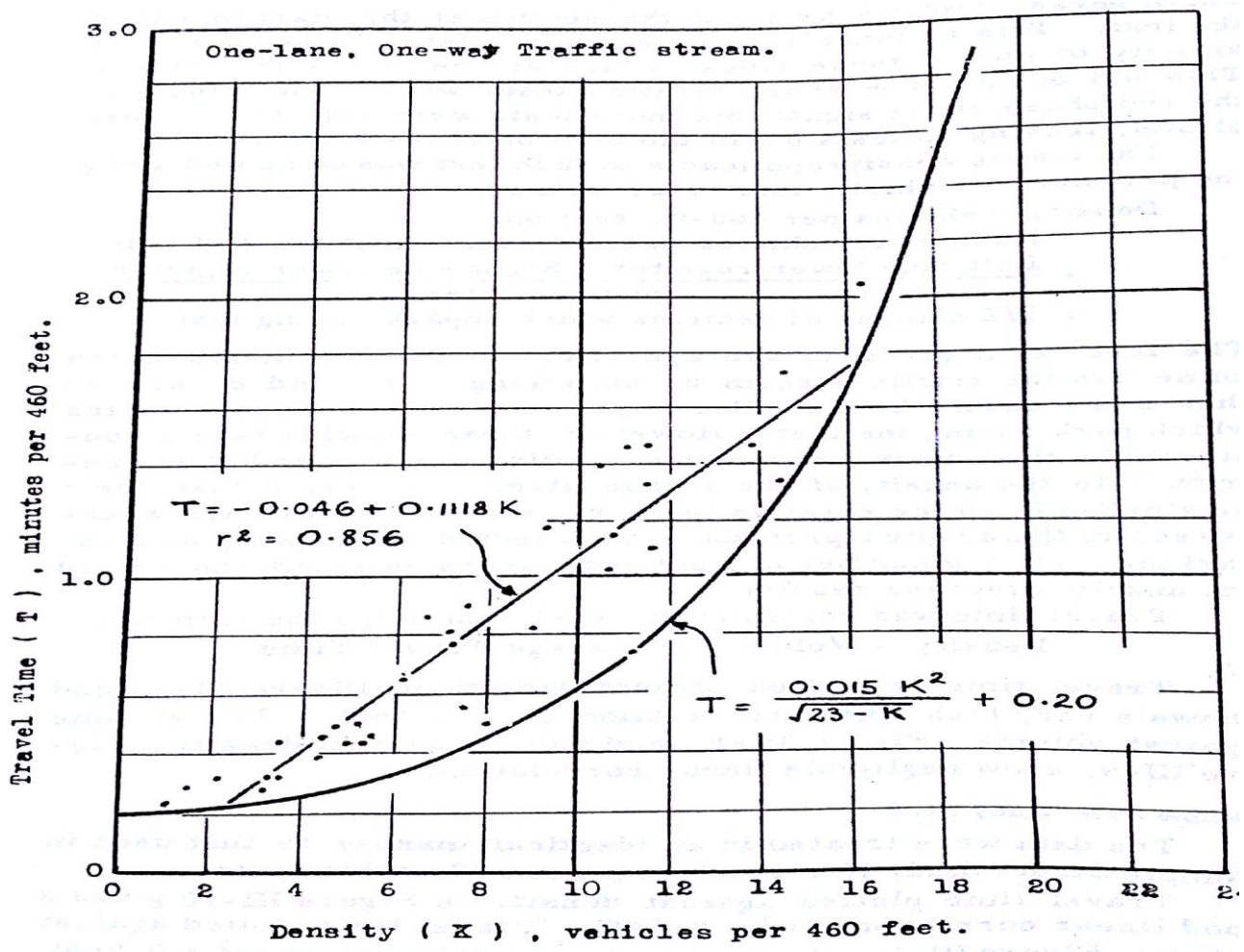

Figure 4. 35: Travel time-density relationship on data taken on Temple Street in USA (Guerin, 1958)

Once the travel time-time density was constructed, Guerin (1958) suggested the use of the equation proposed by Rothrock and Keefer (1957) to define the relationships between travel time and volume as follows:

$$Volume = \frac{Density}{Average\ travel\ time}$$

Figure 4.36 provides an illustration of the travel time-volume relationship on Temple Street as established by Guerin (1958).

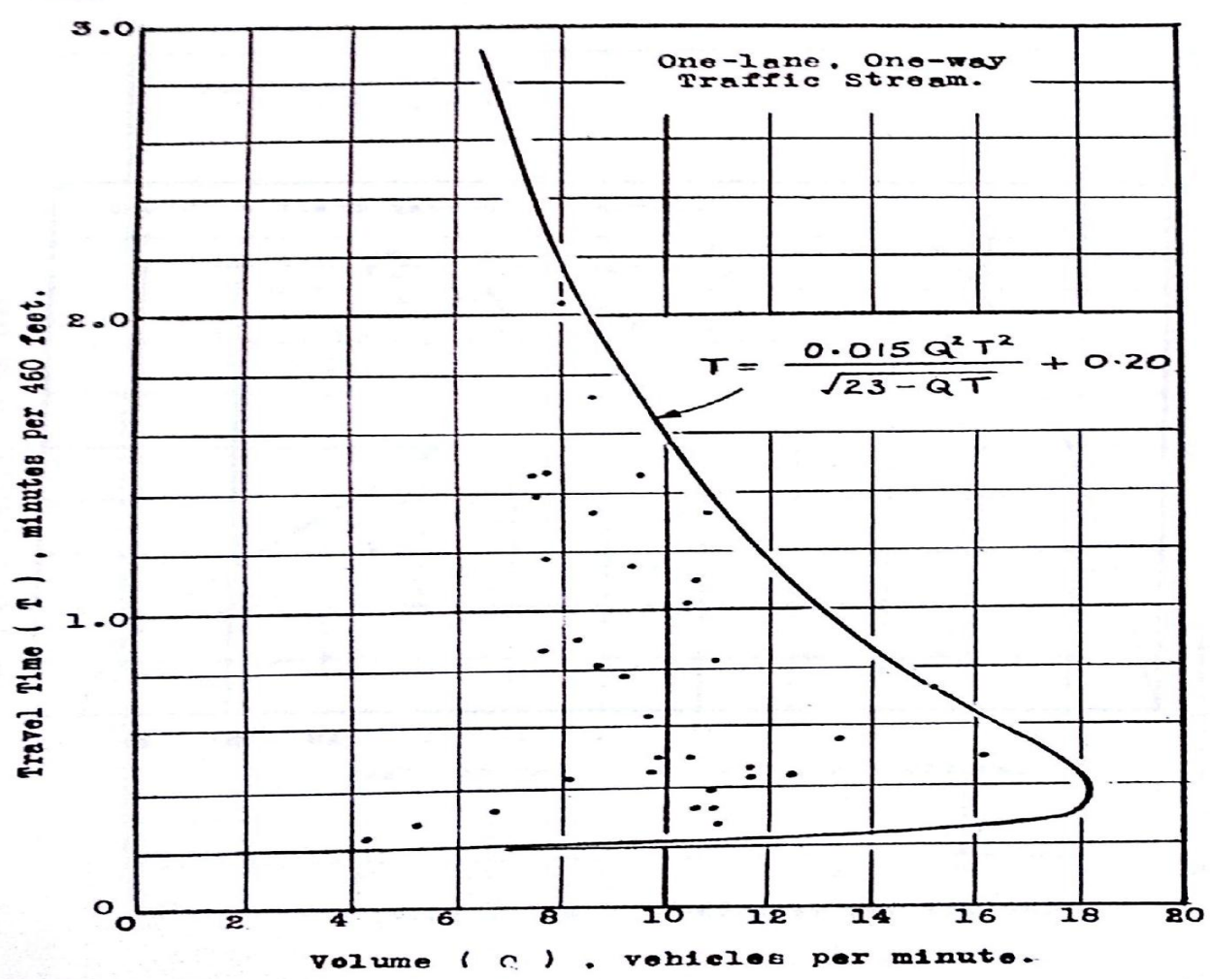

Figure 4. 36: Travel time- volume relationship on Temple Street in USA (Guerin, 1958)

The data from Section 2 in the south bound direction were used to establish relationship between travel time and density (Table 3 in Appendix A). High values of R^2 were

obtained in this section when a linear relationship between travel time and density is applied on the data. However, research has revealed that relationship between travel time and density cannot be linear, but that it has the properties similar to a quadratic equation especially when both volume and density are low. In addition to this, the scatter of the data shows that the later cannot be defined by a linear relationship. The boundary curve proposed by Guerin (1958) was therefore tested since it was found to satisfy all traffic conditions and it was simple to visualise.

Figure 4.37 depicts the travel time-density curves using linear relationship and boundary curve model between density and travel time on Section 2.

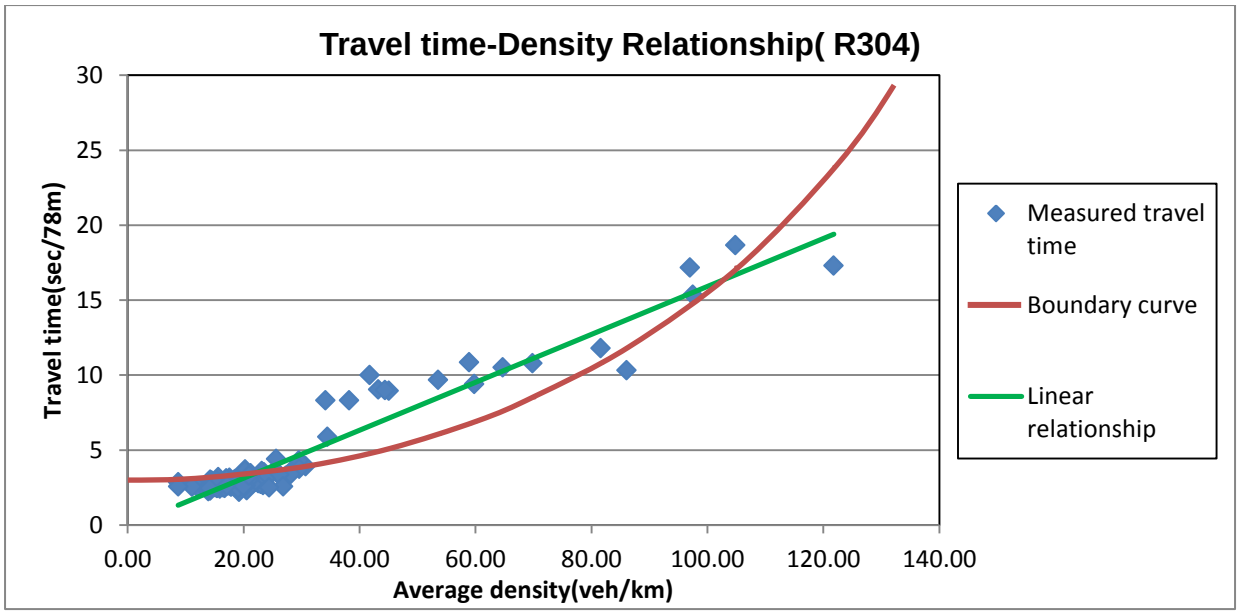

Figure 4. 37: Travel time-Density relationships on Section located on R304

The boundary curve obtained through regression analysis has the following form:

$$T = \frac{0.013.K^2}{\sqrt{(211.8 - K)}} + 2.99 \text{ With } R^2 = 0.810$$

Despite low value of R^2 compared to the value obtained with linear relationship (0.925) between travel time and density, the boundary curve provided more logical representation of the data than the linear relationship. From Figure 4.37, the curve starts with zero slopes and begins to turn upwards away from the minimum travel time

at a rate proportional to the square of the density. As density continues to increase, the curve continues to rise to an unlimited travel times as density approaches to the jammed density, where vehicles are forced to stop.

In contrast to the methodology used by Guerin, in this study the flow obtained using established Speed-Flow relationship (Figure 4.20) were used to derive Travel time-flow relationships. The relationship between travel time and flow obtained from observed data averaged in one-min time intervals is graphically depicted in Figure 4.38.

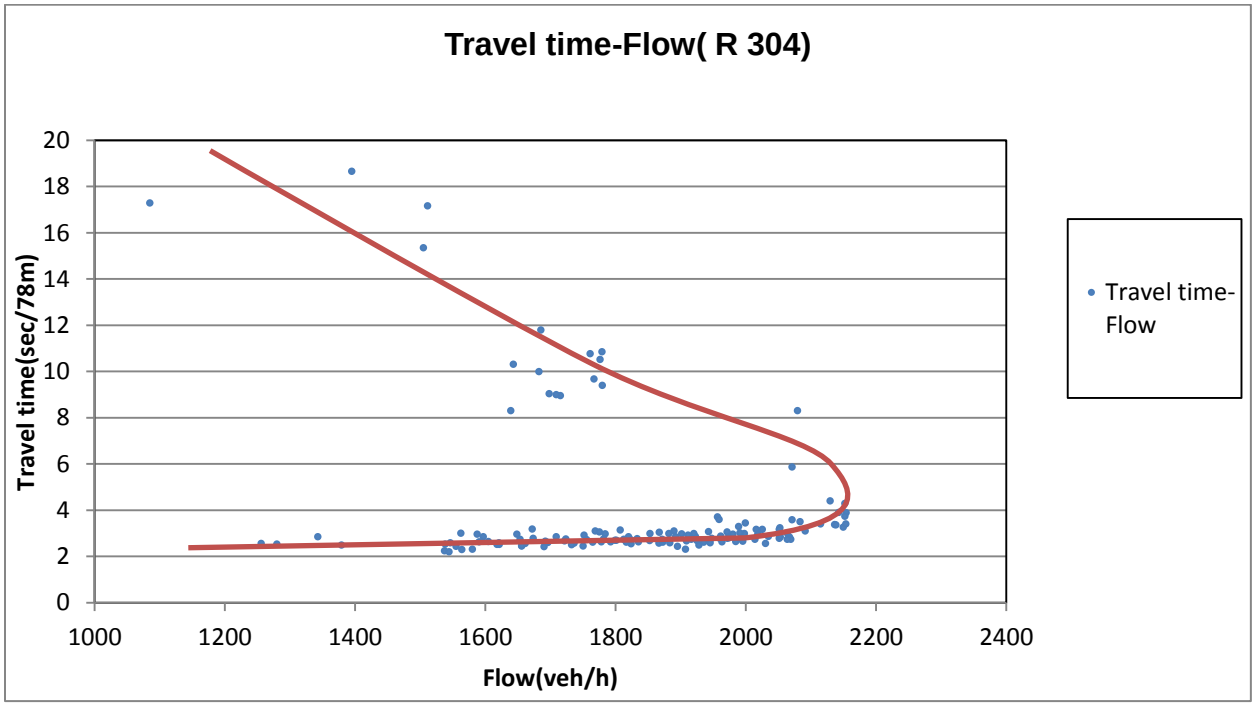

Figure 4. 38: Travel time-Flow relationship on section located on R 304

From Figure 4.38, the first observation of the scatter of data shows that the linear relationship between data is negligible, thus an overall nonlinear pattern is observed. The curve starts in similar way as previous curve with zero slopes, since travel time is practically independent from flow during uncongested conditions. As demand increases, travel time increases slightly with flow up to the point where the maximum flow observable on the section is reached. From that point onwards, travel times increase rapidly while flows decrease up to the point where unlimited travel times are at hand when the flow approaches zero. This is in compliance with traffic stream fundamentals,

according to which low flow rates can stem from either very low density (free flow conditions) or very high density (congested conditions).

The travel time-density and travel-time flow relationships for two-lane highways developed in this research are similar in shape to the relationships developed in many studies done previously in other countries.

4.5 Summary

This section presents the recapitulation of the results obtained in this project as follows:

The available data were aggregated in 1 and 5 minute intervals and analyses were performed separately. During the analysis of data observed over one-min intervals, the composite model was found to provide a best fit of the data with a coefficient of determination close to 0.9 on both sections in the south bound direction. In this model, the Drake et al. model was selected to describe uncongested part of the data while the Greenberg model was found suitable for describing high density part of the data. Again, the free flow speeds close to 125km/h were obtained on both sections. This provides an indication that drivers travel at high speeds on both sections.

Relatively higher values of R^2 greater than 0.9 were achieved in analysis of 5-min data. However, during analysis of data averaged over 5 min time intervals, there were less points relating to congested conditions. This results that, the data are described by using only one model for the whole data set. In the light of this observation, the multi-regime model was selected to describe the data on Section 1 while the Drake et al. model was judged suitable for describing data on Section 2. This made it possible to observe that with less points relating to congested conditions, which results from the change in time interval of observation, a switch from the use of one model to another can be performed.

As it has been found in previous projects and documented in literature, the increase in the time interval of observation results in low value of capacities of the two-lane two-way highways and vice versa. This was observed in this project, where the analyses based

on 5-min time intervals have resulted in reduction of capacity. The differences of capacities of 150 and 60veh/h were obtained for Section 1 and Section 2 respectively in both scenarios.

In this project also, travel time relationships were examined and a model between travel-time and density was established. The boundary curve was found to provide a logical relation between density and travel time despite low value of R^2 compared to R^2 corresponding to a linear relationship between these parameters. The relationship between flow and travel time was proposed as well, where flow data used were obtained from speed-flow curve developed in this study. Finally, all the travel time curves developed in this project were found to be in same shape with the curve developed in previous studies.

CHAPTER 5: APPLICATION OF CURVES

5.1 Introduction

Speed-Flow curves developed in the previous section were used to determine capacity of the study sections. Since the conditions on both sections are the same as the base conditions stipulated in HCM (2010), a comparative analysis was carried out between the values of capacity obtained in this study with the value given in HCM. The comparison between the capacity values determined on both study sections and capacity under base condition provided by HCM is used to determine whether shoulder use increase the capacity of the sections of two-lane two-way highways under consideration or not. This was done because shoulder use was observed during the data collection process.

5.2 Capacity determination

The speed-flow relationship is used in three ways. The upper portion is used to determine the level of service for the users under low density conditions, the right maximum values are used to estimate capacity and the bottom portion of the curve is used to calculate resulting upstream congestion patterns through shock wave analysis. In this project, speed-flow curves developed in the previous sections were used to determine capacity of the study sites.

From Figures 5.1 and 5.2, capacity values of section 1 and section 2 in the south bound direction are estimated to be 1925veh/km and 2154veh/km respectively as shown in following figures:

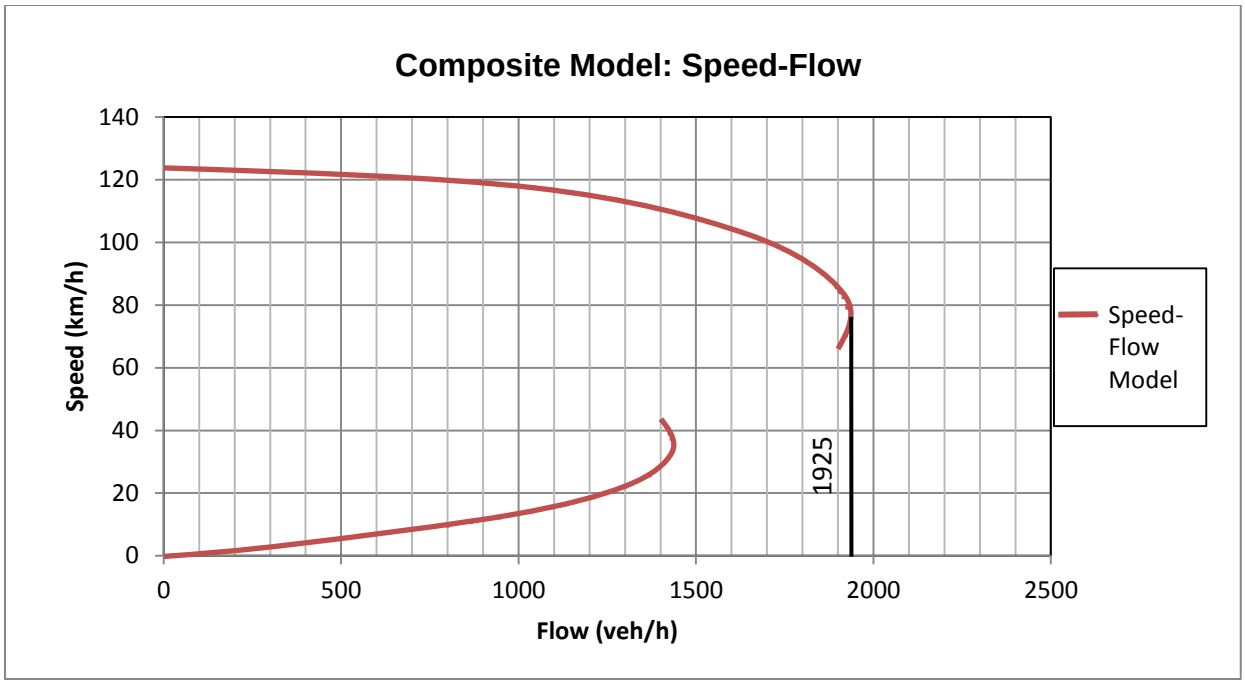

Figure 5. 1: Speed-Flow relationship showing capacity value under 1-min. time intervals on Section 1

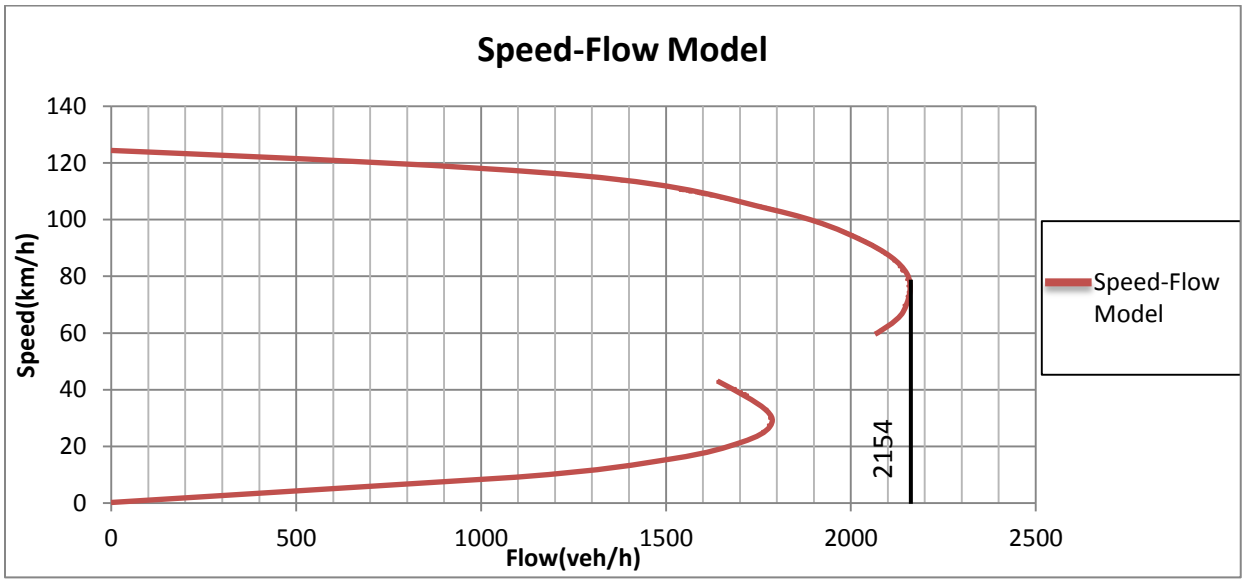

Figure 5. 2: Speed-Flow relationship showing capacity value under 1-min time intervals on Section 2

In both cases, the value of capacity obtained for two-lane highways is greater than 1700veh/h/direction provided as base capacity of two-lane highways in HCM.

It is noteworthy to indicate that both uncongested and congested capacities for Section 2 are higher than the value predicted by HCM, while in Section 1 only the uncongested capacity was found to be higher than 1700 veh/h and that the congested capacity was lower than this value.

5.3 Shoulder use

In some countries where wide paved shoulders are provided, it is a common practice for some drivers to pull onto the paved shoulder, as courtesy, when the latter are in good riding conditions to let the fast following drivers pass them and then return to the travel lane once the overtaking vehicles have cleared the lane. In this context, the wide paved shoulder acts as an informal passing lane which allows slower moving vehicles to be overtaken and queues to be dispersed.

Some researchers have investigated this issue and the influence of the shoulder use on speed and capacity of two-lane two way highways. A study carried out in Germany and Canada has shown that on roads with wide shoulders in Germany, drivers overtake at a rate of 4 times as much as that on standard two-lane highway and that vehicular speed increases considerably. In this case, a rate of increase of 25km/h was observed with the presence of extra-wide highways as shown in Figure 5.3 (Frost & Morrall, 1995)

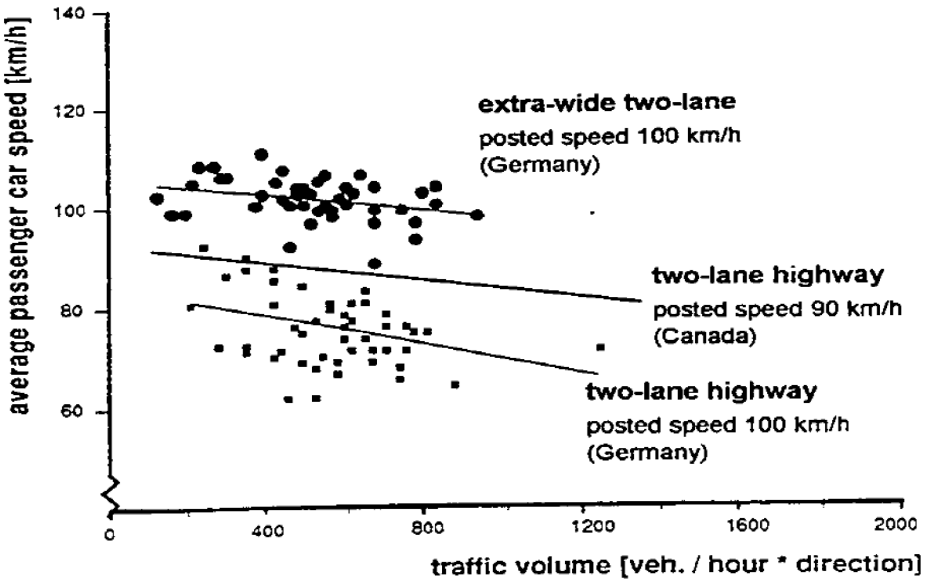

Figure 5. 3: Speed-Flow curves on two-lane highways in Germany and Canada (Frost & Morrall, 1995)

During data collection, this behaviour was observed on both study sections. The shoulder use accounted for 1% and 2% of the total use for sections 1 and 2 respectively.

In this study, the value of capacity provided by HCM is taken as the capacity associated to the normal driving, where drivers are expected to use travelling lane only and shoulders in case of an emergency. This value was to be compared to the values of capacity obtained from speed-flow curves developed in this project, in order to examine the effect of shoulder use on capacity of these highways.

However, as the capacity value provided in HCM was derived from 15-min time intervals, and that the speed-flow curves were developed in analyses based on 1 and 5 min time intervals only, due to limitation of field data to perform an analysis based on 15-min time intervals. This makes it impossible to compare the capacity value given by HCM to the capacities obtained in this study. Therefore, the results obtained in this study are not conclusive with regards to this issue.

From this standpoint, further analysis based on 15-min time intervals is required to highlight if shoulder use increases the capacity of two-lane two-way highways, using comparative assessment between the capacities resulting from that analysis to the HCM capacity as proposed in this study.

CHAPTER 6: CONCLUSIONS AND RECOMMENDATIONS

6.1 Introduction

In this final chapter of the project, the conclusions drawn from results are given and recommendations for further research are proposed.

6.2 Conclusions

Based on the data accumulated in this project and the analysis of the data, the following conclusions can be drawn:

- It was observed that on two-lane two way rural roads, the distance headways between vehicles vary considerably. The traffic may flow with relatively short distance headways for only short periods of time which consequently results in high volumes for that particular time.
- In particular, in the north bound direction on both sites there was no information related to high density conditions, so no clue about congested conditions was available. With this situation, it was therefore impossible to predict capacity of the study sections in this direction: this constrained the model fitting in this direction.
- There is no fixed measure to use for judging whether the data are sufficiently represented by a particular model. Given that models consisted of different parameter types, the confidence limits of parameters were not comparable. Also, the coefficient of determination R^2 which is a singular value representing the overall adequacy of the model. It does not indicate whether the model overestimates (or underestimates) certain areas of the data. Therefore, the decision on whether a particular model constituted a good fit was based on visual observation, after its R^2 value is judged closer to 1. In this study, the models were compared to each other and the best model was chosen as the model giving the best overall fit.
- In the analysis of data aggregated to one-min time intervals, the scatter of the data and the apparent discontinuity between low density data and high density data warrant the use of separate curves to describe the whole range of speed-density data(whole spectrum of densities). Through the use of the composite

model, two separate curves, one for uncongested regime and other for the congested regime provided the best results in each case (based on overall R^2-values and prediction reflected by an adequate visual-fit). The curve resulting from the Drake et al. model consistently gave the best fits for the uncongested domain, while the curve resulting from the Greenberg model proved to describe the congested data satisfactorily.

- In the analysis of data averaged to 5-min time intervals, a reduction of points relating to congested conditions was experienced. This resulted in fitting a curve using a single model for the whole traffic domain. The bell-shaped equation of the multi-regime model and the Drake et al. model provided relatively better representation of the data. Thence, an increase of time interval of observation resulted in a change of model to be used to describe the observed data. Also, the bell-shaped curves were found to adequately describe the data on these highways in most cases, more specifically data relating to the uncongested conditions.
- In most cases, speed-density data were well represented in both uncongested and congested conditions for the data aggregated to one-min time intervals. However, during analysis of data averaged to 5-min time intervals, congested data were not well represented, since the aggregation of the data resulted in less points relating to congested conditions which made the use of the composite curve unfeasible.
- Although the values of capacity obtained in both analyses for both sections are greater than the value provided in HCM. The capacity provided by HCM is derived empirically from data aggregated over 15-min time intervals. This indicates that no comparison could be done between these values, because they are not based on the same time intervals of observation. Again, as the data taken on the study sites could not allow the analysis based on 15-min intervals. Thus, the results from this study are not conclusive with regards to the effect of shoulder use on increase of capacity.

- This study provided a good agreement with previous studies which indicated that the value of capacity is dependent on the time intervals for which data are collected and from which the capacity is calculated.
- The travel time-density and travel time-flow relationships for two-lane two-way highways developed in this study are similar in shape to the relationships developed overseas in many studies carried out to establish these relationships.

6.3 Recommendations

The following recommendations are offered based on the work accomplished during this project and on conclusions given previously:

1. The investigation of speed-flow relationships and thereby capacity for various geometric conditions, terrain and traffic characteristics is required, provided that in this study, only one case was considered since both sections had similar conditions.
2. An investigation of the speed-flow relationships in other provinces and areas in South Africa is required in order to derive general conclusions applicable to all two-lane two-way rural highways across the country.
3. In order to evaluate the effect of shoulder use on capacity, further studies can be performed by comparing the value of capacity obtained on sections with good shoulder conditions to the capacity value of sections where the usage of shoulders is constrained by the conditions which do not allow the use of shoulders.
4. In this study, capacity values were determined from speed-flow curve developed in analyses based on 1 and 5 minutes time intervals only. As the capacity value given in HCM was empirically derived from data based on 15-min time intervals, a further study based on 15-min time intervals is required to verify if this value of capacity is achievable in South Africa.

REFERENCES

Al-Kaisy, A., & Karjala, S. 2008. Indicators of Performance on Two-Lane Rural Highways: Empirical Investigation. *Transportation Research Record: Journal of the Transportation Research Board*, *2071*(1): 87-97.

Allen, B.L., Hall, F.L. & Gunter M.A. 1985. Another Look at Identifying Speed-Flow Relationships on freeways. *Transportation Research Record*: *Journal of the Transportation Research Board*, 1005():54-64.

Baerwald, J.E., Huber, M.J. & Keefer, L.E. 1976.*Transportation and Traffic Engineering Handbook*. New Jersey: Prentice-Hall Inc.

Box, G.E.P., Hunter, W.G. & Hunter, J.S. 1978. *Statistics for Experimenters: An Introduction to Design, Data Analysis, and Model Building*. New York: Wiley & sons.

Chandler, R.E., Herman, R. & Montroll, E.W. 1958. Traffic Dynamics: Studies in car-following. *Operations Research*, 6, (2):165-184.

Chin, H.C. and May, A.D. 1991. Examination of the speed-flow relationships at the Caldecott Tunnel. *Transportation Research Record: Journal of the Transportation Research Board*, 1320, (10): 75-82.

Dey, P.P., Chandra, S. & Gangopadhyay, S. 2008. Simulation of mixed traffic flow on two-lane roads. *Journal of Transportation Engineering*, *134*(9): 361-369.

Drake, T.S., May, A.D., & Schofer, J.L. 1965. A Statistical Analysis of Speed Density Hypotheses. *Highway Research Record*, 154: 53-87.

Drew, D.R. 1968. *Traffic flow theory and control*. New York: McGraw-Hill Book Company.

Edie, L.C. 1961. Car-following and steady-state theory for non-congested traffic. *Operations Research*, 9(1): 66-76.

Frost, U., & Morrall, J. 1995. A comparison and evaluation of the geometric design practices with passing lanes, wide-paved shoulders and extra-wide two-lane highways

in Canada and Germany. In *International Symposium on Highway Geometric Design Practices.*

Garber, N.J. & Hoel, L.A. 2002. *Traffic and Highway Engineering*. Toronto: Thomson Learning.

Garber, N.J. & Hoel, L.A. 2010. *Traffic and Highway Engineering*. Stamford: Cengage Learning.

Gazis, D.C., Herman, R. & Rothery, R.W. 1961. Nonlinear follow-the-leader models of traffic flow. *Operations Research*, 9, (4):545-567.

Greenberg, H. 1959. An analysis of traffic flow. *Operations Research*, 7, (1): 79-85.

Greenshields, B.D. 1935. A study of traffic capacity. *Proc. Highway Research Board*, 14: 448-477.

Guerin, N.S. 1958. Travel time relationships. *Quality and Theory of Traffic Flow*: *69-103.*

Hall, F.L., Hurdle, V.F., &Banks, J.H. 1992. Synthesis of recent work on the nature of speed-flow and flow-occupancy (or density) relationships on freeways. *Transportation Research Records: Journal of the Transportation Research Board*, 1365: 12-18.

Harwood, D.W., May, A.D., Anderson, I.B. & Archilla, A.R. 1999. Capacity and quality of service of two-lane highways. *NCHRP Final Rep. No.3-55 (3)*, Midwest Research Institute.

Hashim I. H. & Abdel-Wahed, T. A. 2011. Evaluation of performance measures for rural two-lane roads in Egypt. *Alexandria Engineering Journal*, 50(3):245-255.

Hurdle, V.F. & Datta, P.L. 1983. Speed and flows on an urban freeway: Some measurements and a hypothesis. *Transportation Research Record: Journal of the Transportation Research Board*, 905:127-137.

Kim, J., & Elefteriadou, L. 2009. Estimation of capacity of two-lane two-way highways using simulation model. *Journal of Transportation Engineering*, *136*(1), 61-66.

Leutzbach, W. 1988. *Introduction to Theory of Traffic Flow*. Berlin Heidelberg: Springer-verlag.

Lighthill, M. J., & Whitham, G. B. 1955. On kinematic waves. II. A theory of traffic flow on long crowded roads. *Proceedings of the Royal Society of London. Series A. Mathematical and Physical Sciences*, *229*(1178): 317-345.

Luttinen, T.R. 2000. Traffic Flow on Two-Lane Highways. An Overview.*TL Research Report*, TL Consulting Engineers, Ltd.

Mannering, F.L., Kilareski, W. & Washburn, S. 2007. *Principles of Highway Engineering and Traffic Analysis*. New York: John Wiley & Sons.

May, A.D. & Keller, H.E.M. 1967. Non-integer car-following models. *Highway Research Records*, 199: 19-32.

May, A.D. 1990. *Traffic Flow Fundamentals*. New Jersey: Prentice-Hall Inc.

McShane, W. R. & Roess, R. P. 1990. *Traffic Engineering*. New Jersey: Pearson Prentice-Hall, Inc.

Montgomery D. C. & Runger G.C. 2007.*Applied Statistics and Probability for Engineers*. United States: Wiley.com.

O'Flaherty, CA 1997, *Transport Planning and Traffic Engineering*. London: Arnold member of Hodder Headline Group.

Pipes, L. A. 1953. An operational analysis of traffic dynamics. *Journal of applied physics*, vol.24: *24*(3), 274-281.

Polus, A., Craus, J. & Livneh, M. 1991. Flow and capacity characteristics on two-lane rural highways. *Transportation Research Record: Journal of the Transportation Research Board*, 1320: 128-134.

Pursula, M. & Enberg, A. 1991. Characteristics and level-of-service estimation of traffic flow on two-lane rural roads in Finland. *Transportation Research Record: Journal of the Transportation Research Board*, 1320: 135-143.

Rothrock, C.A. & Keefer, L.E. 1957. Measurement of urban traffic congestion. *Bulletin 156 Highway Research Board: 7.*

Roux, J. 2001. Establishing and applying speed-flow relationships for traffic on South African freeways. Master's thesis. Stellenbosch: University of Stellenbosch.

Rozic, P. 1992. Capacity of two-lane, two-way rural highways: The new approach. *Transportation Research Record: Journal of the Transportation Research Board*, 1365: 19-29.

Shawky, M. & Hashim, I. 2010. Impact of horizontal alignment on traffic performance at rural two-lane highways. In *Proc. of 4th International Symposium on Highway Geometric Design. Valencia, Spain*.

Tapani, A.2008. Traffic Simulation modelling of rural roads and driver assistance systems. Doctoral dissertation. Linköping: Linköping studies in sciences and technology.

Transport Research Board 1985. *Highway Capacity Manual*. National Research Council.

Transport Research Board 2000. *Highway Capacity Manual* (*metric units*). National Research Council.

Transport Research *Board* 2010. *Highway Capacity Manual* (*U.S Customary units*). National Research Council.

Underwood, R.T. 1960. Speed, Volume and Density Relationships. *Quality and Theory of Traffic Flow*: 143-188.

Van As, C. 2003. The development of an analysis method for the determination of level of service of two-lane undivided highways in South Africa. *Project Summary. South African National Roads Agency*.

Van As, S.C. & Van Nierkerk, A. 2004. The Operational analysis of two-lane rural highways. *Proceedings of the 23rd Southern African Transport Conference* (SATC 2004): 622-633.

Walpole, R.E. & Myers R.H. 1989. *Probability and Statistics for Engineers and Scientists*, New York: Macmillan Publishing Company.

Wardrop, J. G. 1952. Road paper. Some theoretical aspects of road traffic research. In *ICE Proceedings: Engineering Divisions* (Vol. 1, No. 3, pp. 325-362). Thomas Telford.

Yagar, S. 1983. Capacities for two-lane highways. *Australian Road Research*, 13(1): 3-9.

APPENDIX A

Raw data &

Speed/Density/Flow measurements

Table A- 1: Speed/Flow/Density measurements made during consecutive 1 min intervals on Section 1 in the south bound direction

TIME	Average Travel Time	Average Spacing	Average Speed	Average Density	Calculated Flow	Predicted Speed	Predicted Flow
07:24	3.68	93.38	109.57	10.7	1173	114.29114	1224
07:25	3.66	67.79	110.16	14.8	1625	105.56056	1557
07:26	3.96	59	101.82	16.9	1726	100.03255	1695
07:27	3.99	50.24	101.05	19.9	2011	91.964876	1831
07:28	4.25	61.88	94.87	16.2	1533	102.07018	1649
07:29	4.34	54.26	92.90	18.4	1712	96.067614	1771
07:30	4.08	76.71	98.82	13.0	1288	109.51761	1428
07:31	4.14	59.83	97.39	16.7	1628	100.64573	1682
07:32	3.86	65.65	104.46	15.2	1591	104.39202	1590
07:33	3.9	72	103.38	13.9	1436	107.59324	1494
07:34	3.77	93.78	106.95	10.7	1140	114.37731	1220
07:35	4.22	68.09	95.55	14.7	1403	105.71661	1553
07:36	3.75	50.82	107.52	19.7	2116	92.605533	1822
07:37	3.62	67.31	111.38	14.9	1655	105.30702	1565
07:38	4.14	51.94	97.39	19.3	1875	93.794129	1806
07:39	4.75	45.1	84.88	22.2	1882	85.43117	1894
07:40	4.87	36.33	82.79	27.5	2279	69.569889	1915
07:41	5.04	48.27	80.00	20.7	1657	89.651478	1857
07:42	6.77	41.56	59.56	24.1	1433	79.861453	1922
07:43	13.48	27.19	29.91	36.8	1100	38.711504	1424
07:44	22.91	18.64	17.60	53.6	944	25.437217	1365
07:45	40.14	13.92	10.04	71.8	722	15.17109	1090
07:46	33.51	10	12.03	100.0	1203	3.5422163	354
07:47	30.28	12.71	13.32	78.7	1048	11.973725	942
07:48	32.21	12.29	12.52	81.4	1019	10.792237	878
07:49	32.95	14.5	12.24	69.0	844	16.606391	1145
07:50	25.32	22.45	15.92	44.5	709	31.976302	1424
07:51	15.45	30.73	26.10	32.5	849	43.014741	1400
07:52	5.87	36.45	68.69	27.4	1884	69.837917	1916
07:53	5.11	55.79	78.90	17.9	1414	97.440159	1747
07:54	6.17	36.5	65.35	27.4	1790	69.949118	1916
07:55	9.59	30.59	42.04	32.7	1374	54.718865	1789
07:56	31.5	11.82	12.80	84.6	1083	9.4212467	797
07:57	29.7	12.19	13.58	82.0	1114	10.504981	862
07:58	26.55	8.91	15.19	110.0	1671	0.1911103	21
07:59	25.16	16.2	16.03	61.7	989	20.50432	1266

TIME	Average Travel Time	Average Spacing	Average Speed	Average Density	Calculated Flow	Predicted Speed	Predicted Flow
08:00	20.94	30.55	19.26	32.7	630	42.808187	1401
08:01	22.77	25.91	17.71	38.6	683	37.01608	1429
08:02	17.65	16.77	22.84	59.6	1362	21.720164	1295
08:03	8.31	60.54	48.52	16.5	801	101.15319	1671
08:04	5.26	53.33	76.65	18.8	1437	95.18538	1785
08:05	6	35.24	67.20	28.4	1907	67.059867	1903
08:06	3.76	54	107.23	18.5	1986	95.824741	1775
08:07	4.16	62.86	96.92	15.9	1542	102.70888	1634
08:08	4.3	54.9	93.77	18.2	1708	96.653338	1761
08:09	3.48	94.3	115.86	10.6	1229	114.4878	1214
08:10	3.34	102.5	120.72	9.8	1178	116.02483	1132
08:11	3.79	44	106.39	22.7	2418	83.805177	1905
08:12	3.8	95.33	106.11	10.5	1113	114.70164	1203
08:13	3.6	60.2	112.00	16.6	1860	100.9121	1676
08:14	3.43	81.5	117.55	12.3	1442	111.16936	1364
08:15	3.59	63.91	112.31	15.6	1757	103.36497	1617
08:16	3.81	112	105.83	8.9	945	117.41821	1048
08:17	3.9	43	103.38	23.3	2404	82.247291	1913
08:18	3.5	51.38	115.20	19.5	2242	93.207652	1814
08:19	3.85	114	104.73	8.8	919	117.66983	1032
08:20	3.85	84.14	104.73	11.9	1245	111.97039	1331
08:21	3.76	64.22	107.23	15.6	1670	103.55332	1612
08:22	4.23	41	95.32	24.4	2325	78.885643	1924
08:23	3.45	73.45	116.87	13.6	1591	108.2215	1473
08:24	4.43	49.89	91.02	20.0	1824	91.569647	1835
08:25	3.69	68.54	109.27	14.6	1594	105.94727	1546
08:26	3.64	71.5	110.77	14.0	1549	107.36857	1502
08:27	3.88	62.67	103.92	16.0	1658	102.58708	1637
08:28	3.87	54.11	104.19	18.5	1925	95.927847	1773
08:29	3.79	90.67	106.39	11.0	1173	113.67883	1254
08:30	3.94	78.89	102.34	12.7	1297	110.30359	1398
08:31	4.66	97.33	86.52	10.3	889	115.09869	1183
08:32	3.89	51.45	103.65	19.4	2015	93.281807	1813
08:33	3.77	60.33	106.95	16.6	1773	101.00469	1674
08:34	3.74	67	107.81	14.9	1609	105.14071	1569
08:35	4.27	113	94.43	8.8	836	117.54562	1040
08:36	4.11	49	98.10	20.4	2002	90.534351	1848
08:37	3.77	62.5	106.95	16.0	1711	102.47728	1640
08:38	3.76	64	107.23	15.6	1676	103.4199	1616

TIME	Average Travel Time	Average Spacing	Average Speed	Average Density	Calculated Flow	Predicted Speed	Predicted Flow
08:39	3.72	79.67	108.39	12.6	1360	110.57053	1388
08:40	3.52	79.75	114.55	12.5	1436	110.59751	1387
08:41	3.85	77	104.73	13.0	1360	109.62569	1424
08:42	3.69	51.4	109.27	19.5	2126	93.228864	1814
08:43	3.46	68.5	116.53	14.6	1701	105.92693	1546
08:44	3.55	77.5	113.58	12.9	1466	109.80945	1417
08:45	3.75	63.43	107.52	15.8	1695	103.06857	1625
08:46	4.31	44.4	93.55	22.5	2107	84.406797	1901
08:47	3.51	59.67	114.87	16.8	1925	100.52923	1685
08:48	3.58	58.31	112.63	17.1	1931	99.505751	1706
08:49	3.32	55.88	121.45	17.9	2173	97.517984	1745
08:50	3.6	59.33	112.00	16.9	1888	100.27898	1690
08:51	3.88	53	103.92	18.9	1961	94.863151	1790
08:52	3.67	75.14	109.86	13.3	1462	108.91253	1449
08:53	3.27	58	123.30	17.2	2126	99.263864	1711
08:54	3.73	96.75	108.10	10.3	1117	114.98593	1188
08:55	3.8	55.27	106.11	18.1	1920	96.984284	1755

Table A- 2: Speed/Density measurements made during consecutive 1 min intervals on Section 1 in the north bound direction

TIME	Average Travel Time	Average Spacing	Average Speed	Average Density	Calculated Flow
07:24	3.91	45.13	103.12	22.16	2285
07:25	3.44	68.46	117.21	14.61	1712
07:26	3.27	113.00	123.30	8.85	1091
07:27	3.04	78.00	132.63	12.82	1700
07:28	3.51	58.07	114.87	17.22	1978
07:29	3.60	46.20	112.00	21.65	2424
07:30	3.60	50.89	112.00	19.65	2201
07:31	3.14	56.20	128.41	17.79	2285
07:32	3.41	79.33	118.24	12.61	1490
07:33	4.59	36.00	87.84	27.78	2440
07:34	3.28	86.00	122.93	11.63	1429
07:35	3.37	57.00	119.64	17.54	2099
07:36	3.70	61.21	108.97	16.34	1780
07:37	3.40	52.35	118.59	19.10	2265
07:38	3.20	84.50	126.00	11.83	1491
07:39	3.13	58.81	128.82	17.00	2190
07:40	3.94	50.00	102.34	20.00	2047
07:41	3.63	82.25	111.07	12.16	1350
07:42	3.36	54.00	120.00	18.52	2222
07:43	3.37	61.40	119.64	16.29	1949
07:44	3.43	81.00	117.55	12.35	1451
07:45	3.77	44.92	106.95	22.26	2381
07:46	3.27	72.33	123.30	13.83	1705
07:47	3.13	74.00	128.82	13.51	1741
07:48	3.40	50.00	118.59	20.00	2372
07:49	3.41	55.78	118.24	17.93	2120
07:50	3.06	87.00	131.76	11.49	1515
07:51	3.97	43.00	101.56	23.26	2362
07:52	3.37	52.60	119.64	19.01	2275
07:53	3.34	64.25	120.72	15.56	1879
07:54	3.34	77.30	120.72	12.94	1562
07:55	3.49	52.85	115.53	18.92	2186

TIME	Average Travel Time	Average Spacing	Average Speed	Average Density	Calculated Flow
07:56	3.50	49.50	115.20	20.20	2327
07:57	3.17	80.00	127.19	12.50	1590
07:58	3.53	50.00	114.22	20.00	2284
07:59	3.43	70.06	117.55	14.27	1678
08:00	3.23	62.00	124.83	16.13	2013
08:01	3.44	73.00	117.21	13.70	1606
08:02	3.64	56.40	110.77	17.73	1964
08:03	3.39	64.54	118.94	15.49	1843
08:04	3.15	103.33	128.00	9.68	1239
08:05	3.58	102.00	112.63	9.80	1104
08:06	3.89	53.81	103.65	18.58	1926
08:07	3.54	51.54	113.90	19.40	2210
08:08	3.27	66.28	123.30	15.09	1860
08:09	3.52	113.50	114.55	8.81	1009
08:10	3.47	62.00	116.20	16.13	1874
08:11	3.30	83.77	122.18	11.94	1459
08:12	3.25	61.14	124.06	16.36	2029
08:13	3.15	62.67	128.00	15.96	2042
08:14	3.33	50.80	121.08	19.69	2383
08:15	3.15	65.00	128.00	15.38	1969
08:16	3.28	80.00	122.93	12.50	1537
08:17	3.11	71.25	129.65	14.04	1820
08:18	4.17	43.44	96.69	23.02	2226
08:19	3.46	96.25	116.53	10.39	1211
08:20	3.39	50.56	118.94	19.78	2352
08:21	3.54	48.50	113.90	20.62	2348
08:22	3.79	59.20	106.39	16.89	1797
08:23	3.48	75.00	115.86	13.33	1545
08:24	3.65	50.80	110.47	19.69	2175
08:25	3.85	54.20	104.73	18.45	1932
08:26	3.21	71.00	125.61	14.08	1769
08:27	3.24	68.21	124.44	14.66	1824
08:28	3.39	75.00	118.94	13.33	1586
08:29	3.79	57.55	106.39	17.38	1849
08:30	3.27	54.50	123.30	18.35	2262

TIME	Average Travel Time	Average Spacing	Average Speed	Average Density	Calculated Flow
08:31	3.11	69.71	129.65	14.35	1860
08:32	3.52	53.00	114.55	18.87	2161
08:33	3.53	80.25	114.22	12.46	1423
08:34	3.25	56.00	124.06	17.86	2215
08:35	3.38	53.50	119.29	18.69	2230
08:36	3.73	46.80	108.10	21.37	2310
08:37	3.42	86.29	117.89	11.59	1366
08:38	3.50	66.17	115.20	15.11	1741
08:39	3.40	59.00	118.59	16.95	2010
08:40	3.73	60.38	108.10	16.56	1790
08:41	4.30	48.00	93.77	20.83	1953
08:42	3.44	51.00	117.21	19.61	2298
08:43	3.22	76.00	125.22	13.16	1648
08:44	3.28	60.67	122.93	16.48	2026

Table A- 3: Speed/Flow/Density measurements made during consecutive 1 min intervals on Section 2 in the south bound direction

Time	Average Travel Time	Average Spacing	Average Speed	Average Density	Calculated Flow	Predicted Speed	Average Flow
07:31	2.98	58.08	94.23	17.22	1622	103.611	1784
07:32	3.1	58.85	90.58	16.99	1539	104.100	1769
07:33	3.45	47.22	81.39	21.18	1724	94.414	1999
07:34	3.01	43.68	93.29	22.89	2136	90.148	2064
07:35	3.08	50.11	91.17	19.96	1819	97.359	1943
07:36	3.41	40.31	82.35	24.81	2043	85.254	2115
07:37	3.91	32.56	71.82	30.71	2206	69.771	2143
07:38	3.18	46.35	88.30	21.57	1905	93.438	2016
07:39	3.5	42.48	80.23	23.54	1889	88.508	2084
07:40	3.89	34.5	72.19	28.99	2092	74.310	2154
07:41	8.31	29.29	33.79	34.14	1154	60.902	2079
07:42	18.66	9.54	15.05	104.82	1577	13.306	1395
07:43	17.29	8.21	16.24	121.80	1978	8.904	1084
07:44	15.36	10.26	18.28	97.47	1782	15.439	1505
07:45	17.17	10.31	16.35	96.99	1586	15.582	1511
07:46	10.78	14.32	26.05	69.83	1819	25.214	1761
07:47	9.41	16.73	29.84	59.77	1784	29.775	1780
07:48	4.41	39.08	63.67	25.59	1629	54.650	1398
07:49	3.71	49.42	75.69	20.23	1532	61.533	1245
07:50	4.29	33.87	65.45	29.52	1933	50.455	1490
07:51	10.32	11.62	27.21	86.06	2342	19.089	1643
07:52	11.8	12.26	23.80	81.57	1941	20.661	1685
07:53	10.85	16.98	25.88	58.89	1524	30.210	1779
07:54	10.52	15.45	26.69	64.72	1728	27.441	1776
07:55	9.04	23.13	31.06	43.23	1343	39.273	1698
07:56	9.68	18.68	29.01	53.53	1553	33.008	1767
07:57	8.96	22.19	31.34	45.07	1412	38.056	1715
07:58	9	22.53	31.20	44.39	1385	38.502	1709
07:59	8.31	26.16	33.79	38.23	1292	42.882	1639
08:00	10	23.97	28.08	41.72	1171	40.318	1682
08:01	5.87	29.03	47.84	34.45	1648	60.126	2071
08:02	3.27	36.65	85.87	27.29	2343	78.786	2150
08:03	2.79	49.26	100.65	20.30	2043	96.537	1960
08:04	3.38	38.42	83.08	26.03	2162	82.081	2136
08:05	3.74	33.82	75.08	29.57	2220	72.776	2152
08:06	3.19	63.97	88.03	15.63	1376	106.962	1672

TIME	Average Travel Time	Average Spacing	Average Speed	Average Density	Calculated Flow	Predicted Speed	Predicted Flow
08:07	2.97	65.28	94.55	15.32	1448	107.599	1648
08:08	2.88	49.18	97.50	20.33	1983	96.458	1961
08:09	2.56	64.56	109.69	15.49	1699	107.253	1661
08:10	2.74	47.53	102.48	21.04	2156	94.751	1994
08:11	2.62	50.5	107.18	19.80	2122	97.724	1935
08:12	3.11	52.78	90.29	18.95	1711	99.725	1889
08:13	2.86	61.98	98.18	16.13	1584	105.925	1709
08:14	2.55	56.06	110.12	17.84	1964	102.242	1824
08:15	2.49	82.29	112.77	12.15	1370	113.476	1379
08:16	2.52	66.79	111.43	14.97	1668	108.291	1621
08:17	2.66	62.88	105.56	15.90	1679	106.405	1692
08:18	3	47.32	93.60	21.13	1978	94.524	1998
08:19	2.76	61.2	101.74	16.34	1662	105.493	1724
08:20	3.01	70.24	93.29	14.24	1328	109.723	1562
08:21	2.76	58.21	101.74	17.18	1748	103.694	1781
08:22	2.84	43.5	98.87	22.99	2273	89.908	2067
08:23	2.7	57.29	104.00	17.46	1815	103.090	1799
08:24	2.68	51.81	104.78	19.30	2022	98.901	1909
08:25	2.52	67	111.43	14.93	1663	108.384	1618
08:26	2.79	51.61	100.65	19.38	1950	98.726	1913
08:27	3.14	56.91	89.43	17.57	1571	102.833	1807
08:28	2.6	66.83	108.00	14.96	1616	108.309	1621
08:29	2.82	48.5	99.57	20.62	2053	95.772	1975
08:30	2.68	61.32	104.78	16.31	1709	105.561	1721
08:31	2.79	63.91	100.65	15.65	1575	106.932	1673
08:32	2.93	59.75	95.84	16.74	1604	104.651	1751
08:33	3	54.61	93.60	18.31	1714	101.177	1853
08:34	2.71	57.21	103.62	17.48	1811	103.037	1801
08:35	3.24	44.36	86.67	22.54	1954	91.031	2052
08:36	2.58	60.53	108.84	16.52	1798	105.111	1737
08:37	2.3	70.13	122.09	14.26	1741	109.680	1564
08:38	2.77	55.58	101.37	17.99	1824	101.898	1833
08:39	2.59	71.2	108.42	14.04	1523	110.088	1546
08:40	2.85	52.64	98.53	19.00	1872	99.608	1892
08:41	2.73	59.53	102.86	16.80	1728	104.518	1756
08:42	2.51	60.75	111.87	16.46	1842	105.237	1732
08:43	3.17	45.86	88.58	21.81	1932	92.869	2025
08:44	2.69	54.63	104.39	18.30	1911	101.193	1852
08:45	2.25	71.75	124.80	13.94	1739	110.290	1537

TIME	Average Travel Time	Average Spacing	Average Speed	Average Density	Calculated Flow	Predicted Speed	Predicted Flow
08:46	2.46	64.87	114.15	15.42	1760	107.403	1656
08:47	3.07	48.67	91.47	20.55	1879	95.946	1971
08:48	2.62	59.06	107.18	16.93	1815	104.230	1765
08:49	3.07	58.54	91.47	17.08	1562	103.905	1775
08:50	2.58	53.92	108.84	18.55	2018	100.645	1867
08:51	2.78	44.4	101.01	22.52	2275	91.082	2051
08:52	3.59	43.24	78.22	23.13	1809	89.559	2071
08:53	2.87	51.14	97.84	19.55	1913	98.309	1922
08:54	2.6	53.08	108.00	18.84	2035	99.972	1883
08:55	2.61	62.68	107.59	15.95	1716	106.300	1696
08:56	2.75	56.62	102.11	17.66	1803	102.634	1813
08:57	2.84	44.36	98.87	22.54	2229	91.031	2052
08:58	2.99	51.26	93.91	19.51	1832	98.416	1920
08:59	2.74	43.37	102.48	23.06	2363	89.734	2069
09:00	2.43	63	115.56	15.87	1834	106.468	1690
09:01	2.69	51.01	104.39	19.60	2046	98.192	1925
09:02	2.92	51.69	96.16	19.35	1860	98.796	1911
09:03	3.41	35.54	82.35	28.14	2317	76.544	2154
09:04	3.17	44.41	88.58	22.52	1995	91.094	2051
09:05	2.96	46.21	94.86	21.64	2053	93.277	2019
09:06	3.61	49.3	77.78	20.28	1578	96.577	1959
09:07	2.46	59.83	114.15	16.71	1908	104.699	1750
09:08	2.32	51.88	121.03	19.28	2333	98.962	1908
09:09	2.64	68.56	106.36	14.59	1551	109.050	1591
09:10	2.64	57.64	106.36	17.35	1845	103.323	1793
09:11	2.96	68.75	94.86	14.55	1380	109.129	1587
09:12	2.54	71.69	110.55	13.95	1542	110.269	1538
09:13	2.62	53.63	107.18	18.65	1998	100.415	1872
09:14	3.37	38.19	83.32	26.18	2182	81.671	2139
09:15	3.05	53.89	92.07	18.56	1708	100.621	1867
09:16	2.86	44.33	98.18	22.56	2215	90.992	2053
09:17	2.98	52.19	94.23	19.16	1805	99.228	1901
09:18	2.75	51.44	102.11	19.44	1985	98.576	1916
09:19	2.85	68.2	98.53	14.66	1445	108.900	1597
09:20	2.65	48	105.96	20.83	2208	95.252	1984
09:21	2.85	85	98.53	11.76	1159	114.120	1343
09:22	2.86	56.27	98.18	17.77	1745	102.390	1820
09:23	2.75	43.7	102.11	22.88	2337	90.174	2063
09:24	2.62	56.44	107.18	17.72	1899	102.509	1816

TIME	Average Travel Time	Average Spacing	Average Speed	Average Density	Calculated Flow	Predicted Speed	Predicted Flow
09:25	2.72	56.05	103.24	17.84	1842	102.235	1824
09:26	2.64	55.5	106.36	18.02	1916	101.839	1835
09:27	3.11	42	90.29	23.81	2150	87.821	2091
09:28	2.79	48.64	100.65	20.56	2069	95.915	1972
09:29	2.79	49.86	100.65	20.06	2019	97.121	1948
09:30	2.87	45.35	97.84	22.05	2157	92.260	2034
09:31	2.66	47.43	105.56	21.08	2226	94.643	1995
09:32	2.54	90	110.55	11.11	1228	115.168	1280
09:33	2.99	53.15	93.91	18.81	1767	100.029	1882
09:34	3.02	47.67	92.98	20.98	1950	94.902	1991
09:35	2.74	46.45	102.48	21.53	2206	93.553	2014
09:36	2.57	45.58	109.26	21.94	2397	92.537	2030
09:37	2.31	69.17	121.56	14.46	1757	109.300	1580
09:38	2.57	92	109.26	10.87	1188	115.543	1256
09:39	2.96	48.22	94.86	20.74	1967	95.483	1980
09:40	2.65	67.75	105.96	14.76	1564	108.710	1605
09:41	2.47	64.88	113.68	15.41	1752	107.408	1655
09:42	2.2	71.33	127.64	14.02	1789	110.136	1544
09:43	2.74	65	102.48	15.38	1577	107.466	1653
09:44	2.74	53.68	102.48	18.63	1909	100.455	1871
09:45	2.44	52.5	115.08	19.05	2192	99.491	1895
09:46	2.44	70.67	115.08	14.15	1628	109.888	1555
09:47	2.5	50.86	112.32	19.66	2208	98.055	1928
09:48	2.64	49.07	106.36	20.38	2168	96.349	1963
09:49	2.63	58.38	106.77	17.13	1829	103.803	1778
09:50	2.59	50	108.42	20.00	2168	97.255	1945
09:51	3.3	47.77	85.09	20.93	1781	95.009	1989

Table A- 4: Speed/Density/Flow measurements made during consecutive 1 min intervals on Section 2 in the north bound direction

Time	Average Travel Time	Average Spacing	Average Speed	Average Density	Calculated Flow
07:31	2.62	61.5	107.18	16.26	1743
07:32	2.45	62.29	114.61	16.05	1840
07:33	2.85	45	98.53	22.22	2189
07:34	2.73	66.67	102.86	15.00	1543
07:35	2.49	70.25	112.77	14.23	1605
07:36	2.26	83.2	124.25	12.02	1493
07:37	2.61	60.35	107.59	16.57	1783
07:38	2.55	54.25	110.12	18.43	2030
07:39	2.58	68.43	108.84	14.61	1590
07:40	2.5	74.44	112.32	13.43	1509
07:41	2.97	58.13	94.55	17.20	1626
07:42	2.56	59.11	109.69	16.92	1856
07:43	2.7	54.79	104.00	18.25	1898
07:44	2.37	76.25	118.48	13.11	1554
07:45	2.34	82	120.00	12.20	1463
07:46	2.82	68.67	99.57	14.56	1450
07:47	2.94	50.9	95.51	19.65	1876
07:48	2.88	52.91	97.50	18.90	1843
07:49	2.48	54	113.23	18.52	2097
07:50	2.95	43.42	95.19	23.03	2192
07:51	2.92	48.1	96.16	20.79	1999
07:52	2.84	49.5	98.87	20.20	1997
07:53	2.44	49.33	115.08	20.27	2333
07:54	2.73	46.4	102.86	21.55	2217
07:55	2.61	55	107.59	18.18	1956
07:56	2.69	78	104.39	12.82	1338
07:57	2.78	52	101.01	19.23	1942
07:58	2.51	76.6	111.87	13.05	1460
07:59	2.69	44.11	104.39	22.67	2367
08:00	2.65	56.55	105.96	17.68	1874
08:01	2.53	54.29	110.99	18.42	2044
08:02	2.85	55.25	98.53	18.10	1783
08:03	2.42	64.5	116.03	15.50	1799
08:04	2.64	45.58	106.36	21.94	2334

Time	Average Travel Time	Average Spacing	Average Speed	Average Density	Calculated Flow
08:05	2.4	70.86	117.00	14.11	1651
08:06	2.45	49.6	114.61	20.16	2311
08:07	2.47	58.33	113.68	17.14	1949
08:08	2.52	61.3	111.43	16.31	1818
08:09	2.42	67.5	116.03	14.81	1719
08:10	2.46	64.5	114.15	15.50	1770
08:11	2.51	120	111.87	8.33	932
08:12	2.63	56.13	106.77	17.82	1902
08:13	2.3	87	122.09	11.49	1403
08:14	2.54	74.63	110.55	13.40	1481
08:15	2.4	69.89	117.00	14.31	1674
08:16	2.31	58.33	121.56	17.14	2084
08:17	2.18	59.71	128.81	16.75	2157
08:18	2.35	100.5	119.49	9.95	1189
08:19	2.34	63.45	120.00	15.76	1891
08:20	2.36	62.7	118.98	15.95	1898
08:21	2.3	58.83	122.09	17.00	2075
08:22	2.2	57	127.64	17.54	2239
08:23	2.31	52	121.56	19.23	2338
08:24	2.57	62.81	109.26	15.92	1740
08:25	2.31	68.55	121.56	14.59	1773
08:26	2.32	44.25	121.03	22.60	2735
08:27	2.3	81	122.09	12.35	1507
08:28	2.28	60	123.16	16.67	2053
08:29	2.59	52.71	108.42	18.97	2057
08:30	2.43	51.21	115.56	19.53	2257
08:31	2.39	63	117.49	15.87	1865
08:32	2.41	54.13	116.51	18.47	2152
08:33	2.69	46.5	104.39	21.51	2245
08:34	2.54	62.6	110.55	15.97	1766
08:35	2.28	63.7	123.16	15.70	1933
08:36	2.53	66.8	110.99	14.97	1661
08:37	2.95	48.44	95.19	20.64	1965
08:38	2.94	43.2	95.51	23.15	2211
08:39	2.45	68.25	114.61	14.65	1679
08:40	2.53	62.2	110.99	16.08	1784
08:41	2.52	80	111.43	12.50	1393

Time	Average Travel Time	Average Spacing	Average Speed	Average Density	Calculated Flow
08:42	2.18	54.2	128.81	18.45	2377
08:43	2.8	74.89	100.29	13.35	1339
08:44	2.46	52.82	114.15	18.93	2161
08:45	2.35	63.5	119.49	15.75	1882
08:46	2.32	70	121.03	14.29	1729
08:47	2.7	88.38	104.00	11.31	1177
08:48	2.53	54.11	110.99	18.48	2051
08:49	2.29	56.5	122.62	17.70	2170
08:50	2.46	73.5	114.15	13.61	1553
08:51	2.99	41.6	93.91	24.04	2258
08:52	2.54	59.86	110.55	16.71	1847
08:53	2.64	120	106.36	8.33	886
08:54	2.57	47	109.26	21.28	2325
08:55	2.46	68.5	114.15	14.60	1666
08:56	2.36	67.17	118.98	14.89	1771
08:57	2.3	58.25	122.09	17.17	2096
08:58	2.49	47.5	112.77	21.05	2374
08:59	2.66	50.17	105.56	19.93	2104
09:00	2.39	55	117.49	18.18	2136
09:01	2.69	57.83	104.39	17.29	1805
09:02	2.43	69.73	115.56	14.34	1657
09:03	2.48	48.88	113.23	20.46	2316
09:04	2.47	57.75	113.68	17.32	1969
09:05	2.85	115	98.53	8.70	857
09:06	2.63	61	106.77	16.39	1750
09:07	3.03	44.5	92.67	22.47	2083
09:08	2.19	55.5	128.22	18.02	2310
09:09	2.54	55.86	110.55	17.90	1979
09:10	2.43	62.29	115.56	16.05	1855
09:11	2.6	73.93	108.00	13.53	1461
09:12	2.54	63.94	110.55	15.64	1729
09:13	2.3	81.33	122.09	12.30	1501
09:14	2.78	115	101.01	8.70	878
09:15	2.79	42.45	100.65	23.56	2371
09:16	2.35	59.25	119.49	16.88	2017
09:17	2.6	50.57	108.00	19.77	2136
09:18	2.41	61.61	116.51	16.23	1891

Time	Average Travel Time	Average Spacing	Average Speed	Average Density	Calculated Flow
09:19	2.17	76.25	129.40	13.11	1697
09:20	2.64	92	106.36	10.87	1156
09:21	2.5	61.89	112.32	16.16	1815
09:22	2.5	61.06	112.32	16.38	1840
09:23	2.35	63.33	119.49	15.79	1887
09:24	2.64	125	106.36	8.00	851
09:25	2.87	48.88	97.84	20.46	2002
09:26	2.56	46.25	109.69	21.62	2372
09:27	2.47	58.8	113.68	17.01	1933
09:28	2.34	66.4	120.00	15.06	1807
09:29	2.46	70.14	114.15	14.26	1627
09:30	2.77	58.43	101.37	17.11	1735
09:31	2.29	80.5	122.62	12.42	1523
09:32	2.33	50.63	120.52	19.75	2380
09:33	2.21	54	127.06	18.52	2353
09:34	2.21	61.6	127.06	16.23	2063
09:35	2.4	77.17	117.00	12.96	1516
09:36	2.39	69	117.49	14.49	1703
09:37	2.15	56	130.60	17.86	2332
09:38	2.44	58.19	115.08	17.19	1978
09:39	2.23	60.14	125.92	16.63	2094
09:40	2.41	57.33	116.51	17.44	2032
09:41	2.57	63.22	109.26	15.82	1728
09:42	2.47	81	113.68	12.35	1404
09:43	2.69	58	104.39	17.24	1800
09:44	2.54	68.95	110.55	14.50	1603
09:45	3.32	60.75	84.58	16.46	1392
09:46	3.3	67.54	85.09	14.81	1260

Table A- 5: Speed/Flow/Density measurements made during consecutive 5 min intervals on Section 1 in the south bound direction

Time	Average Travel Time	Average Spacing	Average Speed	Average Density	Calculated Flow	Predicted Speed	Predicted Flow
7:24-7:28	3.93	62.0241	102.5954	16.12277	1654	108.10285	1743
7:29-7-33	4.07	64.97917	99.06634	15.38955	1525	111.66741	1719
7:34-7:38	3.89	64.95082	103.6504	15.39626	1596	111.63548	1719
7:39-7:43	7.16	39.26744	56.31285	25.46639	1434	55.985949	1426
7:44-7:48	4.96	53.00962	81.29032	18.8645	1534	93.585733	1765
7:49-7:53	2.72	67.04651	148.2353	14.91502	2211	113.8878	1699
7:54-7:58	3.61	59.94286	111.6898	16.68255	1863	105.28005	1756
7:59-8:03	3.77	54	106.9496	18.51852	1981	95.501896	1769
8:04-8:08	3.79	66.67442	106.3852	14.99826	1596	113.50346	1702
8:09-8:13	3.94	68.03774	102.335	14.69773	1504	114.88063	1688
8:14-8:18	3.85	59.61538	104.7273	16.77419	1757	104.81013	1758
8:19-8:23	3.74	68.82927	107.8075	14.5287	1566	115.64221	1680
8:24-8:28	3.84	55.41935	105	18.04424	1895	98.094939	1770
8:29-8:33	3.6	59.39024	112	16.83778	1886	104.48281	1759
8:34-8:38	3.72	63.7	108.3871	15.69859	1702	110.18419	1730
8:39-8:43	31.7	13.55882	12.71924	73.75273	938	2.411E-05	0
8:44-8:48	16.2	32.29508	24.88889	30.96447	771	29.67717	919
8:49-8:53	19.68	20.07333	20.4878	49.81734	1021	0.5682953	28
8:54-8:56	19.21	29.38971	20.98907	34.02551	714	19.015699	647

Table A- 6: Speed/Density/Flow measurements made during consecutive 5 min intervals on Section 1 in the north bound direction

Time	Average Travel Time	Average Spacing	Average Speed	Average Density	Calculated Flow
7:24-7:28	3.29	62.67742	122.5532	15.954709	1955.30051
7:29-7-33	3.52	46.55263	114.5455	21.481063	2460.55818
7:34-7:38	3.26	67.39286	123.681	14.838367	1835.22381
7:39-7:43	3.12	61.68	129.2308	16.212711	2095.18108
7:44-7:48	3.32	52.82609	121.4458	18.93004	2298.97354
7:49-7:53	3.11	61.92857	129.6463	16.147636	2093.48128
7:54-7:58	3.3	56.94286	122.1818	17.561464	2145.69163
7:59-8:03	3.16	66.11538	127.5949	15.125074	1929.88283
8:04-8:08	3.15	68.70588	128	14.554795	1863.01376
8:09-8:13	3.3	59.34615	122.1818	16.850293	2058.7994
8:14-8:18	3.14	71.72857	128.4076	13.941446	1790.18825
8:19-8:23	3.03	65.77778	133.0693	15.202702	2023.01304
8:24-8:28	3.46	55.6875	116.5318	17.957351	2092.60232
8:29-8:33	3.33	62.31579	121.0811	16.047297	1943.02409
8:34-8:38	3.25	60.5	124.0615	16.528926	2050.60394
8:39-8:43	3.12	67.875	129.2308	14.732965	1903.9524
8:44-8:49	3.27	64.59259	123.3028	15.481652	1908.9303
8:50-8:55	3.36	57.48	120	17.397356	2087.68267

Table A- 7: Speed/Flow/Density measurements made during consecutive 5 min intervals on Section 2 in the south bound direction

Time	Average Travel Time	Average Spacing	Average Speed	Average Density	Calculated Flow	Predicted Speed	Predicted Flow
7:31-7:35	3.13	50.87	89.712	19.658	1764	97.0805937	1908
7:36-7:40	3.56	39.76	78.876	25.151	1984	82.5949865	2077
7:41-7:45	14.75	14.4	19.037	69.444	1322	5.2758122	366
7:46-7:50	6.38	30.96	44.013	32.300	1422	63.0741243	2037
7:51-7:55	10.51	15.99	26.717	62.539	1671	9.59733499	600
7:56-8:00	9.2	22.66	30.522	44.131	1347	34.8361259	1537
8:01-8:05	3.73	36.88	75.282	27.115	2041	77.2119643	2094
8:06-8:10	2.87	55.09	97.840	18.152	1776	100.778121	1829
8:11-8:15	2.88	58.23	97.500	17.173	1674	103.092069	1770
8:16-8:20	2.85	59.55	98.526	16.793	1655	103.970909	1746
8:21-8:25	2.68	58.1	104.776	17.212	1803	103.002682	1773
8:26-8:30	2.84	55.68	98.873	17.960	1776	101.238737	1818
8:31-8:35	2.96	54.97	94.865	18.192	1726	100.68288	1832
8:36-8:40	2.66	59.51	105.564	16.804	1774	103.945027	1747
8:41-8:45	2.74	56.09	102.482	17.828	1827	101.551494	1811
8:46-8:50	2.78	55.99	101.007	17.860	1804	101.475757	1812
8:51-8:55	2.91	50.38	96.495	19.849	1915	96.6003532	1917
8:56-9:00	2.77	51.72	101.372	19.335	1960	97.8868339	1893
9:01-9:05	3.03	45.6	92.673	21.930	2032	91.2416595	2001
9:06-9:10	2.74	58.3	102.482	17.153	1758	103.139986	1769
9:11-9:15	2.97	54.06	94.545	18.498	1749	99.9429507	1849
9:16-9:20	2.83	47.38	99.223	21.106	2094	93.3904736	1971
9:21-9:25	2.75	51.22	102.109	19.524	1994	97.4166276	1902
9:26-9:30	2.84	46.65	98.873	21.436	2119	92.5329456	1984
9:31-9:35	2.82	50.12	99.574	19.952	1987	96.3407877	1922
9:36-9:40	2.64	49.11	106.364	20.362	2166	95.3001303	1941
9:41-9:45	2.58	55.79	108.837	17.924	1951	101.323229	1816
8:46-9:50	2.77	49.06	101.372	20.383	2066	95.2472398	1941

Table A- 8: Speed/Density/Flow measurements made during consecutive 5 min intervals on Section 2 in the north bound direction

Time	Average Travel Time	Average Spacing	Average Speed	Average Density	Calculated Flow
7:31-7:35	2.63	61.28	106.7681	16.31854	1742
7:36-7:40	2.51	68.16	111.8725	14.67136	1641
7:41-7:45	2.63	61.65	106.7681	16.2206	1732
7:46-7:50	2.82	53.43	99.57447	18.71608	1864
7:51-7:55	2.74	49.21	102.4818	20.32107	2083
7:56-8:00	2.69	53.01	104.3866	18.86437	1969
8:01-8:05	2.59	55.87	108.417	17.89869	1941
8:06-8:10	2.47	59.97	113.6842	16.675	1896
8:11-8:15	2.48	65.63	113.2258	15.23693	1725
8:16-8:20	2.31	64.48	121.5584	15.50868	1885
8:21-8:25	2.35	62.1	119.4894	16.10306	1924
8:26-8:30	2.41	52.64	116.5145	18.99696	2213
8:31-8:35	2.46	58.24	114.1463	17.17033	1960
8:36-8:40	2.69	57	104.3866	17.54386	1831
8:41-8:45	2.47	62.3	113.6842	16.05136	1825
8:46-8:50	2.47	64.17	113.6842	15.58361	1772
8:51-8:55	2.62	61.28	107.1756	16.31854	1749
8:56-9:00	2.5	58.12	112.32	17.20578	1933
9:01-9:05	2.49	60	112.7711	16.66667	1880
9:06-9:10	2.72	53	103.2353	18.86792	1948
9:11-9:15	2.5	63.87	112.32	15.6568	1759
9:16-9:20	2.63	51.93	106.7681	19.25669	2056
9:21-9:25	2.43	65.59	115.5556	15.24623	1762
9:26-9:30	2.58	53.12	108.8372	18.8253	2049
9:31-9:35	2.52	61.11	111.4286	16.36393	1823
9:36-9:40	2.31	61.83	121.5584	16.17338	1966
9:41-9:45	2.36	59.48	118.9831	16.81237	2000
8:46-9:50	2.83	65.53	99.22261	15.26019	1514

Table A- 9: Summary of regression analysis data for Section 1 under 1-min time intervals

Model	Equation	Direction	*m*	*l*	U_f	K_j	U_o	K_o	C	n	R^2
Greenshields	$u = u_f\ (1-\frac{k}{k_j})$	South	0	2	121.6	86					0.733
		North	0	2	139.16	104					0.375
Greenberg	$u = u_o \ln\left(\frac{k_j}{k}\right)$	South	0	1		103	52.72				0.786
		North	0	1		6168	19.68				0.304
Underwood	$u = u_f . e^{-k/k_o}$	South	1	2	157.27			32			0.824
		North	1	2	142.56			83			0.391
Drake et al.	$u = u_f e^{\frac{-1}{2}(\frac{k}{k_o})^2}$	South	1	3	124.87			25.45			0.86
		North	1	3	130.15			36.46			0.402
Drew	$u = u_f[1-(\frac{k}{k_j})^{n+1/2}]$	South	0	2/3	173.4	88				0	0.786
		North	0	2/3	123.64	36.46				6.9	0.465
Multi regime	$\ln\left(\frac{U_f}{U}\right) = c.K^{l-1}$ $U^{1-m} = U_f{}^{1-m} + c.K^{l-1}$	South	1	2.050	124.9				2.95E-02		0.818
		North	1.1715	3.523	120				2.16E-06		0.432
Composite	$u = u_f e^{\frac{-1}{2}(\frac{k}{k_o})^2}$ $u = u_o \ln\left(\frac{k_j}{k}\right)$	South (free flow cond.)	1	3	124.87			25.45			0.876
		(Congested cond.)	0	1		110.4	35.16				

Table A- 10: Summary of regression analysis data for Section 2 under 1-min intervals

Model	Equation	Direction	*m*	*l*	U_f	K_j	U_o	K_o	C	n	R 2
Greenshields	$u = u_f\ (1-\frac{k}{k_j})$	South	0	2	121.27	97.48					0.74
		North	0	2	122.94	181.46					0.059
Greenberg	$u = u_o \ln\left(\frac{k_j}{k}\right)$	South	0	1		117.245	53.45				0.842
		North	0	1		24461393	7.85				0.0338
Underwood	$u = u_f . e^{-k/k_o}$	South	1	2	150.3			42			0.861
		North	1	2	123.68			166.67			0.0615
Drake et al.	$u = u_f e^{\frac{-1}{2}(\frac{k}{k_o})^2}$	South	1	3	124.19			28.6			0.879
		North	1	3	119.04			47.21			0.087
Drew	$u = u_f[1-(\frac{k}{k_j})^{n+1/2}]$	South	0	2/3	173.38	100.13				0	0.813
		North	0	2/3	114	28.66				17.18	0.173
Multi regime	$U^{1-m} = U_f^{1-m} + c.K^{l-1}$	South	2	2.999	120				5.49.E-06		0.867
	$\ln\left(\frac{U_f}{U}\right) = c.K^{l-1}$	North	1	3.957	118.37				1.24.E05		0.11
Composite	$u = u_f e^{\frac{-1}{2}(\frac{k}{k_o})^2}$	South (free flow cond.)	1	3	124.19			28.6			0.898
	$u = u_o \ln\left(\frac{k_j}{k}\right)$	(Congested cond.)	0	1		165	29.32				

Table A- 11: Summary of regression analysis data for Section 1 observed in 5-min time intervals

Model	Equation	Direction	*m*	*l*	Uf	Kj	Uo	Ko	C	n	R 2
Greenshields	$u = u_f\ (1-\frac{k}{k_j})$	South	0	2	135.68	63.55					0.693
		North	0	2	157.78	77.13					0.586
Greenberg	$u = u_o\ \ln\left(\frac{k_j}{k}\right)$	South	0	1		77.5	62.25				0.831
		North	0	1		35.3	634.22				0.587
Underwood	$u = u_{f.}e^{-k/k_o}$	South	1	2	199.04			22.72			0.832
		North	1	2	163.2			58.82			0.598
Drake et al.	$u = u_f e^{\frac{-1}{2}(\frac{k}{k_o})^2}$	South	1	3	165			17.33			0.905
		North	1	3	141.5			32.28			0.581
Drew	$u = u_f[1-(\frac{k}{k_j})^{n+1/2}]$	South	0	2/3	210.36	62.12				0	0.771
		North	0	2/3	141.5	52.24				1.31	0.579
Multi regime	$\ln\left(\frac{U_f}{U}\right) = c.K^{l-1}$	South	1	3.643	143.07				1.8 E-04		0.911
	$\ln\left(\frac{U_f}{U}\right) = c.K^{l-1}$	North	1	2.768	144.39				1.06E-03		0.583

Table A- 12: Summary of regression analysis data for Section 2 under 5-min intervals

Model	Equation	Direction	*m*	*l*	Uf	Kj	Uo	Ko	C	n	R 2
Greenshields	$u = u_f\ (1-\frac{k}{k_j})$	South	0	2	131.88	72.87					0.874
		North	0	2	142.2	76.61					0.201
Greenberg	$u = u_o\ \ln\left(\frac{k_j}{k}\right)$	South	0	1		65.27	85.48				0.922
		North	0	1		31.49	586				0.194
Underwood	$u = u_f.e^{-k/k_o}$	South	1	2	185.01			29.41			0.941
		North	1	2	147.17			58.82			0.202
Drake et al.	$u = u_f e^{\frac{-1}{2}(\frac{k}{k_o})^2}$	South	1	3	125.12			27.59			0.928
		North	1	3	127.57			31.95			0.206
Drew	$u = u_f[1-(\frac{k}{k_j})^{n+1/2}]$	South	0	2/3	195.15	76.56				0	0.906
		North	0	2/3	114.95	27.48				6.7	0.222
Multi regime	$\ln\left(\frac{U_f}{U}\right) = c.K^{l-1}$	South	1	2.15	173.4				1.9.E-02		0.933
	$\ln\left(\frac{U_f}{U}\right) = c.K^{l-1}$	North	1	3.764	120				3.16.E-05		0.21

APPENDIX B

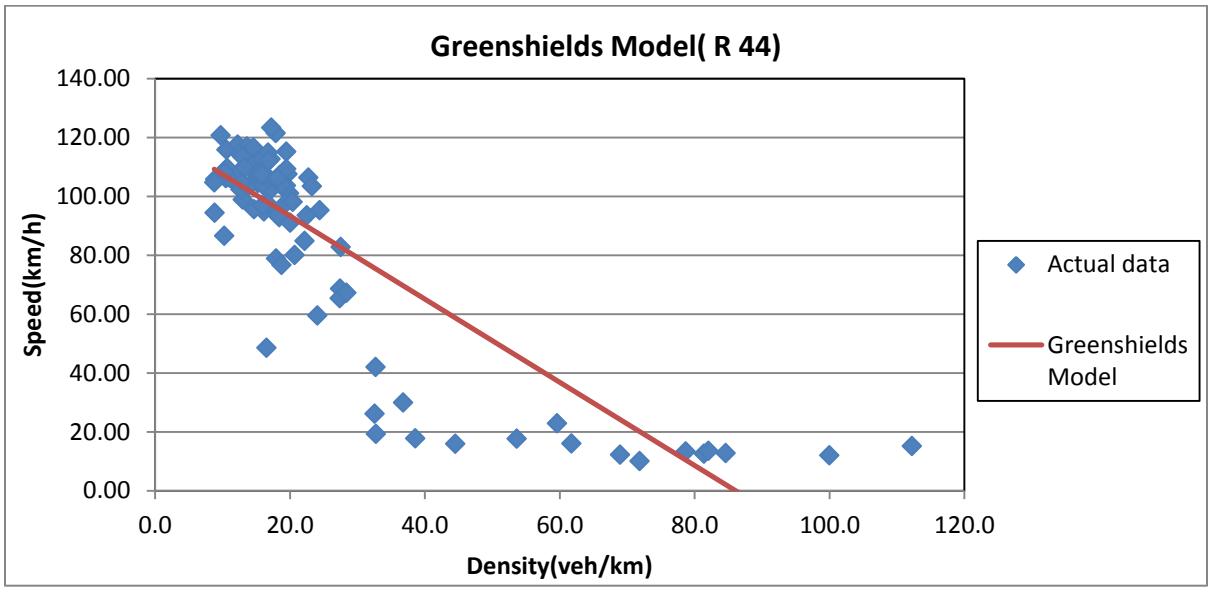

Figure B-1: Greenshields Model fitted to data taken on R44 in the south bound direction

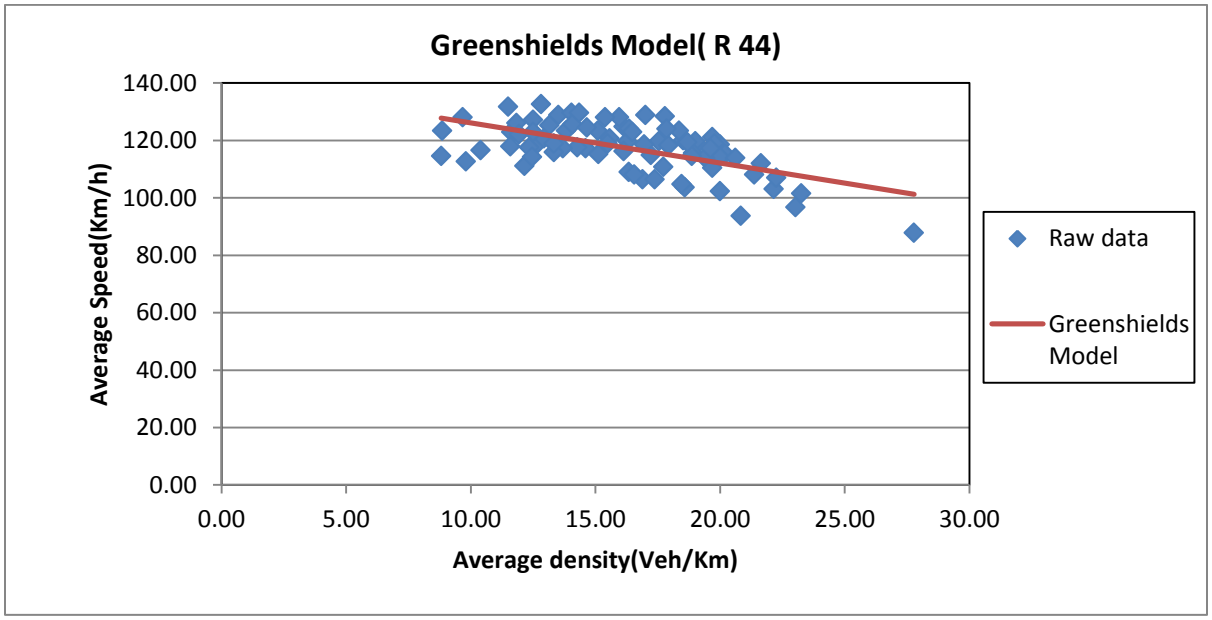

Figure B-2: Greenshields Model fitted to data taken on R44 in the north bound direction

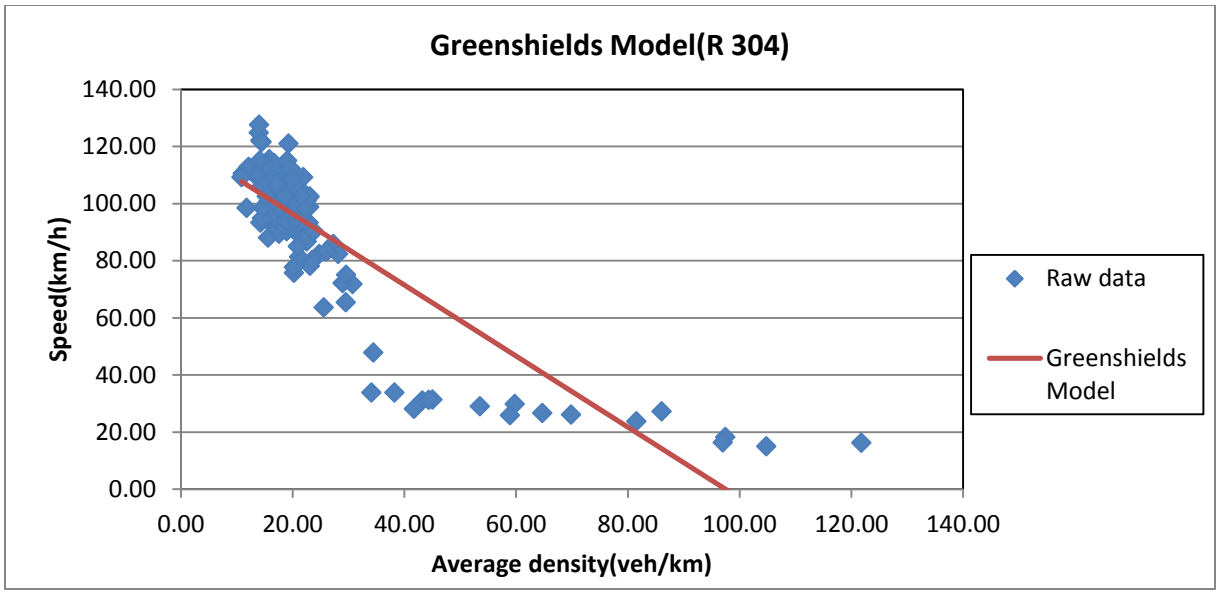

Figure B-3: Greenshields Model fitted to data taken on R304 in the south bound direction

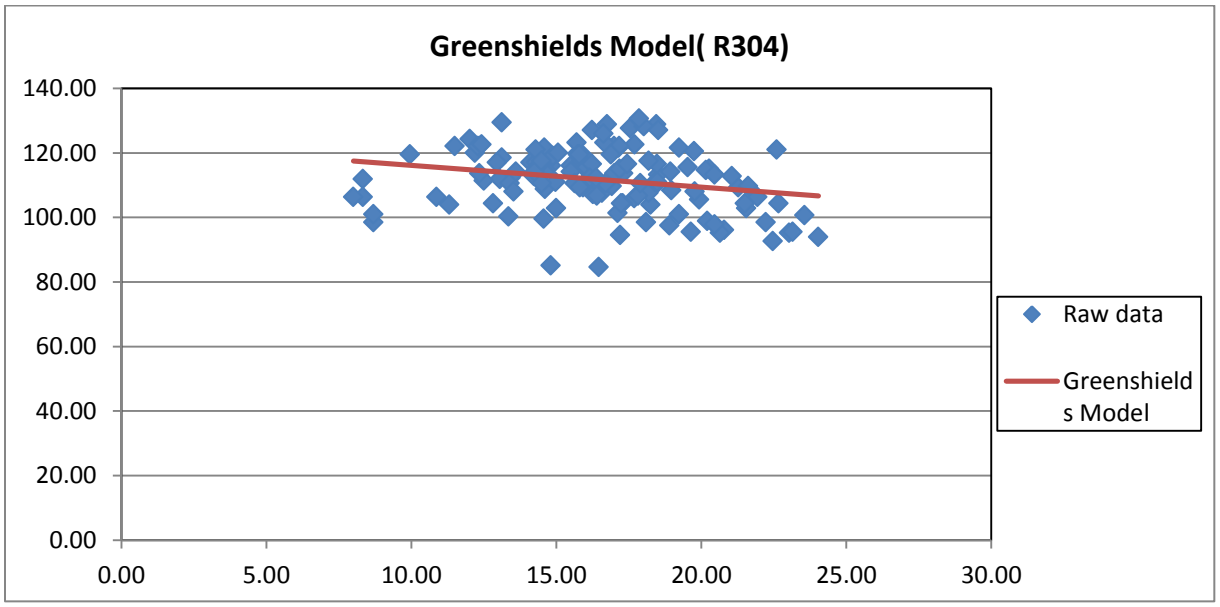

Figure B-4: Greenshields Model fitted to data taken on R304 in the north bound direction

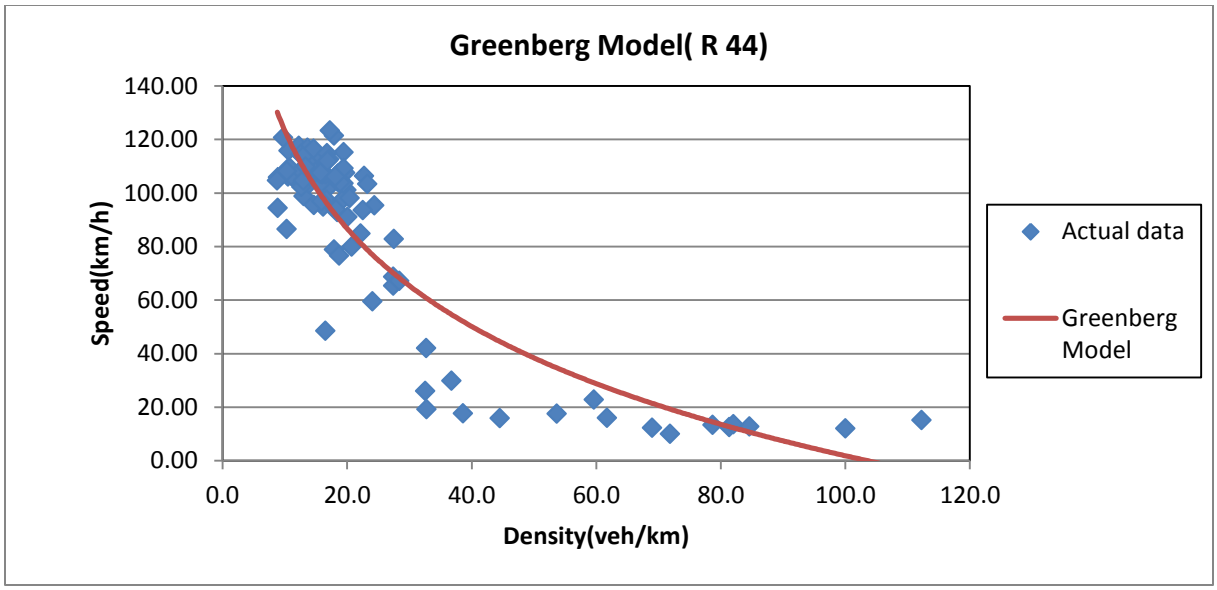

Figure B-5: Greenberg Model fitted to data taken on R44 in the south bound direction

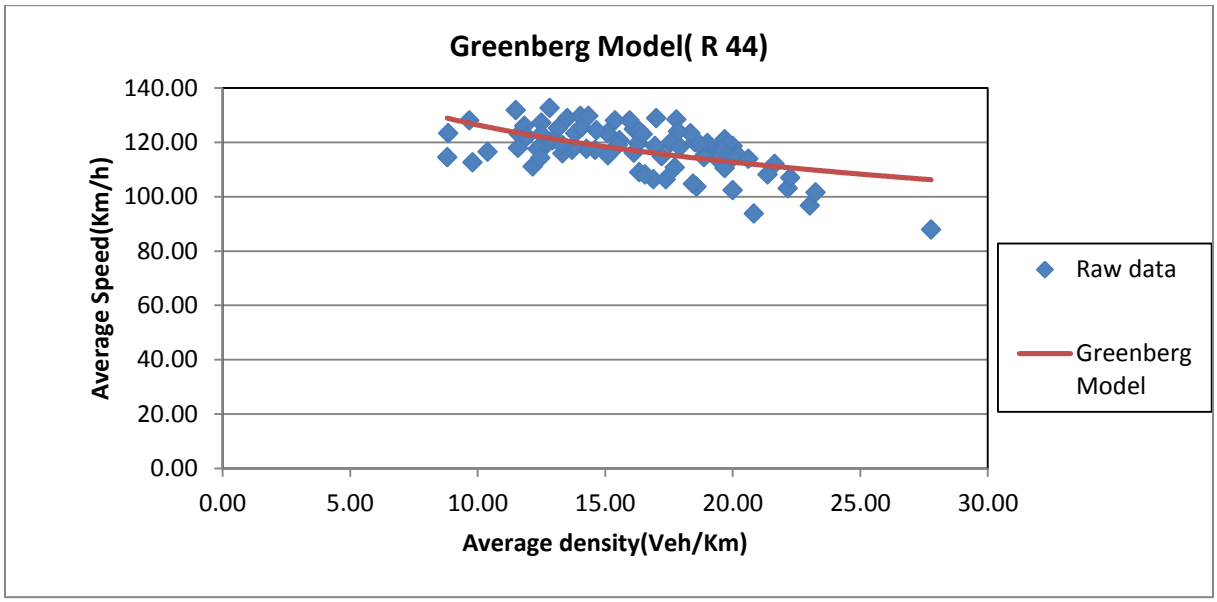

Figure B-6: Greenberg Model fitted to data taken on R44 in the north bound direction

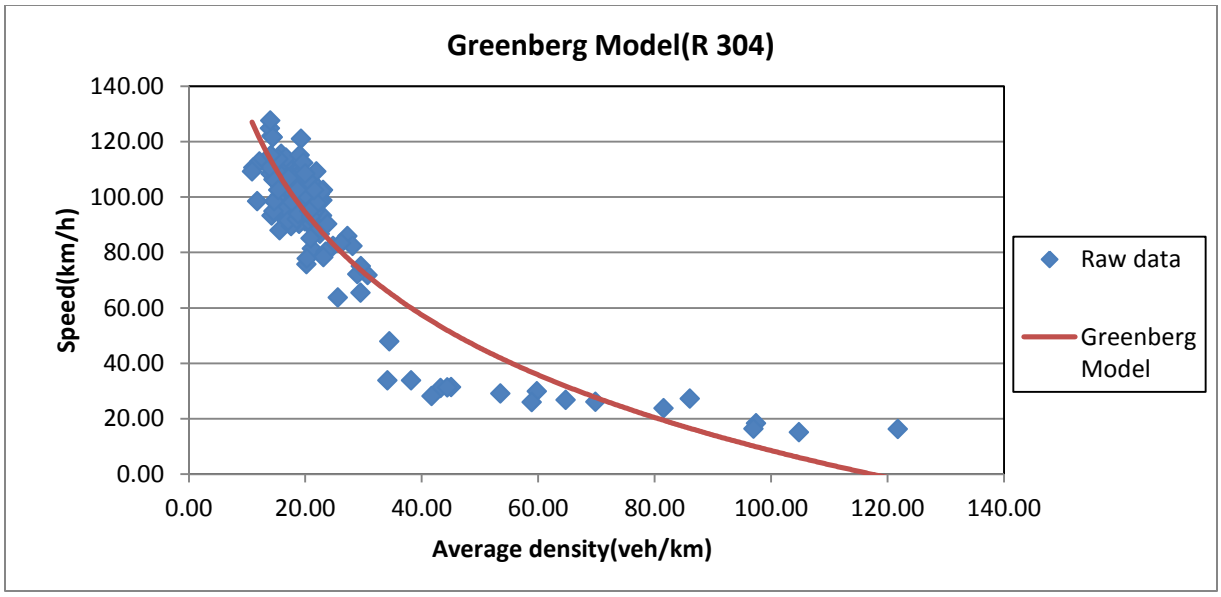

Figure B-7: Greenberg Model fitted to data taken on R304 in the south bound direction

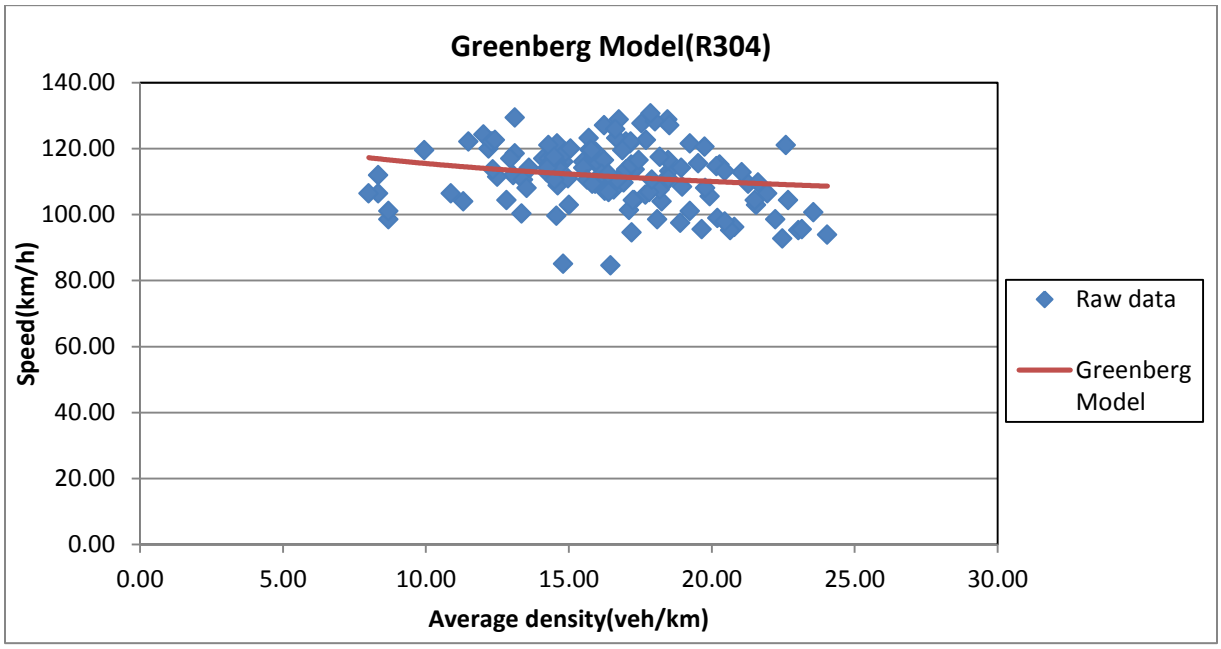

Figure B-8: Greenberg Model fitted to data taken on R304 in the north bound direction

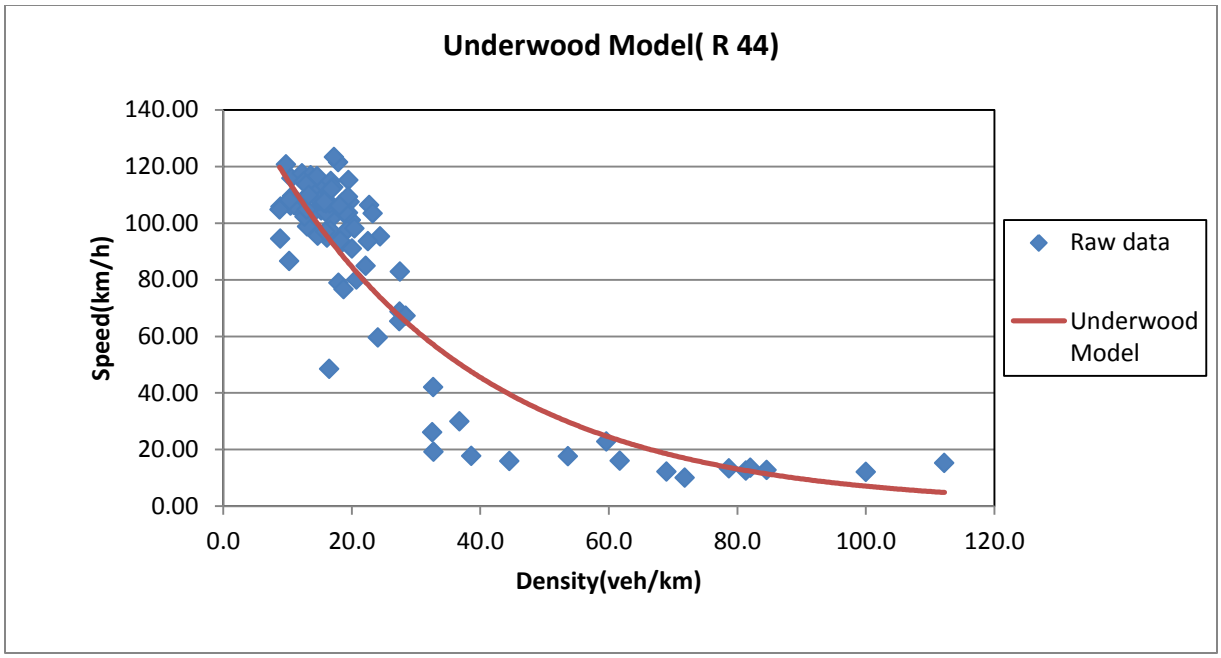

Figure B-9: Underwood Model fitted to data taken on R44 in the south bound direction

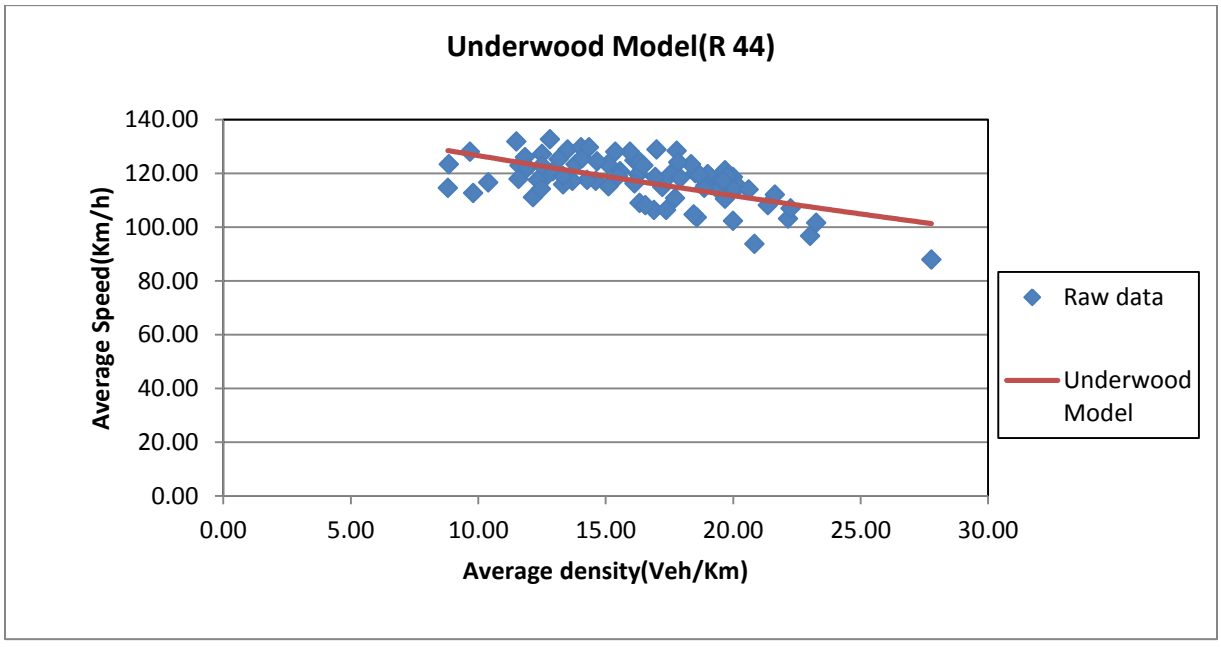

Figure B-10: Underwood Model fitted to data taken on R44 in the north bound direction

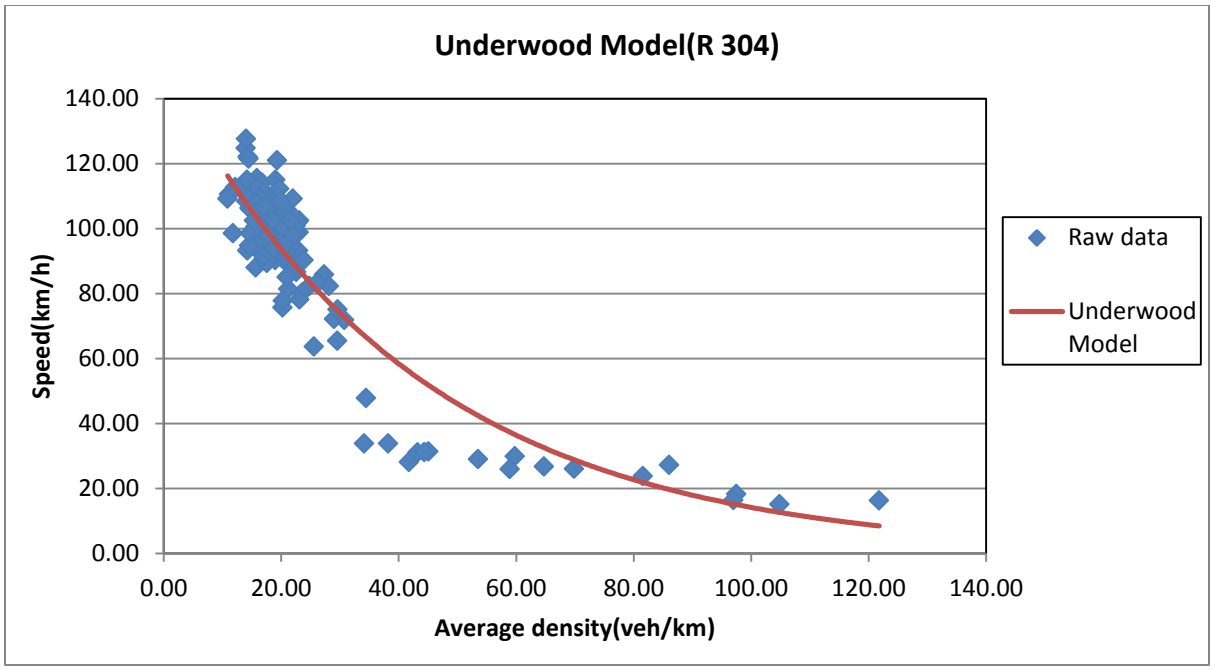

Figure B-11: Underwood Model fitted to data taken on R304 in the south bound direction

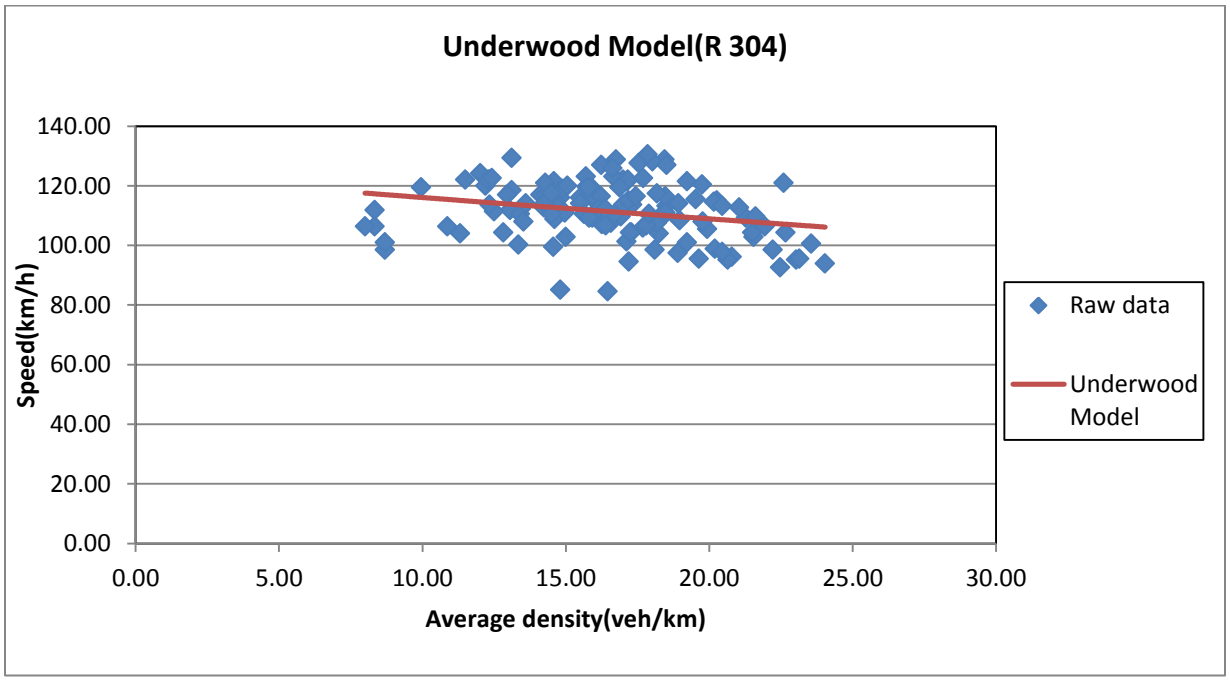

Figure B-12: Underwood Model fitted to data taken on R304 in the north bound direction

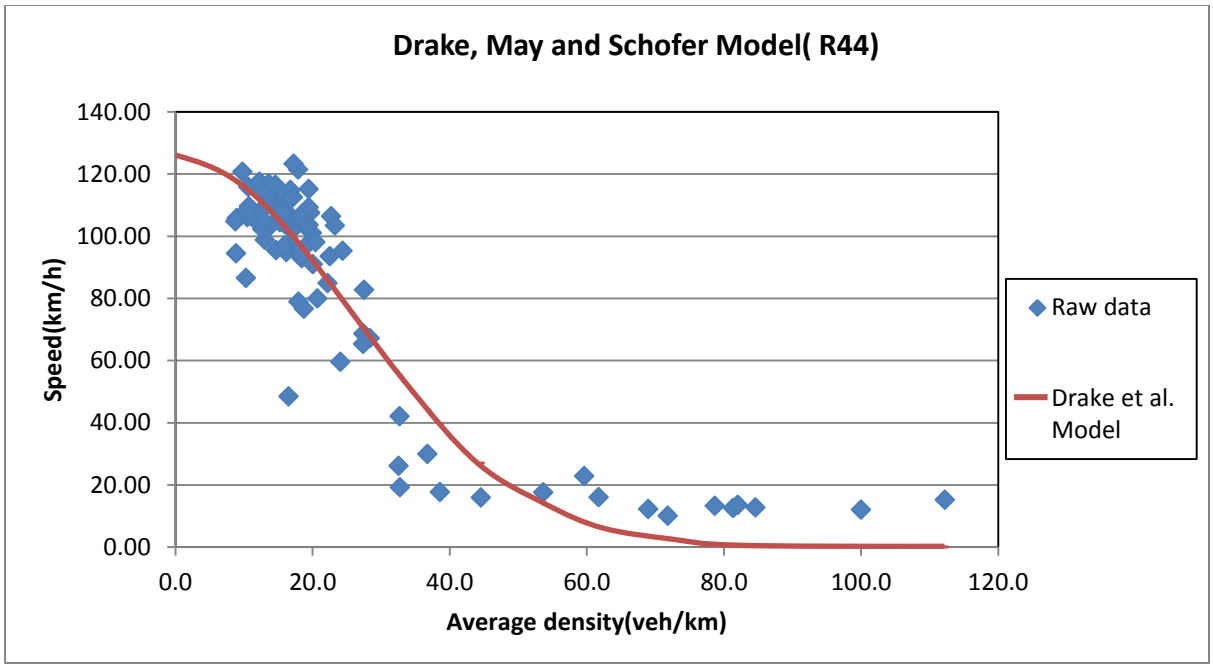

Figure B-13: The Drake et al. Model fitted to data taken on R44 in the south bound direction

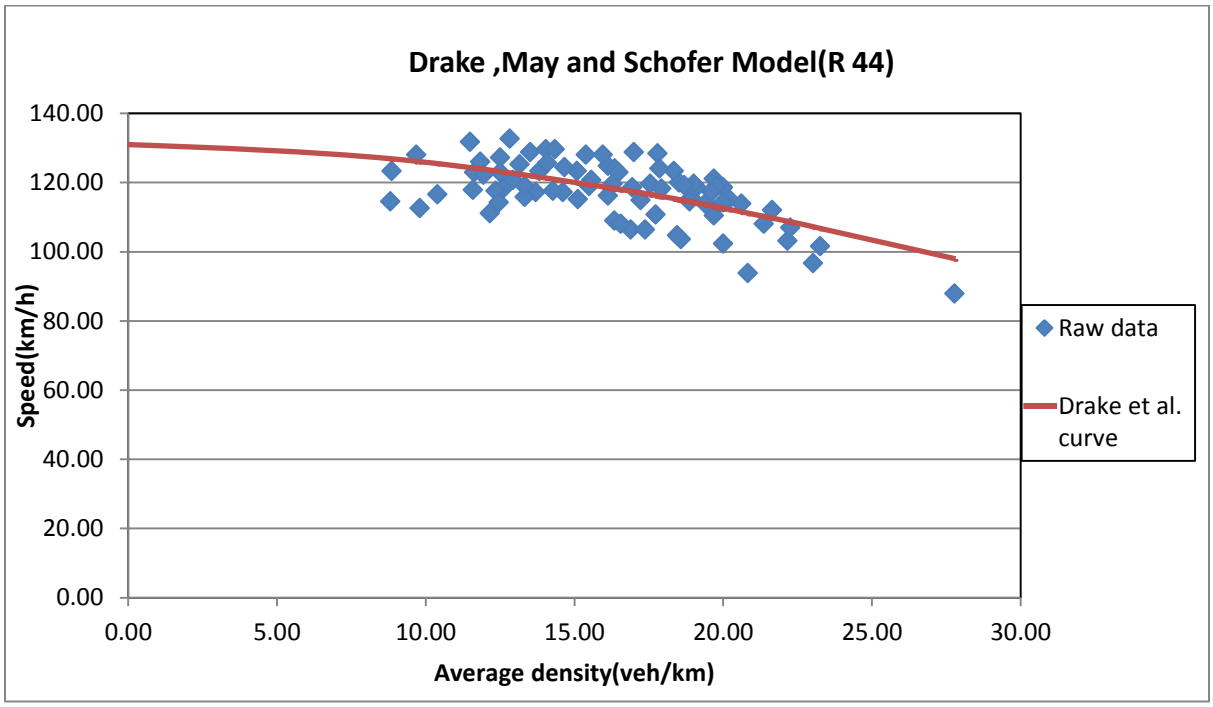

Figure B-14: The Drake et al. Model fitted to data taken on R44 in the north bound direction

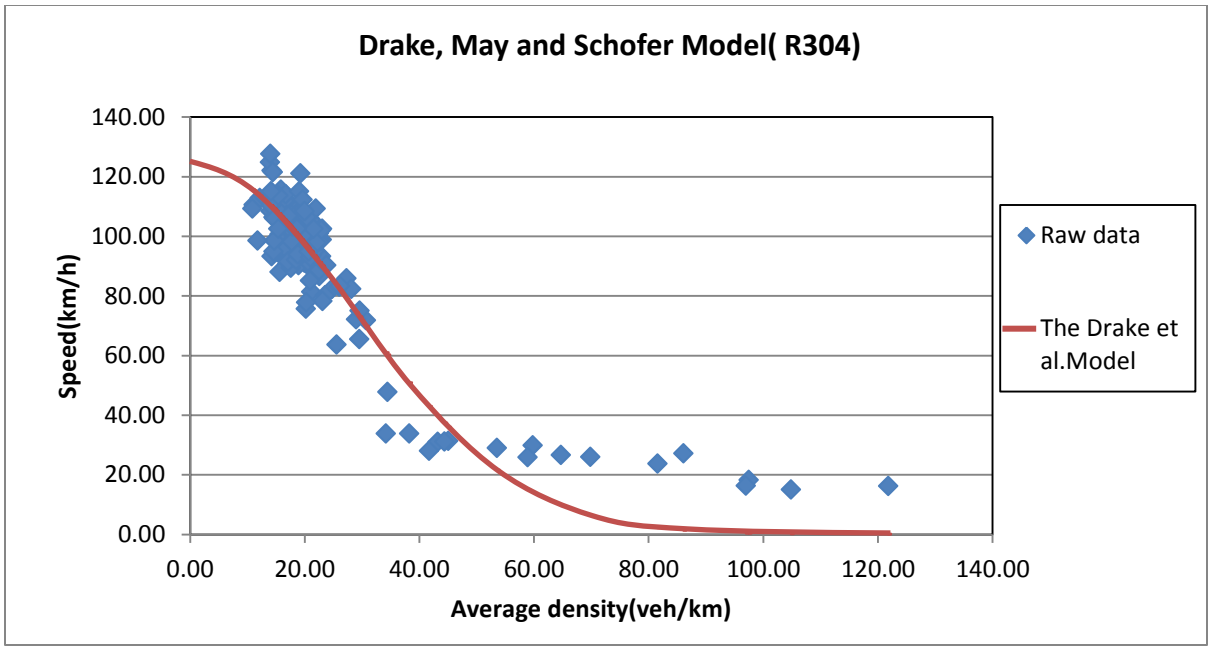

Figure B-15: The Drake et al. Model fitted to data taken on R304 in the south bound direction

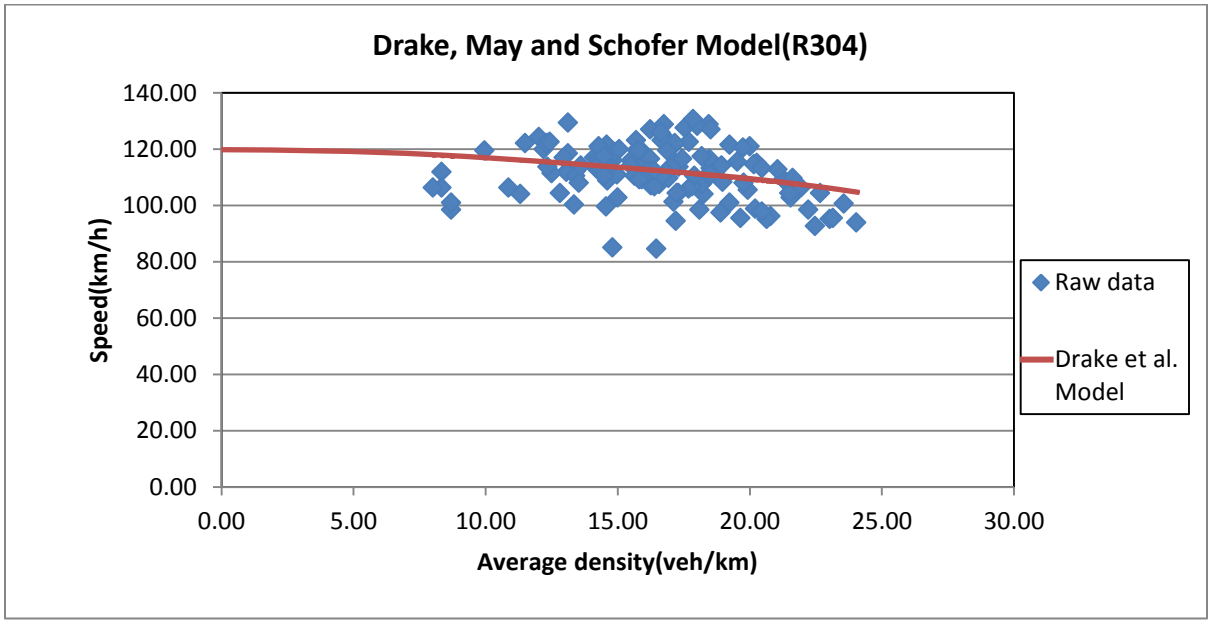

Figure B-16: The Drake et al. Model fitted to data taken on R304 in the north bound direction

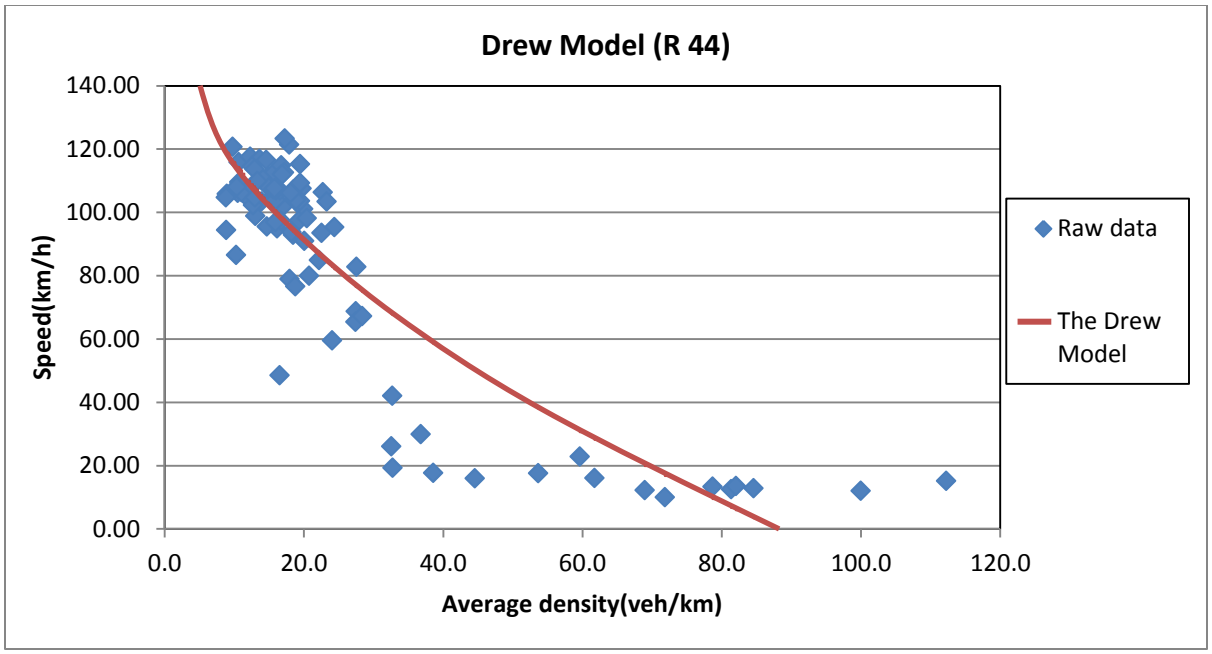

Figure B-17: The Drew Model fitted to data taken on R 44 in the south bound direction

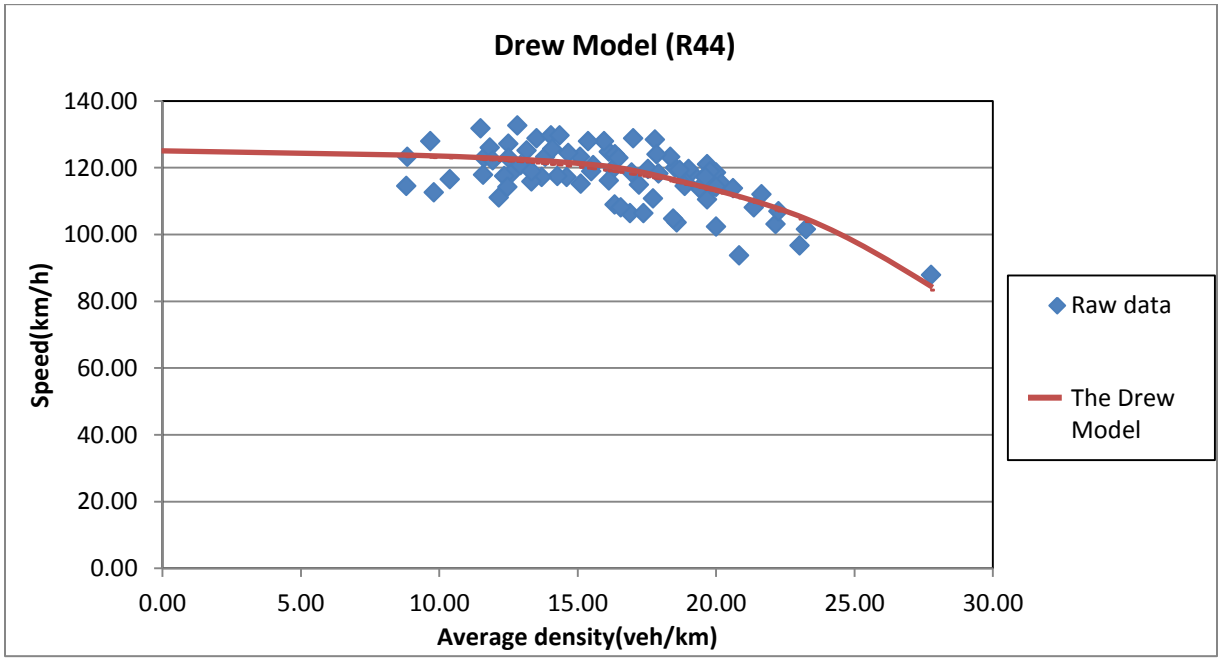

Figure B-18: The Drew Model fitted to data taken on R 44 in the north bound direction

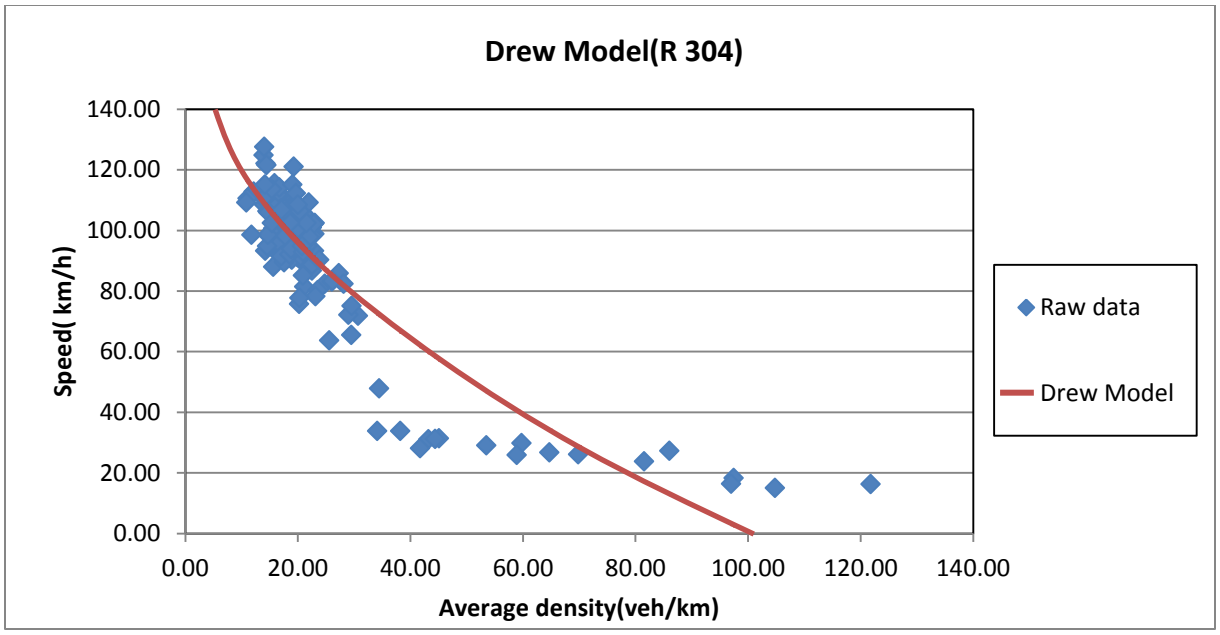

Figure B-19: The Drew Model fitted to data taken on R 304 in the south bound direction

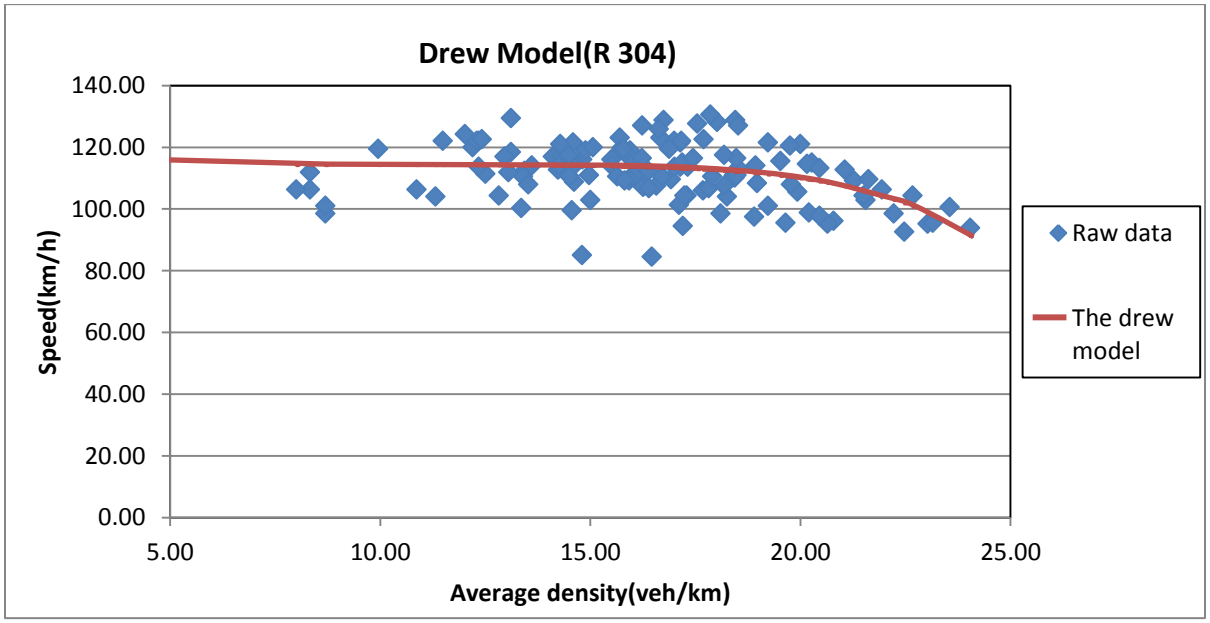

Figure B-20: The Drew Model fitted to data taken on R304 in the north bound direction

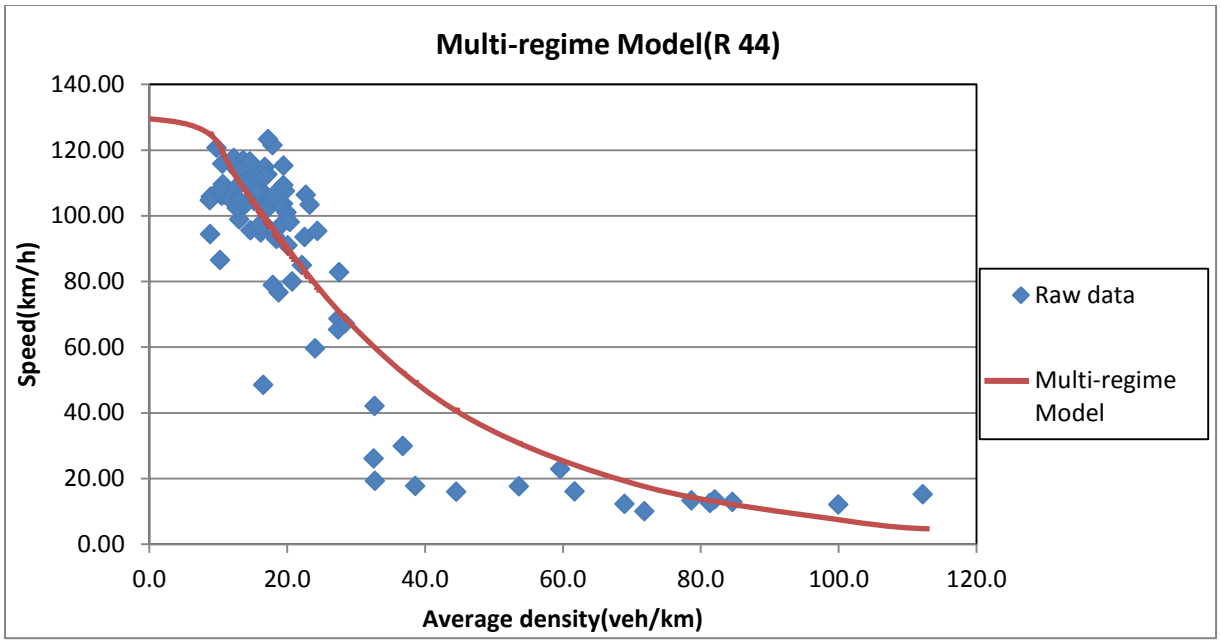

Figure B-21: The multi-regime Model fitted to data taken on R44 in the south bound direction

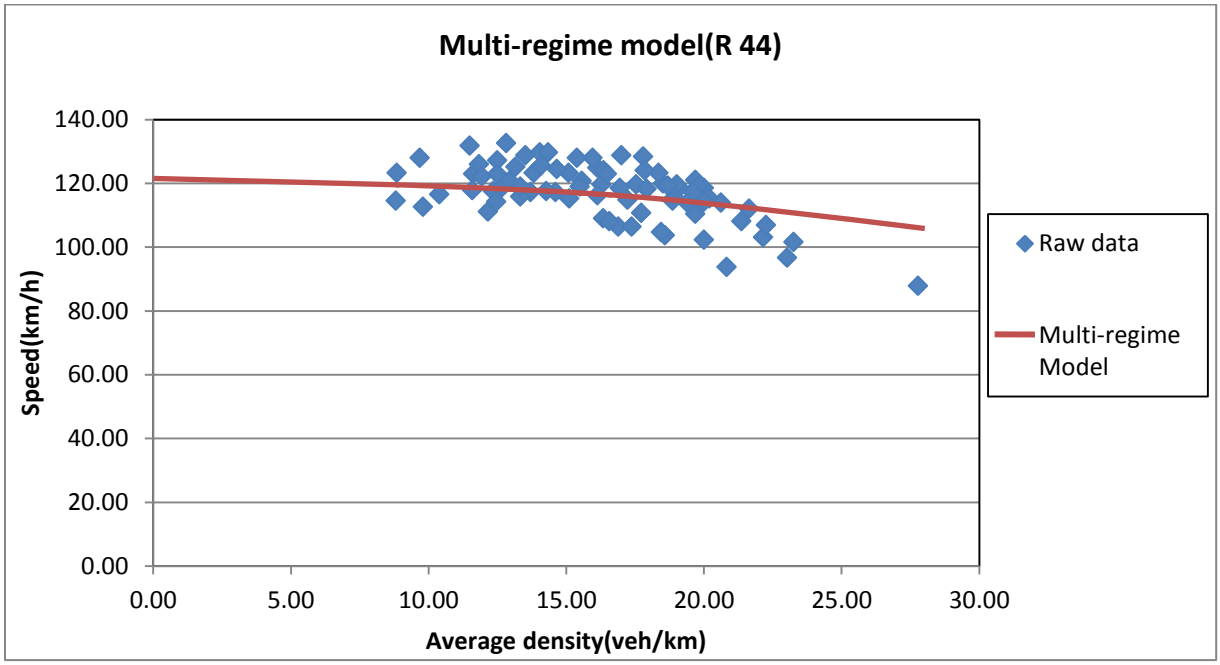

Figure B-22: The multi-regime Model fitted to data taken on R44 in the north bound direction

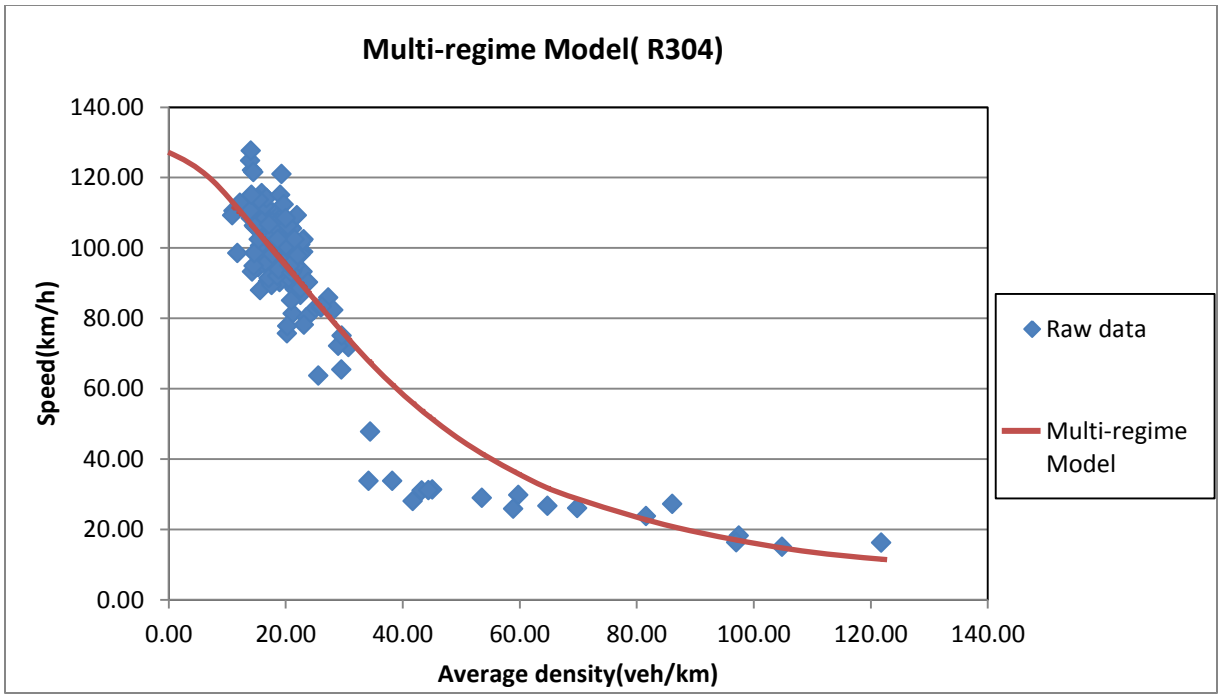

Figure B-23: The multi-regime Model fitted to data taken on R304 in the south bound direction

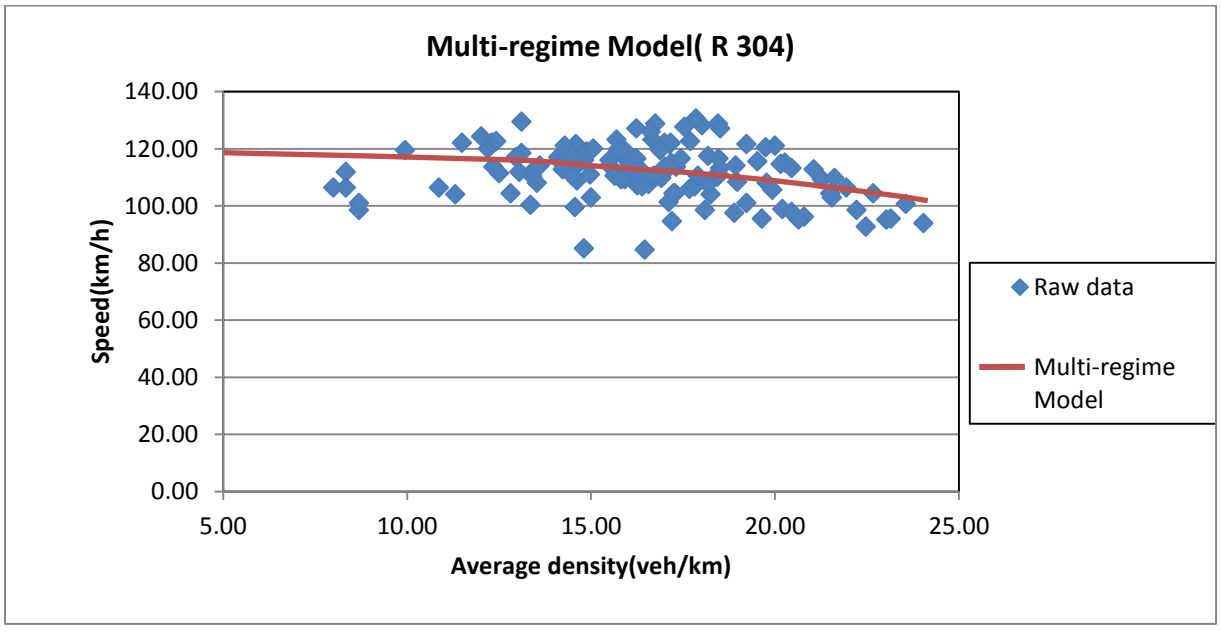

Figure B-24: The multi-regime Model fitted to data taken on R304 in the north bound direction

APPENDIX C

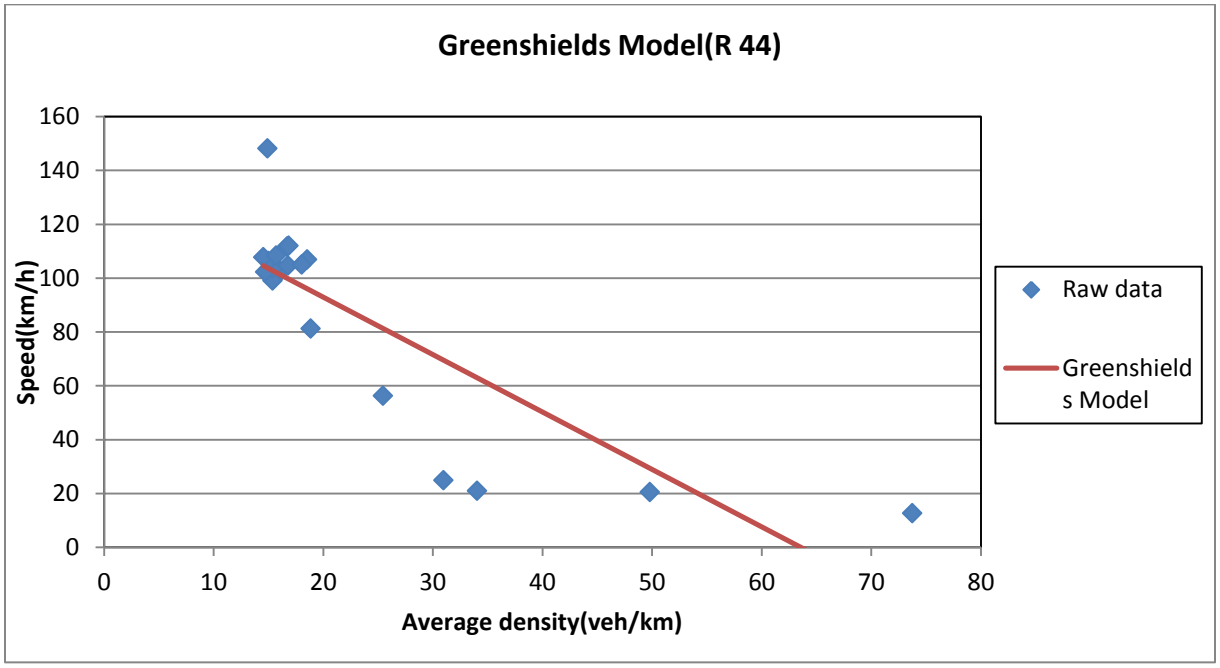

Figure C-1: The Greenshields model fitted to the 5-minutes data taken on R 44 in the south bound direction

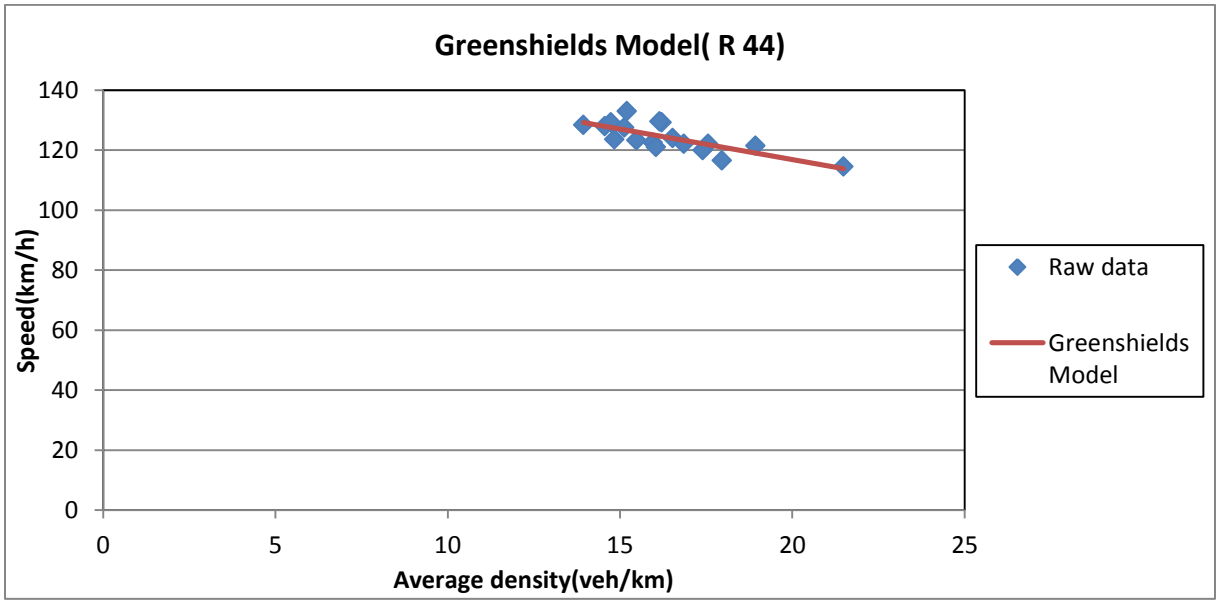

Figure C-2: The Greenshields model fitted to the 5-minutes data taken on R 44 in the north bound direction

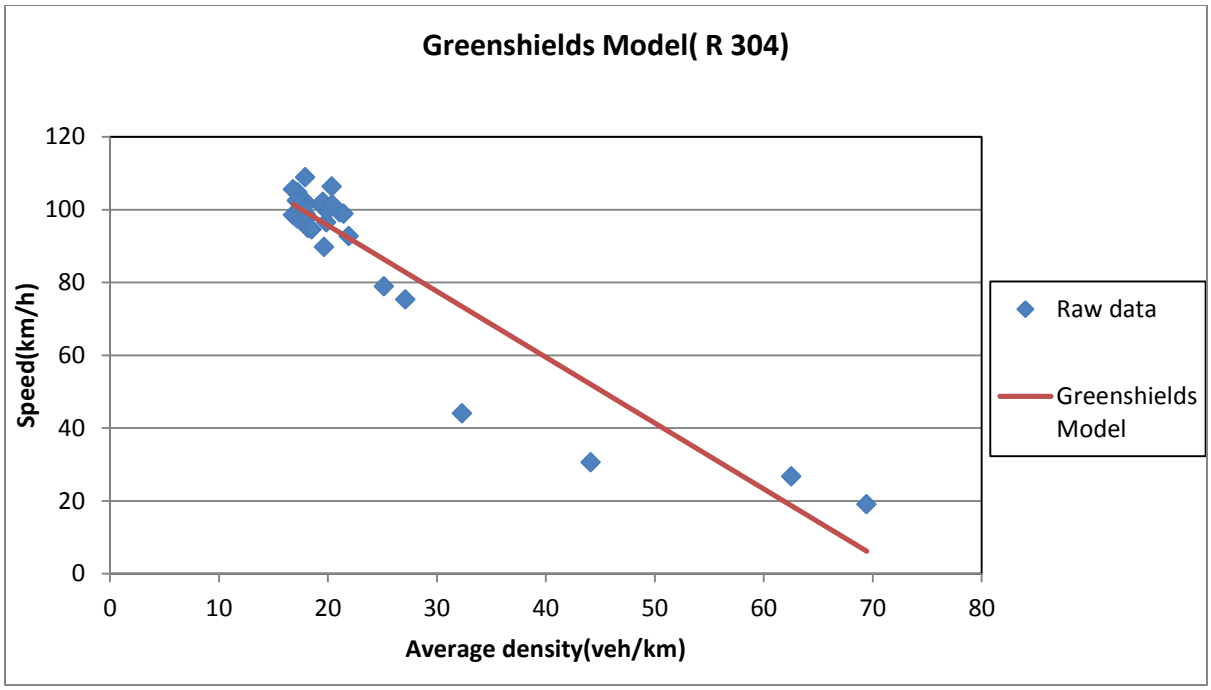

Figure C-3: The Greenshields model fitted to the 5-minutes data taken on R 304 in the south bound direction

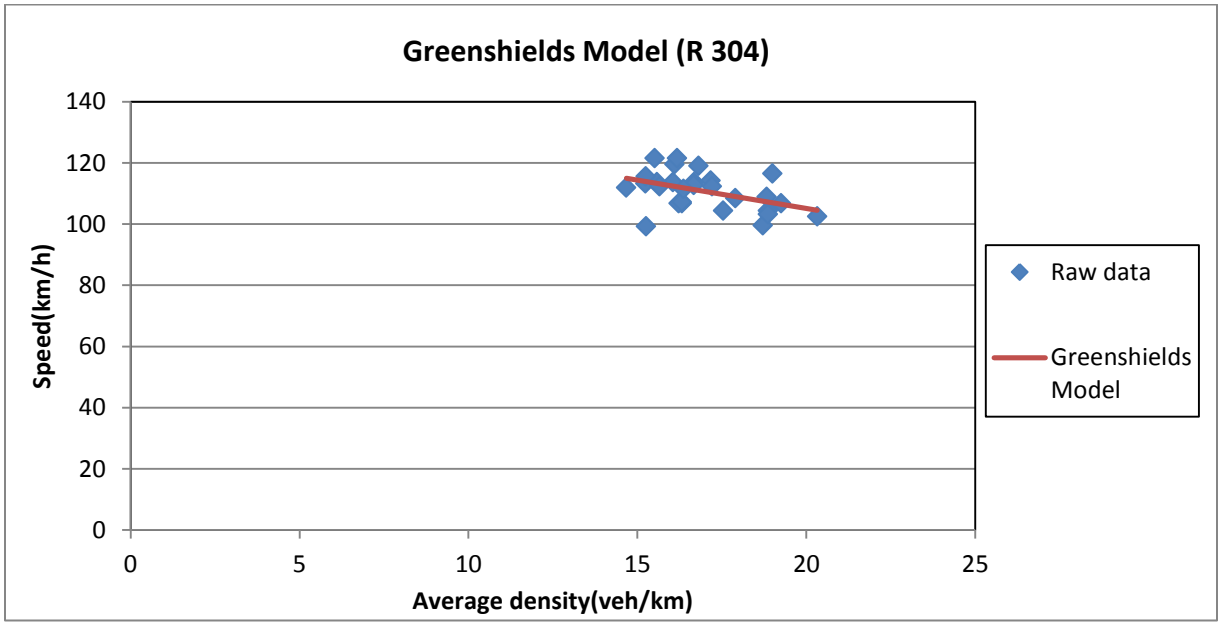

Figure C-4: The Greenshields model fitted to the 5-minutes data taken on R 304 in the north bound direction

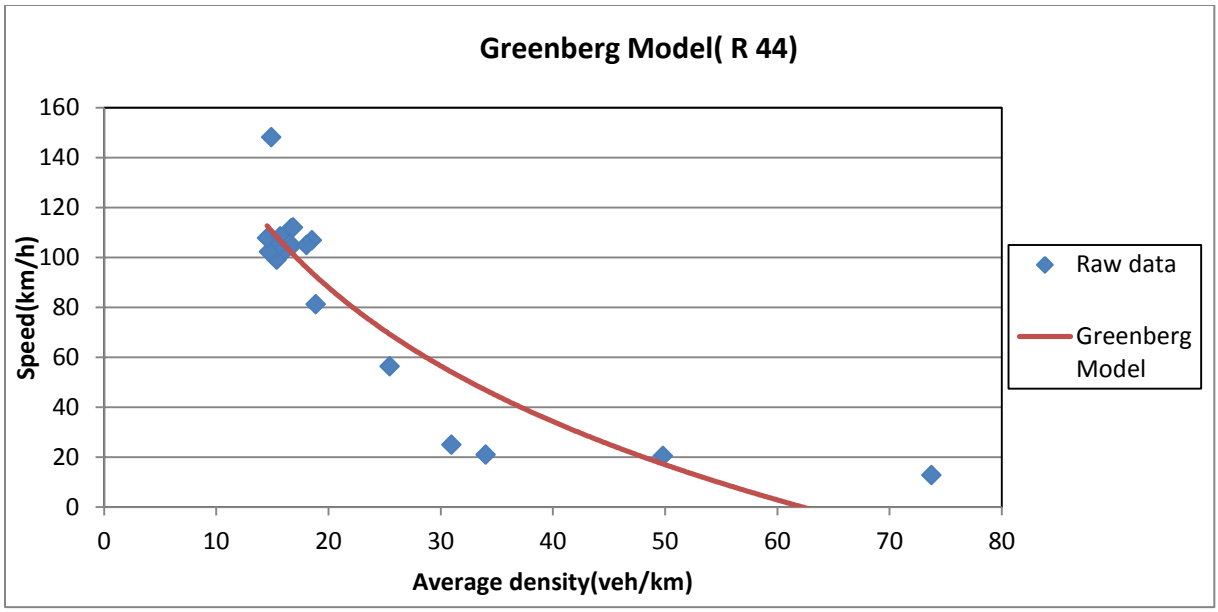

Figure C-5: The Greenberg model fitted to the 5-minutes data taken on R 304 in the south bound direction

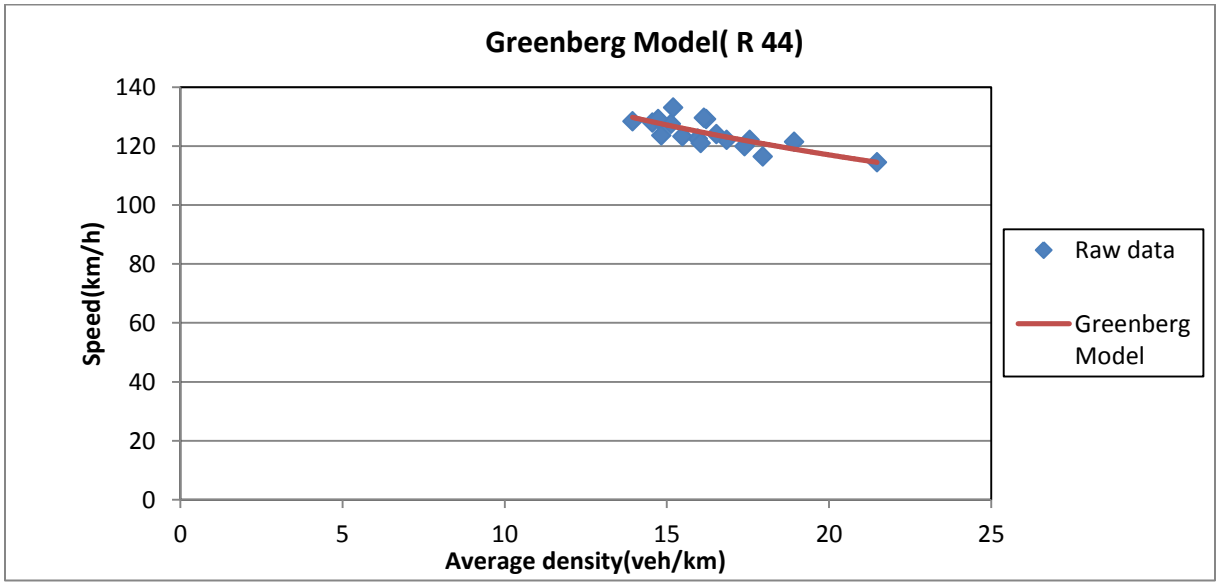

Figure C-6: The Greenberg model fitted to the 5-minutes data taken on R 304 in the north bound direction

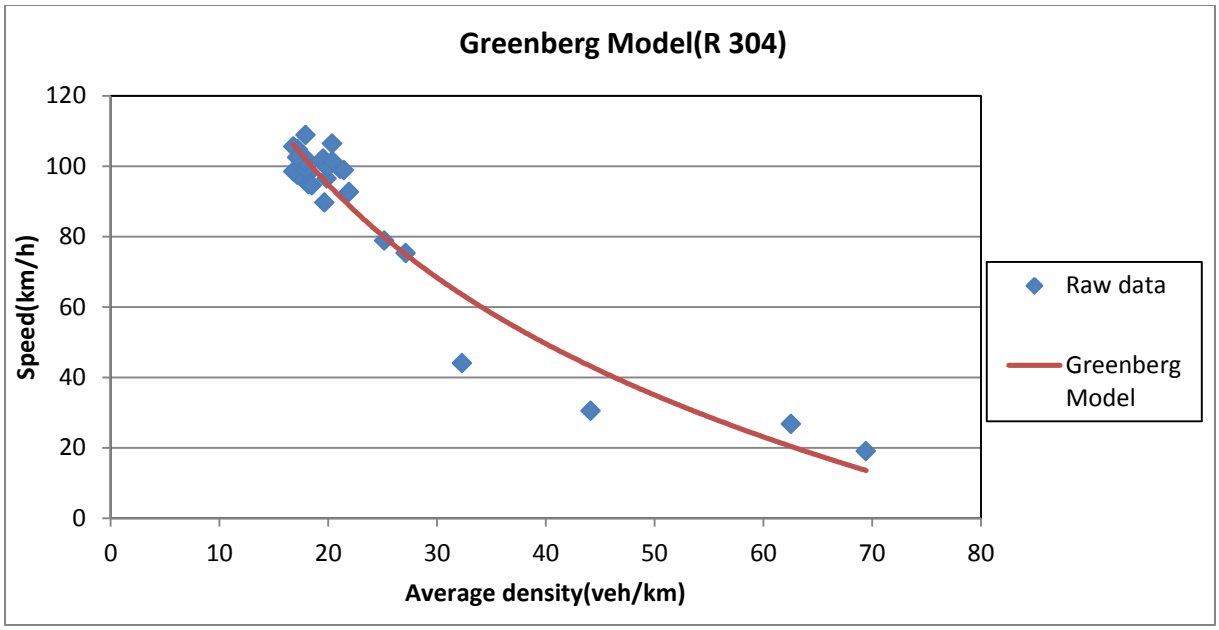

Figure C-7: The Greenberg model fitted to the 5-minutes data taken on R 304 in the south bound direction

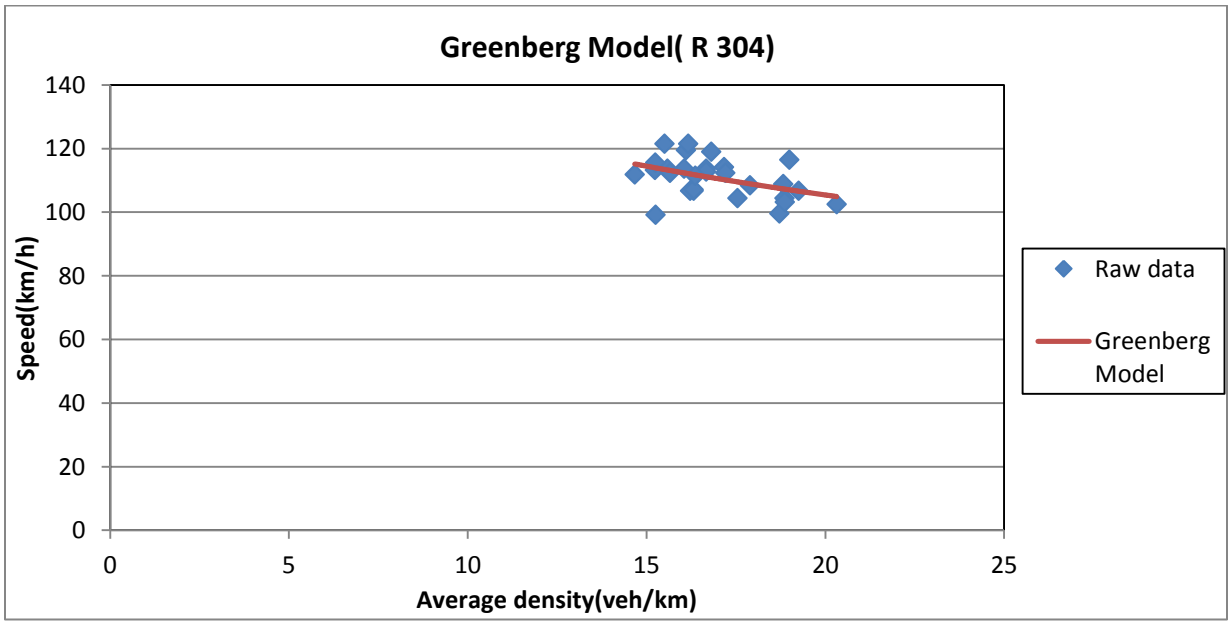

Figure C-8: The Greenberg model fitted to the 5-minutes data taken on R 304 in the north bound direction

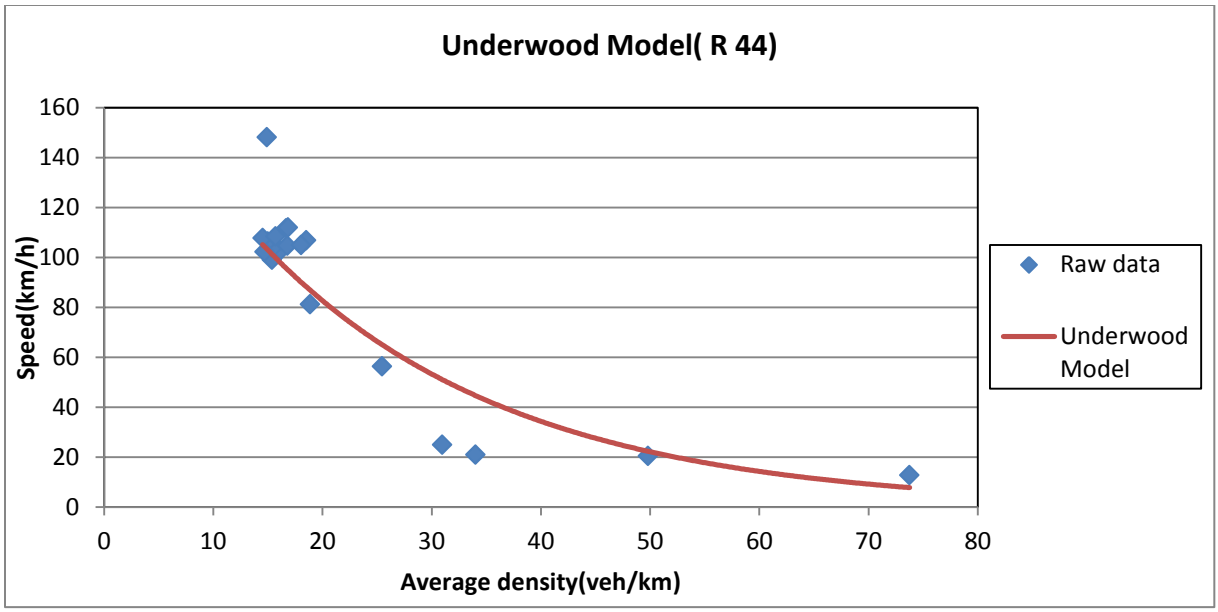

Figure C-9: The Underwood model fitted to the 5-minutes data taken on R 44 in the south bound direction

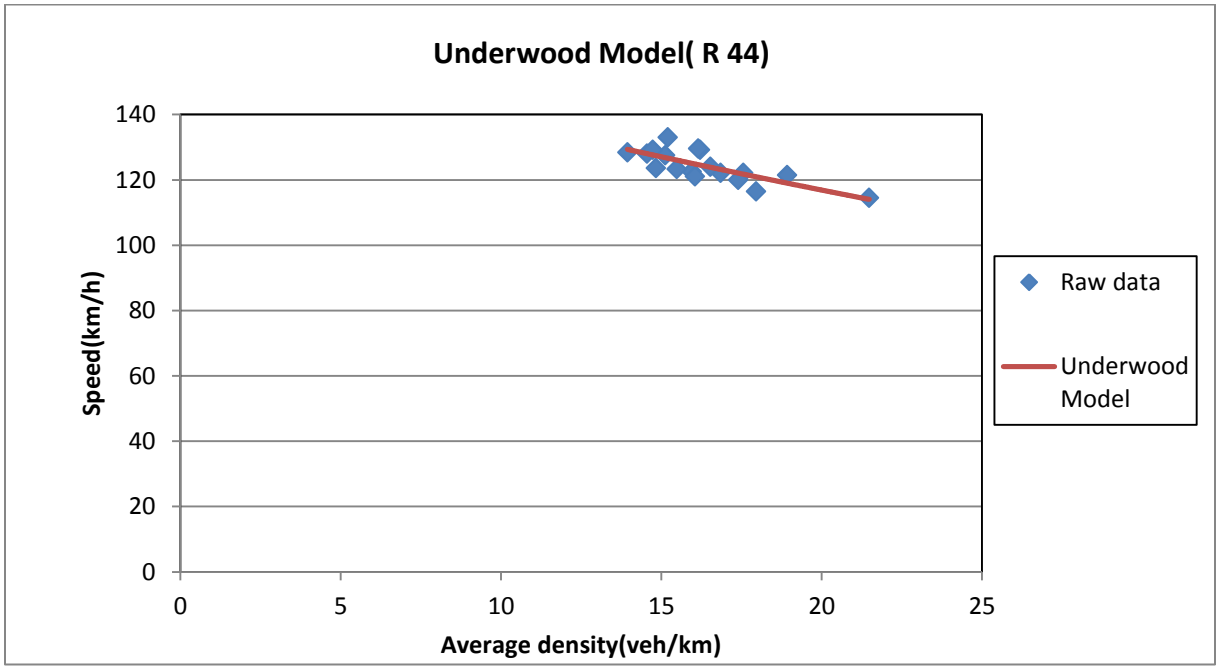

Figure C-10: The Underwood model fitted to the 5-minutes data taken on R 44 in the north bound direction

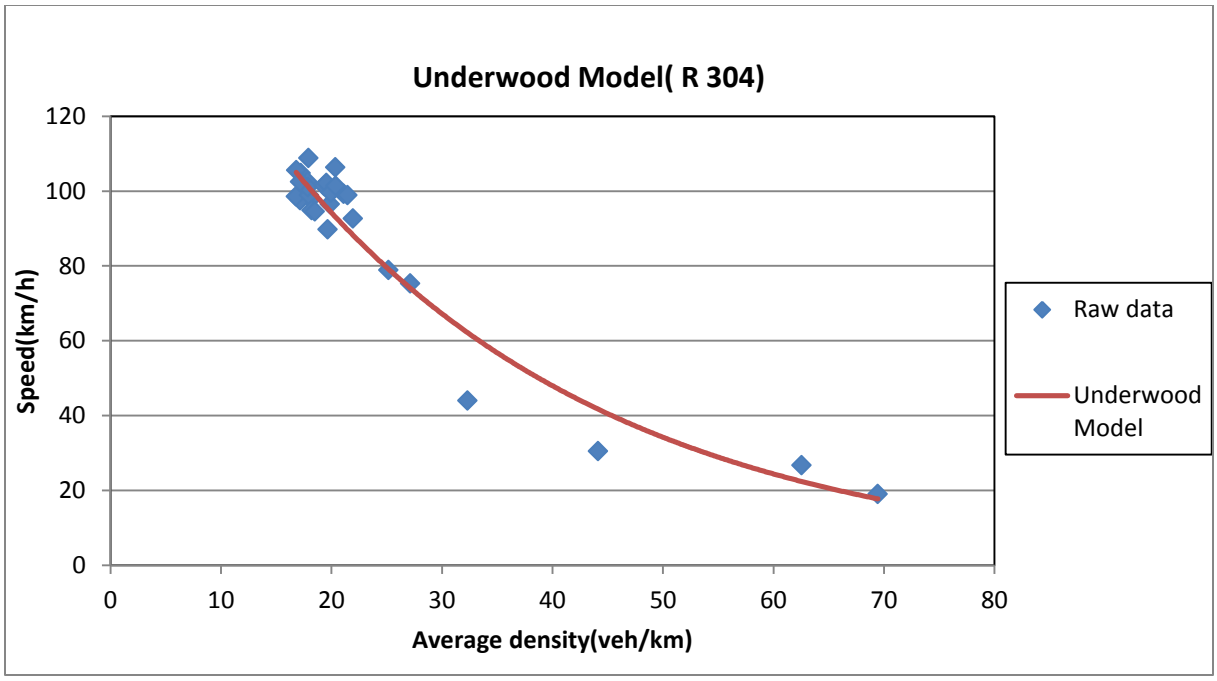

Figure C-11: The Underwood model fitted to the 5-minutes data taken on R 304 in the south bound direction

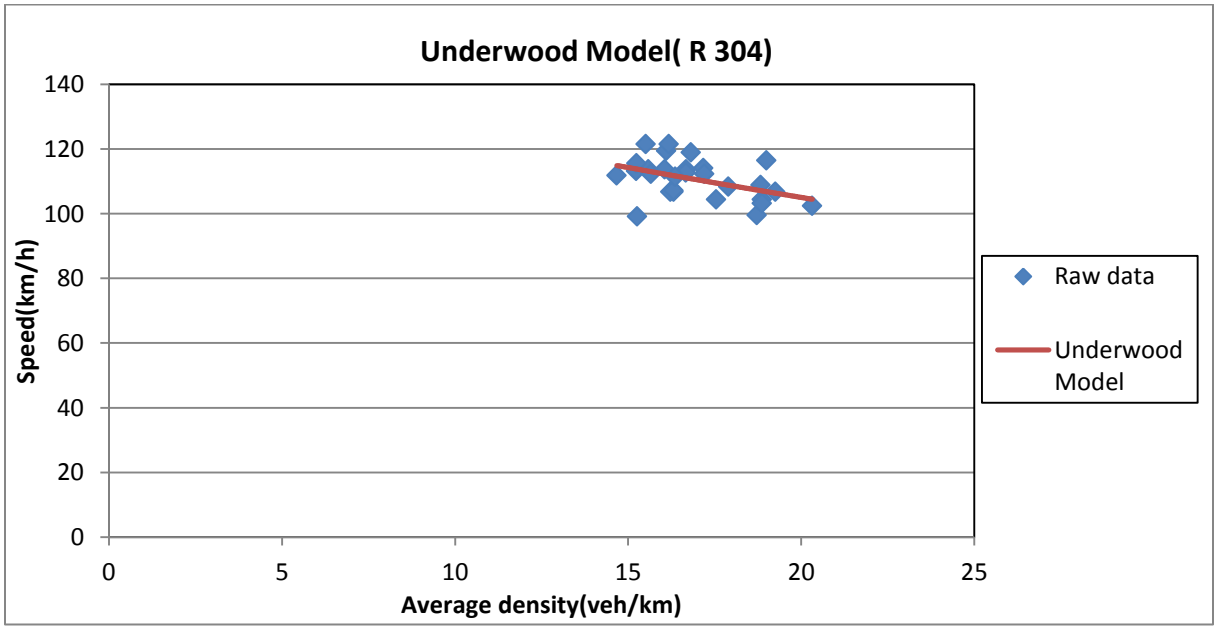

Figure C-12: The Underwood model fitted to the 5-minutes data taken on R 304 in the north bound direction

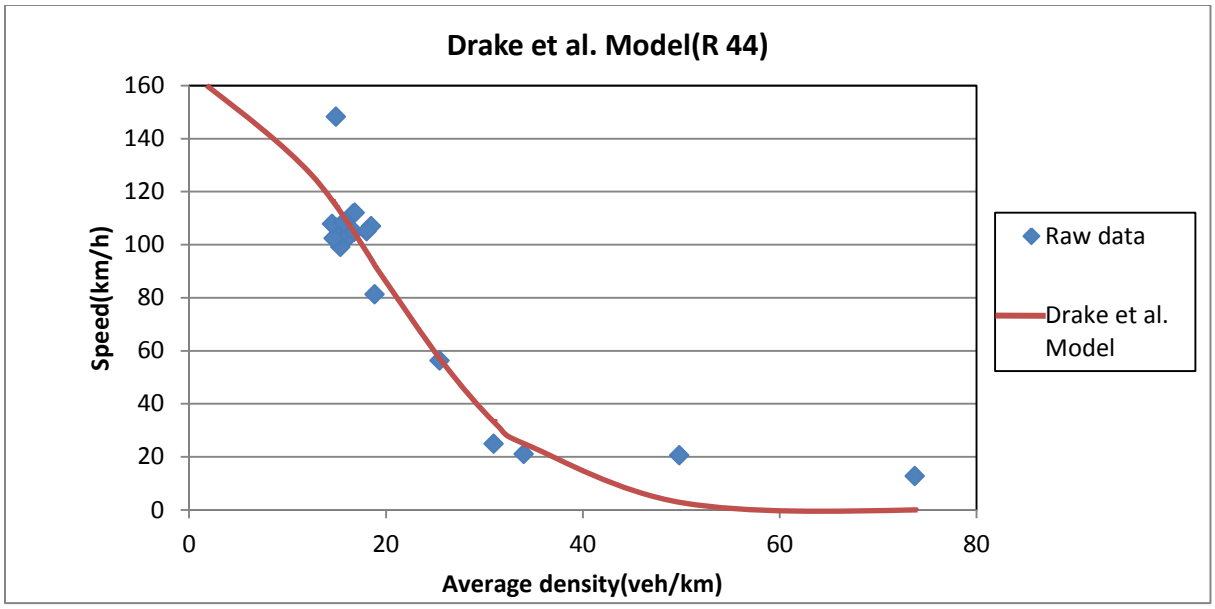

Figure C-13: The Drake model fitted to the 5-minutes data taken on R 44 in the south bound direction

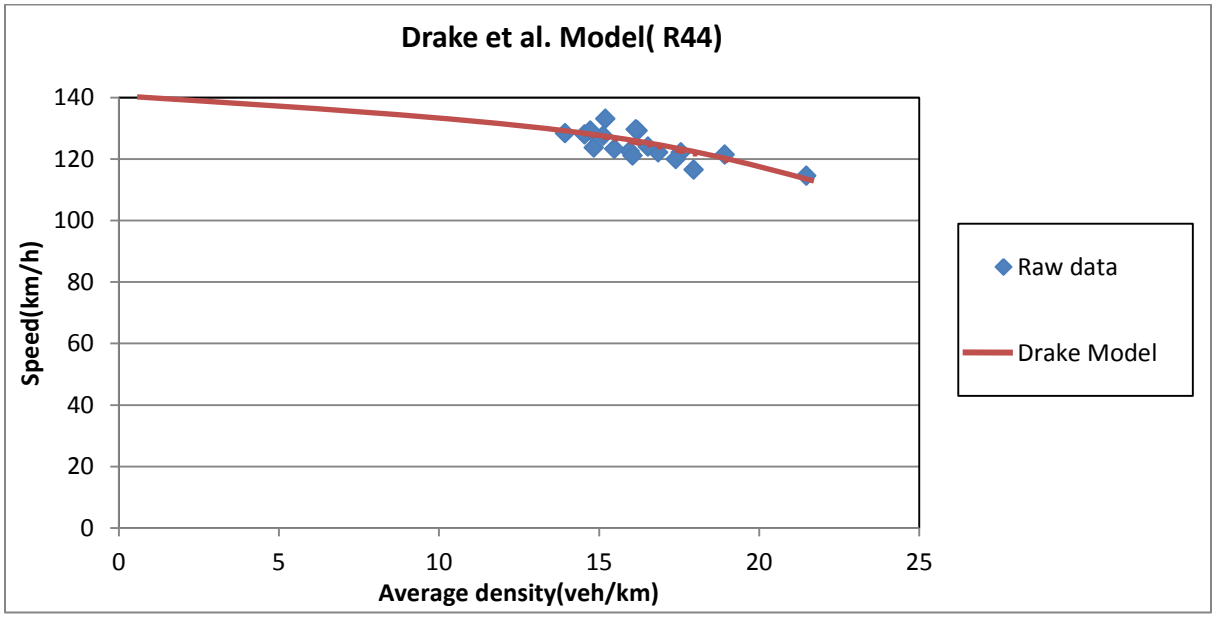

Figure C-14: The Drake model fitted to the 5-minutes data taken on R 44 in the north bound direction

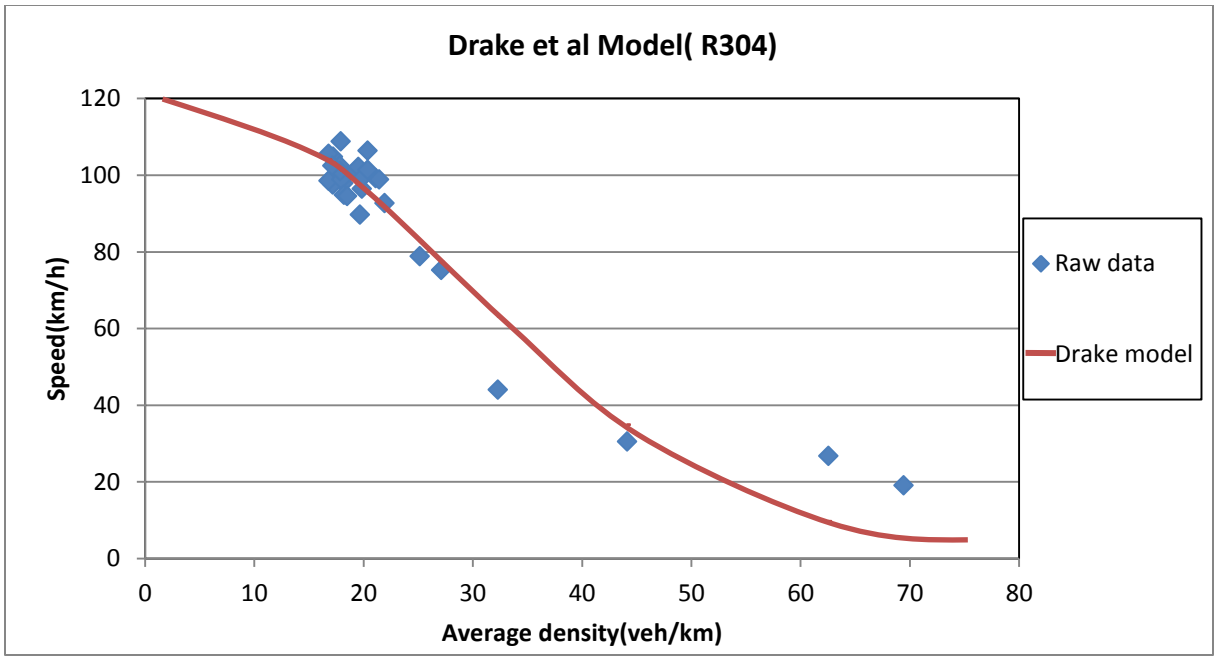

Figure C-15: The Drake et al. model fitted to the 5-minutes data taken on R 304 in the south bound direction

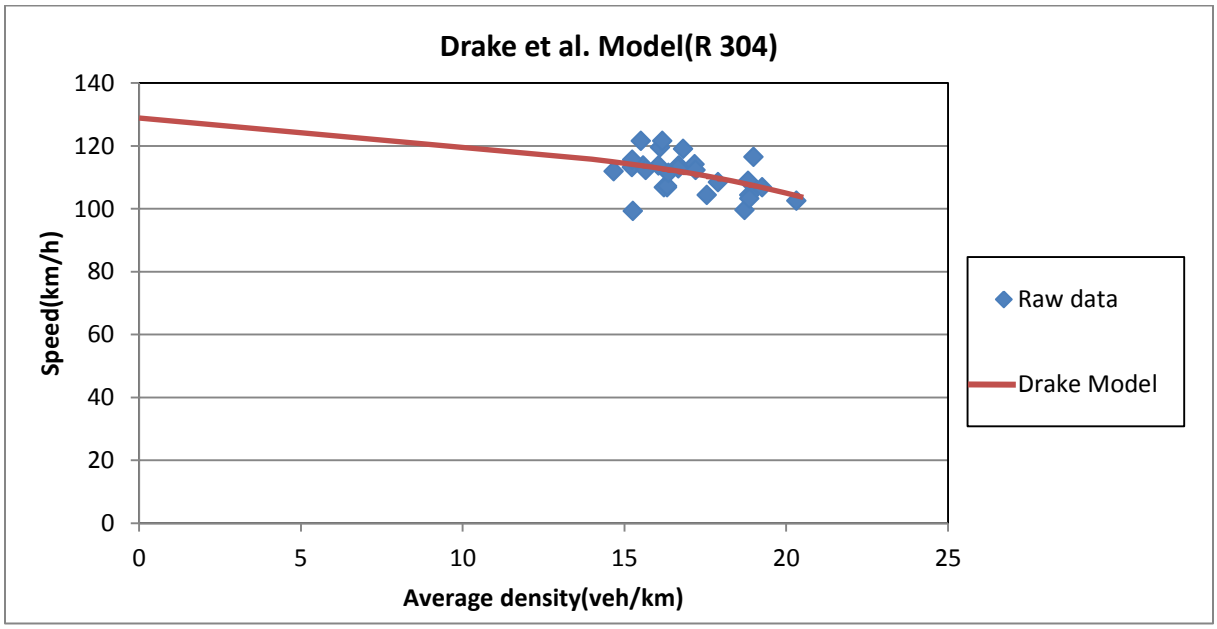

Figure C-16: The Drake et al. model fitted to the 5-minutes data taken on R 304 in the north bound direction

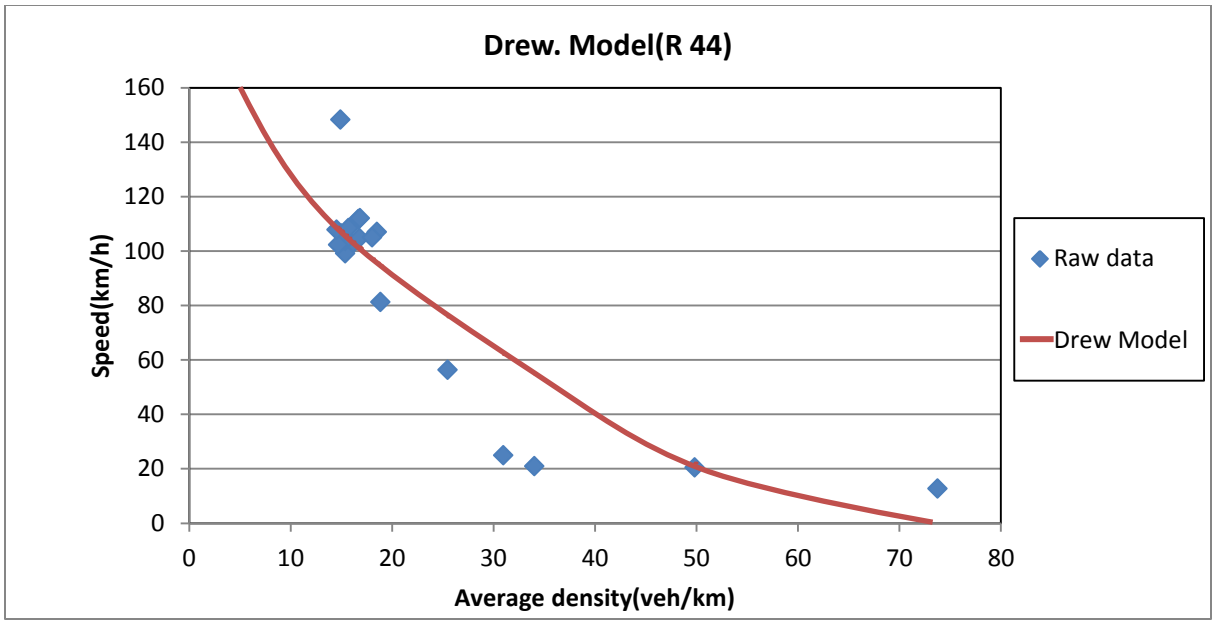

Figure C-17: The Drew model fitted to the 5-minutes data taken on R 44 in the south bound direction

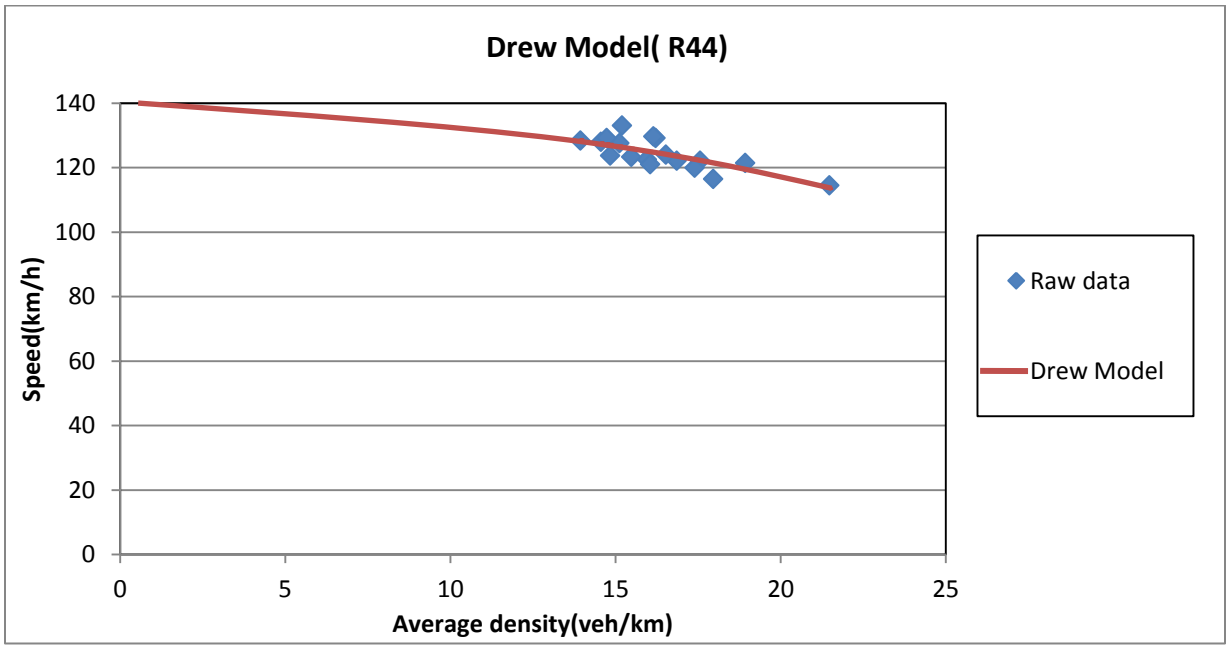

Figure C-18: The Drew model fitted to the 5-minutes data taken on R 44 in the north bound direction

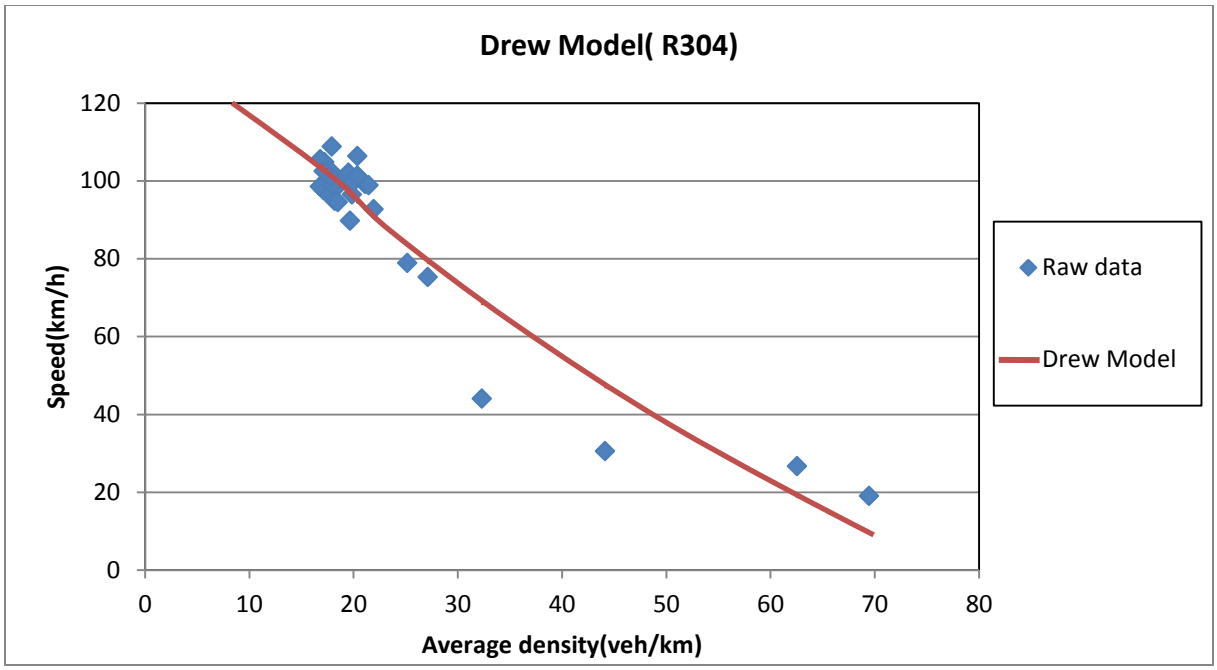

Figure C-19: The Drew model fitted to the 5-minutes data taken on R 304 in the south bound direction

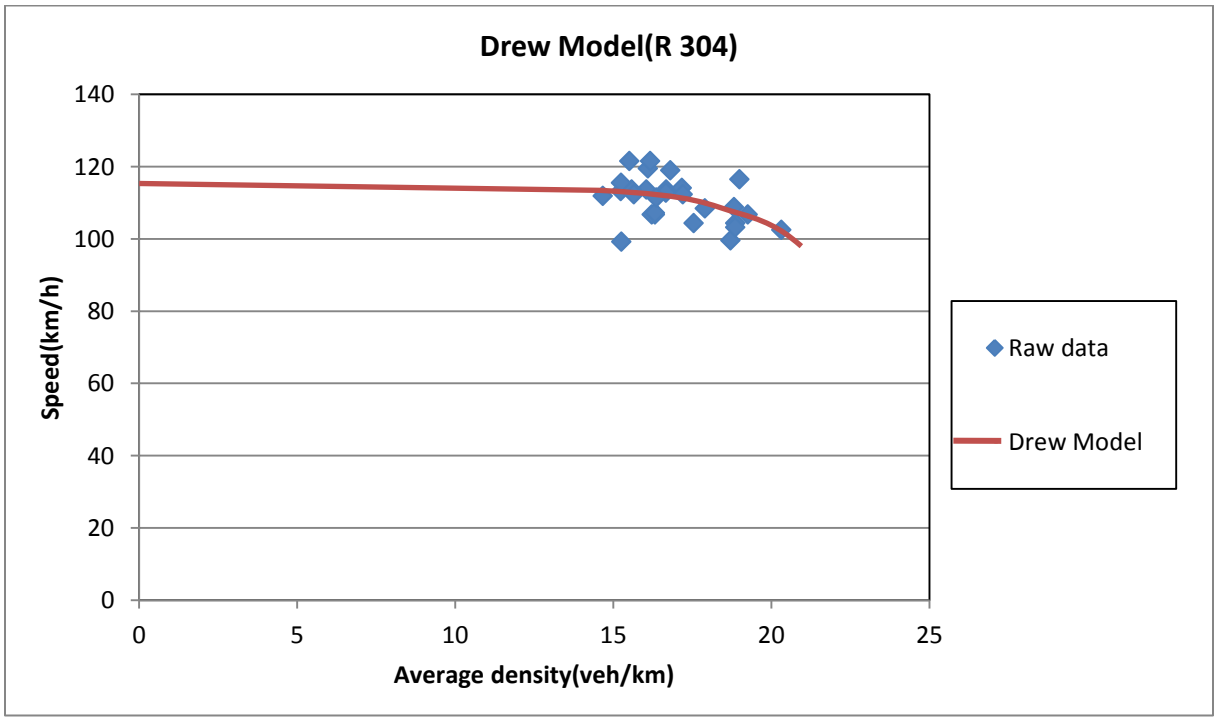

Figure C-20: The Drew model fitted to the 5-minutes data taken on R 304 in the north bound direction

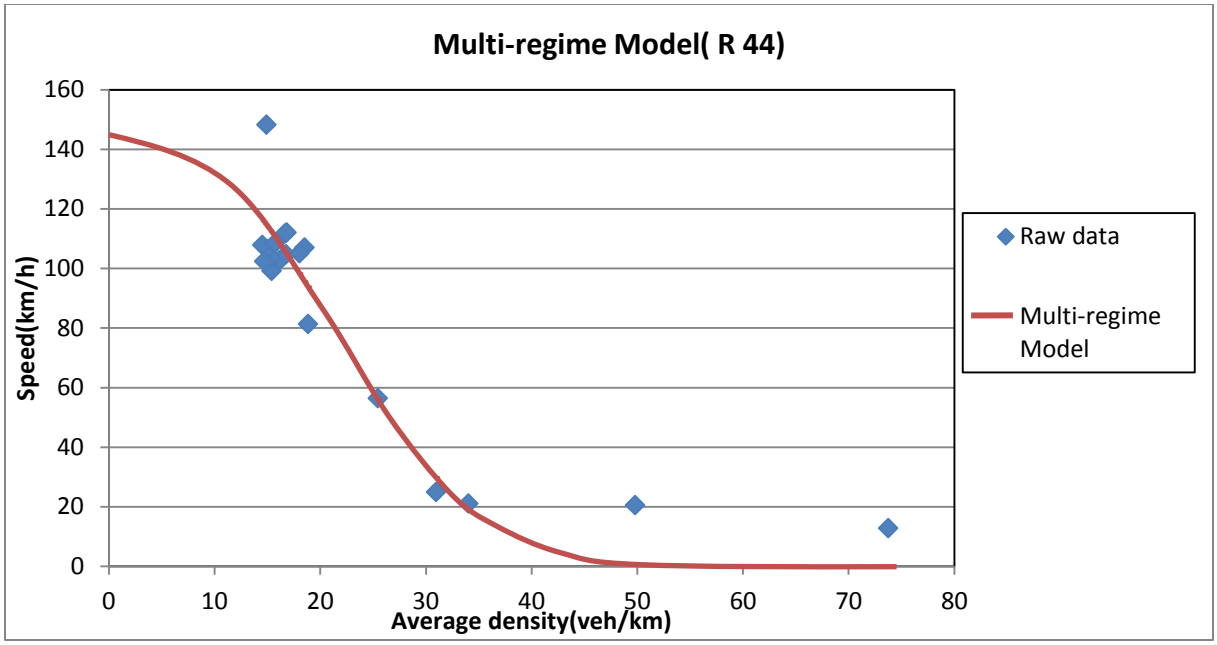

Figure C-21: The multi-regime model fitted to the 5-minutes data taken on R 44 in the south bound direction

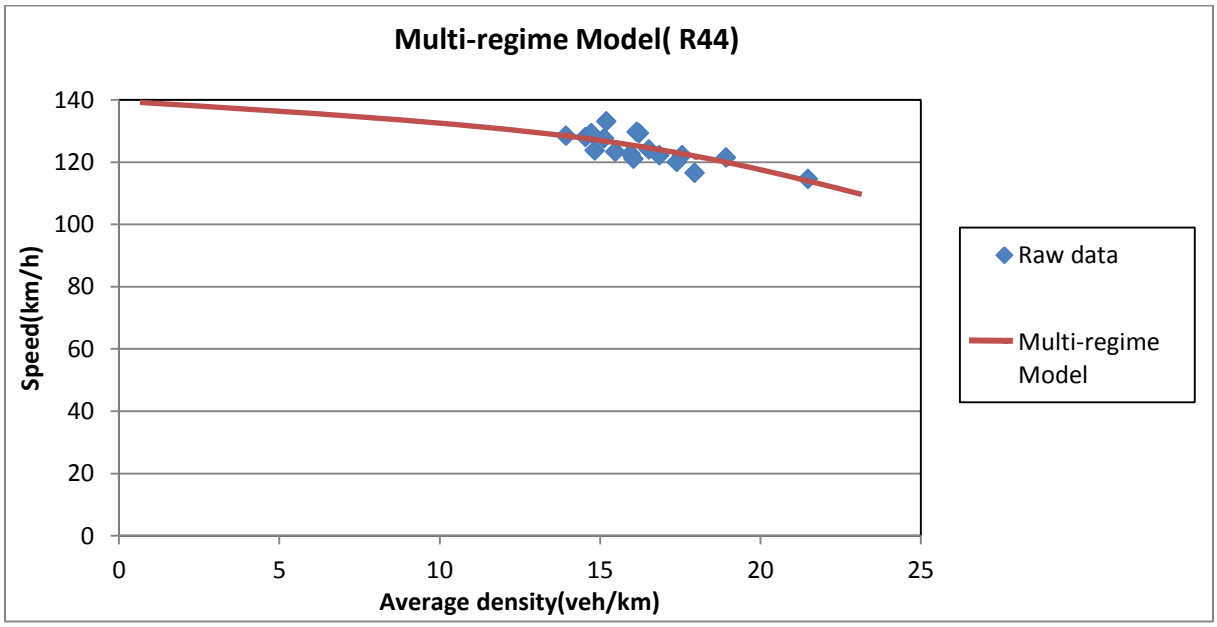

Figure C-22: The multi-regime model fitted to the 5-minutes data taken on R 44 in the north bound direction

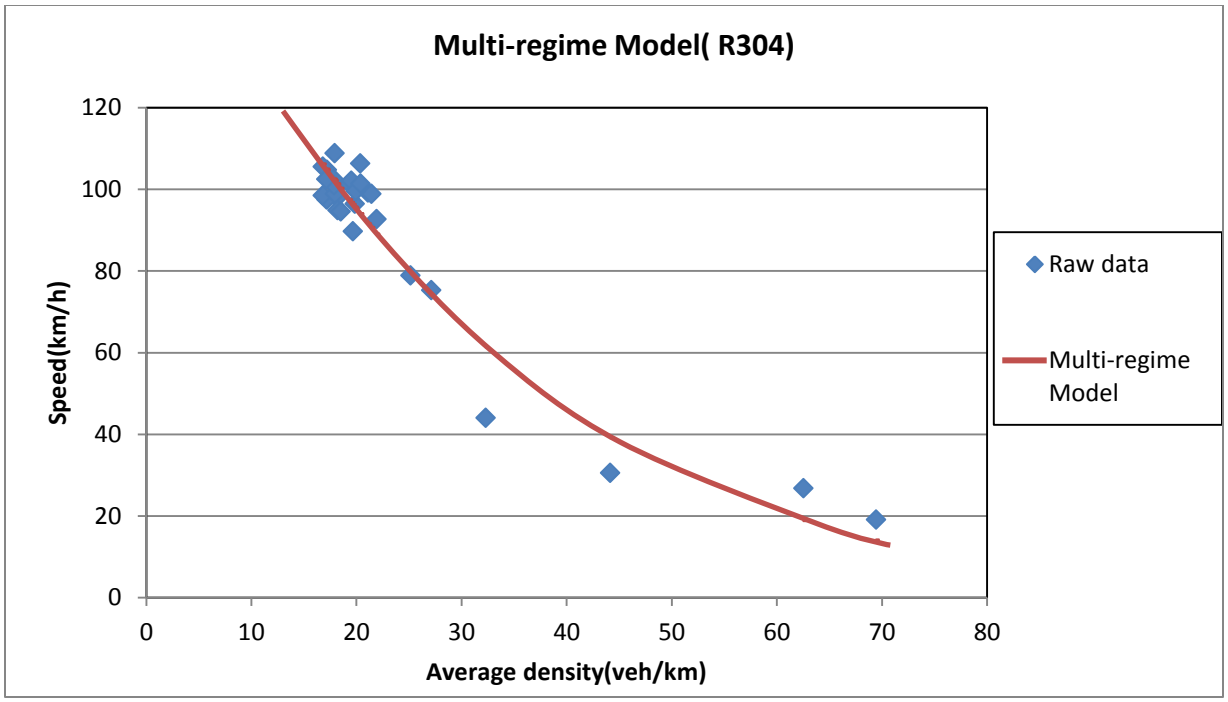

Figure C-23: The multi-regime model fitted to the 5-minutes data taken on R 304 in the south bound direction

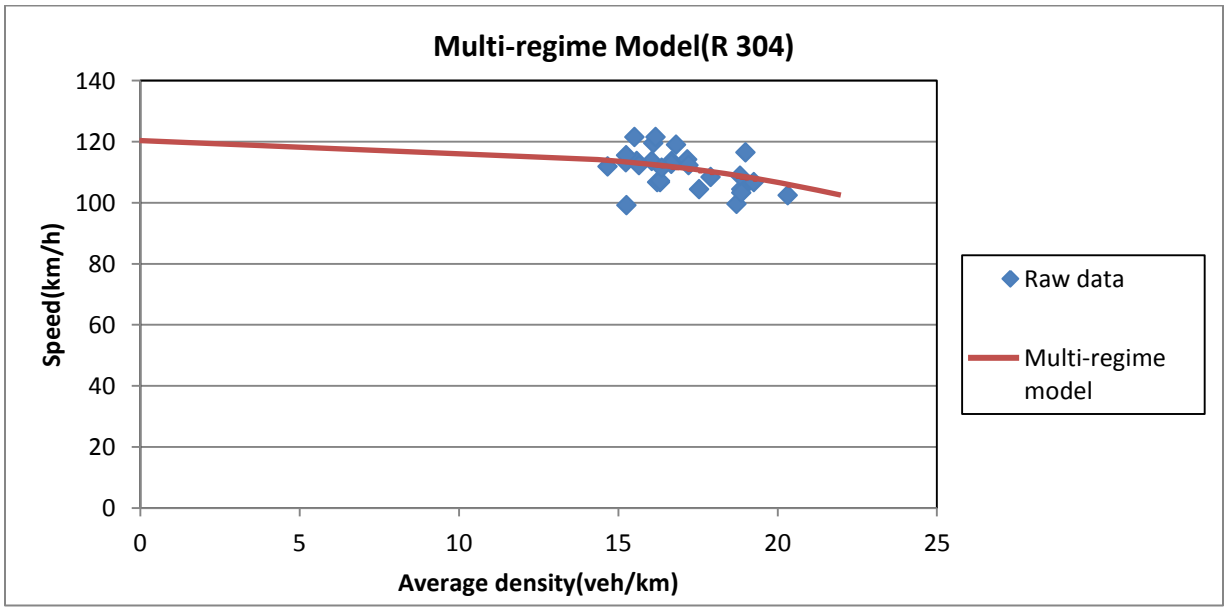

Figure C-24: The multi-regime model fitted to the 5-minutes data taken on R 304 in the north bound direction

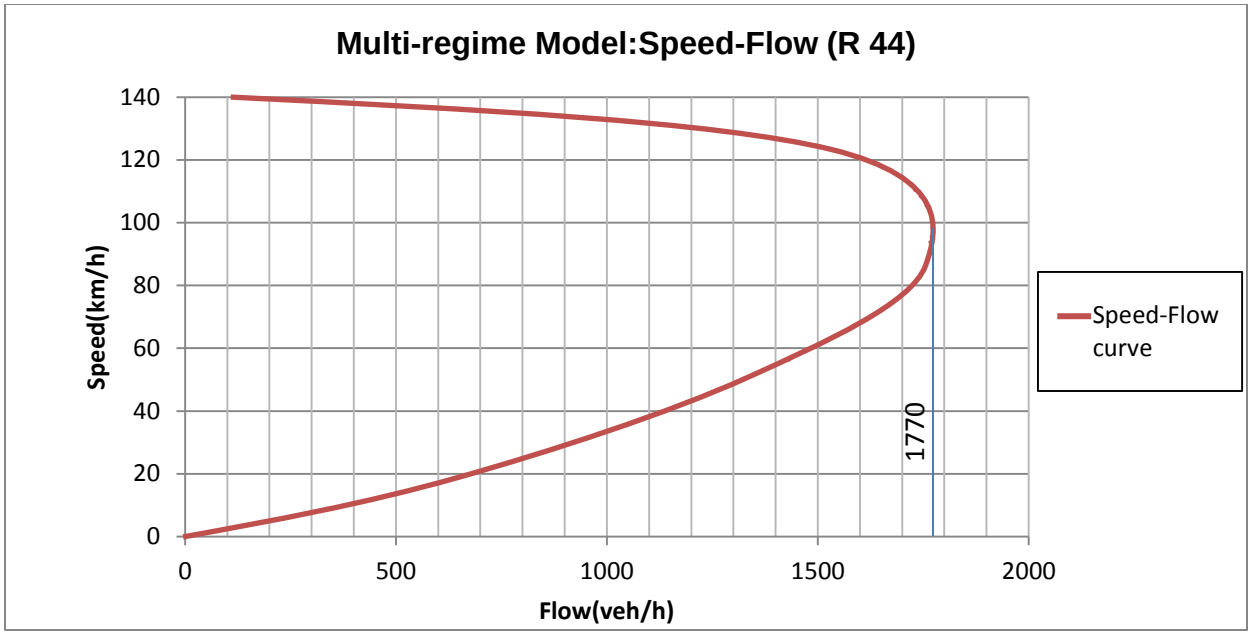

Figure C-25: Speed-Flow relationship showing capacity value on Section 1 for 5-min analysis

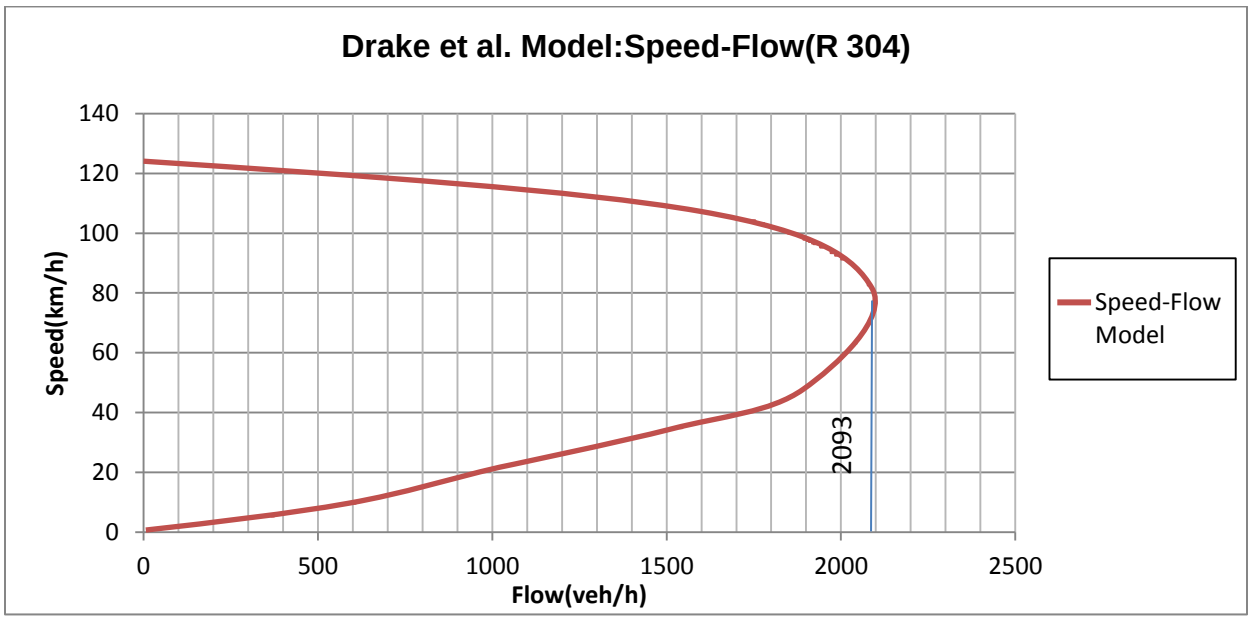

Figure C-26: Speed-Flow relationship showing capacity value on Section 2 for 5-min analysis